THE UNIVERSITY
of EDINBURGH

Assessing the Photoreactivity of Peatland Derived Carbon in Aquatic Systems

Amy Pickard

Thesis submitted for the degree of Doctor of Philosophy

The University of Edinburgh

2016

Declaration

The candidate confirms that the work submitted is her own, except where work which forms part of jointly-authored publications has been included. The thesis contains three chapters which are published, in review or intended for publication in peer-reviewed journals. Details of each publication are given below. The candidate confirms that appropriate credit has been given within the thesis where reference has been made to the work of others. No part of this work has been submitted for any other degree or professional qualification.

The candidate, as lead author, performed the experiments and laboratory analysis, data analysis and writing of the papers. Co-authors provided support and guidance on the scope and design of the project and contributed to the editing of manuscripts.

A.E. Pickard, K.V. Heal, A.R. McLeod and K.J. Dinsmore, Temperature and Filtration Effects on the Photoreactivity of Peatland Carbon. Intended for submission to *Photochemical and Photobiological Sciences* (Chapter 3).

A.E. Pickard, K.V. Heal, A.R. McLeod and K.J. Dinsmore, Temporal Changes in Photoreactivity of Dissolved Organic Carbon and Implications for Aquatic Carbon Fluxes from Peatlands. Published in *Biogeosciences* (doi:10.5194/bg-14-1793-2017) (Chapter 4).

Co-author Andrew Stott contributed laboratory analysis related to the isotope methods in the following paper:

A.E. Pickard, K.V. Heal, A.R. McLeod, K.J. Dinsmore and A.W. Stott, Photochemical and Microbial Processing of Aquatic Carbon in Peatland Pools. Paper in review at *Journal of Geophysical Research: Biogeosciences* (Chapter 5).

Amy Pickard

March 2017

Lay summary

Peatlands are areas of wet, spongy ground which contain decomposing vegetation. The wet conditions typical of peatlands mean that micro-organisms – including bacteria - are unable to digest plant material and so dead plants, instead of decaying fully, become part of the ground as soil. Peatlands are therefore large stores of carbon (C) (the matter which comprises all living things), containing an amount similar to the C stored in the global atmosphere. Water moves on top of the peat or below the surface through water tracks. During this process, water in contact with the peat becomes enriched in C, appearing darker in colour and resulting in water that looks similar to a strongly brewed tea. In time, the C rich water reaches small streams or ponds, which in turn flow into rivers bound for the ocean.

Within these aquatic environments, C can be broken down by micro-organisms and the action of sunlight, and released in the form of gases which can enhance global warming. However, the importance of sunlight on C in aquatic systems is not well known. How much C in aquatic systems reacts with light (is photoreactive) and what factors affect reactivity? Does photoreactivity of C vary between different types of aquatic systems, for example small streams versus large rivers and lakes? How important is the light driven breakdown pathway compared to other pathways? This study aimed to address these questions.

Initial laboratory tests used water samples collected from a stream draining a peatland (Auchencorth Moss, SE Scotland). Exposure to light resulted in gas production from C in the water samples and it was found that the photoreactivity of C is partly controlled by the temperature of the water, with a 13°C temperature increase resulting in a doubling of C photoreactivity. Samples were then collected across a year from the same peatland stream and from a large reservoir draining a peat catchment (Loch Katrine, Central Scotland). Over the course of the year, the peatland stream was a source of photoreactive C, but samples from the reservoir site were less photoreactive. At the stream, samples collected in the winter were the

most photoreactive and heavy rainfall was found to be important in delivering photoreactive C to the system. Finally, the effect of light exposure was also measured in-situ at two peatland pool sites (Red Moss of Balerno, SE Scotland and Cross Lochs, N Scotland). The light driven pathway was responsible for up to 51% of total C breakdown in comparison to breakdown by micro-organisms.

Overall, the results of the study suggest that peatland derived C is reactive to sunlight and that this may be an important part of aquatic C cycles, particularly in small streams and peatland pools. Understanding how much C is released from aquatic systems due to the action of sunlight should be an important focus for future research. This is very important as increasing concentrations of C in aquatic systems have been seen over the past 30 years and inland aquatic systems are expanding due to the melting of previously frozen soils (permafrost). The light driven C breakdown pathway may therefore ultimately provide a positive feedback for climate change.

Abstract

Northern peatlands are a globally important soil carbon (C) store, and aquatic systems draining peatland catchments receive a high loading of dissolved and particulate forms of C from the surrounding terrestrial environment. Once incorporated into the aquatic environment, internal processes occur to modify the C pool. Of these, photo-processing preferentially targets terrestrially derived C and therefore might have a significant effect on the C budget of peatland draining aquatic systems. The overarching aim of this study was to investigate photochemical processing of C in Scottish peatland draining aquatic systems in order to determine the importance of this pathway in aquatic biogeochemical cycles.

For initial laboratory experiments, water samples from a peatland headwater stream (Auchencorth Moss, SE Scotland) were collected. Laboratory based irradiation experiments were conducted at a range of temperatures, and different filtration treatments, including unfiltered samples, were employed to understand the fraction of C most susceptible to photo-processing. UV irradiation and temperature had a significant effect on DOC and gas headspace concentrations, with Q_{10} values of ~1.42 and ~1.65 derived for CO_2 and CO photoproduction in unfiltered samples, respectively. However, filtration treatment did not induce significant changes in gaseous C production between light and dark samples, indicating that the experimental conditions favoured breakdown of DOC rather than POC to CO_2 and CO. In all light treatments a small but significant increase in CH_4 concentration was detected. These data were compared to results from experiments conducted in ambient light and temperature conditions. DOC normalised CO_2 photoproduction was an order of magnitude lower than in laboratory conditions, although relative abundances of C species within overall budgets were similar and these experiments demonstrated that ambient exposure is sufficient to generate photo-processing of aquatic peatland C. Overall these data show that peatland C, particularly the < 0.2 µm fraction, is highly photoreactive and that this process is temperature sensitive.

Further laboratory irradiation experiments were conducted on filtered water samples collected over a 13-month period from two contrasting aquatic systems. The first was the headwater stream draining Auchencorth Moss peatland with high DOC concentrations. The second was a low DOC reservoir (Loch Katrine, C Scotland) situated in a catchment with a high percentage peat cover. Samples were collected monthly from May 2014 to May 2015 and from the stream system during two rainfall events. Significant variation was seen in the photochemical reactivity of DOC between the two systems, with total irradiation induced change typically two orders of magnitude greater and DOC normalised CO_2 production a factor of two higher in the headwater stream samples. This is attributed to longer water residence times in the reservoir rendering a higher proportion of the DOC recalcitrant to photo-processing. Overall the magnitude of photo-induced C losses was significantly positively correlated with DOC concentration in the headwater stream, which varied seasonally with highest concentrations detected in late autumn and winter. Rainfall events were identified as important in replenishing the stream system with photoreactive material, with lignin phenol data indicating mobilisation of fresh DOC from woody vegetation in the upper catchment during a winter rainfall event. Whilst these data clearly demonstrate that peatland catchments generate significant volumes of photoreactive DOC, the degree to which it is processed in the aquatic environment is unclear.

Field investigations were undertaken to address this uncertainty. In-situ experiments with unfiltered water samples in light and dark conditions were conducted in two contrasting open water peatland pool systems. At the high DOC site (Red Moss of Balerno, SE Scotland), DOC concentrations in surface light exposed samples decreased by 18% compared to dark controls over 9 days and light treatments were enriched in CO_2 and CH_4. Photochemical processing was evident in δ^{13}C-DOC and δ^{13}C-DIC signatures of light exposed samples, which were enriched and depleted, respectively, relative to dark controls (+0.23 ‰ and -0.38 ‰) after 9 days of surface exposure. At the low DOC site (Cross Lochs, Forsinard, N Scotland) net

production of DOC occurred in both light and dark samples over the experiment duration, in part due to POC breakdown. δ^{13}C-DIC signatures indicated photolysis had occurred in light exposed samples (-1.98 ‰), whilst δ^{13}C-DOC data suggest an absence of photo-processing, as the signatures in both treatments were similar. Accounting for light attenuation through the water column, 46 ± 4.9 and 8.7 ± 0.5 g C-CO_2 eq m^{-2} yr^{-1} was processed by photochemical and microbial activity in peatland pools within the catchments at the high and low DOC sites, respectively. At both sites, light driven processing was responsible for a considerable percentage (34 and 51%) of gaseous C production when compared to equivalent estimates of microbial C processing and thus should be considered a key driver of peatland pool biogeochemical cycles.

It is clear from this study that temperature, seasonal cycles, rainfall events and water residence time provide strong controls on the photoreactivity of aquatic C in Scottish peatland systems. The photo-processing pathway has the potential to alter the C balance of peatland catchments with a high percentage coverage of aquatic systems. Under climate change scenarios where light, temperature and rainfall conditions are expected to change, this process may become increasingly important in aquatic C cycling, particularly if the upward trend in DOC concentrations in northern aquatic systems continues.

Acknowledgements

Many people have contributed to their time, energy and ideas for the betterment of this PhD and I am grateful to all of them. Firstly I would like to thank my primary supervisor, Professor Kate Heal, for her continued support over the last few years. She has provided guidance, enthusiasm and encouragement from the outset of my PhD through to the finish. I would also like to thank the other members of my supervisory team, Dr Andy McLeod and Dr Kerry Dinsmore, for their guidance and advice.

Laboratory work during this PhD was made much easier with the help of Andy Gray and John Morman, who have been on hand to provide help shifting gas cylinders, to source mysteriously disappearing blue roll and for chats in an otherwise quiet laboratory! Stephen Mowbray helped me to understand the lignin phenol extraction method, from which I have yielded some really interesting data. Thanks also to Jim Smith, who allowed me to monopolise his freeze drier for the summer of 2015, and helped out in the set-up of my irradiation facility. I was awarded a grant from the NERC Stable Isotope Facility, where I worked with Andy Stott and Helen Grant at CEH Lancaster. Thanks to them both for their assistance.

Field work support was provided by the following people: Rebecca McKenzie, Matt Jones, Sarah Leeson, Roxane Anderson and Ian Washborne. Many thanks to each of them. A special mention must go to Laura Parker, who came to Achiemore for a fortnight to help with my extended field campaign in summer 2015. Fraser Leith has been a great source of help through my PhD, especially when Kerry was on maternity leave, and accompanied me on my first trip to Auchencorth. Thank you for passing on your knowledge and enthusiasm for all things peat.

A big thank you to the friends I have made within the GeoSciences department. The coffee breaks, interesting chats and weekends away have made my PhD experience so enjoyable. To

my good friend Ken, thanks for helping out on many early mornings in the lab and for post experiment coffee and muffins.

My family: Mum, Dad, Lucy and James, are a constant source of support and encouragement. I am very grateful for the regular trips they have made to Edinburgh and for everything else they have done for me. To Milton, thanks for putting a smile on my face every day. Finally, I would like to say my biggest thank you to my fiancé, Drew.

This PhD was funded by a Natural Environment Research Council PhD studentship grant and further financial support was provided by a Moss PhD scholarship courtesy of Derek and Maureen Moss.

Table of Contents

List of Tables

List of Figures

List of Abbreviations

Ad	Acid
Al	Aldehyde
C	Carbon
C phenol	Cinnamyl phenol
CDOM	Coloured dissolved organic matter
DIC	Dissolved inorganic carbon
DOC	Dissolved organic carbon
DOM	Dissolved organic matter
FA	Fulvic acid
FI	Fluorescence index
GHG	Greenhouse gas
HA	Humic acid
HMW	High molecular weight
LMW	Low molecular weight
MAT	Mean air temperature
NECB	Net ecosystem carbon balance
P phenol	P-hydroxy phenol
PAR	Photosynthetically active radiation
POC	Particulate organic carbon
S phenol	Syringyl phenol
SOC	Soil organic carbon
SUVA	Specific ultraviolet absorbance
UV	Ultraviolet
V phenol	Vanillyl phenol

Chapter 1 Introduction

The aim of my PhD is to improve understanding of the role of photochemical processing of carbon (C) in the C budgets of peatland draining aquatic systems. Firstly, specific objectives and hypotheses for this study are presented and the thesis structure is outlined. Next, an overview of the types of C found in aquatic systems and the role of peatlands as significant and dynamic sources of C to freshwaters is provided. Finally, the processes by which C is processed in the aquatic environment are reviewed, with particular focus placed on photo-processing, and methods for measuring aquatic C photoreactivity are discussed.

1.1 Thesis objectives and hypotheses

To address the primary aim of my PhD, four principal objectives are investigated, as stated below alongside hypotheses to be tested:

Objective 1: Identification of important factors influencing C breakdown upon irradiation of peatland derived water samples.

H1: Irradiation induced processing of peatland derived organic matter will increase with water temperature, due to the increased activity of photochemically produced reactive oxygen species (ROS) at higher temperatures.

H2: Samples will become progressively less photoreactive as they are filtered with smaller pore size filters, as the filtering process removes both particulate and dissolved carbon which, if present in the sample, could be oxidised by photolysis.

Objective 2: Assessment of natural variation in DOC photoreactivity as a function of DOC source and concentration and catchment position of the aquatic system (a headwater stream vs a standing water reservoir).

H1: Both the headwater stream and lake will exhibit seasonality with regards to the supply of photochemically reactive DOC, with highest concentrations detected in the winter when solar radiation is lowest and thus less in-situ photo-processing has occurred.

H2: Photochemical processing of DOC will be a more significant loss term of C in the headwater stream system than the lake, as samples in the headwater stream will have had a lower light exposure history.

H3: Rainfall events in the headwater stream will replenish the supply of photoreactive DOC from the surrounding catchment due to their flushing effect on peatland soils where DOC is formed. Lignin phenols will be used to infer a soil flushing effect

Objective 3: Quantification of the significance of photo-processing of C in a field setting, through comparison of a high DOC and a low DOC peatland draining aquatic system.

H1: The role of photochemical C turnover will be of similar importance when compared to microbial C processing in the overall C budget within both the high and low DOC pools.

H2: The contribution of photochemically produced C gases to the overall C budget will be greatest in the low DOC system, due to reduced light attenuation effects in the water column.

Objective 4: Application of stable C isotope tracers to allow interpretation of C breakdown pathways.

H1: There will be a change in the stable C isotope ratios ($\delta^{13}C$) of aquatic C upon exposure to sunlight, in both the DOC pool ($\delta^{13}C$-DOC) (where a positive excursion is anticipated) and in the products of photolysis ($\delta^{13}C$-DIC) (where a negative excursion is anticipated).

1.2 Thesis structure

This thesis is composed of three main results chapters based on published, submitted and planned journal papers, each addressing one or two of the objectives listed above by presenting results and discussion from laboratory and field based studies (Figure 1.1). An overview of

the key methods used to generate the data presented in this thesis follows in Chapter 2, with further details provided in the respective results and discussion chapters.

Chapter 3 – Details controlled laboratory irradiation experiments conducted using DOC rich water samples collected from the Black Burn at Auchencorth Moss, Scotland. The experiments were conducted to understand the factors affecting DOC breakdown and the subsequent production of C-based gases, thus addressing Objective 1. Experimental parameters including water temperature, which remains largely unexplored in terms of its effect on photochemistry, and filtration pore size were varied systematically to understand what drives degradation of DOC. Laboratory photo-processing data were compared to data collected from exposure experiments conducted in ambient light conditions to determine the potential importance of the light driven pathway in C processing within peatland draining aquatic systems.

Chapter 4 - Describes temporal variability in photochemical reactivity of DOC in two contrasting peatland draining aquatic systems in order to address Objective 2. Monthly water samples from the Black Burn (a headwater stream) and Loch Katrine (a standing water) were taken from May 2014 – May 2015 for use in laboratory irradiation experiments. These were designed to investigate temporal changes to the aquatic C pool at different positions within a catchment and to understand how DOC concentration and composition were related to susceptibility to photodegradation. At the Black Burn, stream water was also sampled during two rainfall events to determine the role of short term hydrological drivers in controlling DOC photoreactivity. Lignin phenol data measured through these events were used to determine changing plant source contributions to the stream during rainfall, providing a novel data set for a peatland catchment.

Chapter 5 - Investigates the processes of C breakdown in a field setting, using a combination of stable isotopic, optical and chemical analyses. Unfiltered water samples were exposed to ambient sunlight in-situ within two contrasting peatland pool systems (high DOC vs low DOC) in June 2015. Changes to the composition of C species in the water samples were measured

over varying timescales and stable isotopes for DOC and DIC were analysed to provide enhanced process understanding of C breakdown pathways: a first for studies conducted in peatland pool environments. This study aimed to improve understanding of the importance of photochemical processing in relation to other degradation processes and the extent to which aquatic C processing is a loss pathway of C to the atmosphere, thereby addressing Objectives 3 and 4.

Chapter 6 - This chapter brings together the major findings from the above studies to address the over-arching aim of the thesis, whilst putting the results in the context of other contemporary research taking place in peatlands across northern latitudes and assessing the implications of the research results for understanding the contribution of aquatic C processing to peatland C budgets.

Chapter 7 – Finally, ideas for future research based on the findings of this study are discussed and the conclusions of the thesis are presented

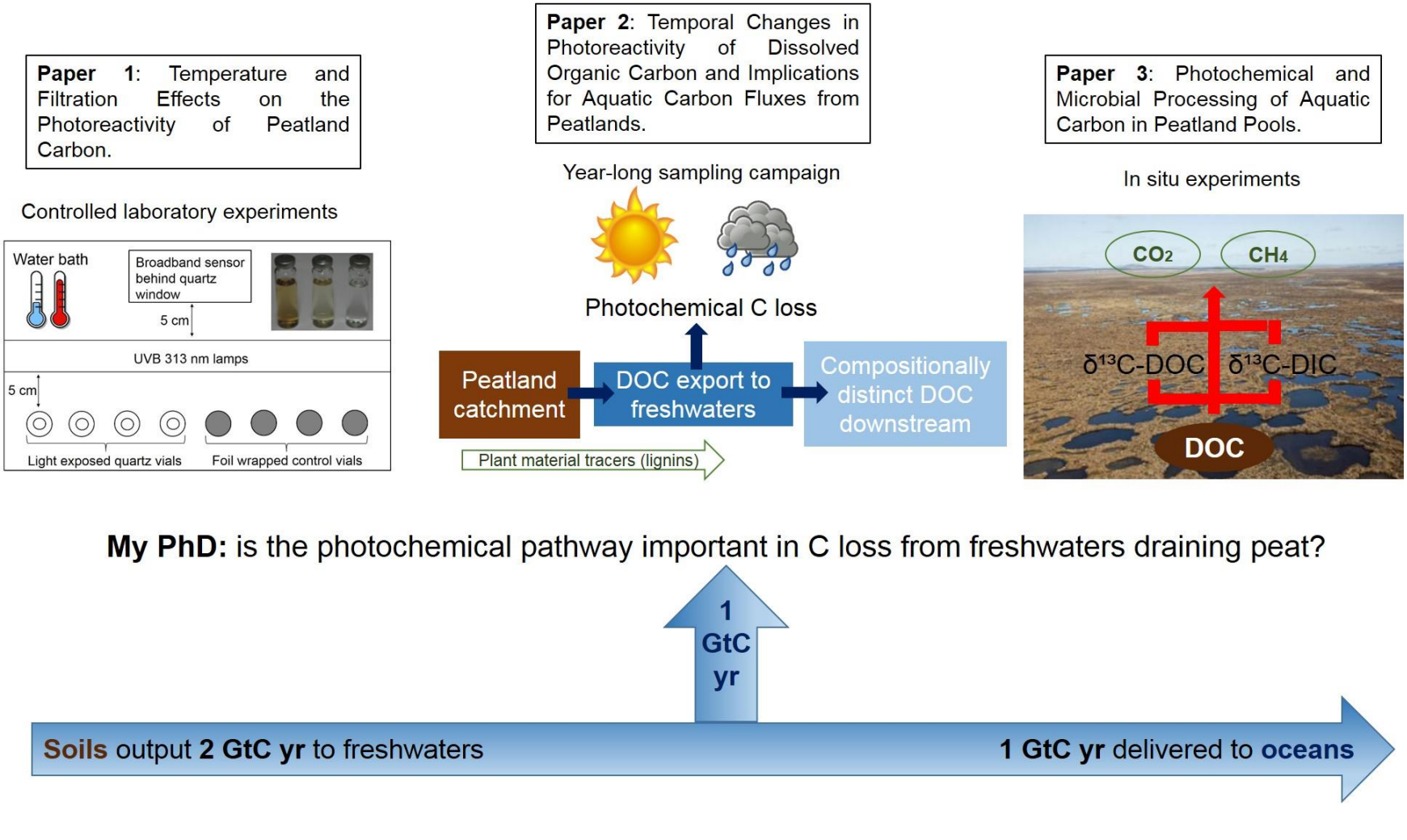

Figure 1.1 Conceptual diagram of the PhD in relation to aquatic carbon cycling, with graphical summaries provided for each paper.

1.3 The form and role of carbon in aquatic systems

Carbon is ubiquitous in freshwater aquatic systems and is present in various compounds. Three primary forms of C, encompassing both organic and inorganic species, can be identified: (i) dissolved i.e. dissolved organic carbon (DOC) and dissolved inorganic carbon (DIC) (ii) particulate organic carbon (POC), and (iii) gaseous, such as CO_2, CO and CH_4. POC is generally defined as the fraction of organic matter which is retained on a 0.45 μm pore size filter (Matilainen et al., 2011) and DOC is defined as the material which passes through the filter. Filtration pore sizes of 0.22 μm (Pokrovsky et al., 2010) and 0.7 μm (Dinsmore et al., 2010) have also been used to distinguish POC from DOC. The relative contribution of dissolved, particulate and gaseous C species to total aquatic C concentration is variable. For example, the relative proportions of some inorganic forms of C present in stream water (DIC and CO_2) are dependent on pH (Palmer et al., 2015). Previous studies in a peatland stream which quantified all C species have identified the following relative mass abundances: DOC > DIC > CO_2 > POC > CH_4 (Billett et al., 2004; Dinsmore et al., 2013), however these are subject to dynamic change driven by a range of climate and land use related factors.

Whilst DOC and POC are useful operational terms, they do not detail the highly variable composition of organic C in aquatic systems (Figure 1.1). It can be comprised of low molecular weight (LMW) and high molecular weight (HMW) substances, ranging from recalcitrant humic acids to labile carbohydrates (Sulzberger and Durisch-Kaiser, 2009).

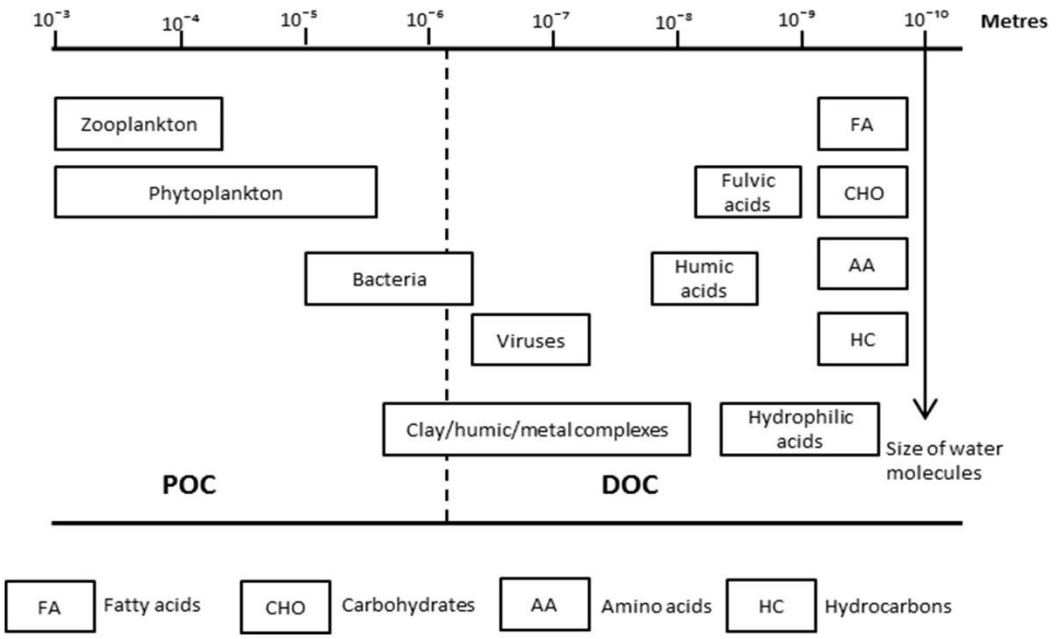

Figure 1.2. Continuum of organic C in aquatic systems. After Robards et al., (1994).

Compositional variation in DOC is partly due to its derivation from two different sources. Autochthonous DOC is produced within aquatic systems through the metabolic activity of microbes, aquatic plants and algae. It is comprised of LMW, labile compounds such as carbohydrates, peptides and amino acids, which can be readily used as an energy source by heterotrophic microbial communities, therefore fuelling aquatic biogeochemical cycles. In a typical riverine system, autochthonous material accounts for ~25% of dissolved organic matter (DOM) (McKnight et al., 2003).

Allochthonous DOC is delivered to aquatic systems via mobilisation of plant and soil derived material from the terrestrial environment. Additional inputs from direct precipitation and leaf fall may also account for a small proportion of allochthonous aquatic DOM (Stockley et al., 1998). It is typically comprised of a suite of HMW aromatic substances such as humic, fulvic and transphilic acids. In a typical river, fulvic acids account for 45 – 65% of DOM, although this can increase to 80 – 90% in wetland environments (McKnight et al., 2003). Allochthonous DOC has been previously considered as biologically inert (Steinberg et al., 2008), however it

is well established as important in aquatic biogeochemical cycles because of its susceptibility to sunlight induced degradation (Opsahl and Zepp, 2001; Cory et al., 2007). Chromophoric components of allochthonous DOC alter the spectrum of radiation penetrating into the water column by absorbing visible and ultraviolet (UV) light (Häder et al., 2014; Williamson et al., 2014), a process which results in the formation of various degradation products, including CO_2, CO and LMW organic substrates (Moran and Zepp, 1997). In addition to directly enhancing aquatic biogeochemical cycling via photodegradation, attenuation by chromophoric (coloured) DOC reduces the penetration depth of harmful UV radiation (Roulet and Moore, 2006). As such, DOC concentration has an indirect effect on primary production of aquatic systems, as it shields aquatic plants from UV radiation which can cause DNA damage and inhibit photosynthesis (Häder and Sinha, 2005).

Determining trends in the relative contribution of autochthonous and allochthonous DOC sources can reveal changes in trophic status of an aquatic system (Smith et al., 2006) and in the rate and mass flux of C cycled in an associated terrestrial system. For example, elevated concentrations of DOC, particularly humic fractions, in aquatic systems have been used to indicate increased rates of soil erosion in the surrounding terrestrial environment and the depletion of soil organic carbon (SOC) stocks (Lal, 2003; Yallop et al., 2010). Measurements of C species within aquatic systems can therefore be used to indicate wider change within a landscape (Schindler and Smol, 2006).

Other motives for investigating trends in aquatic DOC include its negative impact on the quality of drinking water (Clark et al., 2010). DOC not only colours and odourises drinking water so that it requires extensive treatment before human consumption, but has also been associated with the production of carcinogens due to chlorination (Holden et al., 2007), a widespread and cost-efficient means of disinfecting drinking water supplies. This has significant cost and health implications for populations reliant on a DOC-rich water resource. DOC also acts as a complexing agent for potentially toxic elements (such as iron, copper,

aluminium, zinc, arsenic and mercury) and can therefore contribute to their transport to downstream ecosystems (McKnight et al., 1992; Sharp et al., 2006), including the estuarine and marine environment.

The importance of DOC for water quality is widely recognised, but challenges remain in quantifying its role in aquatic biogeochemical cycles and resultant fluxes of C from freshwaters to the atmosphere. The degree to which aquatic organic matter is biogeochemically cycled depends on its concentration and composition, which in turn are dictated by variation in its source material.

1.4 Sources and controls of carbon in peatland draining aquatic systems

The relative contribution of autochthonous and allochthonous sources to the DOC pool varies between aquatic systems. In lacustrine environments, autochthonous material can dominate the DOC budget (Bertilsson and Jones, 2003). However, in most river systems, particularly low order streams, allochthonous inputs are more important due to direct interface and strong hydrological coupling with catchment soils (Lowe and Likens, 2005; Kothawala et al., 2015). Inputs of terrigenous (i.e. allochthonous) organic matter are also suggested to account for a greater proportion of DOC in aquatic systems located in boreal and temporal environments, where peatlands are widespread (Palmer et al., 2001; Stedmon et al., 2007). Northern peatlands are an important store of global SOC, despite covering only 3% of the land surface area, with estimates of total soil C stored in these environments ranging from 450 Gt C (Gorham, 1991) to 270 Gt C (Turunen et al., 2002) to 547 Gt C (Yu et al., 2012). These estimates are comparable to the estimated C store of the global atmosphere (730 Gt C; Ciais et al. (2013)).

Given their capacity to sequester SOC, peatlands are one of the main foci for C cycling research. The Net Ecosystem Carbon Balance (NECB) has been estimated for a range of peatland catchments, providing quantification of the inputs and outputs of all C species from the individual flux pathways within a catchment. A significant flux term identified in peatland

NECB studies is C export via the aquatic pathway, which is estimated to account for 13 – 37% of annual C uptake via Net Ecosystem Exchange (Nilsson et al., 2008; Dinsmore et al., 2010; Koehler et al., 2011; Juutinen et al., 2013).

Typically DOC is the largest term in estimates of the fluvial C export budget, although in eroding peatland catchments POC flux can become a significant term (Table 1.1) and annual POC fluxes of 78.9 MgC km^{-2} a^{-1} have been reported from a degraded peatland catchment in the UK (Pawson et al., 2012). In contrast to less eroded peatlands, POC dominated the C flux relative to DOC within this system and this finding demonstrates the need for site driven characteristics to be considered when evaluating aquatic C export. DOC is mobilised by the movement of pore waters through C rich soil horizons before entering adjacent aquatic systems. Typical DOC concentrations of 20 – 60 mg L^{-1} have been reported in northern peatland draining aquatic systems (Blodau, 2002). Soil C storage and percentage of catchment covered by peatland explained >85% of the variation in DOC concentration recorded in 32 Scottish streams (Aitkenhead et al. (1999).

Table 1.1 Fluvial C export measured for peatland catchments in the UK, Ireland and Sweden. Where available, annual export is defined for C species: DOC, POC, DIC, CO_2 and CH_4.

Reference	Location	Catchment area km^2	Peatland type	Fluvial C export g C m^{-2} yr^{-1}				
				DOC	POC	DIC	CO_2	CH_4
Dinsmore et al., (2010)	Auchencorth Moss peatland, UK	3.4	Ombrotrophic peatland	25.4	3.6	0.7	1.3	0.01
Nilsson et al., (2008)	Degerö Stormyr mire, Sweden	6.5	Mixed acid mire	TOC = 13.0			4.6	0.3
Worrall et al., (2003)	Moor House, UK	11.4	Blanket peatland	9.4	19.9	5.9	3.8	
Dawson et al., (2004)	Glen Dye, UK	46.3	Hill peats (61.7% of catchment)	12-22	1-10		0.2-1	0.001-0.009
Dawson et al., (2002)	Brocky Burn, UK	1-3	Heather moorland	17	2		0.2	<0.001
Koehler et al., (2011)	Glencar, Ireland	7.5	Atlantic blanket bog (85% of catchment)	14.0				

Many studies have reported strong seasonal DOC concentration cycles in in aquatic systems draining peatlands (e.g. Worrall et al., 2006; Dinsmore et al., 2013). As DOC is primarily derived from allochthonous sources in temperate and boreal aquatic environments, these cycles reflect soil properties and are strongly influenced by regional vegetation and climate. Summer and autumn maxima in DOC concentration are observed in many peatland draining aquatic systems (Fenner et al., 2001; Wallin et al., 2015), relating to rates of terrestrial soil decomposition which peak in warm summer months when microbial activity is highest (Fenner et al., 2005). When near surface soil horizons are re-wetted by late summer and autumn rainfall, there is a flushing effect whereby the DOC produced over the summer is entrained and delivered to aquatic environments, thus increasing concentrations (Limpens et al., 2008). The flushing effect can be detected until the soil DOC store is depleted and hence depends on the volume of soil production and the intensity of catchment rainfall events. Post-flushing, DOC concentrations typically decrease to a winter/spring minimum, until warmer temperatures allow further decomposition (Dawson et al., 2008).

Although autochthonous DOC is a smaller term in peatland aquatic C budgets, it also varies seasonally. In northern peatlands, low temperatures, nutrient availability and pH are considered to limit internal DOC production rates for much of the year (Hope et al., 1994). Higher water temperatures and low flow conditions in the summer months may increase microbial activity and water residence time, resulting in a greater contribution of DOC from autochthonous sources.

Superimposed onto the seasonal cycle is the episodic loss of DOC and POC driven by storm event hydrology. A large percentage of the annual DOC export (36 to >50%) can occur during high-intensity rainfall events (Hinton et al., 1998; Eimers et al., 2008; Fellman et al., 2009). In some catchments, up to 66% of the annual DOC export has been attributed to a single storm event (Hinton et al., 1997). Storm events mobilise near surface soil hydrological pathways that are typically inactive during base flow, thus providing a similar catchment flushing effect to

late summer rainfall. However storm events in peat catchments are not always associated with peaks in aquatic DOC concentrations (Clark et al., 2007). Storm driven saturated overland flow which has had minimal soil contact time can have a diluting effect on DOC concentrations, but high flows mean that overall DOC fluxes still increase during storms. Heterogeneity exists in response of DOC concentrations to individual storm events, which needs to be considered when scaling DOC losses from peatland catchments using discharge data (Clark et al., 2007).

1.4.1 Anthropogenic and climatic influences on aquatic DOC

With their high capacity for C storage, DOC export from peatlands has been shown to be affected by anthropogenic disturbance. Burning, cutting for fuel, drainage, afforestation and deforestation in peatlands have been demonstrated to cause increased DOC loss, due to drying of the peat, water table changes and variations in hydrological flow paths (Holden et al., 2007; Billett et al., 2010; Parry et al., 2014). Land management pressures in peatlands are ongoing (Holden et al., 2007), however identifying changes in aquatic DOC loading due to anthropogenic peatland disturbance can be difficult as it is set against a background of already increasing DOC in freshwaters across northern latitudes (Monteith et al., 2007).

DOC concentrations have increased in the majority of monitored surface waters in Europe and North America over the last two decades (Roulet and Moore, 2006; Clark et al., 2010). Evans et al., (2006) reported an average 91% increase in DOC concentrations in UK rivers and lakes since 1988. It is suggested that the dynamics of northern peatlands are primarily responsible for the reported increases in DOC (Freeman et al., 2001; Worrall et al., 2004) and several hypotheses have been proposed to explain the upward trend.

One mechanism proposes that increased air temperature causes accelerated rates of peat decomposition thus releasing more DOC into aquatic environments (Worrall et al., 2004). However studies indicate that DOC concentrations are not sufficiently responsive to warming to account for the magnitude of the detected changes when temperatures have risen by less

than 1ºC (Freeman et al., 2004). Freeman et al., (2004) proposed that DOC increases are caused by elevated atmospheric CO_2 which results in increased terrestrial productivity and litter production and hence a larger available terrestrial DOC store. Tranvik and Jansson (2002) proposed that changes to precipitation affect runoff rates and the volume of DOC transported to aquatic systems. Increased runoff volumes result in greater DOC export, with an expectation that a higher contribution of flow will be derived from near surface soil pathways where DOC is abundant. Monteith et al. (2007) found that widespread DOC increases in surface waters across the northern hemisphere are strongly correlated with a decline in the sulphate content of atmospheric deposition. Atmospheric deposition of sulphur compounds causes soil acidification, thereby decreasing DOC.

Clark et al. (2010) suggest that the varying explanations for observed increases in DOC concentrations are mostly compatible and the phenomenon is probably the result of interacting drivers. Although uncertainty remains about the exact combination of mechanisms responsible for DOC increases, there does appear to be consensus that global change, in the form of atmospheric CO_2 increase (Freeman et al., 2004), hydrological variation (Tranvik and Jansson, 2002) and increasing temperatures (Worrall et al., 2004), will serve to enhance the effect.

The concentration of DOC in peatland aquatic environments clearly relies upon the interplay of many factors. Once incorporated into the aquatic environment, internal processes may occur to modify the DOC pool. The reported changes in DOC concentrations in northern peatlands have served to increase efforts to understand whether DOC is actively transformed in the aquatic systems to which it is delivered (Moody et al., 2013).

1.5 The fate of aquatic carbon

Although DOC export to freshwaters has been identified as a major C output from peatlands (Dinsmore et al., 2010), its fate is unclear since terrestrial derived material accounts for only a small proportion of the marine-DOC pool (Meyers-Schulte and Hedges, 1986; Lalonde et

al., 2014). Resolving the apparent imbalance between reported DOC fluxes in freshwaters and ocean delivery requires identification of the processes by which C is removed.

It is recognised that freshwater systems do not act as passive 'pipes' for organic C transport between land and sea, but are active zones of organic matter transformation (Cole et al., 2007; Battin et al., 2009). Previous studies of DOC processing in freshwaters suggest that up to 50% of the C exported from terrestrial environments is lost to the atmosphere as greenhouse gases (GHGs) (Tranvik et al., 2009). Cole et al. (2007) estimated that of the 1.9 Pg C yr^{-1} that enters rivers globally, 0.8 Pg C yr^{-1} is returned to the atmosphere. A more contemporary study suggests a global evasion rate of 2.1 Pg C yr^{-1}, which is higher than previous estimates due to upward revisions of both terrestrial inputs and the evasion rates of large streams and rivers (Raymond et al., 2013). Recent estimates also indicate that freshwaters are globally significant CH_4 emission sources, emitting around 0.65 Pg C yr^{-1} (Bastviken et al., 2011).

Outgassing from soil water super-saturated with CO_2 and CH_4 entering peatland freshwaters contributes to GHG emissions (Battin et al., 2009a; Billett et al., 2015) but given the disproportionately high loading of allochthonous C to these environments, considerable further biogeochemical processing of C may take place. The driver of biogeochemical aquatic C cycling that this study focuses on is the photochemical processing of C stimulated by exposure to sunlight. An overview of this process follows, with consideration of how it has the potential to enhance microbial processing of C via heterotrophic respiration.

1.5.1 Photochemical processing

The absorption of UV and visible light by coloured (dissolved) organic matter (CDOM) in aquatic environments results in photodegradation (Miller, 1999). Shorter visible wavelengths (< 500 nm) and particularly those in the UV (280 - 400 nm) are primarily responsible for photochemical reactions, as they transfer more energy to the absorbing molecule (Hader, 2000). CDOM in the water column absorbs photons during photolysis, leading to bond

cleavage of the C compound into a variety of photoproducts and a reduction of its molecular mass (Osburn and Morris, 2003).

LMW organic compounds produced during direct photolysis include aldehydes and carboxylic acids (Moran and Zepp, 1997). These products are formed from partial oxidation reactions, whereby the compound is not completely degraded by the reaction to an inorganic state. The importance of partial oxidation is dependent on the aromaticity of the compound, whereby increasingly aromatic compounds are more likely to undergo complete photo-oxidation (Cory et al., 2014).

The most abundant of the inorganic photoproducts is CO_2, formed during photochemical reaction of CDOM with oxygen (Osburn and Morris, 2003). CO and other forms of DIC such as carbonic acid (H_2CO_3) and hydrogen carbonate (HCO_3^-) are also generated by complete photo-oxidation (Bertilsson and Tranvik, 2000; Miller and Zepp, 1995a). It is estimated that 10 to 50% of DOC in various water types can be photomineralised directly to CO_2 and CO (Miller and Zepp, 1995; Anesio et al., 2005) and thus it is important to consider this process in order to quantify aquatic C cycling.

Reactive species, including free radicals, hydrated electrons and reactive oxygen species, are also formed during photolysis which can stimulate secondary reactions in the water column (Paul et al., 2004). Indirect reactions involving reactive species generated by photolysis can result in transformation of non-chromophoric fractions of organic matter (Sulzberger and Durisch-Kaiser, 2009) and it is suggested that these secondary reactions may contribute to most of the observed photodegradation effect (Osburn and Morris, 2003).

As CDOM molecules absorb UV and visible radiation, they reduce the penetration depth of light in the water column. This results in photochemical reactions taking place primarily in the surface water (Köhler et al., 2002; Anesio and Granéli, 2003). Due to preferential light absorbance by CDOM, photoreactions are associated with bleaching of aquatic organic matter

(i.e. loss of colour) (Vecchio and Blough, 2002; Zhang et al., 2013). The penetration depth of light in the water column may increase in aquatic systems with high concentrations of photo-bleached material, resulting in photochemical reactions occurring at greater depths (Benner and Kaiser, 2011).

In addition to water column light availability, pH is another identified environmental factor which affects photoreactivity (Anesio and Graneli, 2003; Molot et al., 2005). Lower pH water samples have typically been found to show increased photoreactivity relative to ambient pH samples (Anesio and Graneli, 2003) and this effect has been attributed to higher production of hydroxyl radicals with decreasing pH (Porcal et al., 2013).

The presence of iron (Fe) in water samples can also have an effect on photoreactivity. Fe absorbs UV light and enhances photo-oxidation of humic substances (Bertilsson and Tranvik, 2000; Molot et al., 2005). Bertilsson and Tranvik (2000) observed elevated DIC production rates in water samples with high Fe concentrations. In acidic water samples, production of hydroxyl radicals is increased by the photo-Fenton reaction (Molot et al., 2005) and therefore there is strong interaction between pH and Fe on overall photoreactivity. The negative relationship between pH and Fe concentration detected by Porcal et al. (2013) in their seasonal study of photoreactivity supports this view.

1.5.2 Interaction of photo-processing with heterotrophic respiration

Heterotrophic bacteria are abundant in aquatic systems and contribute to biogeochemical cycling through re-mineralisation of organic C and nutrients (del Giorgio and Cole, 1998). Re-mineralisation results in production of forms of inorganic C, including CO_2. Simple C in the form of carbohydrates and carboxyl acids is more readily used by bacteria as a substrate for respiration than terrestrially derived C (Kritzberg et al., 2004). The major factors that limit bacterial DOC removal in aquatic environments are temperature, nutrient availability and the organic matter source (Farjalla et al., 2009). However, as allochthonous C is the major DOC

constituent in many aquatic systems, autochthonous C alone does not support bacterial production.

Results from recent studies indicate that chemical quality rather than type of DOC (allochthonous vs. autochthonous) determines bacterial DOC turnover (Koehler et al., 2012; Attermeyer et al., 2015). As photolysis results in the formation of LMW C from previously biologically recalcitrant HMW compounds, it stimulates the activity and growth of aquatic microorganisms (Figure 1.2) (Anesio et al., 2005; Bertilsson and Tranvik, 1998; Moran and Zepp, 1997).

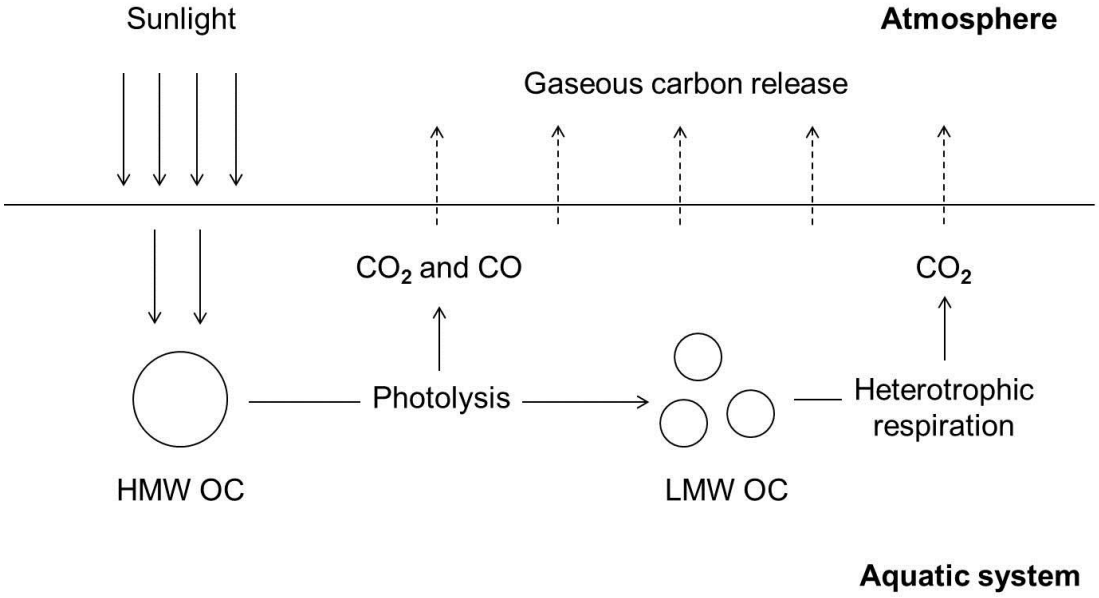

Figure 1.3 Schematic of the interaction of photo-processing and heterotrophic respiration in aquatic systems not limited by oxygen and the potential for C release to the atmosphere.

Interaction between these processes is thought to be greatest in systems with high concentrations of allochthonous DOC. Farjalla et al. (2009) observed that photochemical degradation of DOC in a highly humic tropical lagoon resulted in a threefold increase in both bacterial respiration and production. The relative importance of photochemical and microbial degradation of DOC is not yet well understood in many aquatic environments. However a combination of both processes is likely to be responsible for considerable loss of C from the

aquatic environment to the atmosphere. Freshwater transformations driven by photochemical and microbial degradation also influence on downstream processing of C in marine environments and hence the eventual fate of C.

1.5.3 Potential importance of photochemical processing of carbon in peatland systems

Photochemical processing of C may be significant in peatland draining aquatic systems as they receive a large amount of terrestrially derived chromophoric, aromatic material which is highly susceptible to photochemical decomposition (Osburn and Morris, 2003). For example the 3.4 km^2 catchment of Auchencorth Moss in Scotland inputs 110 ± 63.6 kg DOC yr^{-1} to the peatland stream into which it drains (Dinsmore et al., 2010). Furthermore, low pH conditions associated with peatland aquatic environments have been shown to increase organic matter photoreactivity (Anesio and Graneli, 2003). Consequently the role of photochemical processes in degradation of aquatic C in northern peatland dominated catchments has received increasing recognition (Franke et al., 2012; Cory et al., 2014; Worrall and Moody, 2014).

Moody et al. (2013) conducted photodegradation experiments on DOC rich samples obtained from a peatland headwater and determined mean DOC losses of 73% over 10 days. Jones et al. (2015) observed a significant reduction in DOC concentration (14–17%) in unfiltered peatland stream water after exposure to a dose of solar radiation equivalent to one mid-summer day. Other studies further suggest that DOC photoreactivity may be considerable in low order streams draining peatlands (Köhler et al., 2002; Franke et al., 2012). However, despite high measured photoreactivity, there is still uncertainty as to whether significant in-situ DOC processing takes place in temperate and boreal aquatic systems (Wollheim et al., 2015; Kothawala et al., 2015).

Furthermore, the contribution of photochemical breakdown to total C processing in aquatic environments has been constrained in few studies, often providing contrasting results with regard to its significance. In a study of global lakes and reservoirs, Koehler et al. (2014)

determined that direct sunlight-induced CO_2 emissions accounted for one tenth of the global CO_2 emissions from these systems. However, in a basin-scale Arctic study, Cory et al. (2014) determined that photomineralisation rates exceeded dark bacterial respiration rates by a factor of nearly 5 and accounted for 70 - 95% of DOC processed in the water column of Arctic lakes and rivers. This PhD aims to quantify in-situ DOC photo-processing in an attempt to improve understanding of its relative importance in aquatic C cycling.

There is a clear need for further investigation of the role of photochemical processing in aquatic systems, particularly in peatland draining aquatic systems, due to the increasing concentrations of DOC measured in these inland waters (Clark et al., 2010). Despite increased concentrations of DOC, no increase in DOC export from continents to the oceans has been observed so far (Lapierre et al., 2013). These observations suggest that terrestrially derived C is readily processed in aquatic systems and that aquatic CO_2 emissions resulting from C processing may be globally significant (Lapierre et al., 2013).

Biogeochemical cycling induced C losses from freshwater aquatic environments remain unquantified in the Intergovernmental Panel on Climate Change's (IPCC) estimates of global C cycling (Ciais et al., 2013) and so this emissions pathway has no direct impact upon modelled global GHGs (Worrall and Moody, 2014). In order to accurately predict rates of climate change it is becoming increasingly important to quantify the pathways of C output from aquatic systems. Within the frame of this wider research, this PhD aims to determine the photoreactivity of peatland derived carbon in aquatic systems and place an estimation on the importance of in situ photolysis in comparison to other C loss pathways.

1.6 Measuring photoreactivity of aquatic peatland carbon

Biogeochemical characterisation of water samples prior to and post light exposure has the potential to aid understanding of the photoreactivity of peatland organic matter. A range of

methods can be employed for this purpose, with this section focussing on analytical techniques used in this study to measure photoreactivity.

Most widely used in photochemical studies are changes to bulk measurements of DOC concentration (Köhler et al., 2002; Moody et al., 2013; Jones et al., 2015). Determining the difference in DOC concentration in samples before and after light exposure can show the magnitude of photo-induced change to the aquatic C pool. This is an important technique as it is directly relevant for C budget investigations. Other studies focus on photoproduction of inorganic C species, in dissolved (e.g. Groeneveld et al., 2015) and gaseous form (e.g. Stubbins et al., 2011). However, despite their frequent measurement in photochemical investigations, few studies have tracked mass balances changes to all aquatic C species (gaseous and dissolved) resulting from photochemical transformations. This is important for peatland draining aquatic systems as low pH conditions may mean that loss of DOC to DIC occurs as CO_2 and CO, rather than as dissolved forms such as H_2CO_3 and HCO_3^- (Franke et al., 2012).

Although bulk measurements are useful to understand the magnitude of photoreactivity, they cannot resolve compositional and structural information which enable understanding of inherent susceptibility to photochemical breakdown. A number of methods that yield compositional information can be performed on water samples with no pre-treatment requirements other than filtration. One of these is UV-visible absorbance spectrophotometry.

Due to strong energy absorbance of UV and visible radiation by organic matter, UV-visible (UV-vis) absorbance spectrophotometry can determine both the rough concentration and composition of DOM (Korshin et al., 1997). As the amount of absorbance increases proportionally with the concentration of chromophores in a water sample, this technique can be used as a proxy for DOC concentration. Absorbance at 254 nm is most often used for this purpose, although wavelengths ranging from 250 – 562 nm have also been studied (Peacock et al., 2014). Different chromophores within a sample absorb radiation at different wavelengths allowing inferences to be made regarding DOM composition. Most absorbance

spectra exhibit trends of decreasing absorbance with increasing wavelength, so measurement of absorbance at single wavelengths or wavelength ratios can help to determine specific compositional variations in DOM (Table 1.2).

Table 1.2 Wavelengths at which UV-vis absorbance is measured, and the compositional properties inferred from these measurements.

Measure	Wavelength(s) nm	Inferred property	Reference
SUVA	254 400	Aromaticity	Weishaar et al. (2003) Worrall et al. (2007)
E2:E3 ratio	250 : 365	Aromaticity and molecular weight	Peuravuori and Pihlaja (1997)
E2:E4 ratio	254 : 465	Humification	Park et al. (1999)
E4:E6 ratio	450 : 650 465 : 665	Humification and molecular weight	Wilson et al. (2011) Wallage et al. (2006)

Specific UV absorbance (SUVA) is defined as the UV absorbance of a water sample at a given wavelength, typically 254 nm, normalised for DOC concentration (Weishaar et al., 2003). $SUVA_{254}$ is a useful parameter for estimating the aromatic C content in aquatic systems. Samples with higher $SUVA_{254}$ values on the typical scale range of 0 - 6 are typically enriched in humic substances derived from allochthonous organic C sources (Peacock et al., 2014). E2:E3, E2:E4 and E4:E6 ratios yield information relating to molecular weight, humification and aromaticity of water samples. Examining absorbance parameters upon light exposure can aid understanding of photochemically induced compositional changes (Spencer et al., 2009; Franke et al., 2012).

Fluorescence spectroscopy is used to characterise organic C composition in water samples (McKnight et al., 2001; Fellman et al., 2010). The technique relates the spectral characteristics of a source material at different emission wavelengths to the molecular structure. This allows for distinction between protein-like and humic-like organic compounds, as fluorophores

contained within samples absorb and re-emit radiation at different emission wavelengths (Stedmon et al., 2003). The relative intensity of these wavelength peaks can provide a qualitative assessment of organic matter composition. Within this technique, the Fluorescence Index (FI) and Humification Index (HIX) have been used to identify DOM source material and the extent of humification, respectively (McKnight et al., 2001; Fellman et al., 2010). For the FI ratio, values around 1.8 suggest autochthonous organic material, whereas values around 1.2 indicate terrestrially derived material (Cory and McKnight, 2005), and for the HIX ratio, the larger the number the higher the inferred degree of humification (Ohno, 2002).

Beyond optical and fluorescent techniques, a range of other methods can be used to understand organic C processing in aquatic systems. Lignin phenols are biochemical compounds unique to vascular plants. Whilst they are produced almost exclusively in the terrestrial environment, they are delivered to aquatic environments as part of the bulk DOM pool (Jex et al., 2014). Lignins are highly aromatic molecules which absorb ultraviolet wavelengths strongly and are hence are preferentially photo-processed relative to the bulk DOM pool (Benner and Kaiser, 2011a). Lignin phenols are typically classified into four types: p-hydroxy (P), vanillyl (V), syringyl (S), and cinnamyl (C) phenols (Figure 1.3). The relative abundance of lignin constituents in aquatic systems provides useful information regarding the dominant sources of vegetation on a catchment level, acting as a biomarker from which various vegetation types can be inferred (Jex et al., 2013).

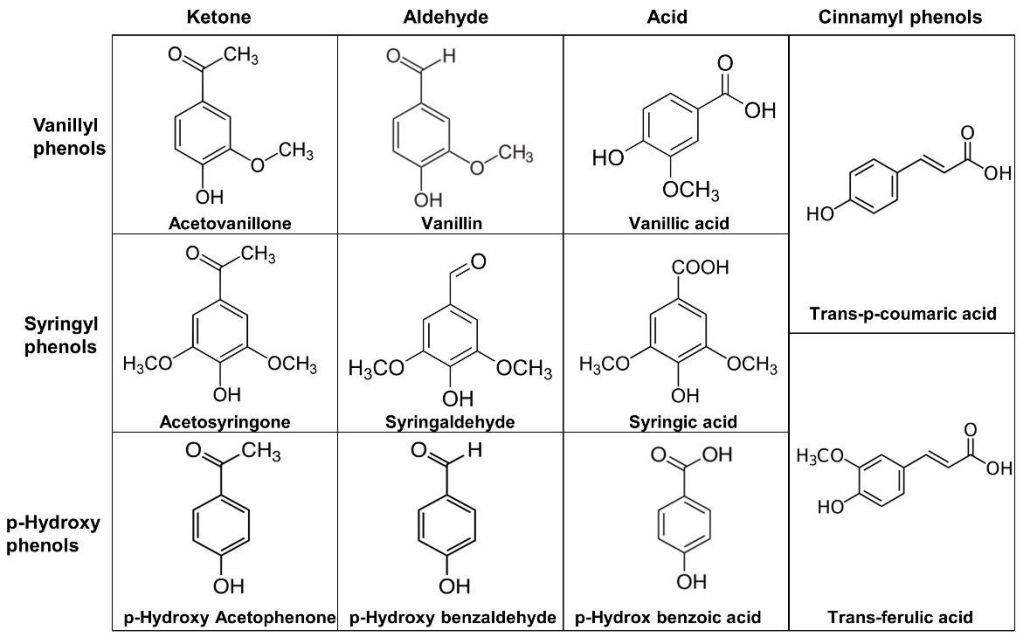

Figure 1.4 Eleven lignin phenols found in peatlands shown in relation to their types (P, V, S and C) and their monomer groups (acid, aldehyde and ketone).

Furthermore they can also indicate the susceptibility of DOM to photo-processing in aquatic environments (Spencer et al., 2009). S and V phenols have been identified in previous studies as particularly photoreactive (Opsahl and Benner, 1998; Benner and Kaiser, 2011b).

Stable C isotope analysis of DOC and DIC in water samples enables determination of the biogeochemical processes that dictate DOM composition (Opsahl and Zepp, 2001; Franke et al., 2012). Previous laboratory exposure studies have shown that photo-processing can lead to enrichment of the δ^{13}C-DOC signature within water samples, related to the preferential loss of aromatic molecules such as lignin phenols (Opsahl and Benner, 1998; Spencer et al., 2009). As photo-processing leads to DIC production, it is likely that evidence of photolysis will also be reflected in the δ^{13}C-DIC, which will be isotopically "light" compared to unexposed controls (Opsahl and Zepp, 2001). This has been observed in freshwaters previously (Opsahl and Benner, 1998; Spencer et al., 2009), but has not been explored within a peatland aquatic context before. Isotopic data from peatland draining aquatic systems collected in this study will provide a novel data set in a previously understudied environment.

Chapter 2 Materials and Methods

This chapter provides an overview of the study sites used in the subsequent chapters (Auchencorth Moss in Chapter 3, Auchencorth Moss and Loch Katrine in Chapter 4, and Red Moss of Balerno and Cross Lochs, Forsinard in Chapter 5). It also gives details of field methods and laboratory irradiation experiments. The main analytical techniques are summarised, with further information regarding study specific methods provided in data chapters 3-5.

2.1 Field sites

Four freshwater study sites were used in this research. The common feature between all sites was their location in a peatland catchment located in Scotland (Figure 2.1). Beyond this, site selection was based on the type of aquatic system, recorded DOC concentrations and degree to which the site had been characterised in previous research (Table 2.1). In the first chapter samples were collected from a well characterised, high DOC system in order to determine maximum photo-processing effects in laboratory conditions. The second chapter compared photoreactivity of samples from a headwater stream and a reservoir over an extended sampling campaign. The final chapter compared organic matter photoreactivity in two peatland pool systems with contrasting DOC concentrations.

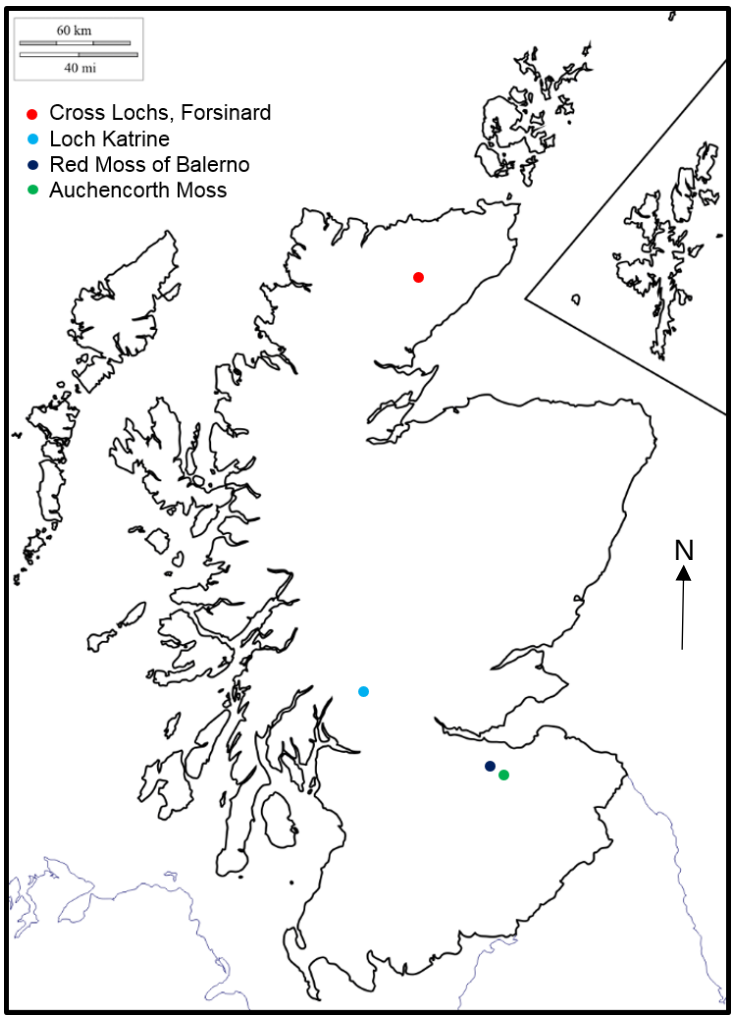

Figure 2.1 Map of Scotland detailing the location of four study sites used in this research. Image sourced from d-maps.com.

Table 2.1 Site characteristics for four peatland catchments containing aquatic systems used in this research.

Site	Peatland type	Catchment area km^2	Peat coverage %	Type of aquatic system	DOC mg L^{-1}	Nature of previous research
Auchencorth Moss	Ombrotrophic	3.4	100	Headwater stream	28.4 ± 1.07[a]	Ongoing research as part of NERC funded Carbon Catchment project
Cross Lochs, Forsinard	Ombrotrophic	1.0	100	Natural peatland pools	13.6 ± 4.58[b]	Ongoing research as part of NERC funded Carbon Catchment project
Loch Katrine	Minerotrophic	96	45	Lake	3.68 ± 0.56[c]	Long term water quality monitoring by SEPA
Red Moss of Balerno	Ombrotrophic	1.6	100	Managed peatland pool	30.5 ± 1.05[d]	Small scale study of terrestrial gaseous emissions[e] Red moss peat soil characterised by multidimensional NMR spectroscopy[f]

[a] Dinsmore et al. (2013), values mean ± standard error
[b] Turner et al. (2016), values mean ± 1 standard deviation
[c] SEPA (pers. comm.), values mean ± 1 standard deviation
[d] Derived from own sampling, values mean ± 1 standard deviation
[e] Hardacre and Heal (2013)
[f] Bell et al. (2015)

2.1.1 Auchencorth Moss

Auchencorth Moss is a 3.4 km² low lying, ombrotrophic peatland catchment 17 km south of Edinburgh, UK (55°47'34"N; 3°14'35"W) (Dinsmore et al., 2010). It is one of the Centre for Ecology & Hydrology's UK Carbon Catchments (www.ceh.ac.uk) (Billett et al., 2010). The catchment has a long term data set regarding both terrestrial and aquatic carbon (C) species, which includes a complete, inter-annual C and greenhouse gas (GHG) budget from 2008 onwards (Dinsmore et al., 2010). The catchment altitude ranges from 250-300 m above sea level (a.s.l).

The peatland is primarily used for low density sheep grazing (Drewer et al., 2010). The vegetation cover over the main body of the peatland consists of grasses, rushes and sedges (*Deschampsia flexuosa*, *Molinia caerulea, Festuca ovina, Eriophorum angustifolium, Eriophorum vaginatum, Juncus effusus)* covering a moss layer of *Sphagnum* and *Polytrichum* (Drewer et al., 2010). Shrubs including *Calluna vulgaris* and *Vaccinium myrtillus* are located in the upper catchment.

The peat catchment is drained by the Black Burn, a small stream with a width of ~1 m and a depth from peat surface to channel bed of ~1.2 m. The stream extends for 4700 m from source to the catchment outlet. The Burn is characterised by low pH, low temperature conditions and a dynamic hydrological response to rainfall events (Billett and Harvey, 2013; Dinsmore and Billett, 2008). Stream water is typically highly coloured (Figure 2.2) and mean long-term DOC concentrations are 28.4 ± 1.07 mg L^{-1} (Dinsmore et al., 2013).

Figure 2.2. Coloured water in the Black Burn at a) high discharge and b) during base flow conditions.

Mean annual air temperature and precipitation measured at the flux tower at the Auchencorth Moss European Monitoring and Evaluation Programme (EMEP) site are 10°C and 1155 mm, respectively (Drewer et al., 2010). Within the stream, mean water temperature is 8.0 ± 3.8°C.

2.1.2 Loch Katrine

Loch Katrine is located in the Loch Lomond and Trossachs National Park, Scotland (56°25'25"N; 4°45'48"W). It is managed by Scottish Water and serves as the primary water reservoir for the city of Glasgow and its surrounding areas. Loch Katrine is located in a peatland catchment and has 88 tributaries that feed into the loch, of which 39 are second order streams or higher. The loch has a surface area of 8.9 km^2 and is approximately 13 km in length and 1 km across at the widest point (Figure 2.3).

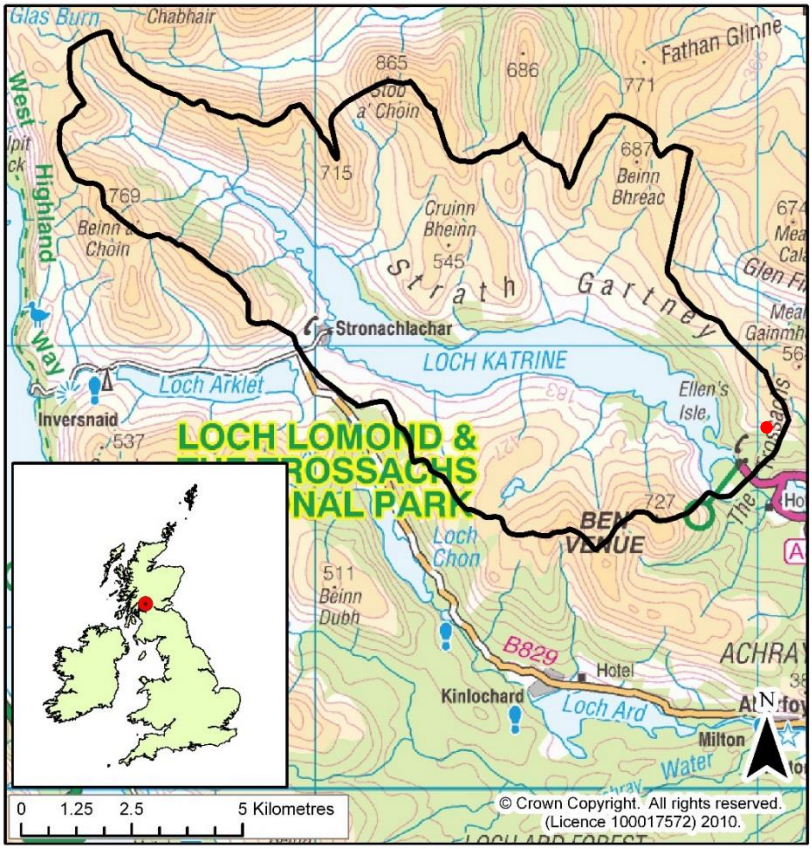

Figure 2.3. Location of Loch Katrine in the UK (inset) and within the Loch Lomond and Trossachs National Park. The black line delineates the hydrological catchment of Loch Katrine. Red dot shows the location of SEPA water sampling point at Ruinn Dubh Aird. Image courtesy of UK Environmental Change Network.

Loch water DOC concentrations, amongst other water quality parameters, have been recorded by the Scottish Environment Protection Agency (SEPA) at Ruinn Dubh Aird, a peninsular located at the south eastern end of the loch. DOC concentrations measured approximately 6 times a year from 2009 - 2014 are consistently very low at 3.68 ± 0.56 mg L^{-1} (SEPA, personal communication). Loch Katrine has a mean pH of 6.53 ± 0.05 and mean water temperature of 10.6 ± 4.13°C.

2.1.3 Red Moss of Balerno

Red Moss of Balerno is a raised peat bog (~1.57 km^2), located 15 km southwest of Edinburgh (55°51”N 3°20”W; 240 m a.s.l) with well-defined hummock-hollow microtopography. Red Moss has an ombrotrophic dome, characteristic of raised peat bogs (Hardacre and Heal, 2013). The peatland site is undergoing restoration coordinated by Scottish Wildlife Trust (SWT), which includes drainage ditch blocking. However due to past drainage and peat extraction water levels are not currently high enough for peat accumulation (Hardacre and Heal, 2013).

The site is drained by an aqueduct that is no longer in commercial use. At the western boundary of the peatland in the topographical low created by the aqueduct, there is a single pool into which the surrounding peat is drained. It has a surface area of 81.4 m^2 and a mean depth of 0.91 m and is actively maintained by SWT through removal of pond vegetation on an annual basis (Figure 2.4).

Figure 2.4. The peat fed pond at Red Moss of Balerno, with high density of aquatic plants in late summer 2014. Photo courtesy of SWT.

In a trial investigation of the site in April 2015, pool DOC concentrations were high (~30.5 mg L^{-1}) (Appendix A). The pool has a surface area of 81.4 m^2 and a mean depth of 0.91 m. No

other large pools are present within the catchment, although there are ephemeral pools of water that collect behind plastic used to block drainage ditches at the site.

2.1.4 Cross Lochs, Forsinard

The blanket bog at Forsinard in the north of Scotland is part of the UK's largest single tract of peatland (~4000 km^2) (www.ceh.ac.uk). It is another of the CEH's UK Carbon Catchments (Billett et al., 2010), with much of the site located within the Forsinard RSPB Reserve. The peatland contains areas dominated by natural bog pool systems. Cross Lochs South is a ~1 km^2 catchment located to the east of the River Dyke and to the west of Forsinard (58°22′N 3°57′W). It has a high density of peatland pools, with ~115 in the catchment of varying size, depth and vegetation coverage (Figure 2.5). The largest pool is 1998 m^2 and the smallest is 7 m^2.

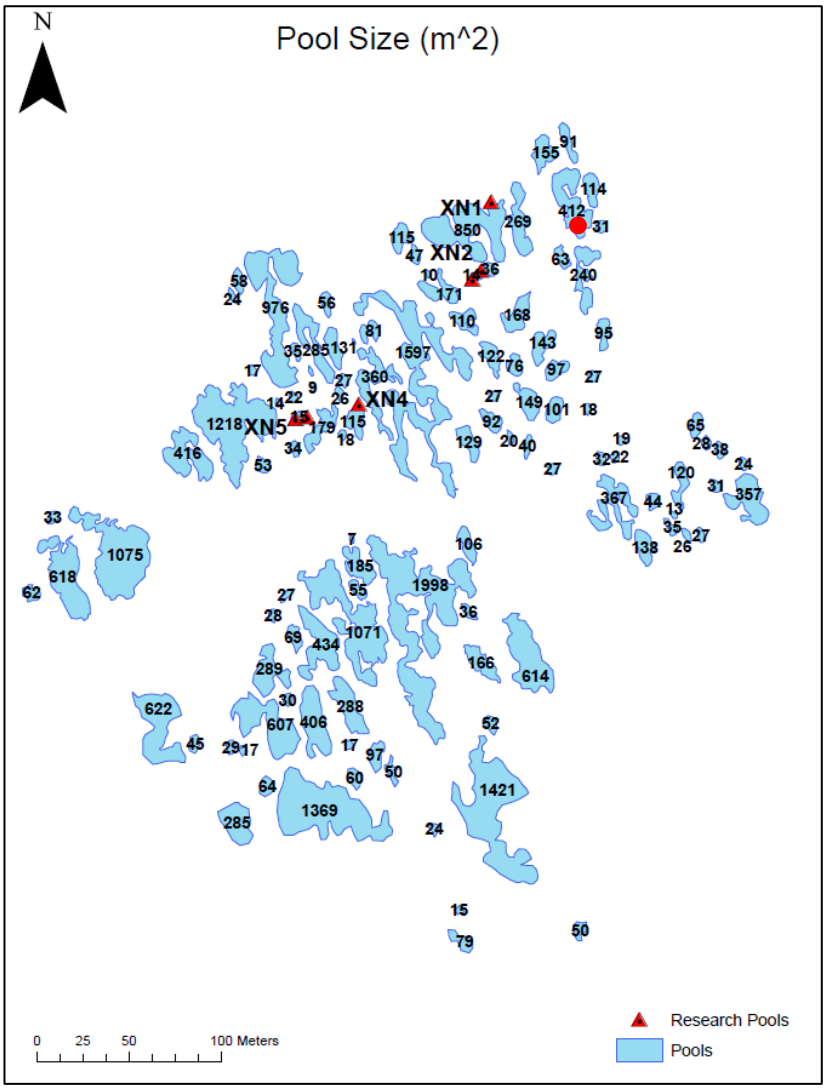

Figure 2.5. Cross Lochs South catchment, with pool surface area in m^2 shown for each of the 115 pools. The red dot marks the pool used in this research (with an area of 412 m^2). Image courtesy of Ed Turner.

DOC concentrations measured in the Flow Country peatland pools are comparatively low compared to the pool at Red Moss, at ~13.6 ± 4.58 mg L^{-1} (Turner et al., 2016). DOC concentrations exhibit a seasonal cycle, with maximum levels recorded in mid to late summer when annual temperatures are highest. A large pool to the north east of the catchment was selected for sampling, as it was sufficiently large (412 m^2) and deep (0.73 m) to house the experimental equipment. In a trial investigation of the site in March 2015, pool DOC concentrations were low (~4.90 mg L^{-1}) (Appendix A).

2.2 Field methods

A range of field methods were used in this study, and here a summary of techniques is provided. Further information regarding field methods can be found in the following data chapters (3-5).

2.2.1 Water sample collection at the Black Burn and Loch Katrine

Water samples were collected from an established sampling site at the Back Burn used in the CEH carbon catchments project and the beach at Ruinn Dubh Aird, Loch Katrine for use in laboratory irradiation experiments.

For laboratory experiments described in Chapter 3, a bulk water sample of 5 L was collected from the Black Burn in October 2013 and again in January 2014. Twelve further 1.5 L samples were collected from 4 August to 16 September 2014 for use in ambient exposure experiments described in the same chapter. From May 2014 to May 2015, 1.5 L water samples were collected on a monthly basis from the Black Burn and Loch Katrine in order to characterise seasonal variation in DOC concentration and composition.

In all instances, water samples were collected approximately 20 cm below the surface of the water, using a screw top sterile 1 L glass bottle. During low flow conditions at the Black Burn where water levels were < 20 cm, the sample was taken at the lowest available point in the water column. The bottles and lids were rinsed twice with site water before collecting the sample. Upon return to the laboratory, samples were refrigerated at 4°C and irradiated within 5 days of collection.

Dissolved oxygen (DO), conductivity, pH and temperature were measured on each sampling occasion at each site with a handheld Hach HQd multimeter (Hach, USA), which was calibrated on site with pH buffers 4 and 7 and an electrical conductivity standard of 1047 $\mu S\ cm^{-1}$.

2.2.2 Rainfall event sampling

The Black Burn, unlike Loch Katrine, showed a dynamic hydrological response to rainfall and it was considered important to determine the effect of such events on stream chemistry and the relative abundance of photoreactive material. Stream water was sampled during two rainfall events, one in winter and one in summer, over the year-long study at the Black Burn. Seasons were defined based on the hydrological year, where winter runs from 1 October to 31 March and summer from 1 April to 30 September (Gordon et al., 2004).

A Teledyne Isco autosampler (Model 3700, Teledyne, USA) was programmed to collect 500 mL of water from the flume at the Black Burn every 30 minutes throughout both rainfall events (Figure 2.6). Two samples of 500 mL were pumped into a 1 L polypropylene sample bottle, so that each hour a composite 1 L sample of water was collected. This allowed characterisation of short term changes in stream water chemistry as a function of rainfall. Upon collection, water samples were transferred into 1 L glass bottles before they were transported to the laboratory for use in irradiation experiments and subsequent organic analyses.

Stream water sampling in the winter rainfall event was conducted from 11:00 GMT on 9 December to 17:00 GMT on 10 December 2014, resulting in 31 samples across the event. Samples were collected during the event after 24 hours in order to replace the bottles and re-set the autosampler to capture the remainder of the event. Stream water sampling in the summer rainfall event started at 14:30 GMT on 1 September and finished at 06:30 GMT on 2 September 2015, resulting in 17 samples.

Figure 2.6. Isco autosampler set up at the Black Burn in the riparian zone, approximately 2 m above the stream channel.

During both events, stream height was measured at 15 minute intervals approximately 2 km downstream from the sampling site on an In Situ Inc. Level Troll pressure transducer with atmospheric correction from a BaroTroll sensor located above the water surface. Stream height readings from the pressure transducer were converted to discharge at the sampling site using manually calibrated rating curves based on dilution gauging measurements (Figure 2.7) (Dinsmore et al., 2013).

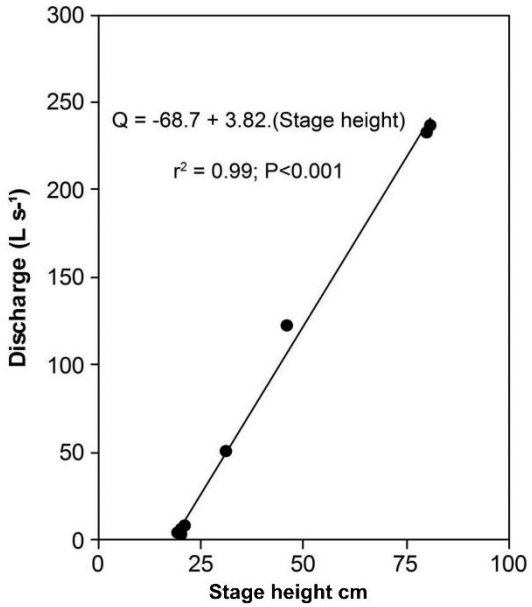

Figure 2.7 Discharge-stage height relationship for the sampling point used in this study at Black Burn, Auchencorth Moss (Dinsmore, pers. comm.)

2.2.3 In situ photo-processing experiments

To quantify the contribution of photochemical processing of C to the overall C budgets of peatland waters, light exposure experiments of varying nature and duration were set up at two peatland pool systems. The first site was the pool at Red Moss, where experiments were conducted from 7-15 June 2015. The second site was the natural bog pool located to the North East of the Cross Lochs South site (Figure 2.5), where experiments were conducted from 21-29 June 2015. The experiments took place at a time of year where maximum irradiation could be expected to produce maximum photo-processing effects and were conducted within the same month so that comparisons were not confounded by seasonal factors.

2.2.3.1 Extended photodegradation experiment

A bamboo cane structure was inserted into the pool sediment the day before experiments commenced to ensure that any disturbance related ebullition fluxes from the systems did not affect results. The structure held 24 Tedlar™ gas bags (1 L volume) in position at the water surface, with approximately 75% of the bag submerged beneath the water surface. At 09:00

GMT on day 1 of the experiment the gas bags were half filled with 500 mL unfiltered water collected from the pool systems using a 60 mL plastic syringe and placed on the pool surface, held in position by the bamboo frame and cable ties. At this time, a 1 L sample of pool water was collected to determine baseline biogeochemical characteristics for comparison with water samples contained in light and dark bags over the experiment duration.

12 bags transmitted sunlight (Figure 2.7) and 12 were covered in foil, acting as dark controls. An ambient headspace of approximately 50 mL was left in the bags to ensure that processing was not O_2 limited. An additional 50 mL of ambient air was added to the headspace of each bag on at 16:00 days 2, 3, 5 and 7 to ensure conditions remained oxygenated throughout the experiment. Two bags of each treatment were removed at 17:00 on days 1, 2, 3, 5, 7 and 9 of the experiment. Replication was limited to two replicates by practical constraints of the number of bags that could be placed at the pool surface.

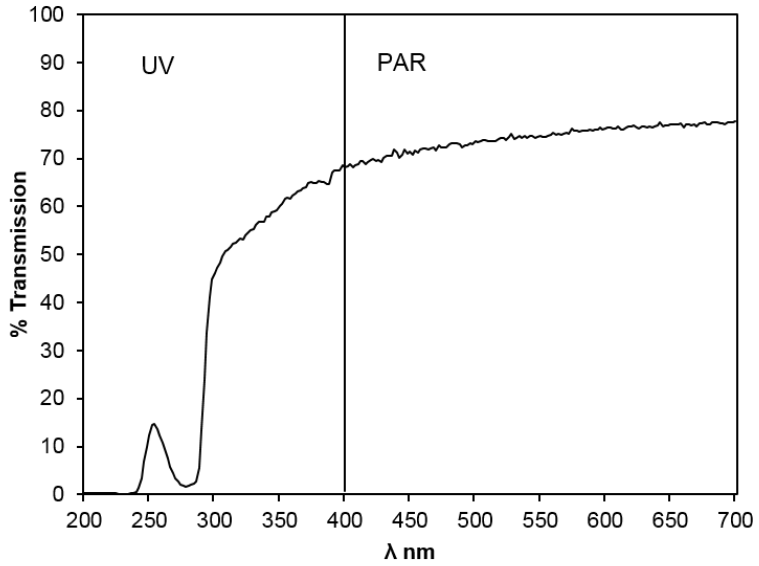

Figure 2.8 Percentage transmission of Tedlar material from 200-700 nm. Results were obtained using a piece of Tedlar in UV-Vis absorbance analysis.

During the experiment, dissolved oxygen (DO), conductivity, pH and water temperature were measured in the surface water of the pool each day at 11:00 and 16:00 GMT with a handheld Hach HQd multimeter. Irradiance from 280 – 700 nm was measured on site at 12:00, 13:00 and 14:00 using a double monochromator scanning spectroradiometer (Model SR9910-V7;

Irradian, UK). Samples from each bag were used in a number of laboratory analyses which are described in the methods section of Chapter 5.

2.2.3.2 Depth attenuation experiments

To quantify the effect of light attenuation on the photo-processing of peatland C in the water column, experiments were conducted with unfiltered water samples contained in Tedlar bags placed at varying depth in the pool systems. Three bamboo cane structures were inserted into the pool sediment the day before experiments commenced. The first structure was designed to hold six gas bags (three transmitting sunlight and three foil covered controls) in place at the surface of the water, the second at a depth of 10 cm and the third at 20 cm below the water surface (Figure 2.9).

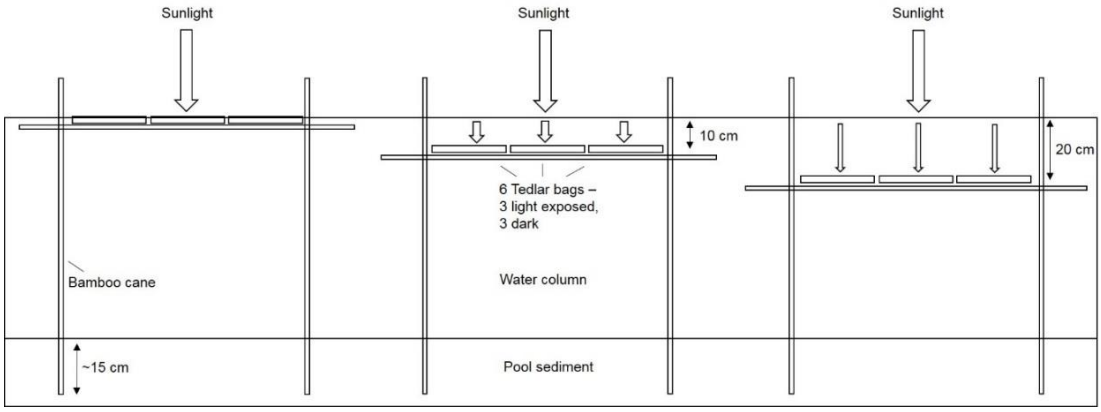

Figure 2.9 Profile view schematic of daily degradation experiment set up.

On the six days that corresponded with sample collection days described in Section 2.2.3.1, 18 bags were half filled with 500 mL water and secured in position on the bamboo structures using cable ties (Figure 2.10). They were exposed to sunlight from 09:00 to 17:00 GMT.

Figure 2.10. Aerial view of Tedlar bags held in position with bamboo frame and cable ties at a depth of 10 cm at Cross Lochs. The three bags in foil are dark controls and the three transparent bags are exposed to sunlight.

After 8 h of exposure the gas bags were collected from their positions in the water column and water samples were used for various laboratory analyses, described in the methods section of Chapter 5.

2.3 Laboratory methods

2.3.1 Irradiation experiments

Water samples collected from peatland aquatic environments in this study were exposed to a known dose of light in a laboratory based irradiation facility to assess photoreactivity of peatland derived C.

2.3.1.1 Sample preparation

Water samples were first degassed in a vacuum system for 20 minutes to remove dissolved gas. Sample aliquots were then prepared for irradiation experiments using three levels of filtration in Chapter 3: unfiltered, and filtered through 0.2 μm MCE filters (Merck Millipore, Germany) and 0.7 μm GF/F filters (Whatman, UK). In Chapter 4, all samples were filtered to

0.2 μm. 15 mL of prepared sample was transferred into 21 mL quartz vials which were sealed with rubber butyl plugs and aluminium crimp tops. The quartz material that comprised the vials was transparent in both the PAR and UV regions of the radiation spectrum (Robson Scientific Technical data). All samples were prepared at room temperature in oxygenated conditions.

2.3.1.2 Irradiation method

Initial laboratory experiments compared water sample photoreactivity after exposure to different lamp types: UV-B 313 and UV-A 351 (Appendix B). It was determined that there was no significant difference between photoproduction of gaseous C from peatland water samples between the two lamp types, if the output of UV-B 313 lamps was adjusted downward to account for its more photochemically effective radiation.

An experimental duration of 8 h was selected following duration experiments in which water samples from the Black Burn were irradiated with UV-B 313 lamps over 1, 2, 4, 8 and 16 h (Appendix C). The results from these experiments showed that significant differences between UV treatment and control samples were generated for headspace CO_2 and CO concentrations after 8 h of irradiation (Table 2.2). As these were photoproducts of interest to this study, the results were used to inform the duration of all further irradiation experiments.

Table 2.2. P values shown for two tailed, paired Student's t-tests conducted between UV treatment and control samples (n=4) at increasing exposure times. Significant differences are determined where p<0.05*

Irradiation time	Headspace CO	Headspace CO_2
+1 h	0.012*	0.852
+2 h	0.006*	0.296
+4 h	0.001*	0.354
+8 h	0.001*	0.017*
+16 h	0.001*	0.015*

Irradiation experiments in data chapters 3 and 4 were performed using UV-B 313 lamps (Q-Panel Com, USA) covered with 125 µm cellulose diacetate (A. Warne, UK) to exclude UV-C (<280 nm) and providing both UV-A (400-315 nm) and UV-B (315-280 nm) exposure. Lamps were mounted inside quartz tubing (Robson Scientific, UK) beneath the water surface in a water bath maintained at a pre-defined temperature (Figure 2.11) and water bath temperatures could be maintained to ± 1 °C of the prescribed temperature. Vials were irradiated sideways while submerged in the water bath below the neck, at a distance of 5 cm from the lamp source. UV irradiance of the samples was modulated to remain constant throughout the 8-h exposure by measurement with a broad-band sensor (Model PMA2102; Solar Light Inc., USA) held beneath the water surface behind a quartz window of the same thickness as the vials. The sensor was calibrated with a double monochromator scanning spectroradiometer (Irradian™, UK), itself calibrated against a secondary deuterium lamp standard (FEL Lamp, F-1297) operated by the NERC Field Spectroscopy Facility, Edinburgh (http://fsf.nerc.ac.uk/).

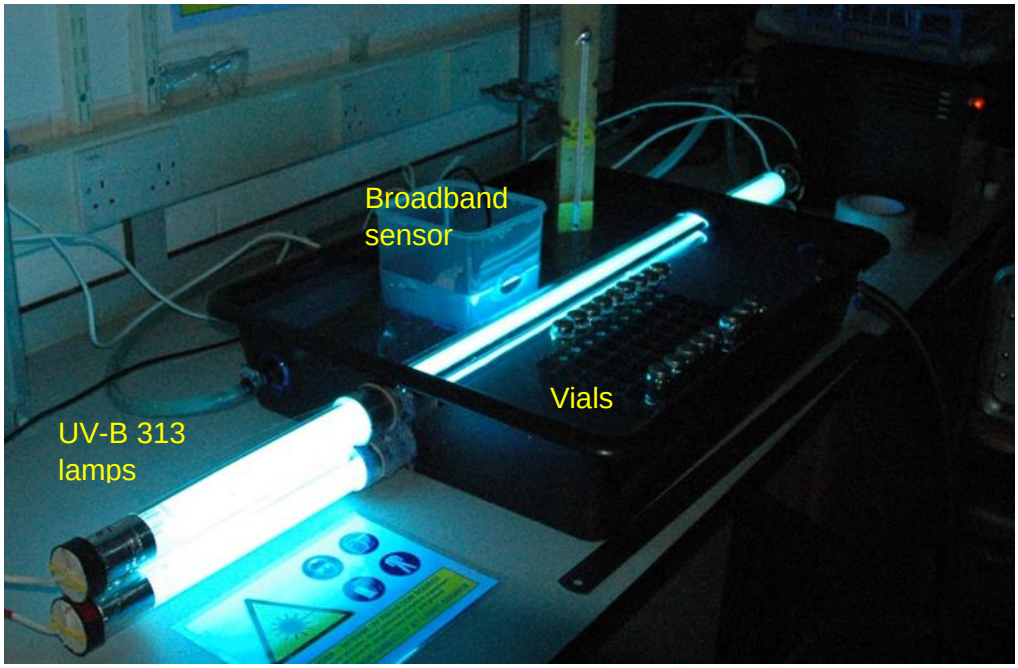

Figure 2.11. Laboratory irradiation facility, showing quartz vials in a temperature controlled water bath. UV irradiance was measured via a broad band sensor on the opposite side of the lamps to the vials.

Control vials wrapped in aluminium foil to exclude irradiation were kept in the water bath for the experiment duration. Four replicates of both the UV-exposed and control samples were used in all experiments. In experiments conducted with samples containing particulate organic carbon (POC), samples were inverted several times every two hours samples to ensure that POC was suspended in the water column. Following irradiation, the samples were first left to equilibrate at room temperature and then used for subsequent laboratory analyses described in the following data chapters (3-4).

Different UV-B 313 lamp outputs were used in various experiments, in order to produce maximum effects (Chapter 3) or to provide irradiance similar to cloudless summertime conditions in the UK (Chapter 4). Table 2.3 shows a summary of the lamp outputs used in laboratory exposure experiments, in relation to measurements of the natural solar spectrum.

Table 2.3. Total unweighted irradiance in the UV-B, UV-A and photosynthetically active radiation (PAR) in experiments in this study.

	UV-B W m^{-2}	**UV-A W m^{-2}**	**PAR W m^{-2}**
Chapter 3 – laboratory experiments[a]	4.45	6.74	2.74
Chapter 3 – ambient exposure[b]	0.36 ± 0.11	17.2 ± 5.44	137 ± 47.9
Chapter 4 – laboratory experiments[a]	2.89	4.63	0.92
Maximum recorded ambient exposure[c]	1.34	35.1	322

[a]Constant values during calibration
[b]Mean ± 1 standard deviation of 12 daily readings from 4 August – 16 Sep 2014
[c]Measured on site at midday at King's Buildings 18/04/2014

2.3.2 Ambient exposure experiments

In Chapter 3, twelve 1.5 L water samples were collected from the Black Burn on separate days between 4 August and 16 September for use in ambient light exposure experiments. These experiments were conducted to detect natural gaseous photoproduction in summer light

conditions. Unfiltered and 0.2 μm filtered sub samples contained in 21 mL quartz vials were placed in an outdoor temperature controlled water bath at 16°C and exposed to sunlight from 09:00 to 17:00 GMT (same exposure period as the laboratory experiments) at the Edinburgh University King's Buildings campus (55°92'2 N; 3°17'47 W), approximately 15 km north of the field collection site. The quartz sample vials were positioned at an angle of ~45° to the lamps to expose the largest possible surface area of the vial to light, following a similar method to that used by Worrall and Moody (2014). As with the laboratory experiments, every two hours samples were inverted several times to ensure that particulate organic matter was suspended in the water column. This process was completed in an identical way for both light and control samples to ensure comparability.

A double monochromator scanning spectroradiometer (Irradian™, Tranent, UK) was used to measure irradiance at each wavelength from 280 -700 nm at 5 nm intervals across the day: 09:00, 11:00, 13:00, 15:00 and 17:00 GMT. Consistent with the laboratory experiment, control vials wrapped in aluminium foil to exclude irradiation were kept in the water bath for the experiment duration. Four replicates of both the light exposed and control samples were used.

2.3.3 Laboratory analytical methods

A range of laboratory analytical techniques were employed to quantify the concentration, composition and photoreactivity of peatland derived C (Table 2.4). These are described in detail in the methods sections of the following data chapters (3-5), with a summary provided here.

Table 2.4. Brief description of laboratory analytical methods used in this study and the chapters in which a detailed method description can be found.

Method	Brief description	Described in		
		Chapter 3	Chapter 4	Chapter 5
Gas chromatography	Measurement of gaseous C species: CO_2, CO and CH_4 in gas bags or vial headspaces	*	*	*
TOC analysis	Determination of DOC concentrations in filtered water samples	*	*	*
TC analysis	Determination of DIC concentrations in filtered water samples	*	*	*
Loss on ignition	Determination of POC concentrations in water samples	*		*
UV-visible spectroscopy	Scan of absorbance of water samples in the UV and visible parts of the spectrum and is commonly used as a proxy for DOC concentration and composition.	*	*	*
$SUVA_{254}$	Uses the absorbance measured at 254 nm and DOC concentrations to estimate the dissolved aromatic C content in water samples	*	*	*
E2:E3	A ratio between absorbance at 254 nm and 375 nm used as an estimation of aromaticity and molecular weight	*	*	
E4:E6	A ratio between absorbance at 465 nm and 665 nm, frequently cited as a measure of water sample humification	*	*	*
Lignin phenols	Measurement of total dissolved lignin phenol concentrations and relative abundance of phenols via GC analysis of extracted water samples to infer sources and composition of terrigenous organic matter		*	
Spectrofluoresence	Measurement of fluorophores within a water sample at different excitation and emission wavelengths in order to determine information about the source and reactivity of DOM		*	
δ^{13}C-DOC	Determination of the isotopic composition of DOC			*
δ^{13}C-DIC	Determination of the isotopic composition of DIC			*

Chapter 3 Temperature and Filtration Effects on the Photoreactivity of Peatland Carbon

Amy E Pickard, Kate V Heal, Andrew R McLeod and Kerry J Dinsmore

Intended for submission to *Photochemical and Photobiological Sciences*.

The candidate performed the experiments, conducted the laboratory and data analyses and wrote the paper. Co-authors provided guidance on project design and contributed to the editing of the manuscript.

Other Acknowledgements: The Irradian™ spectroradiometer used in this study was calibrated by Chris McLellan at the NERC Field Spectroscopy Facility.

Abstract

Laboratory experiments investigating photo-processing of aquatic carbon (C) are typically conducted at higher than ambient temperatures, using filtered samples to exclude particulate C fractions. We aimed to test the effect of temperature and filtration on the photoreactivity of water samples collected from a headwater stream draining Auchencorth Moss peatland, SE Scotland. Laboratory based irradiation experiments were conducted at temperatures ranging from 12 to 24°C on water samples with contrasting DOC concentrations. Two filters with varying pore sizes (0.2 and 0.7 μm) and unfiltered samples were also employed to investigate the fractions of C most susceptible to photo-processing. After exposure to UV irradiation for 8 h in controlled laboratory facilities, C species in solution (DOC, DIC) and gaseous emissions (CO_2, CO and CH_4) were measured in samples exposed to ultraviolet (UV) radiation and in unirradiated controls. Irradiation and temperature had a significant effect on DOC and gas headspace concentrations, with Q_{10} values of 1.42 and 1.65 derived for CO_2 and CO photoproduction in unfiltered samples, respectively. However, filtration did not induce significant changes in gaseous C production between light and dark samples, indicating that the experimental conditions favoured formation of CO_2 and CO from DOC rather than from POC. In all laboratory irradiation treatments a small but significant increase in CH_4 concentration was detected. These data were compared to results from experiments conducted over the same duration in ambient light and temperature conditions. The percentage of DOC photo-oxidised to CO_2 was one order of magnitude lower in ambient conditions, but relative abundances of C species within overall budgets were similar between experiments. CH_4 photoproduction was detected in all samples exposed to ambient light, although this accounted for <0.01% of the total C budget. Overall, these experiments show that the <0.2 μm fraction of C is most photoreactive in peatland draining aquatic systems and is converted primarily to CO_2 and CO. These data further suggest that temperature exerts a strong effect on photoreactivity.

3.1 Introduction

Terrigenous dissolved organic carbon (DOC) is a key component of global carbon (C) budgets, serving to link terrestrial and aquatic biogeochemical cycles (Cole et al., 2007). Light driven processing in the aquatic environment preferentially targets high molecular weight, aromatic fractions of DOC, which are derived from terrestrial sources (Algesten et al., 2004; Hernes, 2003). Photodegradation of DOC has been widely documented to result in production of CO_2 and CO, in addition to low molecular weight forms of DOC which are highly susceptible to microbial decomposition (Lapierre et al., 2013; Moran et al., 2000). CO_2 emissions from streams and rivers are estimated at 1.8 Pg C yr^{-1}, which represents approximately 70% of the global CO_2 emissions from all inland waters (Raymond et al., 2013). Inland waters also emit significant volumes of CH_4, with an estimated source strength of 1.5 Tg CH_4 per year (Bastviken et al., 2011). As freshwaters are a significant C source to the atmosphere, understanding the processes by which DOC is degraded within these systems has become increasingly important. Furthermore, identifying the concentration and composition of DOC delivered to marine environments is key to understanding the coastal ocean C cycle (Hernes and Benner, 2003).

Investigations of DOC photodegradation in freshwaters have focussed on detecting changes in DOC concentration, absorbance properties and terrestrial biomarkers such as lignin phenols (Franke et al., 2012; Spencer et al., 2009). Experiments are either conducted in ambient conditions in situ with natural light and temperature variation (e.g. Worrall and Moody, 2014) or in laboratory conditions where an artificial light source is employed and variables such as temperature are held constant (e.g. Franke et al., 2012; Vachon et al., 2016). In laboratory settings, solar simulators which approximate a natural spectrum (e.g. Franke et al., 2012) or narrow wavelength lamp sources (e.g. Bange and Uher, 2005) have been employed to investigate photo-processing.

Due to positive covariance between light and temperature in the natural environment, temperature corrections are not always explicitly made in laboratory based irradiation studies (Cory et al., 2014; Vachon et al., 2016). However, temperatures selected for laboratory irradiation experiments are, in many cases, considerably higher than ambient conditions in systems from which samples are obtained (25°C in Zhang et al., 2013; 16-18°C in Franke et al., 2012; 24°C in Vachon et al., 2016). Formation of reactive oxygen species (ROS) is enhanced by increasing temperatures, which may result in the development of a non-linear relationship between temperature and sample photoreactivity (Häder et al., 2014; Muller et al., 2008). Whilst temperature effects on photodegradation have recently been explored by Porcal et al. (2015), they did not quantify changes to all C species (dissolved and gaseous), instead focusing on DOC, dissolved inorganic carbon (DIC) and total organic carbon (TOC). All these factors warrant further exploration of the temperature dependence of photochemical processing.

Previous studies examining photo-processing of aquatic C have filtered water samples to 0.2 μm prior to irradiation in order to exclude bacterial biomass (Hernes et al., 2003; Bange and Uher, 2005; Spencer et al., 2009). This process is conducted because microbial activity could lead to additional C processing and thus make distinguishing the relative effect of each process more difficult. However, sample filtration also removes suspended particulate organic matter that is present in aquatic systems and thus the measured response after filtration is not representative of environmental conditions. POC in stream waters draining peatlands generally represents a much smaller component of C export than DOC (e.g. Dinsmore et al., 2010), however it is an important flux term from peatlands via the aquatic pathway, with a maximum annual POC flux of 78.9 MgC km^{-2} a^{-1} reported from a degraded peatland catchment in the UK (Pawson et al., 2012). It is hypothesised that the filtration process, which excludes plant derived particulate material from water samples and therefore decreases the total organic

carbon (TOC) in the sample, will have a significant effect on the magnitude of photo-induced changes in the C pool, resulting in less gaseous C production.

In this study laboratory based irradiation experiments were conducted at a range of temperatures on two water samples with contrasting DOC concentrations collected from the same headwater peatland stream in Scotland. Unfiltered samples were examined together with samples filtered using two different pore sizes (0.2 and 0.7 μm). Samples were tested in conjunction with an organic reference sample obtained from the International Humic Substances Society (IHSS). Changes to dissolved and gaseous C species were analysed in order to understand photodegradation reaction rates as a function of temperature and filtration. Further experiments were conducted in ambient light conditions to compare photo-processing in laboratory versus ambient conditions.

3.2 Methods

3.2.1 Sample collection

Water samples were collected on two occasions in October 2013 and January 2014 from the Black Burn, a brown water stream draining Auchencorth Moss peatland, located in SE Scotland (55°47'34N; 3°14'35W; 254 m a.s.l.) (Billett et al., 2010). Annual mean stream water DOC concentration determined by weekly sampling over a two year period is 28.4 ± 1.07 mg L^{-1} (Dinsmore et al. 2013) although there is strong seasonality, characterised by low DOC concentrations in the spring and high concentrations in summer and autumn. Water samples were collected on both occasions from an established sampling location, where DOC concentrations have been recorded for >9 years as part of the Centre for Ecology & Hydrology (CEH) Carbon Catchments project. The sampling dates were chosen so as to observe the effect of light exposure on samples with different DOC concentrations (above and below the annual mean DOC concentration).

A 5 L water sample was collected approximately 20 cm below the surface of flowing water, using screw top sterile glass bottles. Upon return to the laboratory samples were refrigerated at 4°C and irradiated within four days of collection. Samples were prepared for light exposure experiments using filters with pore sizes 0.2 μm (MCE syringe driven filters; Merck Millipore, Germany) and 0.7 μm (GF/F; Whatman, UK). Unfiltered samples were also prepared. 15 mL of sample was immediately transferred by pipette into 21 mL quartz vials (Robson Scientific, UK) and sealed with Al crimp tops and rubber butyl plugs (Thermo Scientific Chromacol, USA). All samples were prepared at room temperature in oxic conditions.

In the laboratory experiments, a Nordic Aquatic Fulvic Acid (FA) reference sample (IHSS) was prepared at a concentration of 25 mg C L^{-1} by dissolving the lyophilised sample in deionised water (Triple Red Water Technology, UK). The reference sample was adjusted to a pH of 6 using microliter additions of NaOH, with this value selected as it was similar to the measured pH of water samples collected from the Black Burn. It was transferred into quartz vials using the method described above. The reference sample was used to test the comparability of laboratory experiments in which all parameters were held constant except for temperature. A fulvic acid reference sample was selected because fulvic acids represent the dominant fraction of dissolved organic matter (DOM) in typical natural waters (McKnight et al., 2003).

3.2.2 Laboratory UV experiments

Experiments were performed using UV-B 313 lamps (Q-Panel Com, USA) covered with 125 μm cellulose diacetate in order to exclude wavelengths <280 nm. Lamps were mounted inside quartz tubing (Robson Scientific, UK) beneath the surface of a temperature-controlled water bath maintained at temperatures of 12°C, 16ºC, 20ºC and 24°C and vials were irradiated sideways while submerged below the neck. UV irradiance was measured with a broad-band sensor (Model PMA2102; Solar Light Inc., USA) held beneath the surface behind a quartz window of the same thickness as the vials and maintained constant throughout the 8 h

experiments. The sensor was calibrated with a double monochromator scanning spectroradiometer (Irradian^{TM}, UK). Total unweighted UV irradiance was 11.2 W m^{-2} and the biologically-effective irradiance was calculated using the weighting function for UV-driven CH_4 production from plant pectin (McLeod et al., 2008). The weighted value was 6.54 W m^{-2} effective irradiance; within the range of ambient weighted values which reach >30 W m^{-2} for the highest global measured value (McLeod et al., 2008). The higher than ambient intensity was used to reduce irradiation time to accelerate the experimental work, as unfiltered samples were being used which would be subject to microbial processing, and to produce maximum effects for the temperature and filtration treatments. Control vials wrapped in aluminium foil to exclude irradiation were kept in the water bath for the experiment duration. Four replicates of both the UV-exposed and control samples were used for each filtration type and for the IHSS reference samples.

Every two hours, samples of all filtration types in irradiated and control samples were inverted several times to re-suspend particulate organic matter in the water column to ensure comparability.

3.2.3 Ambient sunlight experiments

From 4 August to 16 September 2014 twelve 1.5 L water samples were collected each on a separate day from the Black Burn for use in ambient light exposure experiments. These experiments were conducted to detect natural gaseous photoproduction in summer light conditions. Unfiltered and 0.2 μm filtered sub samples contained in 21 mL quartz vials were placed in a temperature controlled water bath at 16°C and exposed to sunlight from 09:00 to 17:00 GMT (for the same 8-h time period as the laboratory experiments) at the Edinburgh University King's Buildings campus (55°92'2 N; 3°17'47 W), approximately 15 km north of the field collection site. A temperature of 16°C was selected for these experiments, as similar water temperatures had been recorded in the Black Burn in summer conditions. Only two water treatments (0.2 μm filtered and unfiltered) were used in the ambient experiments, as there was

limited time available for sample preparation and these were considered to best represent the fractions of C in the water samples (DOC only and TOC). The quartz sample vials were positioned at an angle of ~45° to expose the largest possible surface area of the vial to light, following a similar method to that used by Worrall and Moody (2014). As with the laboratory experiments, every two hours samples were inverted several times to ensure that POC was suspended in the water column. This process was completed in an identical way for both light and control samples to ensure comparability.

A double monochromator scanning spectroradiometer (Irradian™, UK) was used to measure irradiance at each wavelength from 280 -700 nm at 1 nm intervals across the day: 09:00, 11:00, 13:00, 15:00 and 17:00 GMT. Consistent with the laboratory experiment, control vials wrapped in aluminium foil to exclude irradiation were kept in the water bath for the experiment duration. Four replicates of both the light exposed and control samples were used.

3.2.4 Sample analysis

Following exposure, samples from all experiments were left to equilibrate at room temperature and partitioning of dissolved C gases from the liquid into the vial headspace was encouraged through use of a wrist action shaker for 30 s. An Agilent gas chromatography (GC) system (Agilent Technologies, USA) equipped with an autosampler (HTA, Italy) and a flame ionisation detector (FID) held at 250°C was used to analyse samples for headspace CO_2, CO and CH_4 concentration within 8 h of irradiation. Needle penetration depth was set to a standard depth and 1.5 mL of headspace sample was automatically injected onto the sample loop. Analytical runs lasted for 10.5 mins and the column carrier gas was N_2 at a constant flow rate of 45 mL min^{-1}. CO_2 and CO measurements were made possible by a methaniser fitted between the column and FID. One standard 7-gas mixture (BOC Special Gases, UK) was used for daily detector calibration prior to sample analysis (detection limits: CO_2 78 ppm; CO 1.6 ppm; CH_4 0.8 ppm). Dilutions of 50 and 75% were made from this standard using Zero Grade N_2 to produce a 3 point calibration series for each gas. Post-run peak analysis and integration

were performed using Clarity software (DataApex, Czech Republic). Total dissolved gas was then calculated from the measured headspace concentration using the Bunsen solubility method (Wiesenburg and Guinasso Jr., 1979).

A PPM LABTOC Analyser (Pollution and Process Monitoring Ltd., UK) was used to measure DOC and dissolved inorganic carbon (DIC) concentrations in UV irradiated and unirradiated samples after exposure to experimental conditions. The instrument converts the sample to CO_2 using UV induced persulphate oxidation. CO_2 is then measured by an infra-red gas analyser. Acid sparging allows organic constituents to be determined, with DIC determined from the Total Carbon (TC) minus the TOC concentration. Prior to DOC and DIC measurement, unfiltered irradiated samples were filtered through a 0.7 µm filter to remove particles which would otherwise damage the instrument. LabTOC outputs for TC and TOC are therefore interpreted as the dissolved portion only and do not include POC.

UV-visible absorbance of UV treatment and control samples was measured at room temperature using a Jenway spectrophotometer (Model 7315; Bibby Scientific, UK). Samples were placed into 3 mL UV transparent cuvettes with a path length of 10 mm, and absorbance was measured between 200 and 700 nm at increments of 1 nm. Deionised water controls were used between each sample. Absorption coefficients a_λ were calculated as:

$$a_\lambda = 2.303 \text{ x } \left(\frac{A\lambda}{L}\right) \quad (1)$$

where A is the absorbance at each wavelength and L is the path length (m) of the cuvette (Green and Blough 1994). Specific UV absorbance ($SUVA_{254}$) values, a measure of DOC aromaticity, were determined by dividing the UV absorbance measured at $\lambda = 254$ nm by the DOC concentration (Weishaar et al., 2003). The E2:E3 and E4:E6 ratios were estimated using the absorbance values at 254 nm and 365 nm, and 465 and 665 nm, respectively (Peacock et al., 2014).

Due to previous studies reporting that iron (Fe) affects photoreactivity (Bertilsson and Tranvik, 2000), Fe was measured in UV irradiated and control samples was measured on an iCE 3000 series AA spectrometer (Thermo Scientific, USA) at 248.3 nm using an air/ acetylene flame.

From the remaining unexposed water samples, 250 mL was filtered with 0.7 μm GF/F filters using a vacuum filtration system. The filters were pre-combusted at 450°C for 8 h and weighed (Chanton et al., 2008). The sample was filtered to capture particulate C on the filter which was subsequently dried for 3 h at 105°C and reweighed before combustion at 375°C for 16 h. The paper was then weighed a final time and POC concentration (mg L^{-1}) was calculated by determining the loss on ignition (LOI) (Ball, 1964). A conversion factor of 0.58 (Pribyl, 2010) was applied to the LOI value, which assumes that 58% of organic matter comprises C.

3.2.5 Data analysis

Statistical analyses were conducted using R, version 3.2.1 (R Core Team, 2015). DOC and headspace gas concentrations from the laboratory experiments were used as dependent variates in stepwise multiple regression analyses. Independent variables used included UV treatment, temperature, filtration and DOC concentration (the latter not used when DOC was the dependent variate). This set of independent variables permitted a search for significant linear and nonlinear relationships and subsequent selection of a best fit model for each dependent variate. Best fit was determined by highest adjusted R-sq value. The alpha value, which sets the significance level for entry into the model for individual independent variables, was set at 0.15.

For the ambient experiments, data were used in Pearson correlation analyses and coefficients were derived to determine the significance of various factors in both gaseous C photoproduction and intrinsic photoreactivity of samples. To obtain a standard deviation value for differences between ambient exposed and control samples, the mean control value was determined and subtracted from each of the exposed replicates.

3.3 Results

3.3.1 Laboratory UV experiments

DOC concentrations were significantly higher (by ~17 mg L^{-1}) in the bulk water sample collected in October compared to the January sample (Table 3.1). DIC concentrations in the October sample were also higher than in January. Of the optical parameters, $SUVA_{254}$ values were similar, yet there was variation in the E2:E3 and E4:E6 values, which were both lower in the January sample.

Table 3.1 Water sample chemistry from bulk water samples collected in October 2013 and January 2014 from the Black Burn and the IHSS reference. Values represent the mean value from three replicate measurements ± 1 S.D, unless otherwise stated.

	October 2013	**January 2014**	**Nordic aquatic FA**
DOC (mg L^{-1})	40.1 ± 0.59	23.3 ± 0.96	25.5 ± 0.39
DIC (mg L^{-1})	3.08 ± 0.96	1.73 ± 0.47	0.88 ± 0.23
POC (mg L^{-1})	5.31 ± 0.41	3.47 ± 0.33	---
$SUVA_{254}$	4.83 ± 0.23	4.89 ± 0.30	4.62 ± 0.09
E2:E3	4.40 ± 0.04	4.36 ± 0.08	4.73 ± 0.07
E4:E6	5.63 ± 0.16	5.28 ± 0.44	9.65 ± 0.96
Fe (mg L^{-1})	3.52 ± 0.21	1.17 ± 0.02	0.09 ± 0.01
pH[a]	5.47	5.95	6.00

[a] pH was measured in the field, with one measurement recorded. The Nordic FA sample was prepared to a pre-defined pH.

The FA reference sample was compositionally distinct from bulk water samples collected from the Black Burn, with considerably higher E2:E3 and E4:E6 ratios and very low DIC and Fe concentrations.

Upon experimental exposure, considerable differences emerged between irradiated and control samples for all C species (Table 3.4; Supplementary information). Losses of DOC were detected in all irradiation experiments, with magnitude of loss greatest in Black Burn samples with higher initial DOC concentrations (Figure 3.1). DOC concentrations of irradiated samples

were reduced by 4.62 ± 0.18 mg L^{-1} relative to the control samples in October samples at 24°C (Figure 3.1a). At 12°C, DOC losses were ~ 0.4 mg L^{-1} lower (Figure 3.1b). In the January samples irradiated at 24°C, DOC losses across all filtration treatments were 2.36 ± 0.70 mg L^{-1} (Figure 3.1c).

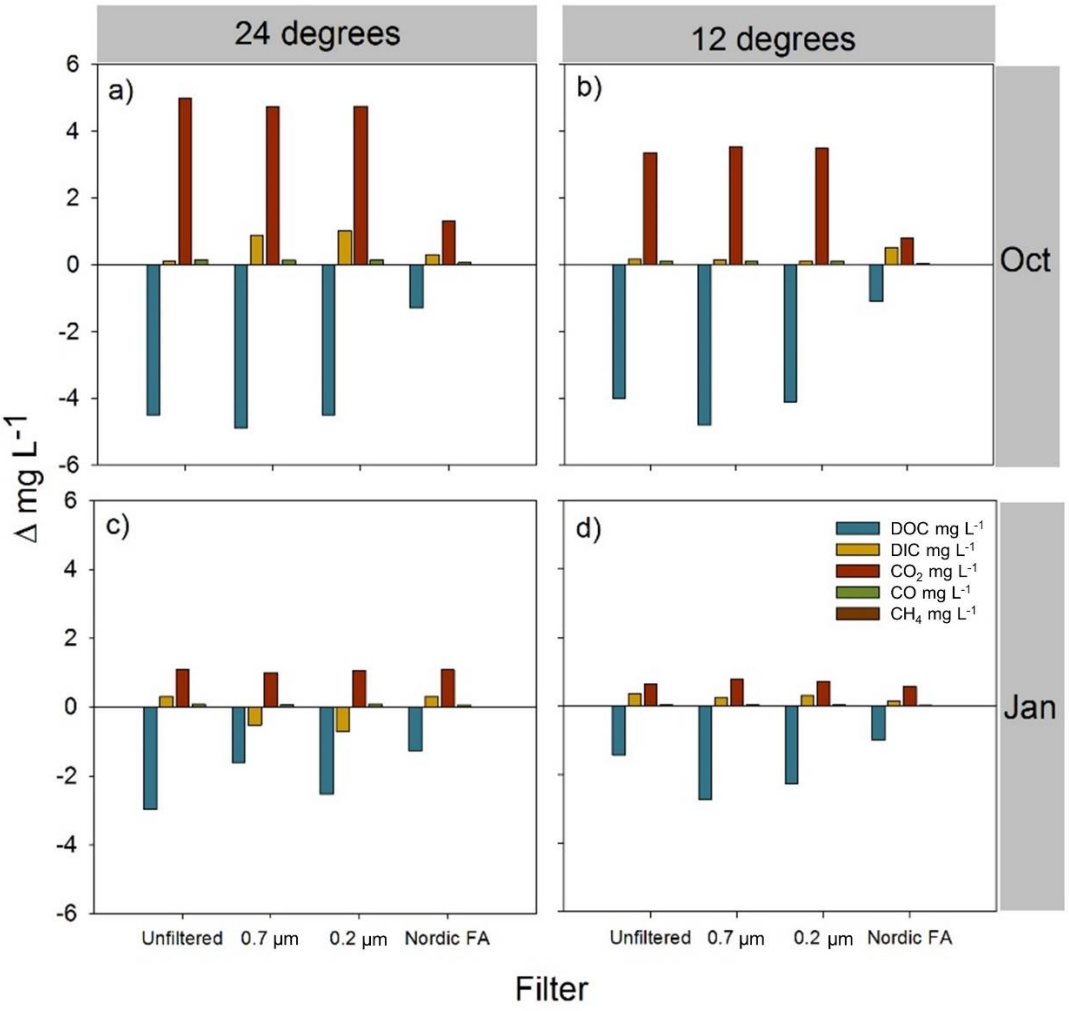

Figure 3.1 Mean irradiation induced changes to C species (determined as difference between UV exposed and unirradiated controls) for the October sample (high DOC) at water bath temperatures of a) 24°C and b) 12°C, and the January sample (low DOC) at water bath temperatures of c) 24°C and d) 12°C. Nordic aquatic FA samples are also shown for each experiment.

UV irradiation resulted in a mean increase in CO_2 concentration of 2.53 ± 1.66 mg L^{-1} relative to the control samples across Black Burn samples at all filtration levels and temperatures. The

increases were similar across filtration treatments, with maximum CO_2 production detected for unfiltered October samples at 24°C (5.0 mg L^{-1}). Lowest CO_2 production (0.6 mg L^{-1}) was detected in unfiltered January samples at 12°C (Figure 3.1d). Although the FA sample had a slightly higher initial DOC concentration, it was similar in terms of overall photoreactivity to the January sample, with CO_2 photoproduction within 3% and 19% of January Black Burn samples at 24°C and 12°C, respectively. In light exposed samples across all filtration treatment and temperatures, CH_4 photoproduction was detected at low concentrations (0.20 ± 0.08 µg L^{-1}).

Stepwise regression analyses were performed to understand how the independent variables UV treatment, temperature, filtration and DOC concentration interacted to produce explanatory models for headspace gas concentrations and DOC (Table 3.2). In both the October and January samples, CO_2-C and CO-C could be adequately explained by two independent variables, UV treatment and temperature. However, the model R-sq values were both higher for the October samples. For DOC, the best fit model used three independent variables, UV treatment, temperature and filtration. However in comparison to the models for the gaseous species, the R-sq values for the DOC model were consistently lower, indicating a reduction in explanatory power.

Table 3.2 Best models found by stepwise multiple regressions for October and January water sample experiments. Independent variate parameters are UV treatment, temperature, filtration and DOC concentration (the latter was not used as an independent variate for dependent variate DOC).

	Dependent variate	Parameter	Coefficient	t value	Model R-sq (adj)
October 2014 samples	**DOC (mg L^{-1})**	*Intercept*	43.641	120.5	92.19
		UV treatment	-4.627	-31.43	
		Temperature	-0.1554	-9.44	
		Filtration	-0.617	-6.85	
	CO_2-C (mg L^{-1})	*Intercept*	0.709	4.51	97.10
		UV treatment	4.1094	55.76	
		Temperature	0.06821	8.28	
	CO-C (mg L^{-1})	*Intercept*	-30.69	-6.53	97.03
		UV treatment	116.94	53.33	
		Temperature	1.796	7.28	
January 2015 samples	**DOC (mg L^{-1})**	*Intercept*	20.986	52.98	66.26
		UV treatment	-2.052	-12.75	
		Temperature	0.0769	4.27	
		Filtration	0.2938	2.98	
	CO_2-C (mg L^{-1})	*Intercept*	1.3419	13.88	82.38
		UV treatment	0.9454	20.87	
		Temperature	-0.01664	-3.28	
	CO-C (mg L^{-1})	*Intercept*	-25.18	-7.53	95.10
		UV treatment	66.10	42.19	
		Temperature	1.451	8.17	

In all instances the t-value, which indicates the relative contribution of each model term to the overall explanatory power of the model, was highest for UV treatment.

Q_{10} temperature coefficients, which measure the rate of change as a consequence of increasing the temperature by 10°C, were determined for gaseous C photoproduction (Table 3.3). The data show variation in temperature sensitivity of photoproduction between the two bulk water

samples and filtration types. For the October sample, Q_{10} values of 1.40 and 1.44 were derived for CO_2 and CO in unfiltered samples, respectively. In comparative filtered samples, Q_{10} values were lower by ~0.11 and ~0.16 for CO_2 and CO, respectively.

Table 3.3 Q_{10} values derived for photoproduction of C gases for bulk water samples.

	Q_{10}	
	CO_2 photoproduction[a]	**CO photoproduction[b]**
October sample		
Unfiltered	1.40	1.44
0.7 μm	1.28	1.25
0.2 μm	1.30	1.31
Nordic aquatic FA	1.57	1.56
January sample		
Unfiltered	1.59	1.72
0.7 μm	1.26	1.52
0.2 μm	1.36	1.61
Nordic aquatic FA	1.51	1.65

[a] Determined as the difference between irradiated and dark CO_2-C concentrations (n=4)

[b] Determined as the difference between irradiated and dark CO-C concentrations (n=4)

In the January sample, Q_{10} values of 1.59 and 1.72 were derived for CO_2 and CO photoproduction in unfiltered samples, respectively. Q_{10} values for comparative filtered samples were consistently lower. The Nordic FA samples showed a greater rate of change for CO production upon temperature increase than for CO_2 in the January sample and the opposite effect in the October sample. Nevertheless temperature sensitivity for Nordic FA photoproduction differed between experiments by <10%.

3.3.2 Ambient sunlight experiments

DOC concentrations in the in the 12 water samples collected 4 August and 16 September 2014 ranged from 20.0 to 37.2 mg L^{-1}, with a mean concentration of 30.5 ± 4.43 mg L^{-1} (Figure 3.2).

DIC concentrations ranged from 2.1 to 9.2 mg L^{-1}, with the highest detected concentrations in samples collected in early August. $SUVA_{254}$ values were stable throughout the sampling campaign, with a mean value of 4.50 ± 0.28, however E4:E6 ratios were subject to variability, ranging from 5.2 to 7.5 (Table 3.5; Supplementary information).

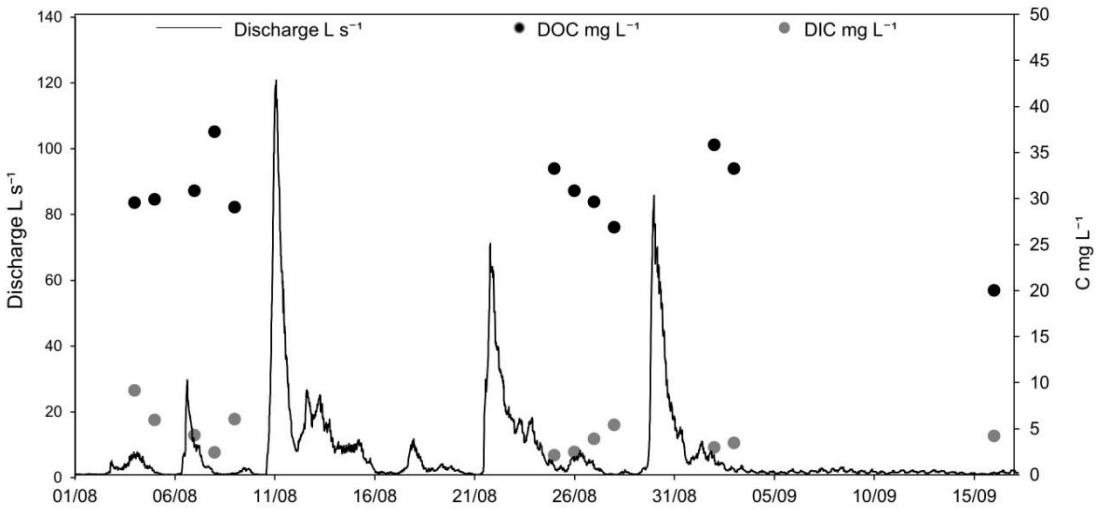

Figure 3.2 DOC and DIC concentrations shown on twelve sampling days in 2014 in the Black Burn in relation to continuous stream discharge data.

Discharge through the sampling period was flashy with four distinct peaks, reaching a maximum of 121 L s^{-1} on 11 August. A notable dry period occurred between 2 and 16 September, where base flow conditions of ~2 L s^{-1} were measured. Daily mean discharge on the sampling days did not exceed 8 L s^{-1}.

Solar radiation conditions measured during the ambient experiments varied considerably over the 12 experimental days, with combined irradiance in the UV and PAR averaging 137 ± 47.9 W m^{-2} (Figure 3.3a). Highest irradiance occurred on 9 August, when a combined irradiance of 201 W m^{-2} was measured. Lowest irradiance occurred on 26 August, when 72.1 W m^{-2} was measured (Figure 3.3b).

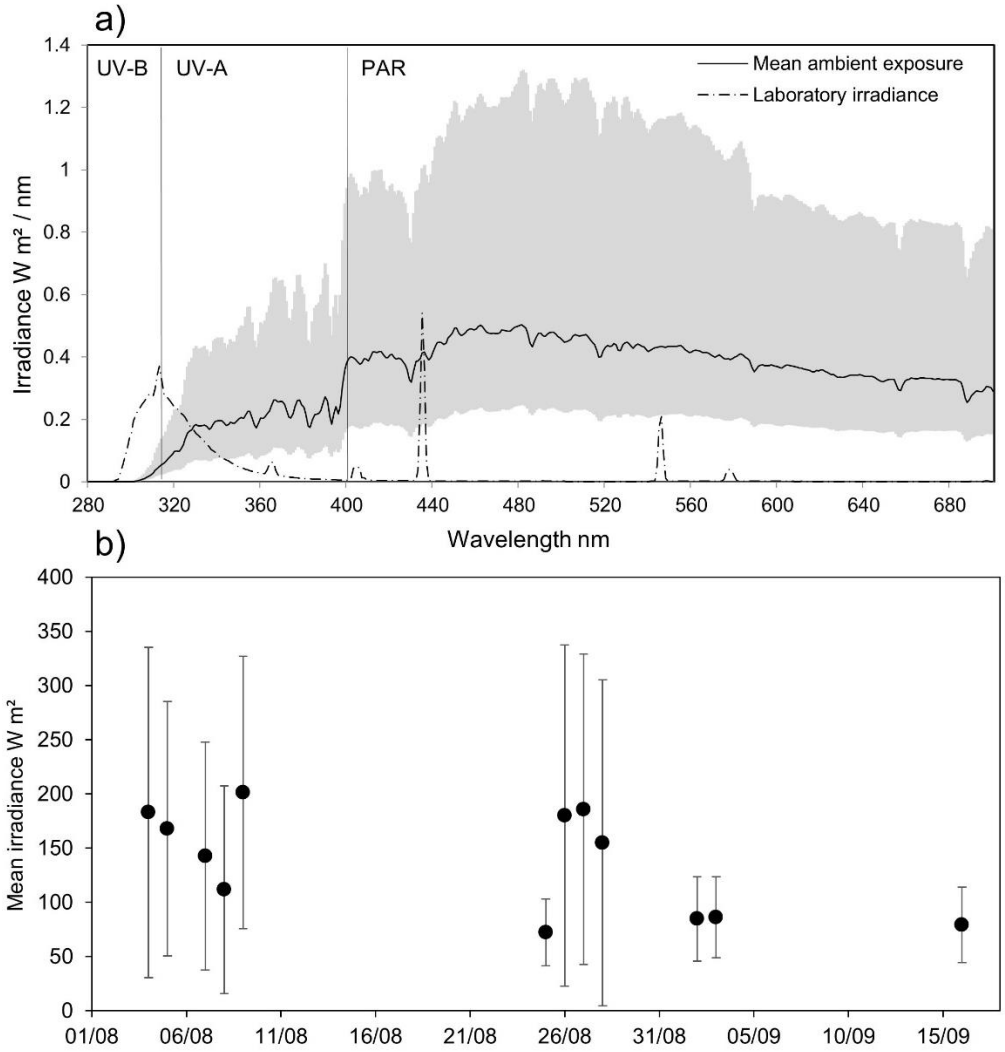

Figure 3.3 a) Mean irradiance (n=12) from 280-700 nm for ambient exposure experiments, shown in relation to irradiance in laboratory irradiation experiments. The grey area shows the minimum and maximum irradiance values measured in the ambient experiments; b) mean total irradiance derived from 5 daily readings (± 1 s.d.) across the measurement period.

Compared to the irradiance of the UV-B lamps used in the laboratory study, ambient irradiance in the UV-A and PAR was a factor of 1 and 2 higher, respectively. However, UV-B irradiance was a factor of 1 lower and was only detectable from 295 nm.

Sunlight was sufficient to generate significant CO_2 production in exposed water samples on all twelve experimental days. Mean CO_2 photoproduction across ambient experiments (0.56 ± 0.14 mg L^{-1}) was low compared to laboratory experiments (2.53 ± 1.66 mg L^{-1}), although it accounted for up to 2.8% of initial DOC concentrations. CO_2 production under ambient

conditions was significantly positively correlated with initial C concentration (Pearson's r 0.41; $p < 0.05$; $n = 24$) (Figure 3.4a). Although this correlation was largely driven by the sample containing 20 mg DOC L^{-1}, similar DOC-ΔCO_2 relationships emerged in Chapter 4 (Table 4.2), where a greater range of DOC concentrations were measured (14.2 to 50.9 mg L^{-1}). Whilst the unfiltered samples had a lower mean photoreactivity than samples filtered to 0.2 µm, the differences were not significant (2-tailed paired Student's t-test; $p > 0.05$).

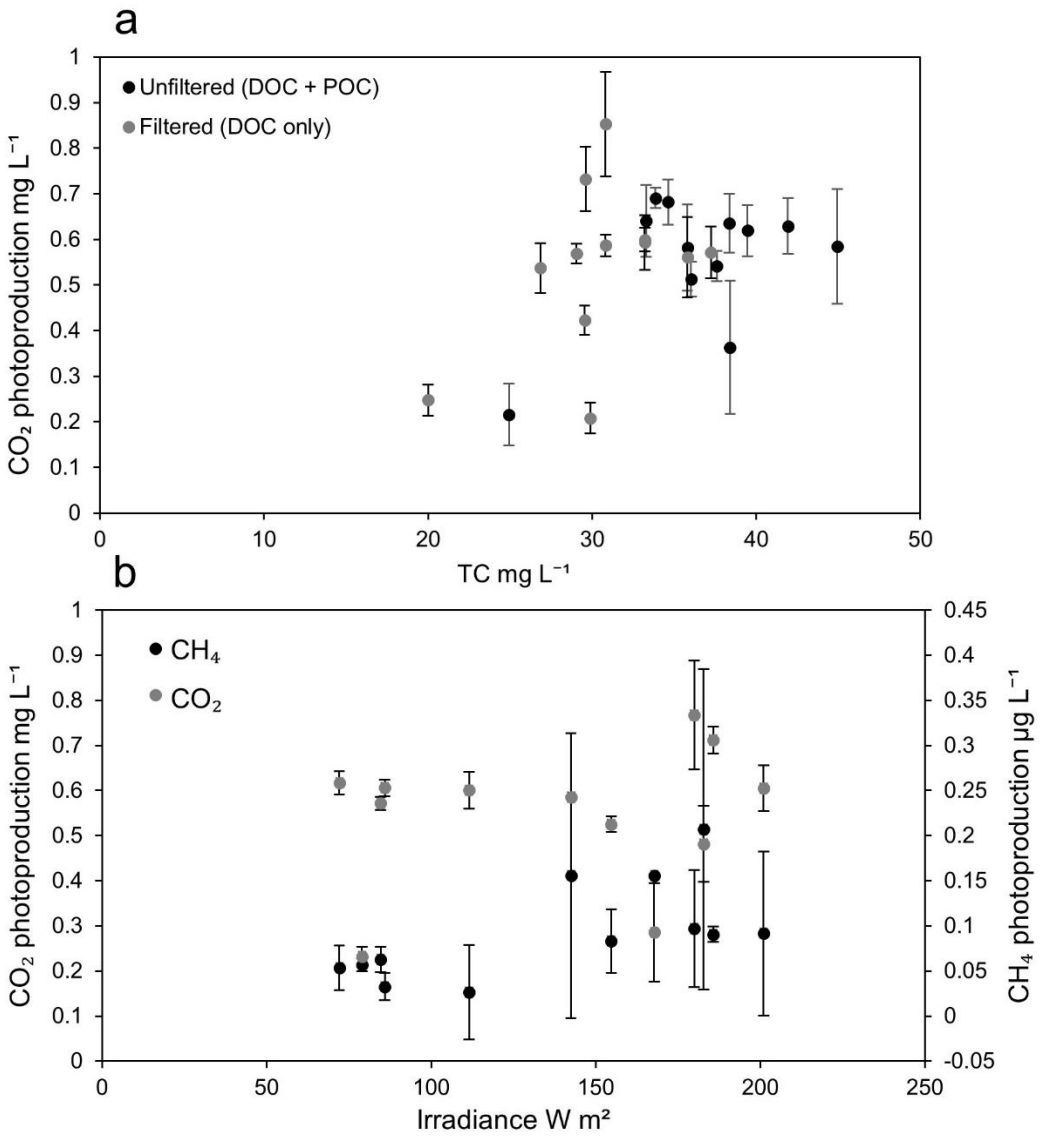

Figure 3.4 Correlations between a) CO_2 photoproduction and total carbon shown for filtered and unfiltered samples, and b) mean CO_2 and CH_4 photoproduction across filtration types and irradiance (UV and visible combined). CO_2 is expressed in mg L^{-1} and CH_4 is expressed in µg L^{-1}. Error bars show ± 1 s.d of the mean production value.

Mean CO_2 production was not significantly correlated with combined irradiance in the UV and PAR (Figure 3.4b). In contrast, CH_4 production was which was significantly positively correlated with irradiance (Pearson's: 0.64; $p < 0.05$, $n = 12$). However, CH_4 production was 3 orders of magnitude lower than CO_2 (0.09 ± 0.05 μg L^{-1}) and standard deviations of the mean were larger.

3.4 Discussion

3.4.1 Temperature and filtration effects on photo-processing of aquatic carbon

The findings of this study suggest that photoreactivity of aquatic C is dependent on temperature. In addition to UV treatment, water temperature was used as an independent variable in all best fit stepwise regression models for dependent parameters DOC, CO_2 and CO in laboratory irradiation experiments (Table 3.2). Variation between the October and January samples was evident, with temperature sensitivity of photo-processing slightly higher in the January samples. This could be a function of differences in the composition of C within the water samples, with higher $SUVA_{254}$ and lower E4:E6 ratios in the January sample suggesting that it was more aromatic and contained larger molecules than the October sample (Table 3.1). Both of these parameters indicate that it was intrinsically more photoreactive, although we lack an explanation for how this would directly affect sample temperature sensitivity. Variation in measured temperature sensitivity also could have arisen from experimental errors, as water bath temperatures varied by ± 1°C. Assuming maximum possible temperature deviations in the January experiments, Q_{10} values for CO_2 and CO production converge to within 6.9% and 14.0% of the values measured in the October samples, respectively.

Q_{10} values for unfiltered samples were higher than in filtered samples (Table 3.3), despite filtration not being selected as a model term in the best fit stepwise models for CO_2 and CO concentrationss (Table 3.2). We determined mean Q_{10} values of ~1.65 and ~1.42 for CO and CO_2 photoproduction, respectively, from unfiltered peatland stream samples compared to mean Q_{10} values of ~1.42 and ~1.30 in filtered samples (0.2 and 0.7 μm). Previous work shows

that lower Q_{10} values are indicative of abiotic process (Lee et al., 2012), and higher values (typically ≥ 2) are indicative of a biotic, microbially driven temperature response (Raich and Schlesinger, 1992). Applying mixing ratio theory, we therefore interpret this to mean that microbial activity in the unfiltered samples resulted in increased temperature sensitivity. A number of studies have demonstrated that bacteria are sufficiently small to pass through filtration pore sizes of 0.45 and 0.2 μm (Hahn, 2004; Wang et al., 2007) and therefore the measured temperature sensitivity in the filtered samples may also be partly due to microbial activity.

Q_{10} values in the Nordic FA reference samples were most similar to the unfiltered samples. This result was contrary to expectation, as samples were prepared in a sterile glassware and thus microbial effects were not anticipated. However, if not entirely sterile, the reference samples might have experienced increased microbial effects due to the low molecular weight (LMW) of fulvic acids relative to other forms of aromatic material (Sutzkover-Gutman et al., 2010). Lower E2:E3 values indicate that the peatland samples were comprised of a greater proportion of high molecular weight (HMW) material, for example humic acids, than the Nordic FA sample (Table 3.1). High quality, LMW substrate may have enhanced microbial lability of the FA reference samples relative to the peatland samples over the short exposure timescales used in these experiments, thereby resulting in higher than expected Q_{10} values.

A study by Porcal et al. (2015) also showed strong dependence of photodegradation on temperature. In headwater stream samples with ~12 mg DOC L^{-1} filtered to 0.45 μm, the sum of the rate constant $k_{DOC \rightarrow DIC}$ almost doubled with a temperature increase of 15°C (Q_{10} = 1.33) (Porcal et al., 2015). However, temperature sensitivity of photo-processing here was considerably higher than in a study by Zhang et al. (2006) in which a ~70% increase in CO was detected in irradiated estuarine samples filtered to 0.2 μm upon a 20°C increase in temperature. Twofold increases in photodegradation rate constants with each 10°C change have been assumed by previous studies (e.g. Molot and Dillon, 1997). Our data suggests that

assigning a Q_{10} of 2 may be an overestimate of the temperature sensitivity of aquatic C to photo-processing. Future laboratory irradiation studies conducted at higher than ambient temperatures should determine Q_{10} values for the photoproduct of interest in order to make appropriate temperature corrections. This may have significant implications for studies such as Cory et al. (2014) where it was estimated that 70 to 95% of total DOC processed in arctic aquatic systems was due to photolysis. This estimate was based on controlled exposure experiments conducted at above ambient temperatures of 10-16 °C. Equivalent bacterial respiration measurements measured by Cory et al. (2014) were conducted at 6-7°C, which was defined as the annual average temperature for non-frozen water at their sampling sites.

Contrary to our expectation, filtration did not have a significant effect on photoproduction of C gases, with concentrations in unfiltered samples (POC and DOC) similar to filtered samples (DOC only). This implies that POC was not as susceptible to direct photo-processing to inorganic species as DOC over the short exposure timescales used in these experiments. Although efforts were made to ensure that POC was suspended in the water column, settling of particles between sample rotations may have meant that they received less exposure than DOC. As such, the presence of POC did not significantly increase photoproduction of C gases, despite accounting for up to 12% of the total C pool (Table 3.1). Particle size distribution analyses of POC in soil pore water from a moderately drained fen show that ~90% of particles were <2.5 µm (Fiedler et al., 2008). Applying Stoke's settling law, and assuming that particles were similarly sized or smaller, we estimate a maximum settling time of 187 s for typical POC particles in the experimental vials. Experimental designs which allow for continual agitation of water samples to ensure POC is suspended in the water column during irradiation might therefore find that unfiltered samples are significantly more photoreactive than filtered samples.

Although filtration did not affect gaseous photoproduction, it was included as a term in the best fit stepwise model for DOC concentration (Table 3.2). Irradiated unfiltered samples

typically had higher DOC concentration than equivalent values for samples filtered to 0.7 and 0.2 μm (Table 3.2). Partial oxidation of POC to DOC may account for this observation, which has been detected in previous photochemical processing studies (Estapa and Mayer, 2010). Although DOC photoproduction did not affect C gaseous production in these experiments, photolysis is known to liberate high quality DOC from biologically refractory compounds and can enhance aquatic heterotrophic respiration, thereby increasing CO_2 concentrations in aquatic systems (Moran and Zepp, 1997).

3.4.2 Photoproduction of carbon species

The relative abundance of photoproducts was consistent between the laboratory and ambient exposure experiments. The contribution of individual C species to overall photoproduction budgets was: CO_2 > DIC > CO > CH_4. In the laboratory experiments, CO_2 photoproduction of up to 5.0 mg L^{-1} was detected in October samples, representing 12% of initial DOC concentrations. In ambient exposure experiments, equivalent photoproduction rates were an order of magnitude lower (~0.6 mg L^{-1}), representing up to 2.8% of initial DOC concentrations. This suggests that peatland derived C is sufficiently photoreactive under ambient light conditions to serve as a source of aquatic CO_2 emissions. In all experiments, CO photoproduction was one order of magnitude lower than CO_2 photoproduction, in agreement with previous observations of photochemical effects on gaseous emissions from organic matter (Osburn and Morris, 2003). DIC photoproduction was inconsistent, with net losses observed in some samples (Figure 3.1). Due to pH being < 7 in peatland water samples used in this study (Table 3.1), we suggest that conversion directly to CO_2 and CO accounted for a greater proportion of inorganic photoproducts than dissolved inorganic species, as has been detected in a previous irradiation study using low pH samples collected from a boreal headwater stream (Franke et al., 2012).

Irradiation initiated small but consistent CH_4 production in water samples under aerobic conditions, in both laboratory and ambient light conditions. CH_4 photoproduction rates were

positively correlated with total irradiance (Figure 3.4b) and were equivalent to <0.02% of CO_2 photoproduction rates, thus constituting a very small part of the overall C budget (<0.01%). However, our finding is in contrast to previous laboratory irradiation experiments conducted by Bange and Uher (2004) in which aerobic CH_4 emissions were not detectable from estuarine water samples. A possible explanation of our result is the observation that plant material, both living and senesced, can emit CH_4 under aerobic conditions when exposed to UV irradiation (McLeod et al., 2008; Messenger et al., 2009; Wang et al., 2011). Peatland water samples used here to detect a significant treatment effect contain particularly high levels of plant derived material, compared to the predominately estuarine water samples used by Bange and Uher (2004). Estuarine environments typically have lower DOC concentrations than headwater systems and hence there is less potential source material for aerobic CH_4 emissions. Furthermore, peatland streams receive the first inputs of DOC from the terrestrial environment and thus material will be less degraded relative to material in downstream aquatic environments (Catalán et al., 2016). Different concentrations and conditions of plant derived material may explain the contrasting results, although more work is needed to define the exact source of CH_4 photoproduction within the water column.

3.4.3 Peatland carbon concentrations and reactivity

Sunlight experiments showed that over 8 h ambient exposure, up to 2.8% of DOC can be photo-oxidised directly to CO_2. These data indicate that peatlands, which export significant volumes of DOC and POC via the aquatic pathway, are important sources of photoreactive C which could be processed in and emitted by aquatic environments. As CO_2 was the largest photoproduction term, understanding the effect of varying DOC and POC concentrations on potential CO_2 emissions from aquatic environments should be an important focus for future research. DOC concentrations in streams and lakes are typically between 0.5 - 50 mg L^{-1} (Aitkenhead et al., 2002), a considerably larger range than measured in Black Burn water samples used in the ambient experiments (20.0 - 37.2 mg L^{-1}). However, despite our limited

DOC concentration range and sampling period, we determined that DOC concentration was significantly positively correlated with maximum daily discharge measured two days prior to sampling DOC concentration (Figure 3.5; Supplementary information) (Pearson's r : 0.66; p value: 0.02, n=12). Clearly hydrological conditions are important in delivering C to peatland draining aquatic systems, with these data suggesting a relatively quick soil flushing response to high discharge in the Auchencorth Moss catchment. Collecting samples over different timescales for use in irradiation experiments would allow the effects of seasonality and hydrology on changes in DOC concentration and composition and subsequent photoreactivity to be further explored (Pickard et al., 2016).

In additional to constraining temporal variation in aquatic DOC and the subsequent effect on photoreactivity, collecting water samples from different types of peatland draining aquatic systems for use in irradiation experiments would yield understanding of spatial variation in DOC photoreactivity (Pickard et al., 2016). Samples in this study were collected from a headwater stream with high DOC inputs (110 ± 63.6 kg DOC yr^{-1}; Dinsmore et al., 2010). Maximum photoreactivity could be expected in these samples as the Black Burn receives DOC directly from the terrestrial environment via leaching from peat soils and thus it has a minimal light exposure history (Cory et al., 2014). In downstream aquatic environments DOC may differ in terms of photoreactivity due to in situ exposure prior to sample collection, rendering it less susceptible to photo-processing. Quantifying DOC photoreactivity along a continuum of inland waters would increase understanding of C processing on the catchment scale.

Supplementary information

Table 3.4. Summary of C species concentrations in irradiated and control samples for the October and January DOC samples collected from the Black Burn for all temperature and filtration treatments at the end of the experiments. Data represent the mean of four replicates.

	Temperature °C	Filtration treatment	CO_2 mg L^{-1}		CO µg L^{-1}		CH_4 µg L^{-1}		DOC[a] mg L^{-1}		DIC mg L^{-1}	
			UV	Control	UV	Control	UV	Control	UV	Control	UV	Control
October sample	24	UF	7.12	2.13	154	1.43	0.81	0.46	34.7	39.2	2.97	2.85
		0.7 µm	6.54	1.82	133	1.96	0.65	0.32	33.9	38.8	3.34	2.46
		0.2 µm	6.83	2.08	140	1.94	0.79	0.50	32.6	37.1	3.97	2.95
	20	UF	6.54	2.10	123	1.32	0.63	0.31	36.6	40.1	1.97	2.35
		0.7 µm	5.92	1.91	117	1.92	0.53	0.27	34.9	39.8	2.57	1.85
		0.2 µm	6.39	1.98	116	1.64	0.60	0.32	33.1	39.2	2.97	1.84
	16	UF	5.80	1.90	107	0.92	0.48	0.21	36.1	40.1	3.02	2.47
		0.7 µm	5.61	1.77	113	0.92	0.39	0.16	35.0	40.1	2.46	2.35
		0.2 µm	5.73	1.82	112	1.31	0.42	0.21	35.3	40.6	2.17	2.09
	12	UF	5.26	1.90	100	1.29	0.42	0.21	36.4	40.4	2.22	2.06
		0.7 µm	5.34	1.82	103	1.50	0.35	0.16	35.1	39.9	2.01	1.87
		0.2 µm	5.49	2.00	102	1.31	0.38	0.21	35.8	39.9	1.97	1.87
January sample	24	UF	1.87	0.77	84.0	0.89	0.37	0.24	20.1	23.1	2.43	2.13
		0.7 µm	1.64	0.63	76.5	0.69	0.26	0.20	21.4	23.0	1.39	1.91
		0.2 µm	1.76	0.71	80.2	*	0.29	0.23	21.2	23.7	0.51	1.22
	20	UF	2.27	1.20	77.1	0.89	0.97	0.77	21.5	22.4	2.5	2.26
		0.7 µm	2.21	1.03	77.0	0.65	0.78	0.56	21.4	23.1	1.5	1.12
		0.2 µm	2.19	1.11	75.7	*	0.79	0.64	20.7	23.1	1.51	1.35
	16	UF	2.22	1.32	61.8	1.34	1.44	1.21	21.7	24.2	2.94	1.27
		0.7 µm	2.13	1.17	66.6	0.72	1.26	1.08	21.4	23.6	3.18	1.78
		0.2 µm	2.20	1.34	62.1	*	1.28	1.20	22.0	24.0	2.61	2.55

Temperature °C	Filtration treatment	CO_2 mg L^{-1}		CO µg L^{-1}		CH_4 µg L^{-1}		DOC[a] mg L^{-1}		DIC mg L^{-1}	
		UV	Control	UV	Control	UV	Control	UV	Control	UV	Control
12	UF	1.80	1.16	45.6	1.10	0.82	0.72	19.1	20.5	2.21	1.85
	0.7 µm	1.80	1.03	47.2	0.66	0.69	0.56	20.2	22.9	2.17	1.93
	0.2 µm	1.77	1.04	46.3	*	0.84	0.68	20.2	22.5	2.03	1.72

*Below detection limit of instrument

[a] Technically there are no unfiltered DOC concentrations as the UF samples were filtered to 0.7 µm before analysis

Table 3.5. Collection dates and chemical properties of water samples used in ambient exposure experiments, shown in relation to measured UV and PAR irradiance.

Date	DOC mg L^{-1}	DIC mg L^{-1}	E2:E3	E4:E6	UV W m^{-2}	PAR W m^{-2}
04/08/2014	29.5	9.2	4.4	5.2	25.9	157
05/08/2014	29.9	5.9	4.3	6.2	21.8	146
07/08/2014	30.8	4.3	4.4	6.8	18.9	124
08/08/2014	37.2	2.4	4.4	6.2	14.8	96.8
09/08/2014	29.0	6.0	4.3	6.5	23.8	177
25/08/2014	33.2	2.1	4.7	7.0	10.3	61.8
26/08/2014	30.8	2.5	4.6	6.9	22.0	158
27/08/2014	29.6	3.9	4.5	7.5	20.3	165
28/08/2014	26.9	5.4	4.5	6.5	19.2	136
02/09/2014	35.8	2.9	4.6	6.6	11.3	73.4
03/09/2014	33.2	3.4	4.5	6.3	11.6	74.4
16/09/2014	20.0	4.2	4.2	7.1	10.8	68.1

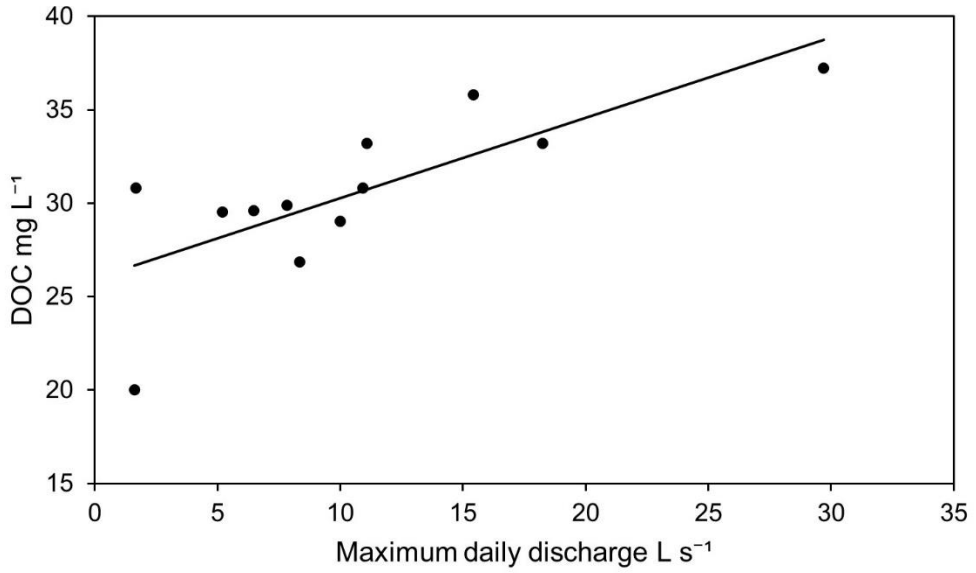

Figure 3.5. Correlation between DOC concentration and maximum discharge measured two days prior to water sampling.

Chapter 4 Temporal Changes in Photoreactivity of Dissolved Organic Carbon and Implications for Aquatic Carbon Fluxes from Peatlands

Amy E Pickard, Kate V Heal, Andrew R McLeod and Kerry J Dinsmore

Published in *Biogeosciences* (doi:10.5194/bg-14-1793-2017). The chapter appears as submitted to the journal, including supplementary information which is provided at the end of the chapter.

The candidate, as lead author, collected field samples, performed irradiation experiments and undertook laboratory analyses. Data analysis and writing of the paper were also carried out by candidate. Co-authors provided guidance on the scope and design of the project, and contributed to the editing of the manuscript.

Other Acknowledgements: The Irradian™ spectroradiometer used in this study was calibrated by Chris McLellan at the NERC Field Spectroscopy Facility. Stephen Mowbray provided assistance with lignin phenol analyses and Andrew Addison helped with fieldwork. Tony Dickinson and Jim Donnelly at the University of Central Lancashire facilitated use of a Horiba FluroMax-4 spectrofluorometer.

Abstract

Aquatic systems draining peatland catchments receive a high loading of dissolved organic carbon (DOC) from the surrounding terrestrial environment. Whilst photo-processing is known to be an important process in the transformation of aquatic DOC, the drivers of temporal variability in this pathway are less well understood. In this study, 8-h laboratory irradiation experiments were conducted on water samples collected from two contrasting peatland aquatic systems in Scotland; a peatland stream and a reservoir in a catchment with high percentage peat cover. Samples were collected monthly at both sites from May 2014 to May 2015 and from the stream system during two rainfall events. DOC concentrations, absorbance properties and fluorescence characteristics were measured to investigate characteristics of the photochemically labile fraction of DOC. CO_2 and CO produced by irradiation were also measured to determine gaseous photoproduction and intrinsic sample photoreactivity. Significant variation was seen in the photoreactivity of DOC between the two systems, with total irradiation induced changes typically two orders of magnitude greater at the high DOC stream site. This is attributed to longer water residence times in the reservoir rendering a higher proportion of the DOC recalcitrant to photo-processing. During the experimental irradiation, 7% of DOC in the stream water samples was photochemically reactive and direct conversion to CO_2 accounted for 46% of the measured DOC loss. Rainfall events were identified as important in replenishing photoreactive material in the stream, with lignin phenol data indicating mobilisation of fresh DOC derived from woody vegetation in the upper catchment. This study shows that peatland catchments produce significant volumes of aromatic DOC and that photoreactivity of this DOC is greatest in headwater streams, however an improved understanding of water residence times and DOC input-output along the source to sea aquatic pathway is required to determine the fate of peatland carbon.

4.1 Introduction

DOC is transported from terrestrial environments to aquatic systems where it plays an important role in carbon (C) cycling. Biogeochemical transformations of DOC via microbial and photochemical pathways impact significantly on aquatic C cycles, with up to 55% of C exported as DOC to freshwaters estimated to be lost to the atmosphere as CO_2 (Cole et al., 2007; Tranvik et al., 2009; Cory et al., 2014). These estimates suggest that the C sink strength of the land surface globally has been overestimated, as the role of freshwater systems in the biogeochemical processing of DOC and the subsequent production of greenhouse gases had not been considered. Understanding of the rate of turnover of DOC in aquatic systems remains incomplete and further efforts are required to quantify the extent to which biogeochemical processes in aquatic systems are a source of C to the atmosphere.

Photochemical reactions in aquatic systems are induced by the absorption of solar radiation, particularly in the UV region of the spectrum, and preferentially affect aromatic, high molecular weight (HMW) molecules derived from allochthonous sources. Upon radiation, HMW DOC is converted to microbially available low molecular weight (LMW) C substrates (Opsahl and Benner, 1998; Sulzberger and Durisch-Kaiser, 2009). Photodegradation of DOC also results in the production of C based gases, primarily CO_2 and CO (Stubbins et al., 2011). Whilst it is understood that input of photochemically reactive terrigenous DOC can regulate C cycling in aquatic systems (Cory et al., 2014; Koehler et al., 2014), the significance of DOC photodegradation processes in these cycles remains poorly constrained over time and space (Franke et al., 2012; Moody et al., 2013). Due to low temperatures and short residence times limiting autochthonous (in situ) DOC production in headwater systems of northern peatlands, photochemical processing may be a disproportionately more important process.

A key control on DOC concentrations in headwater systems is rainfall events which flush young, less degraded plant material within the catchment into streams (Austnes et al., 2010). Rainfall events have been shown to contribute significantly to annual C export from peatland

headwater streams (Clark et al., 2007), yet the degree to which they replenish photolabile material within the aquatic environment is less certain. Stormflows in northern catchments have been associated with increased contribution of humic like material (Fellman et al., 2009), suggesting that DOC photoreactivity may also increase during these events. Several studies have explored seasonal variation in intrinsic DOC photoreactivity in northern aquatic systems (Franke et al., 2012; Vachon et al., 2016) yet, to our knowledge, the contribution of rainfall events to the seasonal cycle of photolabile material has not been previously investigated.

Further uncertainty remains in understanding the variation in DOC photolability at different positions within a watershed (Franke et al. 2012). The increasing residence time of downstream aquatic systems, as headwater streams drain into rivers, lacustrine and marine environments, may mean that photo-processing becomes a more important control on overall C budgets with distance downstream. Conversely, the extent to which the material has already been degraded in the upstream aquatic environment may mean that further processing is limited (Catalán et al., 2016; Vähätalo and Wetzel, 2008). Investigating the susceptibility of DOC to photo-processing in different types of aquatic environments will allow the overall contribution of photochemical processes to C cycling to be understood on a catchment scale.

The primary aim of this study was to assess temporal variation in the photochemical reactivity of DOC from two contrasting aquatic systems draining peatlands and to understand how this variation may impact aquatic C budgets. Controlled UV irradiation experiments were conducted on water samples collected from the two contrasting aquatic systems, one a stream and the other a reservoir. Water from both systems was sampled on a monthly basis over a 1 year period and also from the high DOC stream system during two rainfall events to characterise short term variability in DOC concentration and composition. After experimental exposure, optical, spectroscopic and biogeochemical analyses of the water samples were conducted to explore DOC photoreactivity and the resultant production of C based gases. The results were used to test the following hypotheses:

H1: Both aquatic systems will exhibit seasonality with regards to the supply of photochemically labile DOC, with highest photoreactivity detected in the winter due to limited processing in the aquatic environment.

H2: Photochemical degradation of DOC will be a more significant loss term of C in the high DOC aquatic system.

H3: Rainfall events in the high DOC system will replenish the supply of photolabile material.

4.2 Methods

4.2.1 Study sites

Water samples for the irradiation experiments were collected from two aquatic systems located in peatland catchments. The Black Burn (55°47'34″ N; 3°14'35″ W; 254 m a.s.l.) is a small headwater stream draining Auchencorth Moss, an ombrotrophic peatland located in central Scotland covering 3.35 km^2 (Billett et al., 2010). The stream is fed by a number of small tributaries from the surrounding peatland, part of which is used for peat extraction. Low density sheep grazing is the primary land use within the catchment and vegetation comprises a *Sphagnum* base layer and hummocks of *Deschampsia flexuosa* and *Eriophorum vaginatum*, or *Juncus effusus*. In the upper catchment shrubs are present, including *Calluna vulgaris*, *Erica tetralix* and *Vaccinium myrtillus* (Dinsmore et al. 2010; Drewer et al., 2010).

The Black Burn stream hydrographic record is characterised by a steady base flow and rapid ('flashy') response to rainfall events which typically produce high flow accompanied by elevated DOC concentrations. Annual mean stream water DOC concentrations determined by weekly sampling over a 5 year period were high, at 28.4 ± 1.07 mg L^{-1} (Dinsmore et al. 2013), with a marked seasonal pattern, characterised by low DOC in winter and high concentrations in summer. In this study, water samples were collected from an established sampling site where DOC concentrations have been recorded for >9 years as part of the Centre for Ecology

& Hydrology (CEH) Carbon Catchments project (https://www.ceh.ac.uk/our-science/projects/ceh-carbon-catchments).

The other sampling site was Loch Katrine (56°25'25″ N; 4°45'48″ W; 118 m a.s.l.) in the Loch Lomond and Trossachs National Park, Scotland. Loch Katrine has a surface area of 8.9 km^2 and is fed by ~88 tributaries which predominantly drain a catchment of upland blanket bog (SNH, 2005). Loch water DOC concentrations have been recorded by the Scottish Environment Protection Agency (SEPA) at Ruinn Dubh Aird, a peninsula located at the south eastern end of the loch, which was also selected as the sampling point for this study. DOC concentrations measured approximately six times a year from 2009–2014 were low at 3.68 ± 0.56 mg L^{-1} (SEPA, personal communication).

4.2.2 Sample collection

Water was sampled monthly from both sites from May 2014 to May 2015 inclusive (13 samples over the study duration) to characterise seasonal variation in DOC concentration and composition. Samples were collected at 20 cm below the surface of the water in a screw top sterile clear glass bottle. Upon return to the laboratory, samples were stored in the dark at 4°C and exposed to experimental conditions within a week of collection. Additional water sampling to characterise the effect of rainfall events focused on the Black Burn head water system. Intensive stream water sampling was conducted during two rainfall events, one in winter (defined as 1 October to 31 March) and the other during the summer (1 April to 30 September) (Gordon et al., 2004). An automatic water sampler (Teledyne Isco, USA) was programmed to collect a composite 1 L sample of water from the Black Burn into separate polypropylene bottles every 60 minutes (comprising two 500 mL samples collected each 30 minutes) throughout the rainfall events. Stream water sampling in the winter rainfall event was conducted from 11:00 on 9 December to 17:00 GMT on 10 December 2014, resulting in 31 samples across the event. Stream water sampling in the summer rainfall event started at 14:30 on 1 September and finished at 06:30 GMT on 2 September 2015, resulting in 17 samples.

Water samples were transferred into glass bottles from the automatic water sampler for transport to the laboratory and irradiated within 5 days of collection.

Throughout the year of sampling, the Black Burn water depth was measured at 15 minute intervals approximately 2 km downstream from the sampling site using a Level Troll pressure transducer (In Situ Inc., USA) with atmospheric correction from a BaroTroll sensor (In situ Inc., USA) located above the water surface. Water depth readings from the pressure transducer were converted to discharge at the sampling site using rating curves ($R^2 > 0.90$) based on flows measured by dilution gauging (Dinsmore et al., 2013). Equivalent hydrological data were not available for Loch Katrine.

4.2.3 Sample preparation

Prior to experiments water samples were degassed under a vacuum pressure system for 20 minutes to remove dissolved gas from the water and then filtered using syringe driven pore size filters 0.22 μm (Merck Millipore, UK) to exclude microbial activity. 15 mL of filtered sample was immediately transferred into 21 mL quartz vials (Robson Scientific, UK) which were sealed with aluminium crimp tops and rubber butyl plugs. All samples were prepared at room temperature in oxygenated conditions.

4.2.4 Irradiation experiments

Experiments providing both UV-A and UV-B irradiation were conducted using UV313 lamps (Q-Panel Company, USA) covered with 125 μm cellulose diacetate (A. Warne, UK) to exclude UV-C (<280 nm) and short wavelength UV-B (<290 nm). Lamps were mounted inside quartz tubing (Robson Scientific, UK) beneath the water surface in a water bath maintained at 16°C and vials were irradiated sideways while submerged. UV irradiance of the samples was modulated to remain constant throughout the 8-h exposure by measurement with an erythemally weighted UV-B broad-band sensor with a dimmer (Model PMA2102; Solar Light Inc., USA). The sensor was held beneath the water surface behind a quartz window of the same thickness as the vials. The UV exposure was calibrated with a double monochromator

scanning spectroradiometer (Irradian™, UK), itself calibrated against a quartz halogen standard (FEL Lamp, F-1297) operated by the NERC Field Spectroscopy Facility, Edinburgh (http://fsf.nerc.ac.uk/). Total unweighted irradiance was 2.89 W m^{-2} in the UV-B, 4.63 W m^{-2} in the UV-A, and photosynthetically active radiation (PAR) was 0.92 W m^{-2}. These conditions reflect twice the UV-B irradiance that could be expected over a cloudless summer day in the UK and a significant underestimation of summer time daily ambient UV-A and PAR radiation. Weighting functions derived for a range of photochemical processes were applied to the spectral output (Table 4.1). The time duration of the experiment (8 h) was selected to represent a conservative estimate of the exposure time of surface water during transit through a headwater peatland catchment to a marine outlet. Water temperatures of ~16°C were measured in both field sites in May 2014 prior to commencement of the year-long sampling programme and was employed in the experiments to represent summer time conditions. Controls comprising quartz vials containing water samples and wrapped in aluminium foil to exclude radiation were kept in the water bath for the experiment duration, with four replicates of each of the UV-exposed and control samples.

To select water samples from the rainfall events for use in irradiation experiments, POC concentrations, a_{254} values and E4:E6 ratios were measured within 24 h of sample collection in all samples (using the methods described below). From these results, eight stream water samples were selected from each rainfall event which represented the minimum, maximum and median values of these parameters (Supplementary Information Table 4.3).

4.2.5 Analytical methods

On each monthly sampling occasion the water dissolved oxygen (DO), conductivity, pH and temperature were measured on site with a handheld Hach HQd multimeter (Hach, USA). Measured volumes of water samples were filtered within 24 h of collection through pre-ashed (8 h at 450°C), pre-weighed Whatman GF/F (0.7 μm pore size) filter papers. POC was determined using loss-on-ignition, following the method of Ball (1964).

Following irradiation, partitioning of dissolved C gases from the liquid into the vial headspace was encouraged through use of a wrist action shaker for 30 s. An Agilent gas chromatography (GC) system (Hewlett Packard 6890; Agilent Technologies, USA) equipped with an autosampler (HTA, Italy) and a flame ionisation detector (FID) held at 250°C was used to analyse samples for headspace CO_2, CO and CH_4 concentration within 8 h of irradiation. Needle penetration depth was set to a standard depth and 1.5 mL of headspace sample was automatically injected into the sample loop. Analytical runs lasted for 10.5 min and the column carrier gas was N_2 at a constant flow rate of 45 mL min^{-1}. CO_2 and CO measurements were made possible by a methaniser fitted between the column and FID. A standard 7-gas mixture (BOC Special Gases, UK) was used for daily detector calibration prior to sample analysis (detection limits: CO_2 78 ppm; CO 1.6 ppm; CH_4 0.8 ppm). Dilutions of 50 and 75% were made from this standard using Zero Grade N_2 to produce a 3-point calibration for each gas. Post-run peak analysis and integration were performed using Clarity software (DataApex, Czech Republic).

DOC and total carbon (TC) concentrations were measured using a PPM LABTOC Analyser (Pollution and Process Monitoring Ltd., UK) in UV treatment and control samples after exposure. Dissolved inorganic carbon (DIC) was calculated as the difference between TC and DOC. UV-visible absorbance of UV treatment and control samples contained in 3.5 mL PLASTIBRAND® UV-Cuvettes with a path length of 10 mm was measured at room temperature between 200 and 800 nm at increments of 1 nm using a Jenway spectrophotometer (Model 7315; Bibby Scientific, UK). Deionised water controls were used between each sample. Absorption coefficients a_λ were calculated as:

$$a_\lambda = 2.303\, x\, \left(\frac{A\lambda}{L}\right) \quad (1)$$

where A is the absorbance at each wavelength and L is the path length (m) of the cuvette (Green and Blough, 1994). Specific UV absorbance ($SUVA_{254}$) values, a measure of DOC aromaticity, were determined by dividing the UV absorbance measured at $\lambda = 254$ nm by the

DOC concentration (Weishaar et al., 2003). E4:E6 ratios were estimated using the absorbance values at 465 and 665 nm, respectively (Peacock et al., 2014). Spectral slope (S) was calculated using a nonlinear fit of an exponential function to the absorption spectrum in the ranges of 275–295 and 350–400 nm, where S is the slope fitting parameter. The spectral slope ratio (SR) was calculated as the ratio of S275–295 to S350–400 (Helms et al., 2008; Spencer et al., 2009).

Fluorescence intensity in water samples filtered to 0.2 µm was measured using a FluroMax-4 spectrofluorometer (Horiba Jobin Yvon Ltd., Japan). The instrument was programmed to scan across excitation wavelengths 200-400 nm (5 nm increments) and emission wavelengths 250-500 nm (2 nm increments) with a 1 nm path interval. Data were obtained at room temperature and were blank corrected using deionised water. Intensity ratios derived using these data allow discrimination between different sources of DOC. Here, the fluorescence index (FI), f_{450}/f_{500}, the ratio of fluorescence intensity at the emission wavelength 450 nm to that at 500 nm at excitation wavelength 370 nm, was calculated to help identify dissolved organic matter (DOM) source material. Values around 1.8 suggest autochthonous organic material, whereas values around 1.2 indicate terrestrially derived material (Cory and McKnight, 2005).

Lignin phenol concentrations in unirradiated Black Burn water samples were measured using the CuO oxidation method (Benner et al., 2005; Spencer et al., 2008). After filtration to 0.2 µm, 45 mL of water sample was freeze dried to produce lyophilised DOM which was transferred to stainless steel pressure bombs with 1 g of CuO and 100 mg of $Fe(NH_4)_2(SO_4)_2H_2O$. Under anaerobic conditions, 8 mL of NaOH was added to the bombs before they were sealed. Samples were then oxidised at 155°C for 3 h. Following oxidation, samples were acidified to pH 1 with H_2SO_4, extracted with ethyl acetate three times, and then passed through Na_2SO_4 drying columns. Samples were dried using a flow of N_2 and kept frozen prior to GC analysis. After redissolution in ~200 µL pyridine, lignin phenols were derivatised with bis-trimethylsilyltri-fluoromethylacetamide (BSTFA) and quantified on a GC (Agilent 5890 MkII with twin FID). Specifically, a twin-column split-injection method was

used with Agilent DB1 and DB1701 (both 30 m x 0.25 mm diameter x 0.25 µm film thickness) flow being split in the injection liner with a twin-hole ferrule. Column flow was 1 mL min-1 with a split ratio of 20:1. The chromatographic conditions were 100ºC held for 1.25 min, followed by a heating rate of 4ºC min-1 until 270ºC, then held for 15 min.

Eleven lignin phenols were measured, including three p-hydroxybenzene phenols (P): p-hydroxybenzaldehyde, p hydroxyacetophenone, p-hydroxybenzoic acid; three vanillyl phenols (V): vanillin, acetovanillone, vanillic acid; three syringyl phenols (S): syringaldehyde, acetosyringone, syringic acid; and two cinnamyl phenols (C): p-coumaric acid and ferulic acid. Blank controls, taken through the method from CuO oxidation onwards, were quantified and subtracted from sample concentrations. Quantification was achieved through use of cinnamic acid as an internal standard. In addition to total concentration of lignin phenols (Σ_{11}) and carbon normalised yields (Λ_{11}), the ratio of syringyl to vanillyl phenols (S/V), the ratio of cinnamyl to vanillyl (C/V) phenols, the ratio of p-hydroxybenzenes to vanillyl phenols (P/V) and the ratio of acids to aldehydes ($Ad/Al_{v,s}$) were calculated to aid interpretation of the data. Lignin phenols for Loch Katrine samples were not measured due to insufficient production of lyophilised material using the stated method.

4.2.6 Data analysis

Data collected in the irradiation experiments were tested for normality using the Shapiro-Wilks test and were found to be normally distributed. Unpaired t-tests were conducted between irradiated and unirradiated samples to assess differences in spectral properties, DOC and DIC concentrations, lignin phenol concentration and gaseous production. Pearson correlation coefficients were used to test the potential role of DOC composition and site conditions in regulating photochemical lability, measured as total DOC loss, production of DIC and C gases (CO and CO_2) and change to a_{254} and E4:E6 ratios.

Carbon species DOC, DIC, CO_2 and CO measured each month at the Black Burn and Loch Katrine were included in C mass budgets calculated for irradiated and unirradiated samples.

By converting all data to mg L^{-1}, the difference in C budget between treatment and control samples could be determined (see Table 4.4; Supplementary Information for example calculations). To obtain a standard error value for differences between irradiated and control samples, the mean control value was determined and subtracted from each of the irradiated replicates.

Photoreactivity (mg C / mg DOC) was determined as total change to C species (DOC, CO2 and CO) upon irradiation normalised for initial DOC concentration. For the Loch Katrine samples, where minimal net DOC changes upon irradiation were observed in the sample aliquots, photoreactivity (mg C / mg DOC) is expressed as the sum of gaseous photoproduction (CO2 and CO only) divided by the initial DOC concentration. This is to avoid production of negative photoreactivity values for Loch Katrine which may have been explained in large part by the limited resolution of the PPM LabTOC instrument at very low DOC concentrations.

Correlation coefficients were calculated between intrinsic sample photoreactivity and lignin phenol data. The Durbin-Watson statistic was used to test for the presence of autocorrelation in residuals of lignin phenol analyses of stream water samples collected during rainfall events and showed no correlation between the samples. Minitab v.16 (Minitab Inc., USA) was used for all statistical analyses.

4.3 Results

4.3.1 Climate and water chemistry conditions at time of sampling

Total rainfall measured at the European Monitoring and Evaluation Programme (EMEP) supersite at Auchencorth Moss (Torseth et al., 2012) for the 13 month sampling period was 1015 mm. It varied from lowest monthly values in September and April to the highest in October (Figure 4.1). The mean air temperature of the study period was 7.7°C, similar to the 8 year average of 7.6°C, and reached a maximum of 27.6°C in July 2014 and a minimum of -7.9°C in January 2015.

At Comer meteorological station, located 10 km from the Loch Katrine sampling site, rainfall was considerably higher, totalling 2368 mm over the sampling period (Figure 4.1b) (Met Office, 2012). Seasonal variation in rainfall was clear, with >40% of rainfall falling from December to February. Air temperatures were higher than at the Black Burn, with a mean of 10.2°C.

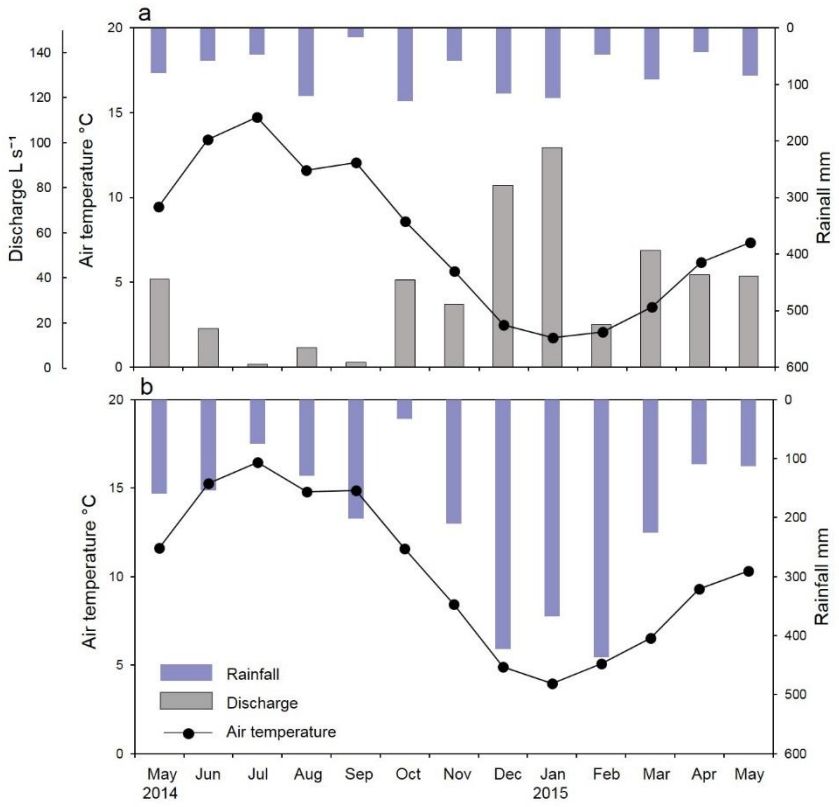

Figure 4.1. Mean monthly air temperature, total rainfall and mean discharge from May 2014 to May 2015 are shown for a) Auchencorth Moss, with discharge of the Black Burn shown on the left hand offset axis. Mean monthly air temperature and total rainfall are shown for the same period for Comer meteorological station, near Loch Katrine. Note inverted right hand y axes.

Water chemistry differed considerably between the two aquatic systems over the year-long sampling (Table 4.1). The water temperatures reflected the difference in air temperature between the sites, with higher mean values at Loch Katrine than at the Black Burn. Mean pH at the Black Burn was 5.4, compared to 6.7 at Loch Katrine. Conductivity was more variable at the Black Burn and was on average 53 μS cm^{-1} higher than at Loch Katrine, although values at both sites were low. POC concentrations at the Black Burn were over double those at Loch Katrine. FI values were slightly higher at the Black Burn, but at both sites were low and stable, indicative of terrestrially derived DOC material (Cory and McKnight, 2005) (see Appendix E for further spectrofluoresence information).

Table 4.1. Mean (n=13 ± 1 standard deviation) water temperature and chemistry parameters including pH, conductivity, POC concentrations, and FI values at the Black Burn and Loch Katrine.

	Black Burn	**Loch Katrine**
Water temperature °C	8.26 ± 4.53	10.9 ± 5.07
pH	5.38 ± 0.85	6.74 ± 0.32
Conductivity μS cm^{-1}	78.2 ± 30.7	25.2 ± 4.01
POC mg L^{-1}	5.78 ± 2.78	2.96 ± 0.63
FI value[a]	1.15 ± 0.13	1.08 ± 0.18

[a]Mean of 12 values as samples missing at both sites (see Appendix E).

DOC concentrations at the Black Burn ranged from 14.2 to 50.9 mg L^{-1} (Figure 4.2) and showed a similar seasonal pattern as described in Dinsmore et al. (2013). Concentrations were lowest in winter (23.2 ± 15.3 mg L^{-1}) and highest in autumn (41.4 ± 12.4 mg L^{-1}); the latter consistent with increased organic matter inputs to the stream from flushing of soils during autumn rainfall events.

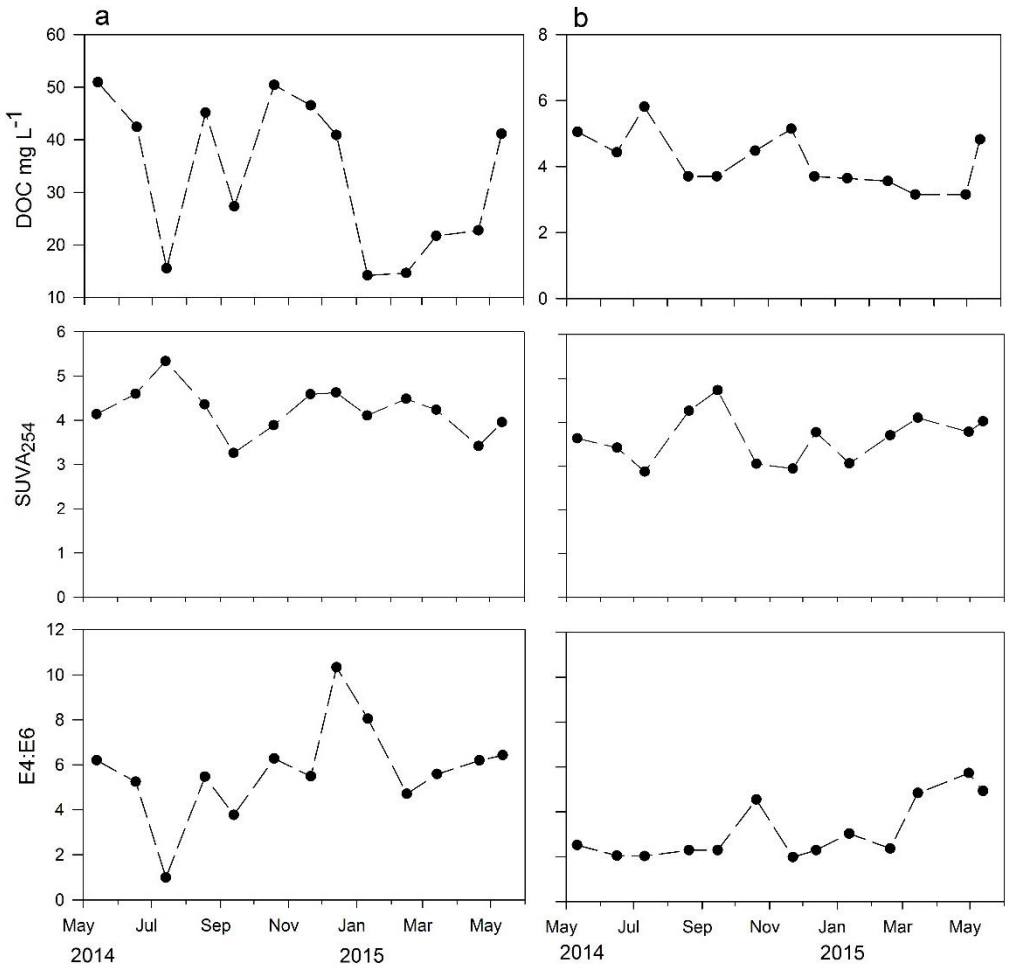

Figure 4.2. Time series at a) the Black Burn and b) Loch Katrine of DOC concentration and parameters for DOC quality: $SUVA_{254}$ and E4:E6 from May 2014 to May 2015. Note different y axis scales for DOC data.

At Loch Katrine, DOC concentrations were low and consistent, ranging from 3.10 to 5.82 mg L^{-1}. Concentrations were lowest in spring and highest in summer. $SUVA_{254}$ values at the Black Burn were higher than at Loch Katrine, suggesting that the DOC pool was comprised of a greater percentage of aromatic material (Weishaar et al., 2003). The E4:E6 ratio at the Black Burn varied considerably over the sampling period, ranging from 1.0 to 10.2. At Loch Katrine, the E4:E6 ratios were lower and less variable, but are a less meaningful parameter in the low DOC concentration Loch Katrine samples due to minimal absorbance in wavelengths greater than 400 nm.

4.3.2 Optical changes in water samples upon irradiation

Absorbance coefficients typically decreased upon irradiation of water samples relative to dark controls, with the strongest decrease occurring in the UV part of the spectrum at ~300 nm (Figure 3). Percentage loss of absorbance upon irradiation was 5% greater in water samples from the Black Burn compared to Loch Katrine samples when averaged across wavelengths 250-400 nm. In the Black Burn, decreases in absorbance were greatest in the summer, whereas at Loch Katrine the decreases in absorbance were greater in the winter and spring.

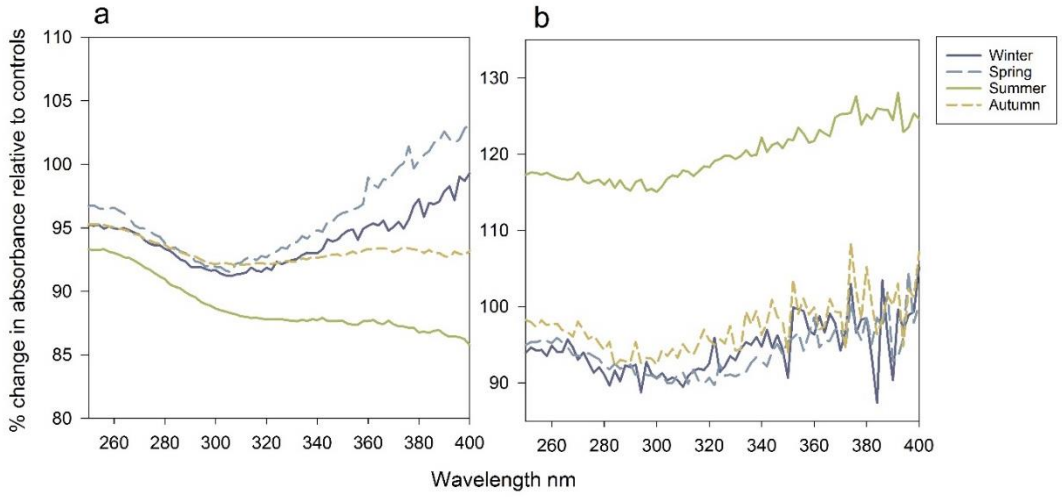

Figure 4.3. Change in absorbance upon irradiation expressed as a percentage of the unirradiated control samples from 250 - 400 nm at a) Black Burn and b) Loch Katrine. Summer is the mean of June, July and August values, autumn is the mean of September, October and November values, winter is the mean of December, January and February values, and spring is the mean of March, April and the combined mean of May '14 and May '15 values. Note different y axis scales.

Percentage values consistently >100% (where UV exposed samples showed an increase in absorbance upon irradiation relative to dark control samples) were recorded for summer water samples from Loch Katrine. E4:E6 ratios decreased by a mean of 1.52 in irradiated Black Burn water samples, indicating accumulation of increasingly humic material in the remaining DOC pool during UV exposure. At Loch Katrine, E4:E6 ratios decreased by a mean of 0.21 upon irradiation.

4.3.3 Carbon budget changes upon irradiation

Typically, DOC concentrations in Black Burn water samples decreased after light exposure compared to unirradiated controls (Figure 4.4a). Mean change in DOC in irradiated samples from the Black Burn for the whole sampling period was -2.14 mg C L^{-1} (ranging from 0.06 to -4.35 mg C L^{-1} for individual months). DOC decreased after irradiation in all Black Burn samples with the exception of September 2014, indicating a photolabile DOC pool for most of the year. In contrast, in water samples from Loch Katrine irradiation induced DOC losses occurred in 5 of 13 samples and small gains were observed in 8 of 13 samples (Figure 4.4b). Whilst these results should be interpreted with caution as small differences in DOC concentrations (<0.5 mg C L^{-1}) are below the instrument detection limit, they suggest that the DOC pool in Loch Katrine was largely recalcitrant to photochemical degradation.

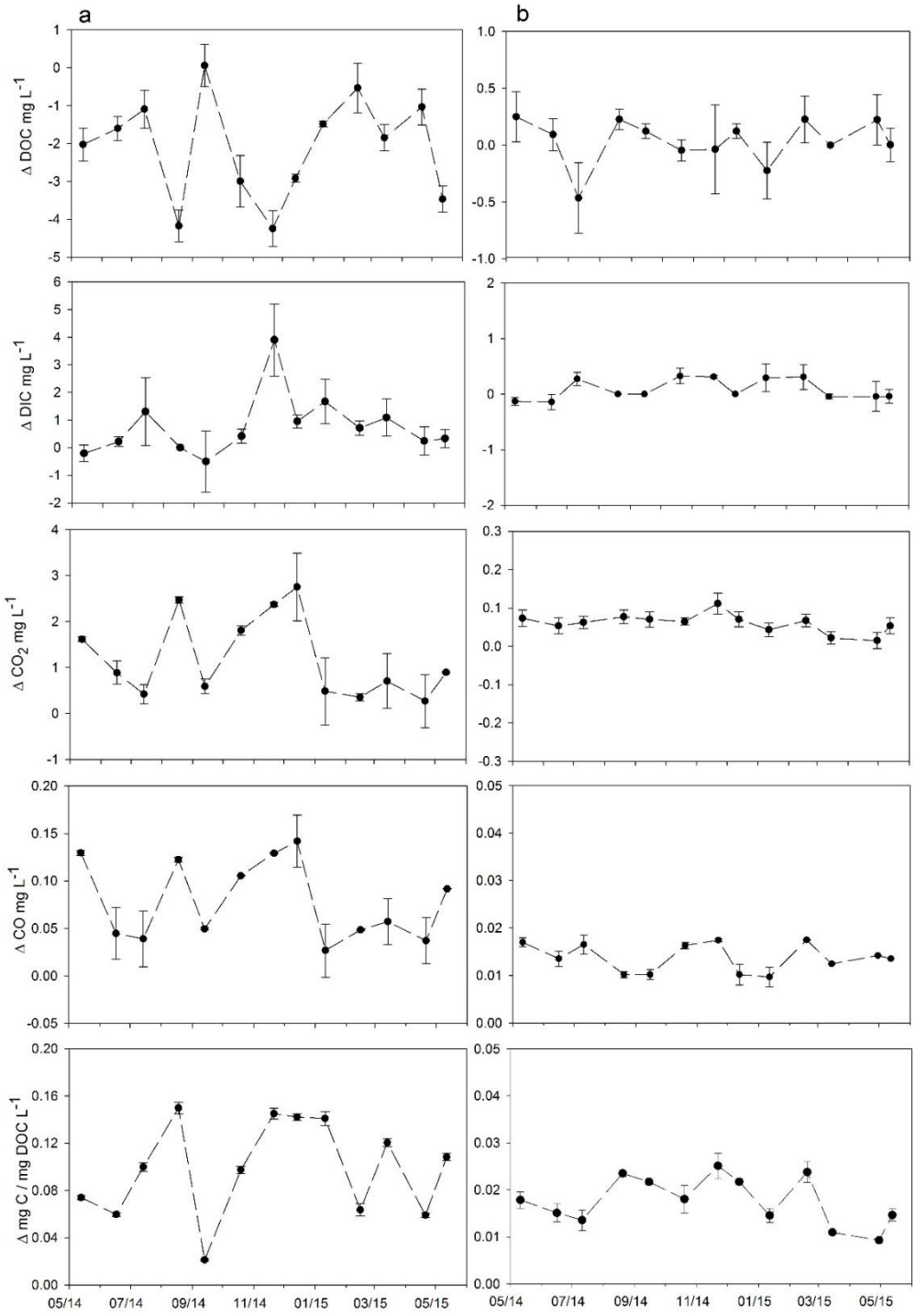

Figure 4.4 Irradiation induced changes to carbon species DOC, DIC, CO2 and CO in monthly water samples from panel Black Burn (panel a) and Loch Katrine (panel b). DOC normalised changes to all C species changes (photoreactivity, quantified as explained in the text) are shown on the bottom row. Data represent the difference between the mean of irradiated and unirradiated control samples. Error bars show the standard error of the mean (n=4). Note different y axis scales for Black Burn and Loch Katrine water samples.

Irradiation resulted in notable photoproduction of DIC, CO_2 and CO from Black Burn samples. DIC concentration increased by a mean of 0.77 mg C L^{-1} for the whole sampling period, although production across the samples was highly variable between months. CO_2 was the most abundant photoproduct and was produced at a mean rate of 1.2 mg C L^{-1} across all monthly samples. At Loch Katrine, CO_2 production was two orders of magnitude lower than in the Black Burn, produced at a mean rate of 0.06 mg C L^{-1}. In all monthly water samples from both sites CO concentrations increased in the irradiation experiments, with mean production rates of 0.07 and 0.01 mg C L^{-1} observed for Black Burn and Loch Katrine samples, respectively.

Carbon mass budgets for DOC loss and photoproduct accumulation (DIC, CO_2 and CO) in water samples were calculated for all the irradiation experiments. Budgets for all monthly water samples from the Black Burn were balanced to within ± 5.1% of the total measured C concentration. For Loch Katrine water samples, budgets were balanced to within ± 11%. The lower accuracy of budget closure in the Loch Katrine samples is likely due to lower overall C concentrations, which are more susceptible to measurement error. CH_4 was detected in all samples at very low levels, with mean concentrations of 0.63 and 0.57 μg L^{-1} detected at the Black Burn and Loch Katrine, respectively, and thus were not included in the mass calculations.

Intrinsic photoreactivity of C in the Black Burn ranged from 0.02 to 0.15 mg C/mg DOC and was highest in August (Figure 4.4a). Photoreactivity peaked again in November and remained elevated until January. Lowest sample photoreactivity was detected in September. At Loch Katrine, mean C photoreactivity was 0.017 mg C/mg DOC, with a maximum of 0.025 mg C/mg DOC L^{-1} detected in November.

4.3.4 Factors influencing carbon budget changes

Factors influencing irradiation induced changes to C species and spectral properties in Black Burn water samples were investigated using Pearson correlations (Table 4.2). Loss of DOC, absorbance at 254 nm and production of both CO2 and CO were significantly positively correlated with initial DOC concentration. Initial E4:E6 ratios had positive coefficient values with all light induced changes to the DOM pool, whilst FI values were all negative, although most of these correlations were not significant.

Table 4.2. Pearson correlation coefficients between irradiation induced changes to aqueous carbon species and spectral properties, and water chemistry of Black Burn water samples from the year-long sampling campaign prior to irradiation and site conditions at Auchencorth Moss (n=13).

	ΔDOC	**ΔDIC**	**ΔCO_2**	**ΔCO**	**Δa_{254}**	**Δa_{350}**	**ΔE4:E6**	**ΔS_R**
DOC	**0.708****	-0.074	**0.773****	**0.824****	**0.766****	-0.168	0.095	-0.547
E4:E6	0.366	0.049	0.463	0.434	0.183	**-0.579***	**0.770****	-0.157
$SUVA_{254}$	0.228	0.460	0.232	0.129	0.231	0.157	-0.098	-0.059
FI	-0.438	-0.161	-0.318	-0.238	-0.115	0.492	-0.485	-0.186
Air temperature[a]	-0.032	-0.379	-0.029	-0.052	0.220	0.402	**-0.571***	-0.405
Rainfall[b]	**0.603***	0.061	0.537	0.445	0.365	-0.389	0.492	-0.226
PAR[c]	-0.161	-0.459	-0.380	-0.267	-0.224	0.054	**-0.662***	-0.489
Discharge[d]	0.132	0.237	0.123	0.088	-0.139	-0.435	**0.767****	-0.072

*** p < 0.05**
**** p < 0.01**
[a] Mean monthly air temperature
[b] Total monthly rainfall (mm)
[c] Mean monthly PAR (μmol m^{-1} s^{-1})
[d] Mean monthly discharge (L s^{-1})

Of the meteorological and discharge variables investigated, air temperature and PAR were significantly negatively correlated with changes to E4:E6 ratios. Total monthly rainfall had positive coefficient values with irradiation induced changes to the DOM pool. Correlations between C species changes and discharge were less consistent, although mean monthly discharge was significantly positively correlated with changes to E4:E6 ratios.

4.3.5 Effect of rainfall events on carbon photo-processing in Black Burn water samples

The Black Burn was sampled hourly during a winter rainfall event, with collection commencing 6 h before peak rainfall (Figure 4.5a). Total rainfall during the event, which we define here as the water sampling period, was 19.6 mm, with an hourly maximum of 3.3 mm and rainfall recorded in 22 of the 31 sampling hours. Stream discharge peaked at 391 L s^{-1} although a separate smaller peak of 266 L s^{-1} also occurred during the sampling period.

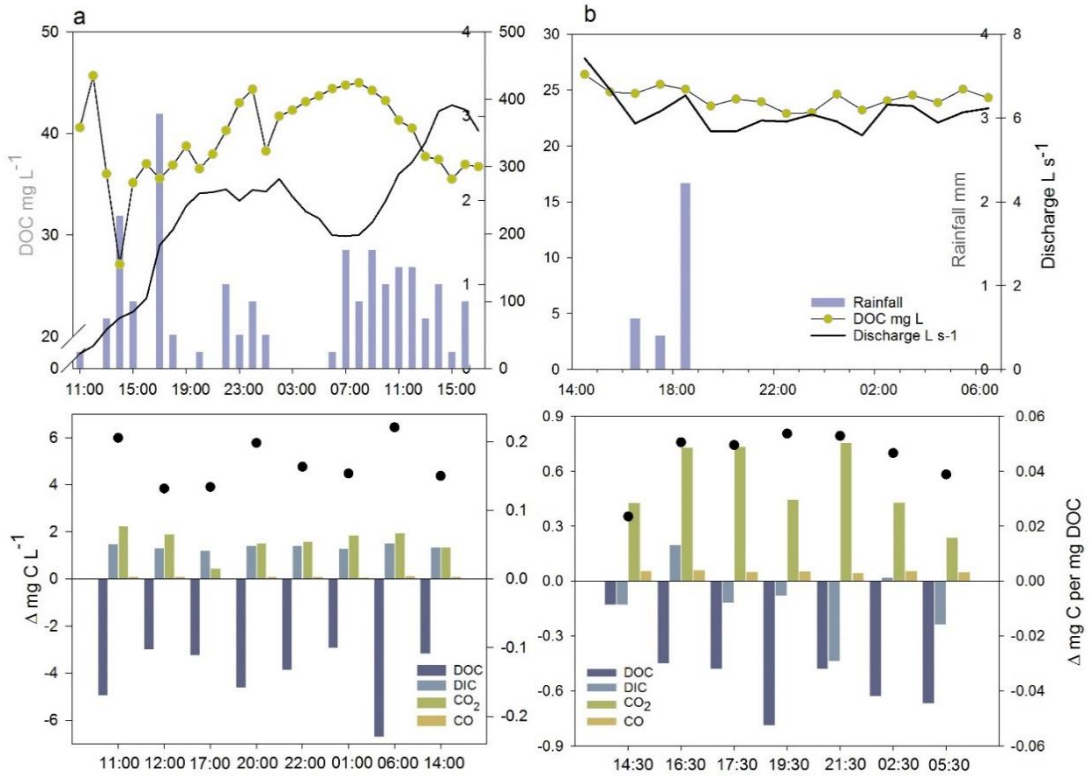

Figure 4.5. Rainfall events sampled on 9-10 December 2014 (panel a) and on 1-2 September 2015 (panel b). Row one shows a time series of hourly rainfall, discharge and DOC

concentrations for each event. Row two shows photo-induced C pool changes of irradiated samples expressed as a total change value per C species in vertical bars (left y axis) and as a DOC normalised value in dots (right y axis). Data represent the difference between the mean of irradiated and unirradiated control samples (n=4). Note different x- and y-axis scales.

During the event, an initial dilution of stream DOC concentrations was followed by recovery to pre-event levels (Figure 4.5a). DOC was most photoreactive at 06:00, with DOC concentration reduced after irradiation by 6.72 mg L^{-1}. DOC loss in this sample was greater than at any time through the year-long study (Figure 4.4a), even though the DOC concentration (44.4 mg L^{-1}) was within the range of measured monthly concentrations. The greatest irradiation induced increase in CO_2 concentration (2.25 mg L^{-1}) occurred in the first event sample at 11:00, collected prior to rainfall input. Photoreactivity was lowest at 12:00, and was similarly low in the sample collected at 17:00, which coincided with peak rainfall.

In the late summer rainfall event occurring at the end of an extended period of base flow in the Black Burn (Figure 4.9; Supplementary Information), 3.2 mm of rainfall was recorded with a maximum hourly total of 2.2 mm. Samples were collected from 14:30 to 06:30, with rainfall only occurring between 16:30 and 18:30. Discharge remained low and relatively stable throughout the event, with a mean flow of 6.14 L s^{-1}. Rainfall marginally diluted the stream DOC concentrations (Figure 4.5b). Photo-induced changes were much smaller than in the winter event and maximum DOC losses were a factor of 2.5 lower than the mean DOC reduction observed in the Black Burn monthly water sample experiments (Figure 4.4a). Photoreactivity was lowest in the initial sample collected at 14:30 prior to rainfall and coinciding with the highest discharge during the sampling period. Photoreactivity was highest in the 19:30 sample collected 3 h after peak rainfall.

4.3.6 Lignin phenol composition of Black Burn water samples

To understand the effect of DOM composition on photolability, lignin phenols were measured in all the Black Burn monthly and rainfall events water samples prior to the irradiation experiments (Appendix D). Dissolved lignin concentrations ranged from 15.3 to 108 μg L^{-1}

(mean = 52.8; n = 28) and were significantly positively correlated with sample DOC concentration (Pearson = 0.831; $p < 0.01$) (Figure 4.10; Supplementary Information). Carbon normalised yields were between 0.71 and 2.66 mg (100 mg OC)$^{-1}$. The contribution of individual phenol groups to the lignin signature varied between monthly samples of the year-long study and the rainfall events (Figure 4.6). In the monthly samples, the P phenols were most abundant, followed by V phenols (Figure 4.6a). Samples in the winter rainfall event contained higher and more variable mean yields for each phenol group, with S phenols most abundant, followed by V phenols and P phenols.

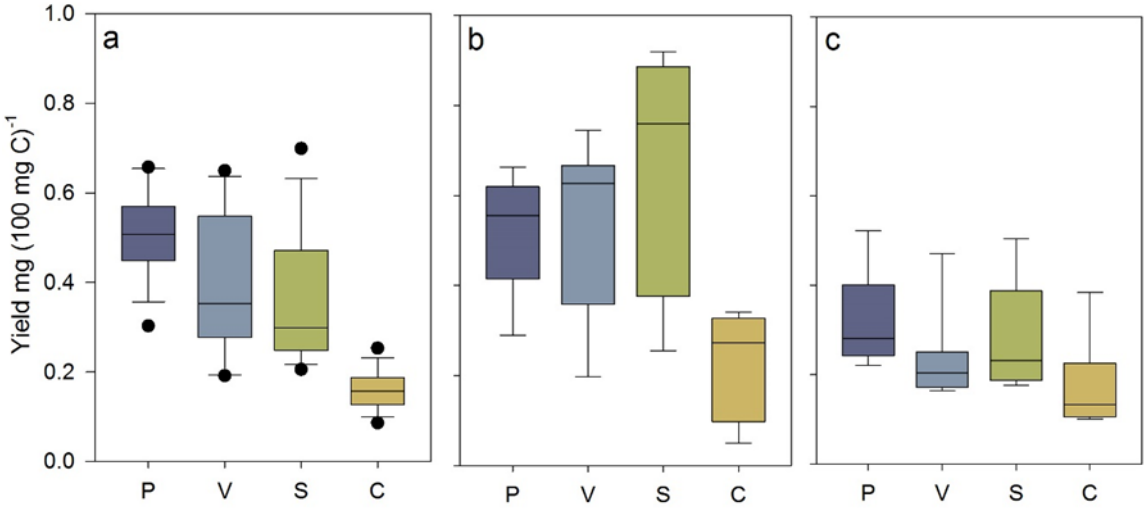

Figure 4.6. Boxplots of carbon-normalised yields of phenols groups for Black Burn water samples collected a) monthly in the year-long study (n=13), b) during the winter rainfall event (n=8) and c) during the summer rainfall event (n=7). P = p hydroxyl, V = vanillyl, S = syringyl and C = cinnamyl. The box spans from the first quartile to the third quartile, with the line showing the median value. Whiskers show the minimum and maximum values, with dots representing outlying values.

Overall yields were significantly lower (1-way ANOVA, $p < 0.01$) during the summer rainfall event. As in the year-long samples, P phenols were the most abundant, followed by S phenols and V phenols. Across all three sampling regimes, the contribution of C phenols to the overall lignin signature was smallest.

P:V ratios, an indication of Sphagnum derived DOC, ranged from 0.83 to 1.69 across all samples, indicating significant temporal variability in DOM source material. Photoreactivity was significantly negatively correlated with P:V ratios when all samples were combined in a correlation analysis (-0.523; $p < 0.01$) (Figure 4.7a). This suggests that the relative abundance of P versus V phenols contributed considerably to sample photoreactivity. The lowest P:V ratios were in winter rainfall event samples, where photoreactivity was highest.

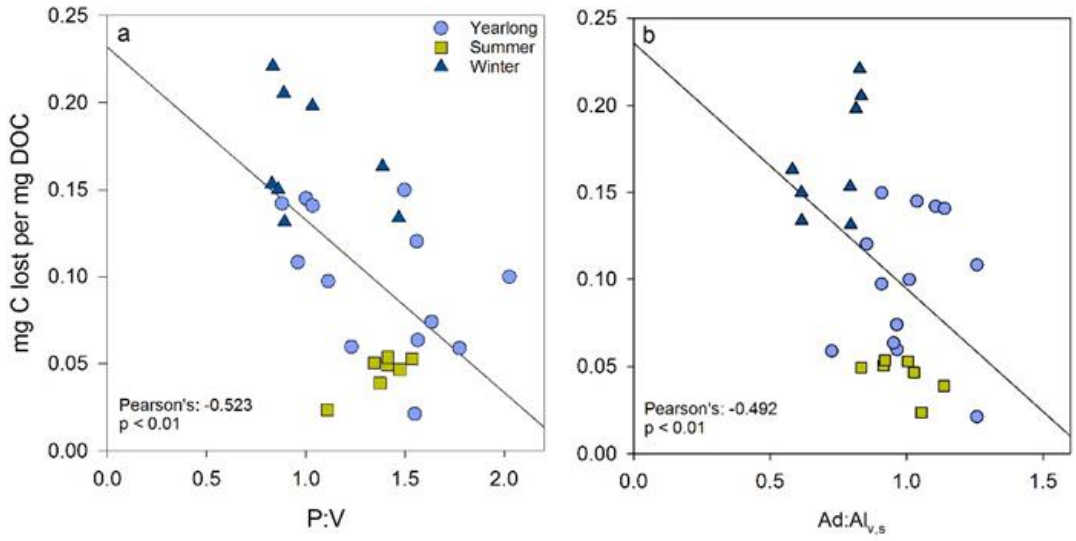

Figure 4.7. Pearson correlation between mg DOC lost upon irradiation per mg DOC and a) P:V ratios and b) Ad:Al$_{v,s}$ (derived from acids and aldehydes from vanillyl and syringyl phenol groups) ratios in all Black Burn water samples analysed (n=28). Lines of best fit for all water samples are also shown. The monthly samples in the year-long study and the winter and summer rainfall event samples are indicated.

Ad:Alv,s ratios, which are an indicator of sample degradation, ranged from 0.58 to 1.26, towards the lower end of reported values in the literature (Winterfeld et al., 2015). Photoreactivity was also significantly negatively correlated with Ad:Al ratios (-0.492; $p < 0.01$) (Figure 4.7b) and again lower ratios typically occurred in winter rainfall event samples.

4.4 Discussion

4.4.1 Peatlands as a source of photochemically labile DOC

Photo-processing resulted in considerable DOC loss from water samples from the Black Burn. Mean DOC loss in the 8-h irradiation experiments conducted on the monthly water samples was 7% relative to initial concentrations. Percentage DOC losses determined here are similar to those reported from irradiation experiments conducted over similar timescales using stream water draining a boreal watershed (3–10 % DOC loss over 10 h; Franke et al., 2012 and 11% TOC loss over 19 h; Köhler et al., 2002). However, photochemical processes are dependent on the spectral composition of irradiation sources and direct comparison of percentage loss rates in this study with those of other experimental studies using different lamp types or ambient sunlight is not possible.

The irradiation source used in this study was selected as UV is the most effective source of radiation in producing photochemical effects (Häder et al., 2007; Zepp et al., 2007). The UV313 lamps provided both UVB and UVA exposures (2.89 and 4.63 W m-2 respectively) which were an appropriate UVB exposure but a lower proportion of UVA and visible wavelengths than ambient sunlight. Cellulose diacetate filters removed wavelengths <290 nm which are absent in sunlight, but lamp outputs used in the irradiation experiments are not directly comparable to the solar spectrum. Consequently, the magnitude of photo-processing determined in this study allows relative comparison of temporal changes and between our sites but do not provide an accurate value of ambient photo-processing.

Photochemical transformations were low in the Loch Katrine samples, with minimal losses to the DOC pool (0.43%; mean from year-long study). Whilst our sites were not located within the same watershed, it seems likely that position within the catchment plays a role in determining the photolability of DOC. The Black Burn headwater stream at Auchencorth Moss receives fresh inputs of DOC from the surrounding peatland catchment and material has less time for solar irradiation exposure in the water column relative to the DOC in the reservoir

system. DOC losses may occur in Loch Katrine soon after water entry into the loch but, due to long water residence times, DOC may have become recalcitrant to photo-processing by the time of sample collection. Catalán et al. (2016) observed a negative relationship between organic carbon decay and water retention time, resulting in decreased organic carbon reactivity along the continuum of inland waters. $SUVA_{254}$ data suggest that DOC in Loch Katrine samples was less aromatic than in the Black Burn (Table 4.1), with values indicating an approximate humic content of 30% based on the findings of Weishaar et al. (2003). As humic molecules are more labile to photo-processing, irradiation had a greater effect on the stream samples relative to the reservoir samples.

Strong seasonal fluctuations in DOC concentration and composition occurred in the Black Burn, in agreement with patterns observed in the same system by Dinsmore et al. (2013). DOC concentrations were highest in the late autumn, consistent with a flushing effect whereby soil organic material produced over the summer is mobilised and delivered to aquatic environments by more intense rainfall after a prolonged, relatively dry period (Fenner et al., 2005). Positive correlation between the irradiation induced change in the E4:E6 ratio and mean monthly discharge suggest that hydrological conditions in the month prior to sampling significantly influence the reactivity of the sample, with high flow delivering more reactive carbon to the stream. Change in the E4:E6 ratio correlated significantly with several other variables, however spectral dependence of absorption photobleaching depends on the spectral distribution of the irradiation source (Del Vecchio and Blough 2002, Tzortziou et al. 2007). UVB-313 exposure may have produced a distinctly different absorption difference spectrum than ambient irradiance, though there is a lack of literature to test this assertion. Hence, whilst the correlations are significant and can be explained theoretically, they should be interpreted with caution.

Overall the magnitude of photo-induced C losses was significantly positively correlated with DOC concentration in the year-long Black Burn dataset. However, despite low DOC

concentrations, photoreactivity remained elevated in January. This suggests that even when lower DOC concentrations are detected in aquatic systems, the DOC may be intrinsically more photoreactive due to its aromatic content and minimal light exposure history.

Lowest DOC concentrations were observed in the late winter and early spring, due to depletion of soil organic C within the catchment by autumn and winter rainfall events. Low rainfall inputs limit the recharge of fresh, photolabile material to the stream and may account for the reduction in DOC photoreactivity detected in September. Furthermore, due to longer residence time in the water column, these samples may have already been degraded by natural light. A previous study at the Black Burn reported ^{13}C enrichment of stream water DOC in September, consistent with increased in-stream processing at this time of year (Leith et al., 2014). Reductions in intrinsic DOC photolability during summer have similarly been reported in northern lakes (Vachon et al., 2016) and a boreal watershed (Franke et al., 2012). Another minimum in photoreactivity occurred in April, where SUVA254 data indicate decreased contribution of aromatic material to C within the stream. Although algal abundance was not measured during this study, production of DOC from such sources would account for the reduction in photolability (Nyugen et al., 2005).

Absorbance increased during irradiation of Loch Katrine samples in summer. A possible explanation for increased absorbance in the irradiated water samples is the formation of an iron (Fe)-DOC complex, since the reaction kinetics of Fe-DOC complexes are directly affected by light exposure (Maranger and Pullin, 2003). Whilst Fe concentrations were not measured in this study, in a SEPA bimonthly measurement campaign (2009-2013) at Loch Katrine peak Fe concentrations in August of up to 0.50 mg L^{-1} were detected, corresponding to the time of year when we found increased absorbance in irradiated water samples. As the data set does not cover the sampling period, the role of Fe-DOC complexes in producing the observed effect cannot be directly determined; however the role of micronutrients in peatland aquatic C cycling should be further investigated.

Prior filtration of samples to 0.22 µm means that the anomalous absorbance increases are unlikely to be the result of microbial DOC production. However, this cannot be entirely discounted as some bacteria can pass through 0.22 µm filters and lacustrine freshwater bacteria colonies are seasonally variable, which may explain why the effect was only observed in summer (Kent et al., 2004; Fortunato et al., 2012). In order to determine microbial effects in the samples, stable C isotope ($\delta^{13}C$) data could be used as it can distinguish microbial activity from photochemical effects due to preferential fractionation of DOC fractions of different molecular weights for each respective process (Opsahl and Zepp, 2001).

4.4.2 Importance of rainfall events in mobilising photolabile material

Dissolved lignin phenol composition indicates that different sources of plant material were mobilised as a result of rainfall in the Auchencorth Moss catchment. High P:V ratios have been used as an indicator of peatland inputs to aquatic systems, as *Sphagnum* acid typical of peatlands is converted into P phenols during lignin extraction (Fichot et al., 2016; Winterfeld et al., 2015). Typically P phenols constituted the largest contribution to the total lignin concentration of the measured phenols, consistent with *Sphagnum* inputs. However, during the winter rainfall event where stream discharge was considerably higher than the year-long mean value, the largest contribution to total lignin concentration was from S and V phenols (Figure 4.6). The former are reported to be the most photolabile phenol (Opsahl and Benner, 1998) and are unique to woody angiosperms. This suggests that hydrological pathways within the catchment were activate upon rainfall, causing DOC release from soil profiles associated with angiosperm plant material. Potential sources within the Auchencorth upper catchment are *Calluna vulgaris*, *Erica tetralix* and *Vaccinium myrtillus*. Further evidence of the operation of variable source areas in the catchment was the observation of delayed input of water, containing high CO_2 concentrations, from the deep peat area in the upper catchment at Auchencorth Moss during a storm event (Dinsmore and Billett, 2008). Low P:V values and high lignin concentrations have been reported during peak flow in Arctic rivers, and the reverse

during base flow (Amon et al., 2012). As samples with low P:V values were typically more photoreactive (Figure 4.7a), our data indicate that rainfall events are important in mobilising photolabile material from this catchment.

Elevated Ad:$Al_{v,s}$ ratios have previously been interpreted as indicators of decomposition of organic matter resulting from preferential degradation of aldehydes relative to acids (Spencer et al., 2009). In the Black Burn water samples, lowest ratios were measured in the winter rainfall event. This implies that DOC mobilised during rainfall is less degraded relative to base flow DOC, in agreement with previous studies of peatland high flow events which detected increased contribution of near surface flow and younger DOC (Clark et al., 2008). The form of the degradation, either microbial or photochemical, cannot be distinguished using these data. However, based on the higher measured photoreactivity of samples with lower ratios (Figure 4.7b), light exposure history may be one of the key moderators of Ad:$Al_{v,s}$ ratios in the Black Burn. High flow events release fresh DOC from soils derived from recent plant material (Evans et al., 2007) and may have significant implications for C processing rates in streams as they are recharged with labile material (Lapierre et al., 2013).

Whilst the samples collected during the winter rainfall event were clearly distinct in composition relative to samples from the year-long study, the summer rainfall event samples had similar P:V and Ad:$Al_{v,s}$ ratios, but significantly lower photoreactivity and overall lignin yields (Figures 4.5b, 4.6c, 4.7). This could be attributed to the timing of sample collection in early September at the end of summer, where considerable degradation may have already occurred across all phenol groups so that the DOC pool remaining was more recalcitrant to further photo-processing. Discharge data indicate that there was no discernible flushing effect during the summer rainfall event, with slight decreases in DOC concentration attributed to dilution of the stream water by direct rainfall inputs or overland flow. The abundance of P phenols within the samples suggest that passive transfer of DOC from the riparian zone, which is dominated by *Sphagnum* and *Juncus* vegetation, to the stream was the dominant mode of

stream DOC recharge at this time of year (Jeanneau et al., 2015). The summer rainfall event samples were notably depleted in V phenols, suggesting that these phenols exert an important control on sample photoreactivity in addition to S phenols.

4.4.3 Implications for photochemical turnover of DOC in aquatic systems

Our 8-h irradiation experiments found 7% of DOC to be labile to photo-processing, with conversion to CO2 as the main loss pathway. Mass budget calculations for Black Burn water samples show that a mean of ~46% of DOC loss in the irradiation experiments was accounted for by production of CO2. Dinsmore et al. (2010) estimate that 108 ± 62.7 kg DOC yr^{-1} is exported to the Black Burn from the Auchencorth Moss catchment. Given the significant volume of DOC produced by the catchment, in-stream photo-processing may be an important term in carbon budgets of peatland draining aquatic systems and may contribute to the high CO2 efflux reported from these systems (Billett et al., 2015). However, determining the volume of material photo-processed both in the stream and in downstream environments relies upon a range of unquantified factors, including optical depth and mixing processes in downstream aquatic environments which are generally poorly understood in relation to photochemical DOC processing.

Due to the effects of bank shading and short transit time of water within the immediate catchment, light driven instream DOC processing is unlikely to be significant. The river continuum concept suggests that increased DOC processing will occur further downstream, where the channel widens (Vannote et al., 1980), and will be partly controlled by the stream water mean transit time (McGuire and McDonnell, 2006; McDonnell et al., 2010). Based on mean velocity (~0.58 m s^{-1}) of a larger nearby river (Ledger, 1981), we estimate a mean water transit time of ~19 h from the Black Burn at Auchencorth Moss to its coastal outlet 34 km downstream, considerably longer than the exposure time in our experiments. However, in a study of 1st to 4th order streams in Sweden no significant change to DOM composition as stream order increased was detected and this was partly attributed to short transit times (<2

days) restricting DOC processing (Kothawala et al., 2015). Peatland derived C in this study is clearly photoreactive, but limited time for in-stream processing may render photo-processing unimportant in the C budgets of some freshwater systems.

Recent studies have determined hotspots of DOC processing within peatland draining systems, which include mixing zones of freshwaters with different pH, conductivity and metal concentrations (Palmer et al., 2015; Jones et al., 2016). In the context of this study, measuring DOC processing at the confluence of the Black Burn, which largely drains peatland, and the River North Esk, which drains a catchment of mixed land use including natural and plantation forestry, 4 km downstream of the point from which our samples were collected would provide a logical starting point for quantifying in situ DOC turnover.

Determining the C cycling implications of this study is further complicated as the most photoreactive material was recorded during a heavy winter rainfall event. The potential for photochemical transformation of DOC within the freshwater aquatic environment would have been limited due to low light availability, extensive cloud cover and decreased stream water transit times associated with the event. During the year-long study period, 12 rainfall events occurred which resulted in similar flow conditions in the Black Burn (stream discharge exceeding 250 L s^{-1}), with a maximum discharge of 2059 L s^{-1} in a late winter storm. Of these high flow events, 11 occurred during winter and one in summer and hence, whilst large quantities of photoreactive material may have been mobilised during heavy rainfall, the likelihood of in-stream processing would remain small. Increases in precipitation, with more frequent and intense rainfall events, are expected with climate change (Capell et al., 2013; Edenhofer et al., 2014) with heavier summer downpours predicted in the UK (Kendon et al., 2014). Thus, although the contribution of rainfall events to photochemically induced C cycling in this study is likely to be minimal, they could become more significant if heavy rainfall events occur more frequently in summer.

Supplementary information

Table 4.3. Selection parameters for rainfall event samples from the Black Burn used in irradiation experiments. Top row denotes winter rainfall event values and bottom row denotes summer rainfall event values.

	Rainfall event	**a_{254}**	**E4:E6**	**POC mg L^{-1}**
Median	Winter	1.63	6.70	11.0
	Summer	1.36	6.73	5.83
Maximum	Winter	1.98	8.63	63.5
	Summer	1.47	11.0	10.6
Minimum	Winter	1.34	3.57	4.10
	Summer	1.30	4.62	3.88

Table 4.4. Carbon budget calculations for individual C species and total C balance in samples collected in May 2014 at the Black Burn and Loch Katrine. CH_4 concentrations are not included in budget calculations as they were < 0.05% of the total budget. Differences are expressed as % of non-irradiated samples. Values are means of 4 replicates. LOD = limit of detection

	DOC mg L^{-1}	DIC mg L^{-1}	CO_2 mg L^{-1}	CO mg L^{-1}	**$\sum$ C mg L^{-1}**
Black Burn					
Irradiated	48.9	1.18	2.82	0.13	**53.0**
Non irradiated	50.9	1.38	1.20	<LOD	**53.5**
Difference	-3.9%	-14%	135%	---	**-0.8%**
Loch Katrine					
Irradiated	5.30	1.42	0.82	0.02	**7.56**
Non irradiated	5.05	1.55	0.80	<LOD	**7.40**
Difference	5.0%	-8.4%	2.5%	---	**2.2%**

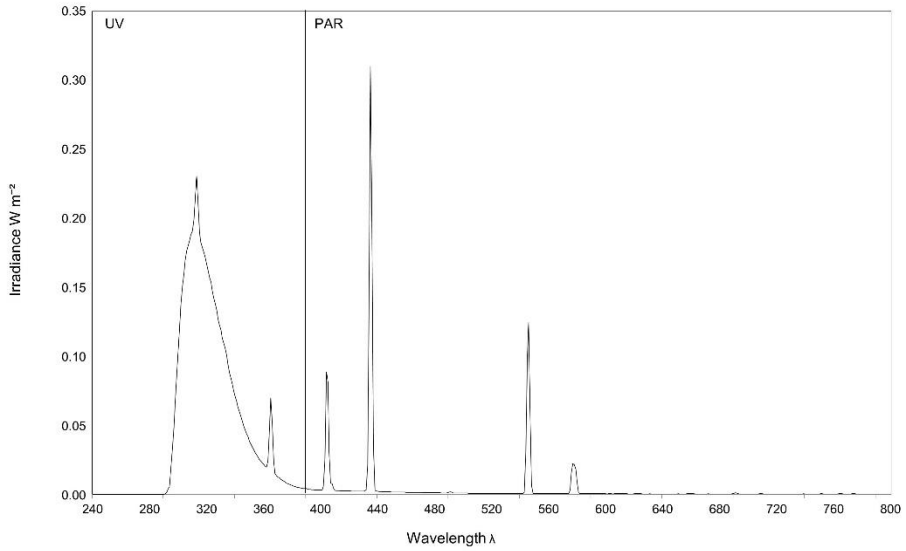

Figure 4.8. Spectral output (240-800 nm) of UV-B 313 lamps employed in irradiation experiments in this study.

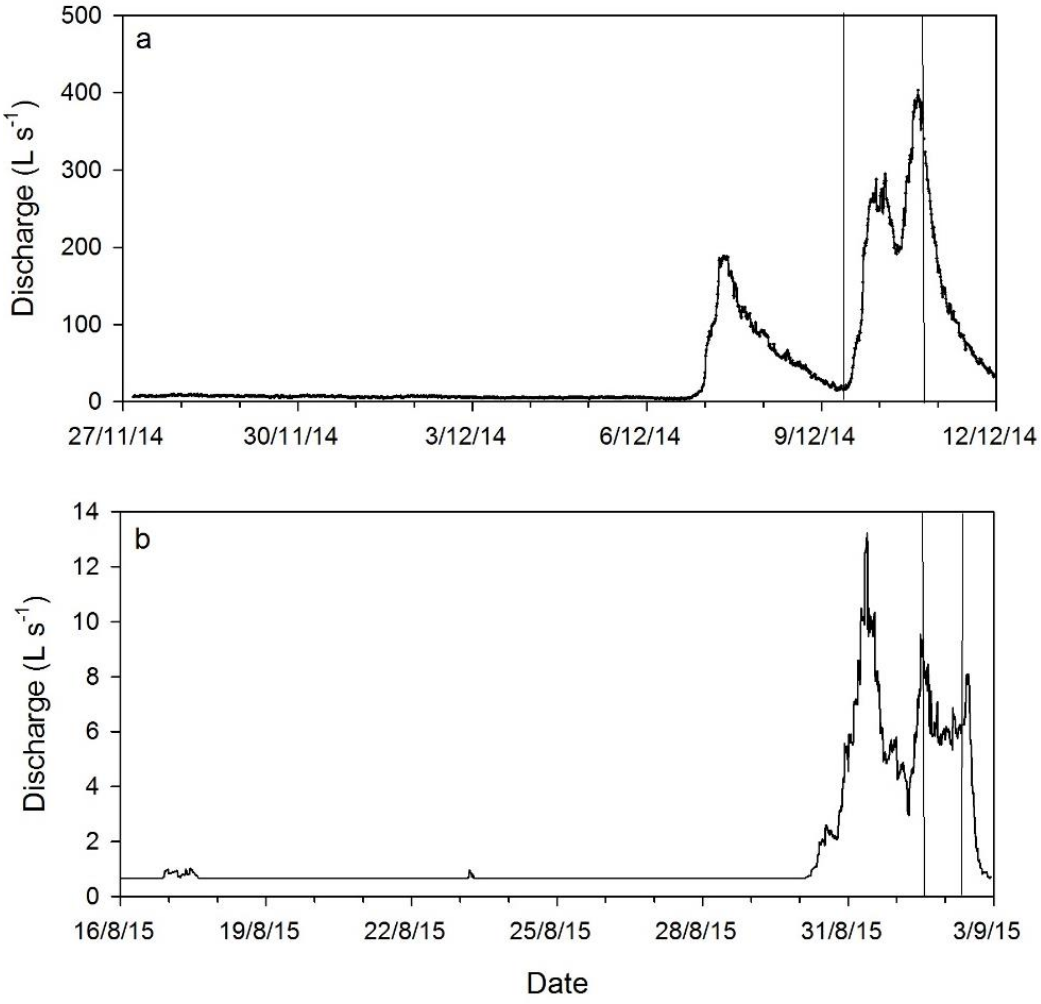

Figure 4.9. Black Burn discharge during and 2 weeks before a) winter and b) summer rainfall events. The events are demarcated by two vertical lines on each of the plots.

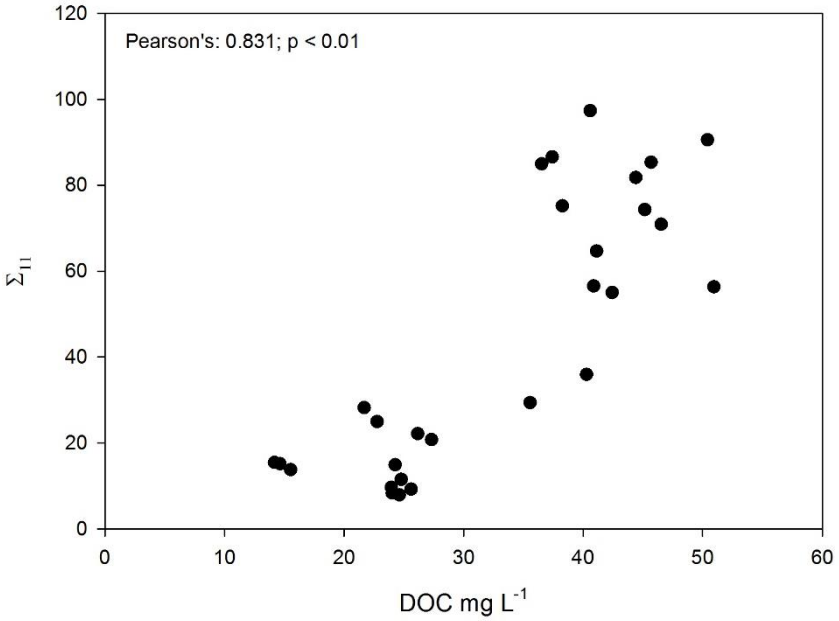

Figure 4.10. Pearson correlation between total concentration of lignin phenols Σ_{11} (µg L^{-1}) and DOC concentration in all Black Burn water samples (n=28), including monthly and rainfall event samples.

Chapter 5 Photochemical and Microbial Processing of Aquatic Carbon in Peatland Pools

Amy E Pickard, Kate V Heal, Andrew R McLeod, Kerry J Dinsmore and Andrew W Stott

Paper in review stage at *Journal of Geophysical Research: Biogeosciences.* The chapter appears as submitted to the journal, including supplementary information which is shown at the end of the chapter.

The candidate, as lead author, conducted field experiments and undertook laboratory analyses. Andrew Stott provided assistance with isotopic analyses. Data analysis and writing of the paper were also carried out by candidate. Other co-authors provided guidance on the scope and design of the project, and contributed to the editing of the manuscript.

Other Acknowledgments: Permission to use Red Moss of Balerno and Cross Lochs, Forsinard as study sites was obtained from the Scottish Wildlife Trust and the Royal Society for the Protection of Birds, respectively. Field work assistance was provided by Andrew Addison and Laura Parker. Stable isotope analyses were made possible by a grant-in-kind from the NERC Stable Isotope Facility.

Abstract

Open water pool systems are widespread in Northern peatlands despite often being neglected in catchment scale carbon (C) budgets. Whilst pool systems are a known net source of C to the atmosphere, the contribution of photochemical and microbial processes to C cycling in peatland pools is poorly constrained. In this study, in-situ experiments with water samples in light and dark conditions were conducted at two peatland pools in Scotland with contrasting dissolved organic carbon (DOC) concentrations. At the high DOC site, DOC concentrations in surface light exposed samples decreased by 18% compared to dark controls over 9 days. Photochemical processing was evident in δ^{13}C-DOC and δ^{13}C-DIC signatures of light exposed samples, which were enriched and depleted, respectively, relative to dark controls (+0.23 ‰ and -0.38 ‰) after 9 days of surface exposure. At the low DOC site net production of DOC occurred in both light and dark samples over the experiment duration, in part due to POC breakdown. δ^{13}C-DIC signatures indicated photolysis had occurred in light exposed samples (-1.98 ‰), whilst δ^{13}C-DOC data suggest an absence of photo-processing, as the signatures in both treatments were similar. Accounting for light attenuation through the water column, 46 ± 5.0 and 8.8 ± 0.5 g C-CO_2 eq m^{-2} yr^{-1} was processed by photochemical and microbial activity in peatland pools within the catchments at the high and low DOC sites, respectively. At both sites, light driven processing was responsible for a considerable percentage (33 and 51%) of gaseous C production and should be considered a key driver of peatland pool biogeochemical cycles.

5.1 Introduction

Peatlands are recognised as significant for global carbon (C) cycling as they store disproportionally large amounts of soil C compared to other ecosystems, at a rate of up to 70.6 g C m^{-2} yr^{-1} (Dinsmore et al., 2010; Yu et al. 2013). Aquatic systems in peatlands are subject to high loading of dissolved and particulate forms of C from the surrounding terrestrial environment. Recent research in peatlands has been concerned with understanding the rate of turnover of C in aquatic systems and quantifying the extent to which biogeochemical processes in these systems are a source of C to the atmosphere (Worrall and Moody, 2014; Billett et al., 2015). This is becoming an increasingly important question, particularly in relation to climate change where both concentrations of aquatic C and potential for its microbial and photochemical transformation are increasing (Clark et al., 2010). The limited number of studies mean that it is difficult to evaluate whether aquatic losses of C from peatlands significantly undermine their capacity to sequester C and the potential for photochemical transformation of C in aquatic systems remains poorly understood.

Open water pool systems are common features of peatlands which act as a net source of C to the atmosphere in the order of 23–419 g C m^{-2} yr^{-1} (Hamilton, et al., 1994; Repo et al., 2007; McEnroe et al., 2009; Pelletier et al., 2014). Inputs from the surrounding peatland of dissolved and particulate forms of C are processed in-situ in pools via microbial and photochemical pathways, resulting in gaseous release (*Turner et al., 2016*). However, to our knowledge, no studies have directly measured rates of light driven C turnover in peatland pools. The residence time of water in pools, although poorly constrained, is thought to be much longer than in streams draining peatlands (*Carrer et al., 2015*), and thus there is more time over which internal processing of C can occur. Constraining the drivers of C dynamics over varying time scales in pools is fundamental to understanding the role they play in peatland C cycling.

Evidence from previous studies suggests that photochemical processing could contribute to C loss from peatland pools (Cory et al., 2014; Koehler et al., 2014). Pelletier et al. (2014)

reported a significant positive relationship between the amplitude of the diurnal pattern in dissolved CO_2 concentration at the surface and cumulative daily photosynthetic active radiation (PAR) in one of their study pools. However, determining the contribution of photodegradation processes to overall C cycling in pools is difficult as it has largely the same effect as microbial processing on both dissolved organic carbon (DOC) and dissolved CO_2 concentrations, decreasing the former and increasing the latter.

Peatland pool systems have been identified as significant sources of CH_4 (McEnroe et al., 2009; Pelletier et al., 2014). Breakdown of aromatic compounds can result in the formation of compounds which are labile to microbial processing (Moran and Zepp, 1997) and therefore light exposure may indirectly increase microbially induced CH_4 production. The effects of photolysis on CO concentrations are well established and it has been identified as the second most abundant carbon-containing photoproduct, after CO_2 (Hong et al., 2014; Stubbins et al., 2011). By quantifying photo-induced changes to the full range of dissolved and gaseous C species, the contribution of photochemical processing to C loss from peatland pools may be better understood. Stable carbon isotope analysis of DOC and dissolved inorganic carbon (DIC) have been used to determine the biogeochemical processes that dictate DOC composition (Opsahl and Zepp, 2001; Spencer et al., 2009; Waldron et al., 2007). Previous studies using DOC rich water samples have shown that photo-processing enriches the δ^{13}C-DOC signature, due to the preferential photo-induced loss of aromatic molecules such as lignin phenols (Spencer et al., 2009). Microbial degradation is associated with the removal of ^{13}C enriched molecules such as carbohydrates and thus has the opposite effect on the residual δ^{13}C-DOC signature (Opsahl and Zepp, 2001). As photodegradation leads to enhanced DIC production, evidence of light driven processing is also reflected in the δ^{13}C-DIC signature, which becomes isotopically "light" (Zepp et al., 2003). Measurement of changes to the isotopes of C species over time allows the contribution of photochemical processes to C cycling in peatland pools to be better understood.

The primary aim of our study was to determine the role of photochemical processing in C cycling at two peatland pools with contrasting DOC concentrations. Our secondary aim was to understand how important photochemical processing is in relation to microbial processing on a catchment C budget basis.

We characterised changes to C species DOC, DIC, CO_2, CO and CH_4 and isotopic carbon species δ^{13}C-DOC and δ^{13}C-DIC in light and dark treatments in order to address our first aim. Additional depth attenuation experiments were conducted using light and dark treatments in order to derive site specific water column attenuation coefficients. These data were used in upscaling calculations in order to address our second aim. Accounting for light attenuation through the water column is critical when scaling to the aquatic system as a whole, as the effects of photolysis are limited to near surface water, particularly in humic systems with high organic carbon concentrations.

5.2 Site Descriptions

Experiments were conducted at two peatland pool sites in Scotland (Figure 5.1). Characteristics of the individual pools studied at each site are given in Table 5.1.

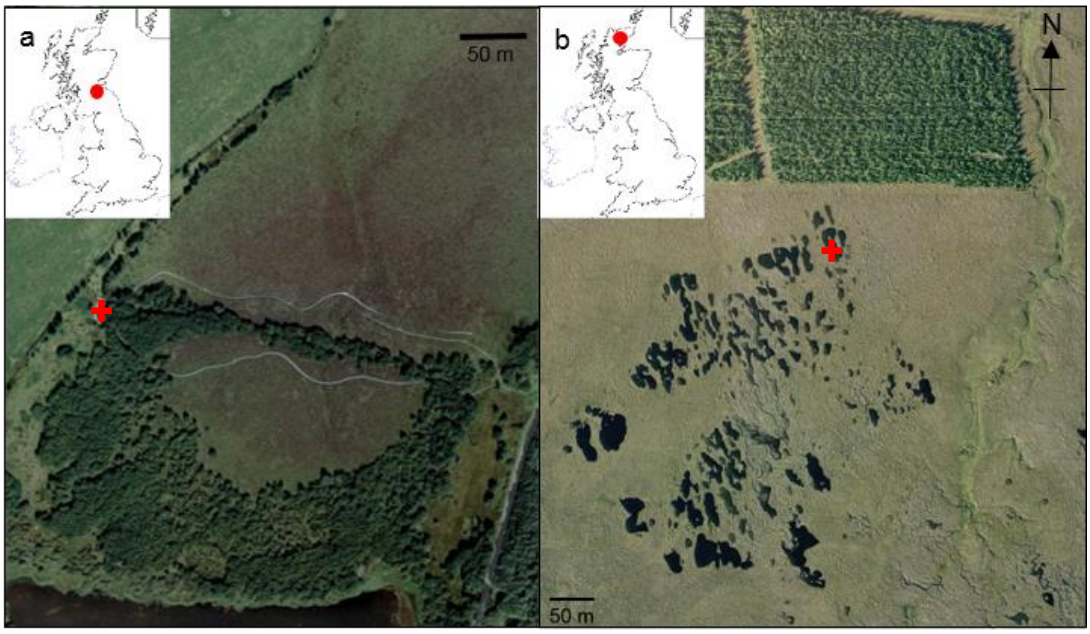

Figure 5.1 Satellite images of field sites **a)** Red Moss and **b)** Cross Lochs, with location shown

in relation to the United Kingdom. The red cross indicates the exact location of the pool. Source: Google Earth™

Red Moss of Balerno (Figure 1a; 55°51′N 3°20′W) is a raised peat bog (~0.16 km^2), located 15 km southwest of Edinburgh with well-defined hummock-hollow micro topography (Hardacre and Heal, 2013). The site is undergoing restoration primarily in the form of drainage ditch blocking and is managed to prevent tree regeneration in order to maintain the ecosystem as a raised peat bog (Hardacre and Heal, 2013). The open water pool that was the focus of this study drains the surrounding peat and has a high coverage of aquatic vegetation (~40% surface area), dominated by *Equisetum spp.*

Cross Lochs South (Figure 1b ; 58°37′N 3°95′W) is a ~1 km^2 peatland catchment located 2 km west of Forsinard in northeast Scotland. It is part of the internationally-important Flow Country patterned blanket bog system, the UK's largest store of terrestrial C and its largest single tract of peatland (~4000 km^2) (Turner et al., 2016). The catchment is comprised of an extensive pristine bog-pool system that drains west to the River Dyke. The site used in this study was a mainly unvegetated open water pool located in the north east of the catchment.

Biogeochemical characteristics of both sites were investigated in laboratory experiments prior to the field study (Table 5.1.) (Appendix A).

Table 5.1 Physical and chemical Characteristics of study catchments and experiment pools

Site name	Catchment area ha	Percentage coverage of open pools	Experiment pool surface area m^2 [a]	Experiment pool mean water depth m [b]	Site elevation (m a.s.l)	DOC mg L^{-1}
Red Moss	157	0.09%	81.4	0.91	240	25.1[c]
Cross Lochs	1000	2.38%	412	0.73	210	13.6[d]

[a] Determined from on-site measurements at Red Moss and from data from Turner (Pers. Comm., 2015) for Cross Lochs

[b] Derived from on-site measurements where a meter rule was inserted into the pool at 10 random points located <1 m from the pool perimeter

[c] Determined from mean concentration measured on two site visits in March and April 2015 prior to experiment

[d] Mean concentration of DOC in 6 study pools in Cross Lochs catchment (Turner et al., 2016)

5.3 Methods

5.3.1 Surface exposure experiment

To quantify the contribution of photochemical processing of C to the overall C budget, experiments of different designs and duration were set up in the two peatland pools. Two treatments were applied in the experiments using unfiltered water samples inside new 1 L bags of 25-µm UV-transparent polyvinylfluoride (Tedlar™) normally used for gas sampling (SKC Inc., Eighty Four, USA). One treatment exposed bags to ambient light conditions and the other used bags covered in foil to act as dark controls. These treatments distinguish between the combined effect of photochemical and microbial activity in the pool systems (light exposed bags) and the effect of microbial activity only (dark bags). Experiments were conducted at Red Moss from 7 to 15 June 2015 and at Cross Lochs from 21 to 29 June 2015. The experiments took place at the time of year when maximum irradiation could be expected to produce maximum photo-induced C cycling effects and were conducted within the same month to compare results.

A bamboo cane structure was placed in the pool sediment the day before experiments commenced, to ensure that any disturbance related ebullition fluxes did not affect results. The structure held the gas bags in position at the water surface, with approximately 75% of the bag submerged beneath the water. At 08:00 British Summer Time (BST) on day 1 of the experiment the gas bags were half filled with 500 mL unfiltered water collected immediately beforehand from approximately 10 cm below the pool water surface using 60 mL polyethylene syringes. A total of 24 bags were placed at the pool surface, half exposed to ambient light conditions and the other half covered in aluminium foil. At this time, a 1 L sample of pool water was collected to determine baseline characteristics for comparison with water samples contained in light and dark bags over the experiment duration. 50 mL of ambient air was added to the headspace of each bag on at 16:00 days 1, 2, 3, 5 and 7 to ensure conditions remained oxic.

Two bags of each treatment were removed at 16:00 on days 1, 2, 3, 5, 7 and 9 of the experiment, so as to capture the expected initially rapid decrease in photo-reactive C (Worrall and Moody, 2014). Replication was limited to two replicates by practical constraints of the number of bags that could be placed at the pool surface. Upon removal from the pool, excess headspace gas was emptied and a 10 mL water sample was taken from each bag for δ^{13}C-DIC analysis. Gas bags were then filled with 490 mL of O_2-free N_2 and shaken to equilibrate the water sample with the gas headspace, using a water to headspace ratio of 1:1. Gas samples from the headspace were analyzed for CH_4, CO_2 and CO concentration using a Hewlett Packard 6890 series gas chromatography (GC) system equipped with a flame ionisation detector (Agilent Technologies Ltd, USA). The remaining water in the gas bag was filtered using 0.7 μm Whatman GF/F filters (GE Healthcare, UK) on an acid-washed vacuum filtration system and analysed for DOC and DIC using a PPM LABTOC Analyser (Pollution & Process Monitoring Ltd, UK), with a limit of detection equivalent to 1% of the calibration standard concentration (50 mg C L^{-1}). DIC was calculated as the difference between total carbon (TC) and DOC.

UV-visible absorbance of water samples from the light exposed and dark bags was measured between 200 and 700 nm at increments of 1 nm at room temperature using a Jenway spectrophotometer (Model 7315; Bibby Scientific Ltd, UK). Deionized water blanks were used between each sample. Specific UV absorbance ($SUVA_{254}$) values, a measure of DOC aromaticity, were determined by dividing the UV absorbance measured at $\lambda = 254$ nm by the DOC concentration (Weishaar et al., 2003). The E2:E3 and E4:E6 ratios were estimated using the absorbance values at 254 nm and 375 nm, and 465 and 665 nm, respectively (Peacock et al. 2014). The remaining water contained in the gas bag (~450 mL) was used to produce lyophilized DOM samples for δ^{13}C-DOC analysis, as described below.

During the experiment, dissolved oxygen (DO), conductivity, pH and water temperature were measured in the surface water of the pool every day at 9:00 and 15:00 with a handheld Hach

HQd multimeter (Hach, USA). Sunlight irradiance from 280 – 800 nm was measured at the water surface at 11:00, 12:00 and 13:00 using a double monochromator scanning spectroradiometer (Model SR9910-V7; Irradian, UK).

Continuous measurements of mean air temperature, rainfall and PAR were taken at 30 minute intervals at the weather station at the Auchencorth Moss European Monitoring and Evaluation Programme (EMEP) flux tower, 9.68 km from Red Moss of Balerno and at a similar elevation (270 m a.s.l). The same parameters were measured at a flux tower at Cross Lochs South site, 0.92 km from the experimental pool.

After experimental exposure, water samples were prepared for δ^{13}C-DOC analysis using the method described in Hood et al. (2009). Briefly, 450 mL of sample from each gas bag was filtered through pre-ashed 0.7 μm GF/F filters and transferred to acid-washed 500 mL polypropylene bottles. Samples were then frozen at -80°C and transferred to a freeze dryer maintained at -50°C until all that remained of the sample was the lyophilized DOM. The lyophilized DOM was stored in a desiccator prior to isotopic analysis.

After drying at 105ºC for 1 hour and cooling in a desiccator the $^{13}C/^{12}C$ ratio of lyophilized samples was measured at the Natural Environment Research Council (NERC) Life Sciences Mass Spectrometry Facility located at CEH, Lancaster, UK. For $^{13}C/^{12}C$, 0.5–2.5 mg of each sample (amount depending on the concentration of carbon in the individual sample) was weighed using a high precision microbalance and then sealed into a 6 x 4 mm tin capsule. Samples were then combusted in an automated Eurovector elemental analyzer coupled to an Isotope Ratio Mass-Spectrometer (IRMS, Isoprime Ltd, UK). An in-house working standard of vegetation (flour) was analysed after every twelfth sample resulting in an analytical precision of 0.11‰. Resultant CO_2 from combustion was analysed for δ^{13}C using an Isoprime Ltd IRMS.

Samples for δ^{13}C-DIC analysis were prepared using the headspace method of Waldron et al. (2007). 10 mL of water sample from a gas bag was injected into a 12 mL acid-washed pre-evacuated exetainer containing 100 µL of phosphoric acid. Drawing in of the syringe barrel during sample transfer was used as a quality control measure to indicate the exetainers had retained vacuum with minimal contamination from atmospheric CO_2. The shaken exetainer was then stored upside-down with the liquid in contact with the septa, thus minimizing headspace CO_2 ingression or egression, and transported in this manner to the laboratory to await isotopic analysis. δ^{13}C-DIC values of were measured using an Isoprime Ltd Tracegas Preconcentrator coupled to an Isoprime Ltd isotope ratio mass spectrometer. Between 100 and 400µls of headspace was introduced into the injection port of the Preconcentrator, whereupon water is removed by a magnesium perchlorate chemical trap and the CO_2 cryogenically focussed before entering the IRMS via an open split. The isotope ratio of the resultant CO_2 is compared to pulses of known reference CO_2. The instrument was calibrated on each day of analysis. Blanks were run prior to each analytical batch, in addition to a quality control reference CO_2 standard and duplicate analysis after every 15th sample. Precision was better than or equal to ± 0.1‰.

5.3.2 Depth attenuation experiments

Depth experiments were conducted to aid upscaling attempts of the importance of C photo-processing on an ecosystem scale. Daily exposure experiments testing the effect of light attenuation with depth on C processing were conducted in the study pools at Red Moss and at Cross Lochs at the same time as the experiments described above. At 08:00 BST on days 1, 2, 3, 5, 7 and 9, 500 mL water samples were collected from approximately 10 cm below the pool water surface using 60 mL plastic syringes and decanted into Tedlar gas bags, with a 50 mL ambient air headspace. Six bags were placed at the pool surface, where half of the bags transmitted sunlight and the other half were covered in aluminium foil, acting as dark controls. Further sets of six bags were placed at 10 cm and at 20 cm below the water (Figure 2.9). The

bags were removed at 16:00 on the same day after an 8-hour exposure. The range of depths were selected based on the widely held view that photochemical breakdown of C is limited to the top 10 cm of the water column (*Vähätalo et al., 2000*). The same methods as described above for the surface exposure study were used to provide samples for CH_4, CO_2 and CO analysis by GC, DOC and DIC analysis and UV visible absorbance analysis.

5.3.3 Data analysis

In order to generate a measure of variability with two replicates of each sample, the difference between light and dark samples was calculated by subtracting the individual light exposed samples from the mean of the dark controls. $\delta^{13}C$ data are all reported relative to the Vienna Pee Dee Belemnite standard. Data from the surface exposure experiment were analyzed using Pearson's correlation coefficients to improve understanding of causes of changes to C and $\delta^{13}C$ over the duration of the experiment. Unpaired 2-sample Student's t-tests were conducted between dark and light exposed samples to ascertain differences in spectral properties, and DOC, DIC and POC concentrations.

Data collected in the depth attenuation experiment were tested for normality using the Shapiro-Wilks test and were found to be normally distributed. A two-way analysis of variance (ANOVA) was used to assess the significance of two factors (position in water column and light or dark treatment) and their interaction. Significant differences were identified where $p<0.05$. All statistical analysis was conducted using the Minitab statistical package (version 16, Minitab Ltd., UK).

5.4. Results

5.4.1 Light and temperature conditions

Air temperature and PAR measured at the sites during the experiments are shown in Figure 5.7 (Supplementary Information). Mean air temperature for Red Moss, recorded at the Auchencorth EMEP site, was 11.4°C across the experiment duration, reaching a maximum of

24.8°C on 11 June. Mean PAR exposure was 414 μmol m^{-2} s^{-1} peaking at 1770 μmol m^{-2} s^{-1}. At Cross Lochs, mean air temperature was also 11.4°C during the experiment, although temperatures varied less over time than at Red Moss, and had smaller diurnal variation. Mean PAR exposure was significantly lower at Cross Lochs, averaging 235 μmol m^{-2} s^{-1} over the experiment duration.

5.4.2 Changes to aquatic carbon over the surface exposure experiment

DOC concentrations measured at the start of the degradation experiment at Red Moss were one order of magnitude higher than at Cross Lochs. At Red Moss, DOC concentrations were significantly different in the light exposed and control water samples at the end of the experiment ($p < 0.05$). Light exposure resulted in the depletion of DOC at Red Moss from 34.6 ± 0.13 to 30.2 ± 2.31 mg L^{-1} by day 9. An increase of 2.51 mg L^{-1} was detected in the DOC concentrations of the dark control samples over the same period, suggesting in-situ production of DOC during the experiment. At Cross Lochs, DOC concentrations in both the light exposed and control water samples increased over time and light treatment did not result in significant differences from the dark treatment bags (Table 5.2).

Table 5.2. Optical and chemical properties of both light exposed and control (dark) water samples at the end (day 9) of the degradation experiment, and changes relative to the baseline pool water sampled at 08:00 on day 1. Values are means and standard deviation of 2 replicates, unless otherwise stated.

Sample	DOC (mg L^{-1})	$SUVA_{254}$[a]	a350 m^{-1} [b]	a350 (m^{-1} mg DOC^{-1})[c]	E4:E6[d]	DIC (mg L^{-1})	POC (mg L^{-1})
Red Moss							
Baseline (Day 1)	34.6 (± 0.13)	5.42 (± 0.02)	146 (± 1.47)	4.22 (± 0.03)	5.67 (± 0.36)	0.82 (± 0.04)	5.61 (± 0.31)
Day 9 Control	37.1 (± 0.60)	4.82 (± 0.07)	139 (± 0.16)	3.75 (± 0.06)	5.44 (± 0.05)	0.59 (± 0.06)	4.46 (± 0.11)
% change	7.22%	-11.0%	-4.61%	-11.2%	-4.06%	-28.0%	-20.5%
Day 9 Exposed	30.2 (± 2.31)	4.70 (± 0.36)	106 (± 22.1)	3.51 (± 0.36)	3.89 (± 0.23)	2.02 (± 0.29)	3.78 (± 0.28)
% change	-12.7%	-13.3%	-27.4%	-16.8%	-31.4%	147%	-32.7%
Cross Lochs							
Baseline (Day 1)	8.41 (± 0.03)	2.76 (± 0.01)	15.6 (± 1.30)	1.85 (± 0.05)	4.10 (± 2.12)	0.96 (± 0.44)	4.53[e]
Day 9 Control	10.4 (± 0.13)	2.36 (± 0.06)	15.9 (± 0.01)	1.52 (± 0.01)	4.83 (± 1.37)	0.77 (± 0.77)	3.14 (± 0.42)
% change	23.7%	-14.5%	1.9%	-17.8%	17.8%	-19.8%	-30.7%
Day 9 Exposed	9.77 (± 0.11)	2.04 (± 0.13)	10.9 (± 0.81)	1.12 (± 0.07)	4.65 (± 1.38)	2.26 (± 0.85)	3.79[e]
% change	16.1%	-26.0%	-30.1%	-39.5%	13.4%	136%	-16.4%

[a]$SUVA_{254}$, the ratio of A_{254} to DOC concentration.

[b]a350, absorption coefficient where a350 = (2.303*A_{350})/0.01 (A_{350} is absorbance at 350 nm and 0.01 is the cuvette path length in m).

[c]a350, absorption coefficient where sa350 = a350/DOC mg L^{-1}

[d]the ratio of absorbance at two wavelengths: 465 nm (E4) and 665 nm (E6)

[e]n=1 as replicate data not available

The mean DOC concentration of light exposed samples at Red Moss declined steeply initially, with 83% of total photo-induced DOC degradation occurring by day 3 (Figure 5.2). By day 9 of the experiment, DOC concentration in the dark (control) samples was 37.1 ± 0.60 mg C L^{-1} compared to 30.2 ± 2.31 mg C L^{-1} in the light exposed samples, representing a percentage difference of 19%. At Cross Lochs, percentage DOC loss at day 9 was lower, at 6% relative to the dark samples.

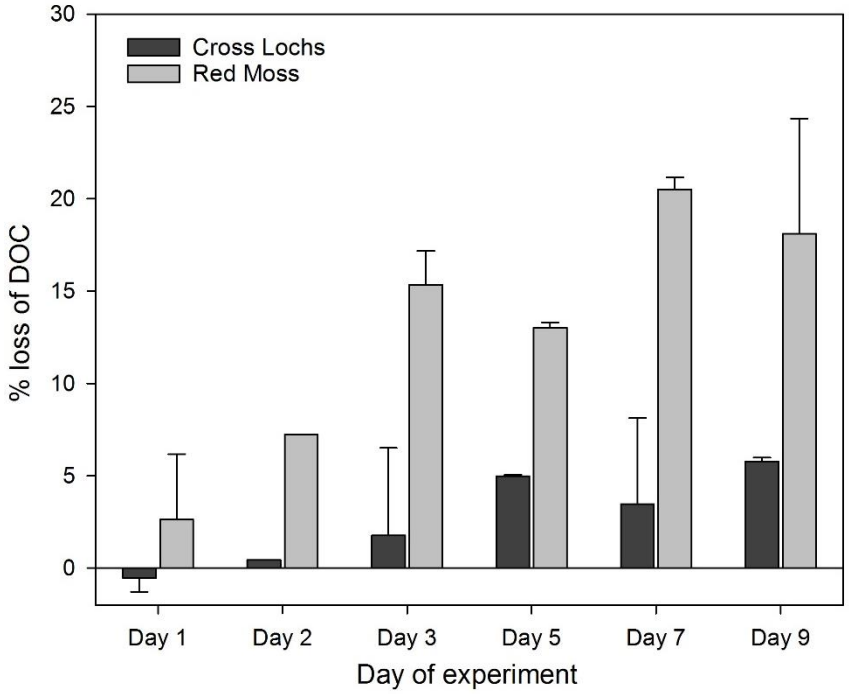

Figure 5.2. Mean percentage difference between DOC concentrations of light exposed and dark control samples for Cross Lochs and Red Moss over the experiment duration. Error bars represent the standard error of the mean (n=2).

Exposure induced changes to absorption properties of the samples also occurred during the experiments. $SUVA_{254}$ values differed between the sites, with higher values at Red Moss indicating that DOC was more humified at this site (Table 5.2). SUVA values in both light exposed and control water samples decreased over the experiment duration, with percentage losses relative to the baseline greatest at Cross Lochs. Absorption coefficients at 350 nm were reduced by 27% and 30% in light exposed samples at Red Moss and Cross Lochs, respectively. When normalized to DOC concentration, absorption coefficients at 350 nm (a350) decreased

by 17% at Red Moss during the experiment, indicating a depletion of chromophoric forms of dissolved organic matter (CDOM) in the remaining pool (Opsahl and Zepp, 2001). At Cross Lochs, a350 decreased by 40%, indicating a higher degree of CDOM removal from the light exposed samples. E4:E6 ratios, indicating the humicity of samples, decreased at Red Moss in the light exposed samples but increased in Cross Lochs samples during the experiments (Table 5.2).

Exposure to light resulted in DIC production in samples at Red Moss and Cross Lochs (Table 2), although concentrations measured at both sites were low across all treatments. DIC concentrations in dark control samples decreased over the experiment, although the decreases detected were small. POC concentrations decreased at all sites, across all treatments, with greatest percentage losses detected in light exposed samples at Red Moss.

Irradiation induced changes to DOC, absorbance at 254 nm and 350 nm were described by an exponential decay model (Table 5.3). Using the method of Spencer et al., (2009), we applied a single, three-parameter exponential decay model to our data: ($C(t) = C_{\infty} + z_0 e^{-kt}$). Here, C(t) represents the modelled value (t); C_{∞} represents the non-photoreactive component remaining at the experiment end; z_0 represents the photoreactive component at time = 0; k is the rate of decay, t is the time in days and e is the base of the natural logarithm. Model data show that rates of decay (k) were higher for optical parameters than for DOC at both study sites. The highest detected decay rate, 0.046 d^{-1}, was observed for a350 m^{-1} at Cross Lochs.

Table 5.3 Exponential decay model with rate of decay k for DOC, a254 and a350 for the 9 day exposure experiments shown for both sites.

	Red Moss			**Cross Lochs**		
	DOC	a254	a350	DOC	a254	a350
C_∞	30.2	329	106	9.77	46.7	10.9
z_0	34.6	426	146	8.46	54.8	15.6
k (d^{-1})	0.015	0.032	0.037	-0.019	0.017	0.046
R^2	0.87	0.88	0.84	0.87	0.60	0.89

5.4.3 Dissolved gas production

During the experiment CO_2-C in water samples ranged from 0.56 to 0.89 mg L^{-1} at Cross Lochs and from 2.04 to 4.28 mg L^{-1} at Red Moss. CO_2-C accumulated over time relative to the baseline at Red Moss by 1.37 mg L^{-1} and 1.03 mg L^{-1} at day 9 in light and dark control treatments, respectively. Increases of 0.31 mg L^{-1} and 0.19 mg L^{-1} were also observed at Cross Lochs in the light and dark treatments, respectively. Higher CO_2-C concentrations were detected in light exposed samples relative to the control samples throughout the experiments at both sites, with one exception on day 2 of the experiment at Cross Lochs (Figure 5.3).

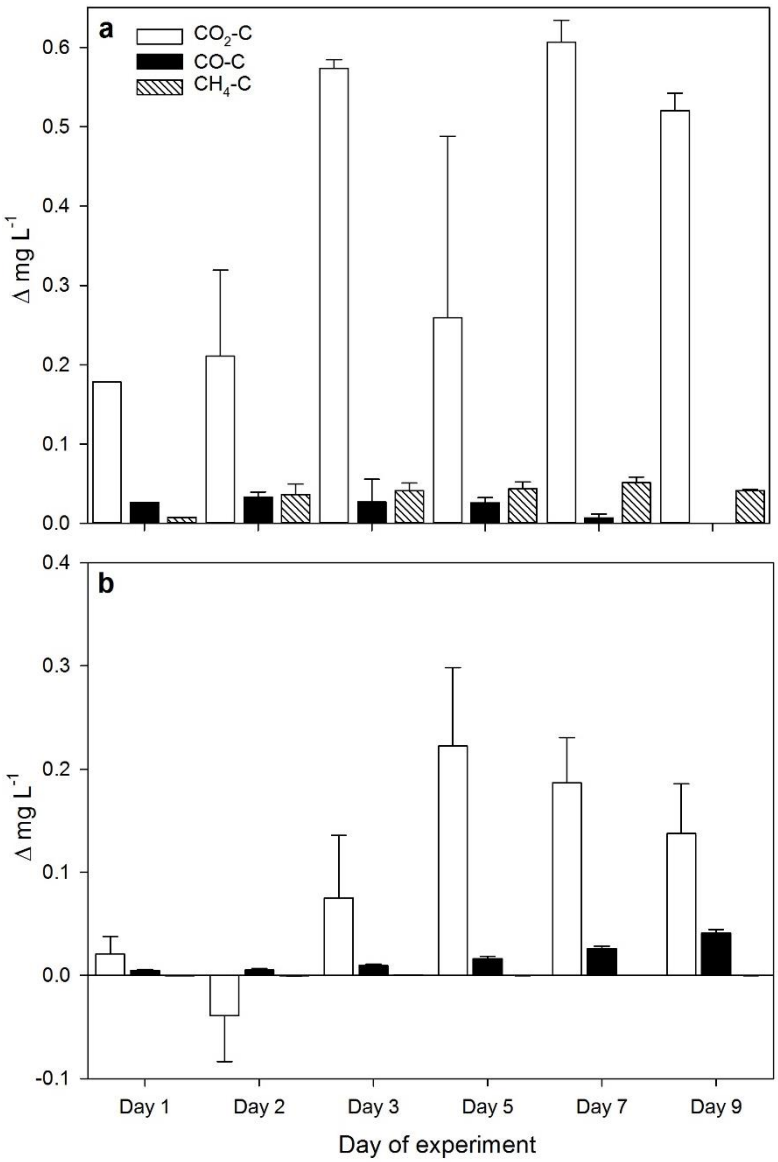

Figure 5.3. Mean difference between CO_2, CO and CH_4 concentrations of light exposed and dark control samples for a) Red Moss and b) Cross Lochs over the experiment duration. CH_4 concentrations at Cross Lochs are too small to be visible in Figure 4b. Error bars represent the standard deviation of the mean (n=2). Note different y-axis scales.

Dissolved CO and CH_4 in both pools also varied temporally over the study period. Concentrations of CO decreased over time at Red Moss by 28.2 and 1.31 μg L^{-1} in the light exposed and control samples, respectively. CH_4 concentrations also declined over time, however the overall decrease was much greater in the dark control samples (66.0 μg L^{-1}) than in the light exposed samples (32.6 μg L^{-1}). Dissolved CO increased over time at Cross Lochs

in the light exposed samples, with a maximum dissolved concentration of 43.8 μg L^{-1} recorded on the final day. CH_4 concentrations increased over the experiment duration in both the light exposed and control samples by 1.02 and 0.97 μg L^{-1}, respectively. There were no clear differences in CH_4 concentrations between the treatment types at Cross Lochs and, for four out of six samples, concentrations in the dark control samples were higher than comparative light exposed samples.

The difference in CO_2-C between light and dark samples was negatively correlated with treatment induced changes to DOC concentrations at both sites (Table 5.4), suggesting that pool water DOC processing is the main source of CO_2 over the experiment duration. ΔCO-C was also significantly negatively correlated with ΔDOC at Cross Lochs, whereas at Red Moss this correlation was positive. A significant negative correlation between ΔCH_4-C and ΔDOC indicates that light exposure enhanced CH_4 production in the water column at Red Moss.

Table 5.4. Pearson correlation coefficients between mean changes in gaseous C species over 9 days between light exposed and dark samples and changes in aqueous C and key environmental variables during the experiment (n=6 at each site). The first row denotes coefficients for Red Moss and the second row for Cross Lochs.

	ΔCO_2-C	**ΔCO-C**	**ΔCH_4-C**
ΔDOC	-0.924** -0.833*	0.744 -0.872*	-0.855* -0.117
Δa350	-0.503 -0.790	0.704 -0.887*	-0.657 -0.386
ΔE4:E6	-0.651 0.456	0.642 0.299	-0.728 -0.141
ΔDIC	0.836* 0.918*	0.620 0.779	0.701 0.294
PAR[a]	0.616 0.670	-0.863* 0.991**	0.714 0.064
Temperature[b]	0.442 0.251	-0.580 0.873*	0.724 -0.263

*$p < 0.05$

**p < 0.01
[a]Cumulative PAR W m^2 over experiment duration
[b]Mean air temperature

At Red Moss, ΔCO_2 and ΔCH_4 were negatively correlated with changes to the humicity of the pool water as indicated by E4:E6 ratios. ΔCO_2 was positively correlated with ΔDIC at both sites, suggesting that they were produced synchronously by photolysis. ΔCO_2 and ΔCH_4 were positively correlated with PAR and air temperature at Red Moss. However, the direction of the correlation for ΔCO was negative when measured against the same environmental variables. At Cross Lochs, ΔCO was significantly positively correlated to PAR and air temperature.

5.4.4 Isotopic composition of dissolved carbon species

Mean carbon isotopic composition of DOC (δ^{13}C-DOC) in the water samples during the experiment ranged from -29.4 to -28.7 ‰ at Red Moss and -26.1 to -25.4 ‰ at Cross Lochs (Table 5.6; Supplementary Information). At Red Moss the isotopic signature shifted towards an enriched DOC over the experiment duration, whilst at Cross Lochs δ^{13}C-DOC became increasingly depleted over time, although measurements were subject to considerable noise (Figure 5.4).

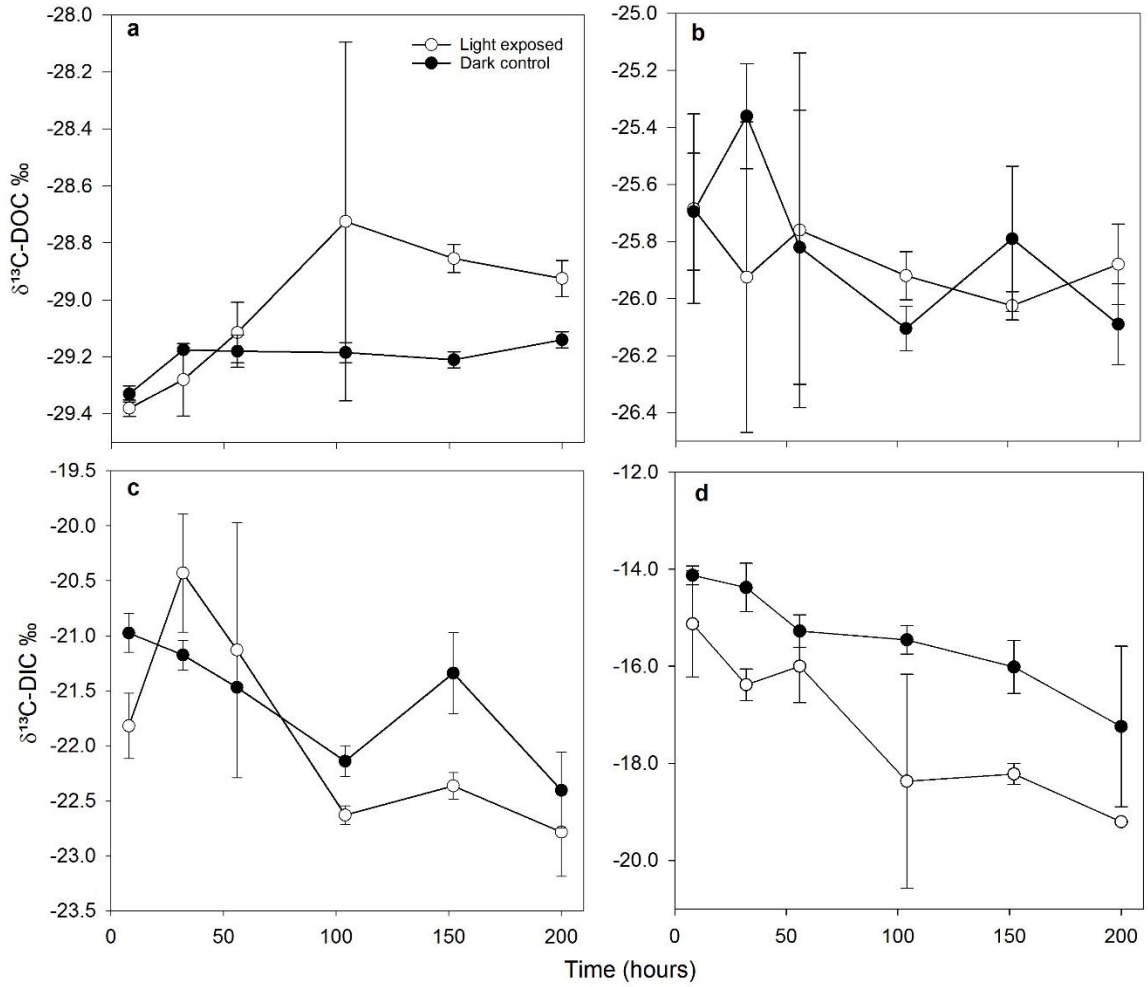

Figure 5.4. Stable carbon isotope ratios of DOC and DIC during exposure experiments over 9 days. a and b show δ^{13}C-DOC changes over time at Red Moss and Cross Lochs, respectively, and c and d show δ^{13}C-DIC changes over time at Red Moss and Cross Lochs, respectively. Error bars show the standard deviation (n=2). Note different y-axis scales.

Positive DOC (δ^{13}C-DOC) excursions were detected in the light exposed samples relative to the dark controls by the end of the experiment of +0.23 ‰ and +0.22 ‰ at Red Moss and Cross Lochs, respectively, with error terms larger for Cross Lochs.

Mean carbon isotopic composition of DIC (δ^{13}C-DIC) ranged from -23.1 to -20.1 ‰ at Red Moss and -19.9 to -13.9 ‰ at Cross Lochs (Figure 5.4 c-d). At both sites, the range of δ^{13}C-DIC values during the experiment was greater than the range of δ^{13}C-DOC values. δ^{13}C-DIC became increasingly depleted over time at both sites. At Red Moss, a negative excursion of -0.38 ‰ emerged in the light exposed samples relative to the dark controls by the end of the

experiment. At Cross Lochs, the negative excursion was much larger (-1.98 ‰) and light exposure resulted in notable differences in the δ^{13}C-DIC values in light exposed samples compared to the dark controls.

Changes to δ^{13}C-DOC values were positively correlated to changes in DOC concentrations of all experimental samples from both sites (Figure 5.5a). The correlation between changes in δ^{13}C-DIC values and changes in DIC concentrations (Figure 5.5b) was in the opposite direction to the DOC data, suggesting that increased DIC concentrations were related to the accumulation of LMW molecules. None of the correlations detected were statistically significant.

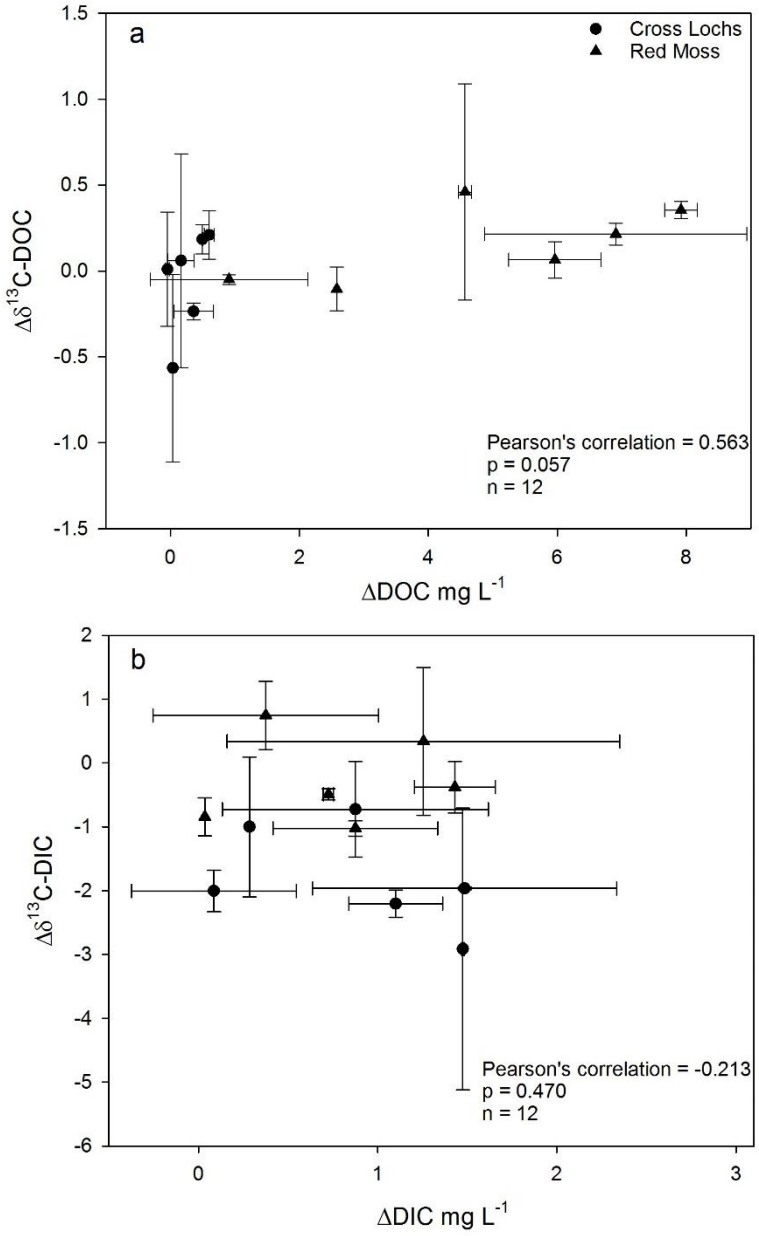

Figure 5.5. Correlations between mean a) $\Delta\delta^{13}$C-DOC and ΔDOC and b) $\Delta\delta^{13}$C-DIC and ΔDIC between control (dark) and light exposed samples from both sites pooled together. Error bars show the standard deviation (n=2).

4.5 Depth attenuation experiment

In the depth attenuation experiment the DOC concentrations of light exposed samples held at the water surface were lower than the corresponding dark control samples at Red Moss, with a mean reduction of 1.69 ± 1.04 mg L^{-1} per day (Figure 5.6a). However, mean differences in DOC concentrations detected between light exposed and dark water samples held at 10 cm

and 20 cm below the water surface were smaller than at the surface by a factor of 1.5 and 2.2, respectively. At Cross Lochs no significant differences in DOC concentration were detected between light and dark treatments at any position in the water column. DOC concentrations were lowest in the surface samples at both sites and a 2-way ANOVA revealed that at Red Moss, position in the water column was significant in determining DOC concentrations ($F=4.372$; $p=0.015$, Table 5.5; Supplementary Information).

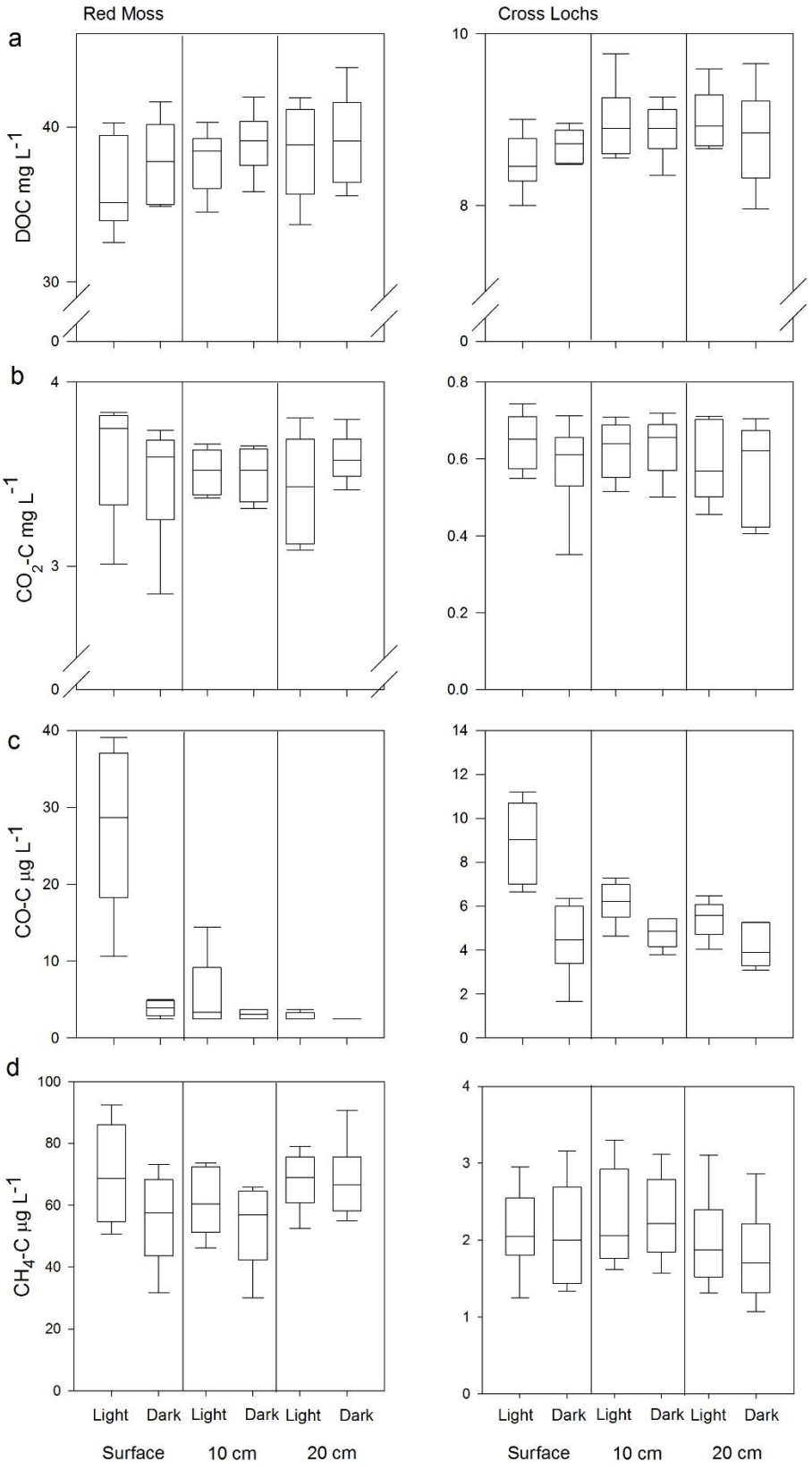

Figure 5.6 Box plots showing median, upper and lower quartile (a) DOC, (b) CO_2-C (c) CO-C and (d) CH_4-C concentrations in light and dark treatments at three depths in the water column:

surface, 10 cm and 20 cm depth. Input data for the plots represent the mean value from three replicates on 6 repeated days of 8 hour exposure experiments (n=6). Error bars represent minimum and maximum values. The left hand panel of each figure shows data for Red Moss and the right hand panel shows data for Cross Lochs. Note different y-axis scales.

Dissolved CO_2-C ranged from 2.97 to 3.83 mg L^{-1} at Red Moss and from 0.35 to 0.74 mg L^{-1} at Cross Lochs in the depth experiments. At the surface, CO_2-C concentrations in light exposed samples at Red Moss were 0.14 ± 0.05 mg L^{-1} higher than in the dark treatment samples across the six experimental days.

CO-C concentrations varied most in the depth experiments, with significant differences detected between light and dark samples at the surface, 10 cm and 20 cm depths at both sites (Table 5.5; Supplementary Information). Mean CO-C concentration decreased between the light exposed samples at the surface and samples held at 10 cm depth by a factor of 5 at Red Moss and a factor of 1.5 at Cross Lochs. The reduction in CO-C concentration between 10 and 20 cm depth was smaller at both sites for light exposed samples, with a factor of 2 and 1.1 decrease detected at Red Moss and Cross Lochs, respectively.

CH_4-C concentrations at Red Moss were subject to attenuation through the water column, with surface production of 14 μg L^{-1} decreasing by a factor of 1.9 by 10 cm depth. By 20 cm the difference in concentration between light and dark controls was negligible. At Cross Lochs, the difference in CH_4-C concentrations between light exposed and dark controls was minimal at all positions in the water column.

5.5 Discussion

5.5.1 Exposure induced changes to aquatic carbon

Light exposure resulted in decreased DOC concentrations in the pool at Red Moss due to the effects of photochemical processing. Losses were strongly concentrated in the first 3 days of light exposure, in agreement with Worrall and Moody (2014) who observed a non-linear rate of DOC loss over time, with 59% loss occurring over the first 30 h of ambient light exposure

of stream water samples from a peat-covered catchment. DOC loss rates in the light exposed samples were lower than in comparative studies, where photo-induced losses of up to 75% have been observed over similar durations in ambient conditions (Cory et al., 2014; Moody and Worrall 2015). Lower rates observed in these data may be partly due to transmission limitations of the Tedlar sample bags (Figure 5.8; Supplementary Information), where a maximum of 69% of total irradiance was transmitted in the UV part of the spectrum (280 – 400 nm). Previous studies have established UV as the most effective type of irradiation for inducing photolysis (Moran and Zepp 1997; Zepp et al., 2003), and thus photochemically induced DOC losses reported here are likely to be conservative.

At Cross Lochs light exposure did not result in photochemical losses of DOC. $SUVA_{254}$ data suggest that the DOC at this site was less humic than at Red Moss (Table 5.2), with values indicating an approximate humic content of 25% based on the findings of Weishaar et al. (2003). As humic molecules are more labile to photo-processing, it may be that photodegradation is a secondary driver of biogeochemical cycling at this pool site relative to microbial processing, as there is less available photoreactive DOC.

Whilst light induced changes to DOC concentrations were smaller in comparison to other studies, changes in absorbance characteristics were more substantial. Reductions in absorbance at 350 nm were >25% at both sites in light exposed samples, suggesting that photochemical processing of C had occurred at rates comparative to other laboratory based photodegradation studies (Spencer et al., 2009). That this effect was not observed as clearly in the DOC data is likely due to the confounding effects of simultaneous DOC production in the water samples. In-situ DOC production may also explain why the rates of decay (k) detected in the exposure experiments were higher for optical parameters than for DOC at both study sites (Table 5.3). DOC production has been observed in previous studies using peatland water samples (Moody and Worrall, 2015) and can be attributed to two main sources.

Strong coupling between the particulate and dissolved fractions of C can result in DOC production (He et al., 2016; Porcal et al., 2013). As POC concentrations decreased, DOC concentrations increased in dark samples at both pool sites and in the light exposed samples at Cross Lochs (Table 5.2), suggesting that microbial and photochemical conversion of POC to DOC has occurred. Whilst these data indicate that release from POC may be an important DOC source, the budgets do not balance, with DOC gains greater than the equivalent POC losses at both sites. Production from algal sources (e.g. Nguyen et al., 2005) may also have contributed to the observed DOC increases, although data regarding algal abundance and activity in the samples were not collected. These findings suggest that C budgets for peatland pools should consider POC as a labile fraction of aquatic C, which can be subject to turnover into DOC and further lost to the atmosphere as C based gas. Studies which neglect POC in budget estimations may be underestimating C turnover in peatland waters.

The dominant fate of DOC in freshwaters remains unclear (Cole et al., 2007; Vonk et al., 2015) although the dissolved CO_2-DOC relationships detected in this study suggest that complete oxidation to CO_2 is the one of the primary loss pathways in peatland pools. In budget calculations, CO_2 production accounts for up to one-third of the total DOC loss detected in light exposed samples at Red Moss. DIC, CO and partially oxidized molecules in the remaining fraction of DOC are the other identified products of photochemical processing. There is consensus emerging that light driven processes are responsible for significant release of CO_2 from inland aquatic systems (Koehler et al., 2014). From combined field measurements and experiments, 55% of DOC processed in the water column of aquatic ecosystems was estimated to be oxidized to CO_2 across the 8140 km^2 Kuparuk River basin in the Canadian Arctic (Cory et al., 2014). In our experiments light exposure resulted in CO_2 concentrations 15% and 16% higher than in dark control samples by the end of the exposure period at Red Moss and Cross Lochs, respectively, demonstrating the importance of photochemical processing of C in the production of CO_2 in peatland pools. These data are likely to be a

conservative estimate of photo-induced gaseous C production due to the emptying of the bag headspace during the experiment, which was undertaken in order to ensure that conditions remained oxygenated.

5.5.2 Isotopic signatures of aquatic carbon species

This study has provided the first isotopic insight into DOC processing in peatland pools. The range of δ^{13}C-DOC values measured here (-29.4 to -25.4 ‰) is similar to those reported in studies of freshwater DOC transformation (Opsahl and Zepp, 2001; Spencer et al., 2009) and are consistent with C3 plant material acting as the primary DOC source. In comparison to δ^{13}C-DOC values derived specifically from soil pore water and stream samples collected across UK peatland environments (Billett et al., 2007; Leith et al., 2014), the range detected in this study is wide due to the quantification of in-situ δ^{13}C-DOC transformation over time.

The δ^{13}C-DOC values at the start of the experiment were significantly different between sites, with more enriched δ^{13}C-DOC evident at Cross Lochs. The degree to which the enriched δ^{13}C-DOC signature is a function of the light exposure history of the aquatic C cannot be distinguished using these data, however water residence times in the two pools may be contrasting. As such, the water at Cross Lochs could have been exposed to light over a longer duration than at Red Moss prior to the start of our experiments, resulting in a remaining C pool which was recalcitrant to further photochemical processing. Water residence time is clearly a key factor in moderating C cycling within aquatic environments (Cory et al., 2007; Vähätalo and Wetzel, 2008) and requires further investigation within peatland pool systems to constrain the timescales over which labile C is removed and subsequently replenished.

The accumulation of enriched DOC in light exposed samples at Red Moss shows that photo-processing has changed the isotopic signature. These results are consistent with other studies of DOC photo-processing, where a positive isotopic excursion has been explained by preferential loss of lignin phenols (Opsahl and Zepp, 2001; Spencer et al., 2009). At Cross Lochs, a clear δ^{13}C-DOC excursion in light exposed samples was not apparent relative to the

dark controls. However, a shift towards a depleted δ^{13}C-DOC signature in both treatments either suggests that microbial processing of DOC has occurred over the experiment duration, resulting in depletion of isotopically heavy fractions such as carbohydrates in the remaining DOC pool.

Isotopic data suggest that processing pathways of C are different at the two sites, with the effects of DOC photo-processing more apparent at Red Moss. However the relative contribution of photochemical versus microbial activity to C cycling at each site cannot be distinguished quantitatively due to interacting effects between the two processing pathways. Photochemical degradation has been widely reported to produce biologically labile substrates from recalcitrant forms of aquatic C (Remington, 2011; Miller and Moran, 1997). Such substrates could have stimulated production of DOC from POC or algal sources within the samples, thereby masking the effect of decreased DOC concentrations upon light exposure. In order to quantify the extent of coupling between the two processes, a third treatment where inoculated samples are exposed to light could be employed. This would allow differentiation between photodegradation of C, microbial processing of C and the degree to which the former enhances the latter. However, use of sterilizing substances such as $HgCl_2$ in experiments conducted in pristine systems could pose a potential risk to aquatic flora and fauna.

5.5.3 Accounting for depth attenuation effects

In the depth attenuation experiments conducted at varying positions in the water column clear differences in gaseous production emerged, both between experimental sites and between the selected depths. At Red Moss, CO data suggest that photochemical breakdown occurred predominantly in the top 10 cm of the water column and was negligible below this depth, as reported by numerous previous studies (e.g. Vähätalo et al., 2000). At Cross Lochs, CO and CO_2 production rates were lower than at Red Moss across water samples at all depths and attenuation with depth was less pronounced due to lower DOC concentrations. For gases other than CO, production rates did not display statistically significant depth dependence at either

site. This could be due to simultaneous microbial production of CO_2 and CH_4 introducing noise into the measured depth response.

The overall significance of aquatic C photo-processing within the catchments was estimated by using measured attenuation rates through the water column to determine gaseous production per liter of water and multiplying by the open water pool surface area (see Supplementary Information Text S1 for details of the calculations). Corrected for mean monthly PAR data and catchment surface area, 2.91 ± 0.36 and 96.3 ± 8.59 mg C m^{-2} yr^{-1} was converted to CO_2 via photo-processing in the water column at Red Moss and Cross Lochs, respectively. Production rates were higher at Cross Lochs despite significantly lower measured values in the field experiments (Figure 5.6) due to the much larger percentage coverage of open pool systems within the catchment (Table 5.1) and the reduced effects of light attenuation through the water column relative to Red Moss. When converted to a rate of per m^2 based on the total peatland pool surface area within the catchment, photo-processing rates at Red Moss were similar to Cross Lochs (3.17 ± 0.39 relative to 4.18 ± 0.42 g C m^{-2} yr^{-1}). Both of these estimates are comparable to those reported by Algesten et al. (2004) who used DIC concentrations to determine C photo-processing rates of 3.8 ± 0.04 g C m^{-2} yr^{-1} in seven Swedish lakes with an average DOC concentration of 16 mg C L^{-1}.

Accounting for measured concentrations of CO and CH_4 in addition to CO_2, photo-processing rates for the total peatland pool surface area within the catchment increase to 15.3 ± 1.98 and 4.63 ± 0.13 g C-CO_2 eq m^{-2} yr^{-1} at Red Moss and Cross Lochs, respectively. CH_4 emissions, corrected for 100 year global warming potentials derived from the most recent IPCC report (Edenhofer et al., 2014), constitute the largest part of the budget at Red Moss and these data demonstrate the importance of measuring non-CO_2 terms to fully constrain aquatic C cycling.

In both catchments light driven processes were responsible for a considerable percentage of total C processing (33% and 51% of total aquatic C turnover at Red Moss and Cross Lochs, respectively) when compared to equivalent estimates of dark microbial respiration, which were

derived from gaseous production rates in dark control bags (see Supporting Information Text S1 for details of calculations). Incorporating both photochemical and microbial C processing terms into the C budget corrected for total pool surface area within the catchments, a total of 45.8 ± 4.95 and 8.84 ± 0.47 g C-CO_2 eq m^{-2} yr^{-1} was processed in pools at Red Moss and Cross Lochs, respectively. Whilst these figures are at the lower end of previous estimates of peatland pool C release of 23–419 g C m^{-2} yr^{-1} (Hamilton, et al., 1994; Repo et al., 2007; McEnroe et al., 2009; Pelletier et al., 2014), they do not directly account for CO_2 which enters the aquatic environment from de-gassing of supersaturated soil pore water. Instead they offer an insight into the internal production pathways of C gases within peatland pools of varying C concentrations.

The greenhouse gas (GHG) balance of Cross Lochs was constrained by Levy and Gray (2015) through multi-year eddy covariance measurements, with the site determined as a net sink of C in the order of −50 g C-CO_2 eq m^{-2} yr^{-1}. Assuming full evasion of dissolved gases into the atmosphere, our data suggest that the combined effect of photochemical and microbial C processing in pool environments within the Cross Lochs catchment reduce the C sequestration potential of the peatland by 0.20 g C-CO_2 eq m^{-2} yr^{-1}. This estimate is within the same order of magnitude as a recent catchment scale study by Cory et al. (2014), which determined that ~0.4 g C m^{-2} yr^{-1} was mineralized to CO_2 in the water column. Whilst the term is small in comparison with the overall GHG budget for Cross Lochs, it does not include estimates of C processing in downstream aquatic environments which may constitute a significant loss term. It also has implications for peatlands which have a high percentage cover of pool environments (>30%) in areas such as the Hudson Bay lowland (Moore et al. 1994), as the sequestration potential of these systems is likely to be significantly reduced by C cycling in the aquatic environment.

5.6 Conclusions

This study has shown that C in peatland pools is labile to photochemical and microbial processing, as changes to C species occurred in light exposed and dark control sample bags over the experiment duration. Interaction between the particulate and dissolved forms of aquatic C was detected at both study sites and POC should be considered as a labile C fraction. Significant differences in biogeochemical cycling of C were detected between the high and low DOC sites, confirming that inter-site variability in peatland pool biogeochemistry is high (Turner et al., 2016). Accounting for light attenuation effects through the water column, we estimate that 45.8 ± 4.95 and 8.84 ± 0.47 g C-CO_2 eq m^{-2} yr^{-1} was processed by photochemical and microbial activity in the pools at the high and low DOC sites, respectively. These data, whilst insufficient to alter the GHG balance of the surrounding peatland catchments from a sink to a source, should be considered in a global context where rapid increases in surface coverage of open water pools have been observed in the Arctic, due in part to melting permafrost (Jorgenson et al. 2001; Laurion et al. 2010; Vonk et al. 2015). By understanding what drives individual gaseous production rates within aquatic GHG budgets, models will be able to better predict the GHG source strength of peatland pool environments under climate change.

Supplementary Information

Text S1. Photochemical and microbial C processing calculations

Water column rates of photochemical C processing were estimated using measured production rates of CO_2, CO and CH_4 at the water surface and at depths of 10 and 20 cm. Best fits between depth and production rate, as determined by the highest R^2 value, were produced to describe the attenuation effects at both systems, using exponential functions for CO_2 and CO data, and a linear function for CH_4 data (Table 5.7). The mean production rate measured through the upper 20 cm of the water column was then established for each C gas species. Production below 20 cm water depth was considered negligible at both study sites. In order to incorporate uncertainty into depth integrated production estimates, the standard deviation of production rate at each depth was calculated and propagated through the upscaling method.

CO_2, CH_4 and CO concentration data collected from the 8 hour depth attenuation experiments were corrected for day length (in hours) for each month. Correction factors were also applied to account for the limited transmission properties of the Tedlar bags used in the experiments (Figure 5.9). The percentage transmission measured for each wavelength across photochemically relevant range of 280–600 nm (Koehler et al., 2014) of the Tedlar bags was applied to measured irradiance data for both sites at the corresponding wavelength (Figure 5.9). The corrected values were summed and compared with the original uncorrected irradiance data to determine the mean percentage of light transmitted by the bags across all wavelengths. At Red Moss, 72% of light was transmitted and at Cross Lochs 71% was transmitted, and these site specific correction factors were applied to the data. Whilst this is simplistic as UV light is the most effective in driving photo-reactions and is subject to the greatest attenuation in the water column, since no underwater measurements of light penetration were made, it was considered the best approach to yield estimates of water column C processing with the available data.

PAR data measured during the experiment was averaged and compared against mean monthly PAR data for both sites from 2008 - 2015 (Table 5.8). Production rates were corrected for PAR for each month of the year, assuming a linear relationship between the two variables. For Cross Lochs, photoproduction of C gases was assumed negligible in the months of December and January, as pools are often ice covered during these months. PAR corrected production measurements for each month were summed and the standard deviation of PAR data were added and subtracted to the mean monthly value to generate an error term around the total C processing estimates. As PAR and air temperature positively co-vary at Red Moss and Cross Lochs (R^2 = 0.675 and 0.615, respectively), correcting production rates for PAR was assumed to account for the sensitivity of photochemical reactions to temperature (Häder et al., 2014).

To determine an annual areal rate of C processing per m^2 for the total catchment land area (g C m^{-2} yr^{-1}), production rates were then multiplied by the surface area of peatland pools within the catchment and this value was divided by the total catchment area (Table 5.1).

In order to understand the contribution of microbial C processing to overall budgets for the pools, areal rates of C photo-processing were compared to an areal estimate of dark bacterial respiration. This was generated from mean water column production rates of C gas species in dark control samples. Rates measured at the surface were assumed to be constant through the water column. Data were scaled using mean air temperature measured during the experiment compared against mean monthly air temperature data for both sites from 2008 - 2015 (Table 5.8; Supplementary Information 4). A Q_{10} value of 2 was assumed, whereby a 10°C change in temperature results in a factor of 2 variation in reaction rate (Bloom et al., 2010), as bacterial activity has been shown to correlate weakly with water temperature in such systems (Adams et al., 2010; Bloom et al., 2010; Cory et al., 2014).

Temperature corrected production rates were then multiplied by the surface area of peatland pools within the catchment and this value was divided by the total catchment area (Table 5.1).

As with the photo-processing estimate, bacterial C processing was assumed negligible in December and January at Cross Lochs.

To express production rates in terms of CO_2 equivalents, production values for both CH_4 and CO were weighted using 100 year global warming potentials (GWPs) from IPCC estimates (Edenhofer et al. 2014). 100 year GWPs were selected to ensure comparability with other peatland studies which have calculated greenhouse gas balances (Dinsmore et al., 2010; Beetz et al., 2013). Radiative forcing factors of 34 for CH_4 and 1.9 for CO were employed. These factors were converted using the atomic mass of CH_4 (16) and CO (28) relative to CO_2 (44) to get atomic mass based factors (12.4 and 1.21 for CH4–C and CO-C, respectively).

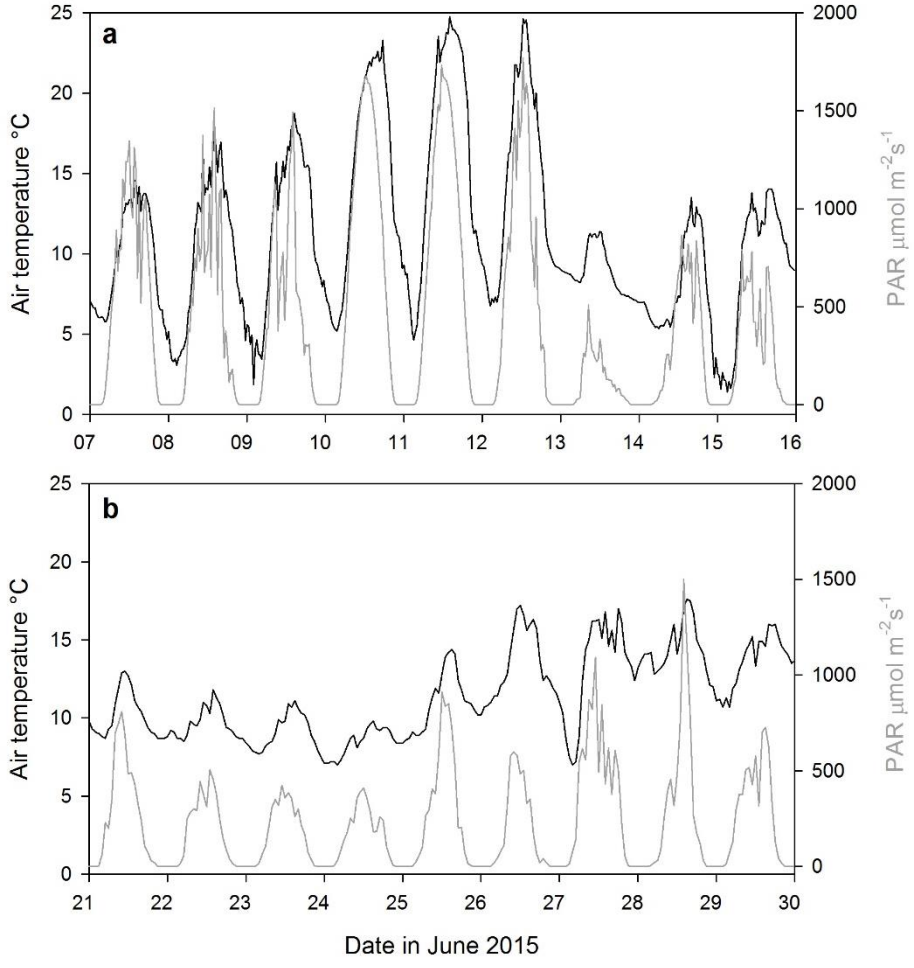

Figure 5.7. Time series of air temperature (black line) and PAR (grey line) over the experiment duration in June 2015 at a) Red Moss and b) Cross Lochs.

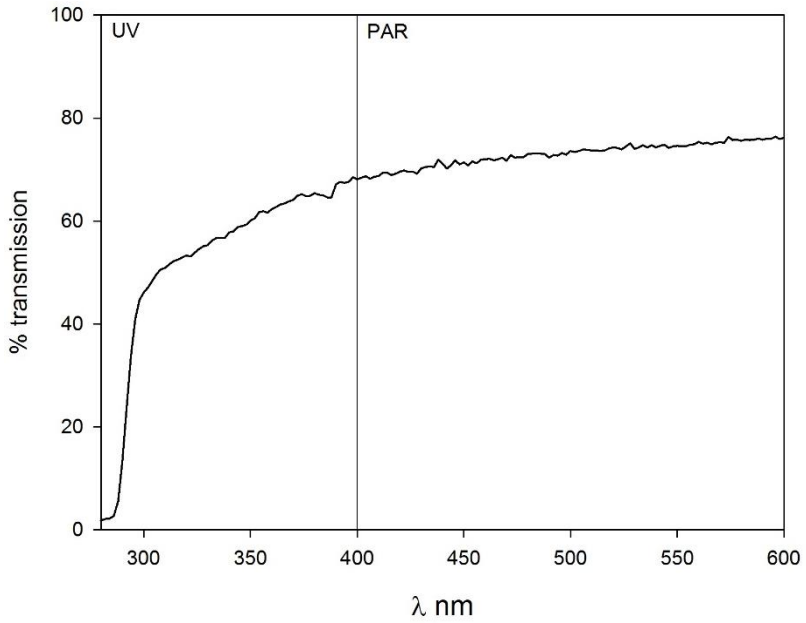

Figure 5.8. Percentage transmission of Tedlar material from 280-600 nm. We obtained the data using a piece of Tedlar™ bag in UV-Vis absorbance analysis.

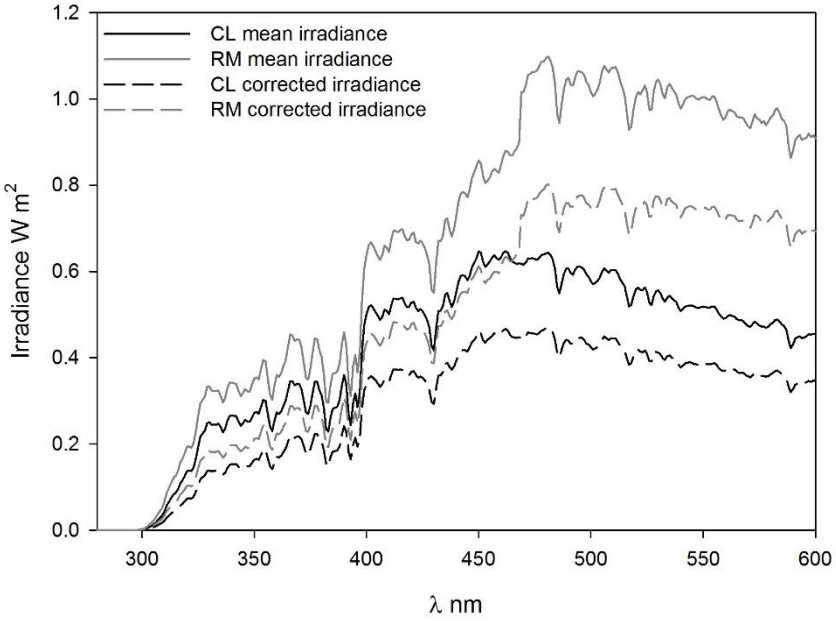

Figure 5.9 Mean irradiance data from 280 – 600 nm collected at midday on 6 experimental days at Cross Lochs (CL) and Red Moss (RM), compared to Tedlar™ transmission corrected irradiance data.

Table 5.5 Summary of 2-way ANOVA analysis looking at the dependence of DOC, CO_2-C, CO-C and CH_4-C concentrations on position in water column, light treatment and the interaction between the two factors (n=18).

	Red Moss		**Cross Lochs**	
DOC				
	F value	*P value*	*F value*	*P value*
Position	**4.372**	**0.0153***	2.695	0.0728
Light Treatment	1.703	0.1717	0.074	0.7864
Interaction	0.066	0.9988	0.876	0.4199
CO_2-C				
	F value	*P value*	*F value*	*P value*
Position	1.086	0.342	1.133	0.326
Light Treatment	1.066	0.367	0.359	0.550
Interaction	1.594	0.157	0.707	0.495
CO-C				
	F value	*P value*	*F value*	*P value*
Position	**60.10**	**0.000****	**15.03**	**0.000****
Light Treatment	**32.55**	**0.000****	**68.11**	**0.000****
Interaction	**20.56**	**0.000****	**12.74**	**0.000****
CH_4-C				
	F value	*P value*	*F value*	*P value*
Position	**4.823**	**0.0101***	0.591	0.556
Light Treatment	2.129	0.1016	0.457	0.501
Interaction	0.765	0.5990	0.380	0.685

Table 5.6. All stable carbon isotope data from this study. RM denotes Red Moss and CL denotes Cross Lochs, the first number refers to day of experiment, the '+' indicates light treatment and the second number refers to the replicate. Control (dark) treatments are denoted by '-'.

Sample	δ^{13}C-DOC ‰	Publication code	δ^{13}C-DIC ‰	Publication code
RM 1+1	-29.36	S-177785	-22.03	SE164863
RM 1+2	-29.40	S-177786	-21.61	SE164864
RM 1-1	-29.35	S-177787	-20.85	SE164865
RM 1-2	-29.31	S-177788	-21.10	SE164866
RM 2+1	-29.19	S-177805	-20.81	SE164867
RM 2+2	-29.37	S-177806	-20.05	SE164868
RM 2-1	-29.17	S-177807	-21.08	SE164869
RM 2-2	-29.18	S-177808	-21.27	SE164870
RM 3+1	-29.04	S-177809	-21.95	SE164871
RM 3+2	-29.19	S-177810	-20.31	SE164872
RM 3-1	-29.22	S-177811	-21.47	SE164873
RM 3-2	-29.14	S-177812	-21.47	SE164874
RM 5+1	-29.17	S-177789	-23.14	SE164875
RM 5+2	-28.28	S-177790	-23.02	SE164876
RM 5-1	-29.21	S-177791	-22.24	SE164877
RM 5-2	-29.16	S-177792	-22.04	SE164878
RM 7+1	-28.82	S-177793	-22.28	SE164879
RM 7+2	-28.89	S-177794	-22.45	SE164880
RM 7-1	-29.19	S-177795	-21.08	SE164881
RM 7-2	-29.23	S-177796	-21.60	SE164882
RM 9+1	-28.99	S-177797	-23.07	SE164883

Sample	δ^{13}C-DOC ‰	Publication code	δ^{13}C-DIC ‰	Publication code
RM 9+2	-28.86	S-177798	-22.50	SE164884
RM 9-1	-29.12	S-177799	-22.16	SE164885
RM 9-2	-29.16	S-177800	-22.65	SE164886
CL1+1	-25.92	S-177817	-14.35	SE164839
CL 1+2	-25.45	S-177818	-15.90	SE164840
CL 1-1	-25.84	S-177819	-14.26	SE164841
CL 1-2	-25.55	S-177820	-13.99	SE164842
CL 2+1	-25.54	S-177821	-16.15	SE164843
CL 2+2	-26.31	S-177822	-16.61	SE164844
CL 2-1	-25.23	S-177823	-14.73	SE164845
CL 2 -2	-25.49	S-177824	-14.02	SE164846
CL 3+1	-26.2	S-177825	-16.53	SE164847
CL 3+2	-25.32	S-177826	-15.47	SE164848
CL 3-1	-26.16	S-177827	-15.51	SE164849
CL 3-2	-25.48	S-177828	-15.04	SE164850
CL 5+1	-25.86	S-183452	-19.93	SE164851
CL 5+2	-25.98	S-183453	-16.81	SE164852
CL 5-1	-26.16	S-183454	-15.66	SE164853
CL 5-2	-26.05	S-183455	-15.25	SE164854
CL 7+1	-26.06	S-183456	-18.37	SE164855
CL 7+2	-25.99	S-183457	-18.07	SE164856
CL 7-1	-25.61	S-183458	-15.63	SE164857
CL 7-2	-25.97	S-183459	-16.40	SE164858
CL 9+1	-25.98	S-183460	-19.19	SE164859
CL 9+2	-25.78	S-183461	-19.22	SE164860

Sample	δ^{13}C-DOC ‰	Publication code	δ^{13}C-DIC ‰	Publication code
CL 9-1	-26.19	S-183462	-18.41	SE164861
CL 9-2	-25.99	S-183463	-16.07	SE164862

[a]RM denotes Red Moss, the first number refers to day of experiment, the '+' indictes light treatment and the second number refers to the replicate.

[b]Control (dark) treatments are denoted by '-'.

[c]CL denotes Cross Lochs.

Table 5.7 Regression equations and R^2 values used to describe attenuation effects through the water column for gaseous C species at Red Moss and Cross Lochs.

	Red Moss	Cross Lochs
CO_2	$y = 0.1805e^{-0.241x}$ $R^2 = 0.998$	$y = 0.0603e^{-0.079x}$ $R^2 = 0.977$
CO	$y = 22.805e^{-0.215x}$ $R^2 = 0.999$	$y = 3.7161e^{-0.061x}$ $R^2 = 0.789$
CH_4	$y = -0.7197x + 14.523$ $R^2 = 0.999$	N/A[a]

[a]Production rates of CH_4 were negligible at Cross Lochs

Table 5.8. Mean monthly PAR and air temperature data for Red Moss and Cross Lochs, 2008 – 2015. Error terms represent the standard deviation of the mean. Data were collected from the EMEP supersite at Auchencorth Moss for Red Moss and from the flux tower for Cross Lochs and represent the monthly means of measurements made every 30 minutes.

	Red Moss		**Cross Lochs**	
	PAR μmol m^{-2} s^{-1}	Air temperature °C	PAR μmol m^{-2} s^{-1}	Air temperature °C
January	31.3 ± 4.10	2.4 ± 1.0	31.5 ± 4.99	2.5 ± 1.1
February	69.2 ± 7.99	2.9 ± 1.5	80.3 ± 8.98	3.0 ± 1.3
March	146 ± 12.1	4.1 ± 2.0	162 ± 9.41	4.0 ± 1.5
April	249 ± 38.1	6.6 ± 2.0	273 ± 20.7	5.9 ± 1.5
May	326 ± 29.3	9.1 ± 1.0	361 ± 45.7	7.8 ± 0.9
June	346 ± 41.7	12.2 ± 1.2	345 ± 35.8	10.0 ± 0.9
July	328 ± 49.8	13.9 ± 1.6	340 ± 32.3	11.9 ± 1.1
August	254 ± 33.7	13.2 ± 1.1	268 ± 13.0	11.3 ± 0.8
September	182 ± 22.3	11.3 ± 0.8	190 ± 15.9	10.0 ± 0.7
October	94.1 ± 8.98	8.2 ± 1.6	99.4 ± 4.34	7.3 ± 1.2
November	43.5 ± 5.17	5.0 ± 1.7	42.7 ± 5.22	4.9 ± 1.7
December	22.9 ± 4.14	2.3 ± 2.3	20.0 ± 2.57	1.7 ± 2.0

Chapter 6 Discussion

This discussion brings together the findings from Chapters 3-5 to address the aim of the PhD as set out in Chapter 1, by considering the overall role of photochemical processing of carbon (C) in C budgets of aquatic systems draining peatlands. Firstly, an assessment of the concentration and composition of C found in peatland draining aquatic systems is made. This is followed by a discussion of controls on DOC photoreactivity, classified here into spatial and temporal factors. The next section attempts to determine the importance of photochemical processing of aquatic C in catchment scale peatland C budgets. Finally, the wider implications of the study are examined in the context of both future climate change and anthropogenic impacts on peatlands.

6.1 Concentration and composition of carbon in peatland draining aquatic systems

There was considerable variation in both concentration and composition of C in the peatland draining aquatic systems investigated in this study. DOC concentrations were high in the peatland pool at Red Moss of Balerno (32.5 ± 2.87 mg L^{-1}), although limited sampling means that these values do not reflect annual mean concentrations. Comparable DOC concentrations were detected at the Black Burn, with a mean concentration of 33.4 ± 14.2 mg L^{-1} in the year-long study. This is slightly higher than the 5-year mean reported in the CEH carbon catchments project (28.4 ± 1.07 mg L^{-1}; Dinmore et al., 2013), which employs a bi-weekly sampling regime. During the year-long study, DOC measurements were being made at the same site at the Black Burn as part of the long term CEH project. Although data from this study resolved annual maximum and minimum concentrations in addition to the seasonal cycle of DOC when compared to the CEH carbon catchments project data (Figure 6.1), monthly sampling places a limit on determining the full range of C composition within aquatic systems.

DOC concentrations were lowest at Loch Katrine and varied considerably less in the year-long study than at the Black Burn. In comparison to SEPA DOC data collected bi-monthly from

2008-2013 (3.71 ± 0.54 mg L^{-1}), this study detected a slightly higher mean concentration of 4.17 ± 0.83 mg L^{-1}, comparative to other studies of northern lakes (Sobek et al., 2007; Koehler et al., 2014).

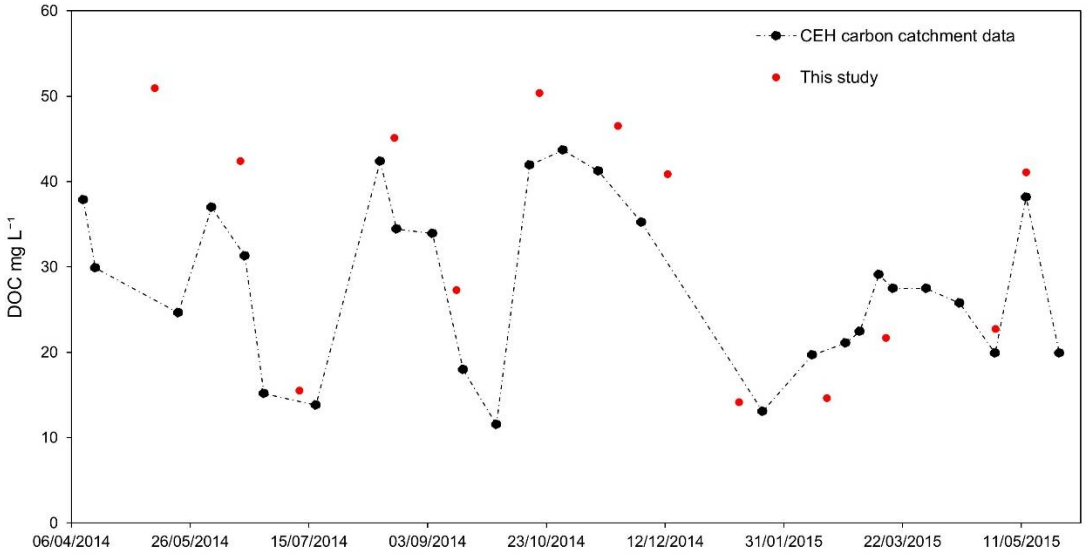

Figure 6.1 DOC concentrations measured in the Black Burn during the year-long study, compared to CEH Carbon Catchment data over the same period.

The peatland pool at Cross Lochs had a mean DOC concentration of 6.66 ± 2.49 mg L^{-1}, based on samples collected on two sampling occasions in March and June 2015. A survey of DOC concentrations in pools within the wider Flow Country of Scotland (Turner et al. (2016) determined a mean concentration of 13.6 ± 4.58 mg L^{-1} in September 2013, suggesting that samples in this study were not collected at the time of year where maximum concentrations could be expected. Turner et al. (2016) also reported low intra-site variability in DOC concentrations, indicating that the pool used in this study is largely representative of pools in the wider Cross Lochs catchment.

Across all sites investigated in the present research, absorbance at 254 nm was significantly positively correlated with DOC concentration (Figure 6.2). This correlation has been previously reported in other peatland draining aquatic systems (Peacock et al., 2014; Turner et al., 2016) and demonstrates strong association between the coloured dissolved organic

matter (CDOM) pool and the DOC pool (Spencer et al., 2012). Tight coupling between light absorbing CDOM and DOC suggests that C in peatland draining aquatic systems is highly photoreactive.

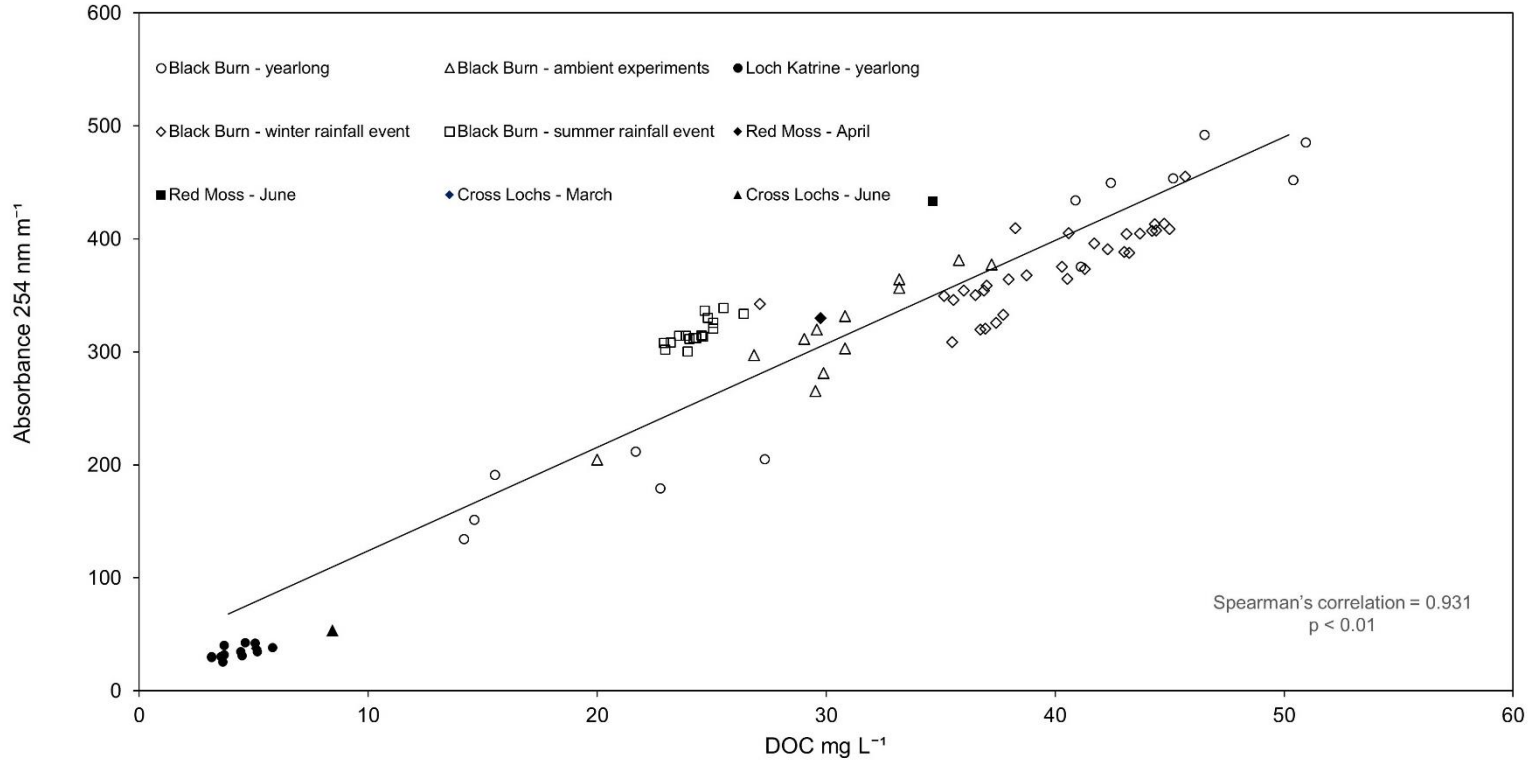

Figure 6.2 Spearman rank order correlation between absorbance at 254 nm m^{-1} (a_{254}) and DOC concentration across different sites and sampling regimes used in this study (n = 90).

Further investigations of DOC composition showed that the peatland pool at Red Moss was biogeochemically most similar to the Black Burn at Auchencorth, both of which exhibited relatively high $SUVA_{254}$ values suggesting that material was aromatic (Table 6.1). Comparative values for Loch Katrine and Cross Lochs were lower by ~0.43. E4:E6 ratios were also lower at these sites, indicating that the DOC pool was derived from well-humified material (Thurman, 1985). Higher values (>8) have been previously interpreted to indicate a dominance of less-humified fulvic acids and thus the relatively higher E4:E6 values at the Black Burn and Red Moss suggest a greater contribution of fresher, less-humified material than at Loch Katrine and Cross Lochs. This interpretation is supported by the E2:E3 values, which show that molecule size was greatest at Cross Lochs and Loch Katrine.

Table 6.1 Biogeochemical characteristics of water sampled at the sites used in this study, prior to use in exposure experiments. Values represent the mean ± 1 standard deviation.

	Black Burn, Auchencorth[a]	**Loch Katrine[b]**	**Red Moss of Balerno[c]**	**Cross Lochs, Forsinard[d]**
DOC mg L^{-1}	33.4 ± 14.2	4.17 ± 0.83	32.5 ± 2.87	6.66 ± 2.49
POC mg L^{-1}	5.78 ± 2.78	2.96 ± 0.63	4.43 ± 1.37	3.78 ± 0.46
δ^{13}C-DOC ‰	---	---	-29.3 ± 0.03	-26.1 ± 0.09
E2:E3	4.22 ± 0.62	4.45 ± 0.99	4.40 ± 0.08	5.29 ± 0.21
E4:E6	5.76 ± 2.16	3.14 ± 1.34	5.95 ± 0.39	2.96 ± 0.28
$SUVA_{254}$	4.23 ± 0.54	3.71 ± 0.63	5.07 ± 0.49	3.80 ± 0.42

[a] Mean concentration determined from year-long study (n = 13)
[b] Mean concentration determined from year-long study(n = 13)
[c] Mean concentration determined from two sampling occasions (for March see Appendix and for June see Chapter 5) (n=2)
[d] Mean concentration determined from two sampling occasions (for April see Appendix and for June see Chapter 5) (n=2)

Clearly, there is significant variability in the concentration and composition of peatland derived C in the aquatic systems investigated in this study. Nonetheless, together these findings demonstrate that the inherent chemical composition of C in peatland draining aquatic systems renders it susceptible to photo-processing.

6.2 Spatial variation in peatland carbon photoreactivity

In Chapter 4 DOC photoreactivity was reported to be considerably higher at a headwater stream, the Black Burn, than at a reservoir, Loch Katrine. During the year-long experiment, conversion to CO_2 accounted for 3.3 ± 1.6% of initial DOC concentrations at the Black Burn, whereas 1.4 ± 0.5% of DOC was converted under the same experimental and exposure conditions in the Loch Katrine samples. In samples at the Black Burn collected during a winter rainfall event, up to 5.5% of initial DOC was converted to CO_2, suggesting that the stream was loaded with photoreactive C input from the peatland catchment. Since Loch Katrine is located in a catchment that is not characterised by 100% peat coverage, contribution of DOC from other soil types may have caused differences in the intrinsic photoreactivity of C delivered to the loch. With increasing catchment area, downstream water bodies receive inputs from multiple sources and, furthermore, this input is not necessarily directly received from the terrestrial environment, instead delivered via other aquatic systems where already exposed and processed to a degree.

This observation informs discussion of the wider question of how C photoreactivity alters through the continuum of inland aquatic systems. In downstream aquatic systems such as Loch Katrine, organic C may have already been subject to in-situ degradation as a function of increased water residence times and processing in upstream systems including headwater streams. Although this study investigated only one headwater and one downstream system, the data collected indicate that this model helped to explain the differences in C composition and photoreactivity between the Black Burn and Loch Katrine. Lower E4:E6 ratios (Table 6.1) suggest that material in the loch was humified relative to the Black Burn, where inputs were fresher and less humified. Decreasing organic C decomposition rates with increasing water retention times have been observed in previous studies (Weyhenmeyer et al., 2012; Catalán et al., 2016). Weyhenmeyer et al. (2012) determined that both C and colour decreased exponentially from freshwaters during transport to marine outlets, yet the rate of decrease of

colour was about twice as fast as the bulk C pool. Photo-processing in aquatic systems may contribute to decoupling between bulk DOC and light absorbing CDOM with increasing water residence time. If the correlation between a_{254} (a proxy for CDOM) and DOC concentrations shown in Figure 6.2 is calculated for water samples from Loch Katrine only, the correlation coefficient decreases to 0.52 (n=13). This suggests decoupling between DOC and CDOM, thereby further supporting the view that C in the loch had already been subject to processing at time of sample collection, as the photoreactive component of DOC is depleted.

In contrast to lakes and larger rivers, headwater streams such as the Black Burn receive input directly from the terrestrial environment. This material is considered 'fresh' and labile to processing in the aquatic environment. Photoreactivity data show that DOC from the Black Burn was highly susceptible to photo-processing, in both ambient and laboratory conditions. In the year-long study, it was estimated that 3.5 ± 2.0 kg CO_2 yr^{-1} could be produced from aquatic photo-processing of DOC derived from the 3.4 km^2 Auchencorth Moss catchment. However, in-situ measurements of photo-processing were not made at the Black Burn during this study. Previous investigations of DOC composition in boreal and temperate streams have suggested that in-situ DOC processing is minimal (Kothawala et al., 2015; Palmer et al., 2015; Wollheim et al., 2015) due to high flows and short transit times (<2 days) (Kothawala et al. 2015). The Black Burn is incised deeply (~1.2 m) into the peat profile (Figure 2.2) and bank shading restricts light exposure, rendering photo-processing unlikely at least within the immediate catchment. Palmer et al. (2015) determined that 5–44% of DOC could be removed during transit from peatland headwaters to sea, yet for the majority of measurements in their multiple catchment study, DOC concentrations were within the range expected based on conservative transport.

However, quantifying the net transformation of C through the continuum of aquatic systems is difficult because losses can be quickly balanced by new sources (Palmer et al., 2015). Furthermore there are contrasting in-situ studies which suggest that up to 20% of aquatic

DOC can be removed in in streams draining peatland headwater catchments (Dawson et al., 2001; Billett et al., 2006). In Arctic aquatic environments, Cory et al. (2014) also showed that in-situ photochemical processing of DOC accounted one-third of the total CO_2 released from surface waters. Combined, these studies demonstrate that more in-situ measurements of C processing, via photochemical and heterotrophic microbial pathways, are required to understand whether inland aquatic systems are a major loss pathway for peatland derived C.

Peatland pools present a unique biogeochemical environment which, due to their headwater location, receive the same C inputs as systems such as the Black Burn, yet have much longer residence times over which transformations can occur. They are well documented as sources of CO_2 and CH_4 to the atmosphere, with reported annual C release from open water pools in boreal environments of >100 g C m^{-2} yr^{-1} (Pelletier et al., 2014). In this study, upscaling from in-situ exposure experiments over 9 days, photochemical production of CO_2 accounted for 3.2 ± 0.4 and 4.2 ± 0.4 g C m^{-2} yr^{-1} in pools with high and low C concentrations, respectively. Furthermore, photo-processing accounted for up to 51% of total C processing in peatland pool systems at one study site (Cross Lochs). Within the continuum of inland waters, peatland pools therefore appear to be a hot spot for photochemical processing (Figure 6.3).

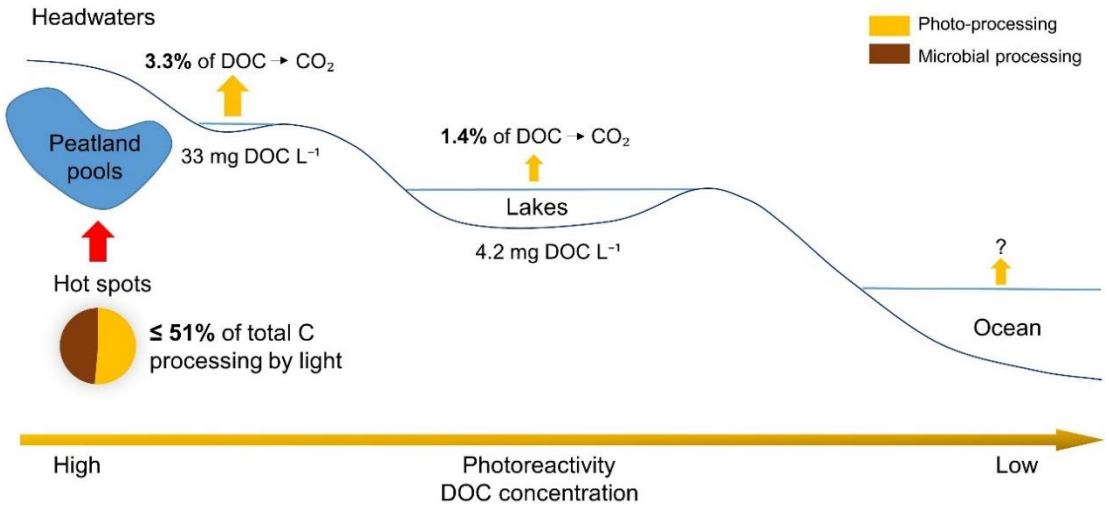

Figure 6.3 Conceptual model of photo-processing of aquatic DOC based upon the results of this research. Peatland pools are shown as a potential hot spot for in-situ processing within

the continuum of inland waters. DOC concentrations and DOC-CO_2 percentage conversions in the headwater versus the lake are derived from data collected in the year-long study in Chapter 4. After Cory et al. (2014).

In-situ experiments conducted in this study determined light driven processing to account for between 33 and 51% of total C processing (in peatland pools at Red Moss and Cross Lochs, respectively). These estimates can be directly compared to studies by Cory et al. (2014), who determined that a higher percentage (70-85%) of C cycling could be attributed to light driven processing in arctic aquatic systems, and by Koehler et al. (2014) who determined that <10% of C processing was due to light exposure in a Swedish study of lakes and reservoirs. Clearly there are large variations in these percentage estimates, which could be attributed to variation in baseline biogeochemical conditions between these systems.

Although the up-scaled estimates for photochemical production of CO_2 were similar between the two peatland pools studied in Chapter 5, there were considerable differences in biogeochemical conditions at the start of the in-situ experiments (Table 6.1). Isotopic values of DOC and DIC in peatland pools were measured in situ for the first time in this study and baseline isotopic values shown to be contrasting, with significantly depleted δ^{13}C-DOC (-29 ‰) values at Red Moss relative to Cross Lochs (-26 ‰). This indicates that the water at Cross Lochs could have been exposed to light over a longer duration than at Red Moss, resulting in a C pool which was recalcitrant to further photochemical processing. The E4:E6 data support this interpretation, with lower values at Cross Lochs suggesting that material was more humified. Further investigations are required within peatland pools and aquatic systems more widely to constrain the timescales over which reactive C is removed and subsequently replenished.

High inter-site variability in biogeochemistry has been reported for peatland pools, with pool morphology suggested as a potential driver of variability (Turner et al., 2016). Although pool depths were comparable, the pool surface areas in this study were considerably different (81

m^2 and 412 m^2 at Red Moss and Cross Lochs, respectively), with the smaller pool having a greater exposure to the surrounding terrestrial environment from which photoreactive peatland C is derived. Spatial variation in water body size is likely to impact pool biogeochemistry, although, with only two pools examined in this study, further investigation is required to understand the indirect impact pool morphology may have on C photo-processing.

6.3 Temporal variation in peatland carbon photoreactivity

A seasonal cycle in photoreactivity at the Black Burn was detected during the year-long study (Chapter 4). Intrinsic photoreactivity was typically higher in the winter, due to the combined effects of increased rainfall mobilising labile material from the peat soil profile and minimal light exposure. This seasonal pattern has been observed in previous studies of C photoreactivity in headwater systems (Franke et al., 2012; Vachon et al., 2016) and is further supported by studies which have detected a winter peak in $SUVA_{254}$ (Wallin et al., 2015). Seasonal peaks in irradiance occur in the summer months and therefore there is disparity between the time of maximum photoreactivity of aquatic material and potential for it to be transformed. Cory et al. (2015) suggest that low flow conditions on clear sunny days provide the optimum conditions for photoreactivity, yet these conditions are atypical of Scottish peatland environments for much of the year.

During the year-long study at the Black Burn, there was a summer peak in photoreactivity measured in August, which coincided with low flow conditions and relatively high PAR (Figure 6.4). This occasion may have provided an opportunity for in-situ photo-processing within the headwater system and the downstream environments into which it drains. Elevated water temperature measured at this time of year (13.6°C compared to year-long mean of 8.3 ± 4.5°C) may have further enhanced potential for photo-processing, as one of the key findings of Chapter 3 was that temperature exerted a significant control on photoreactivity of Black Burn water samples. However, due to lack of in-situ measurements of photo-processing and use of temperature controlled experimental conditions in the year-long study, these assertions

remain speculative and further investigation would be required to determine temperature driven hot moments for photo-processing within peatland draining aquatic systems.

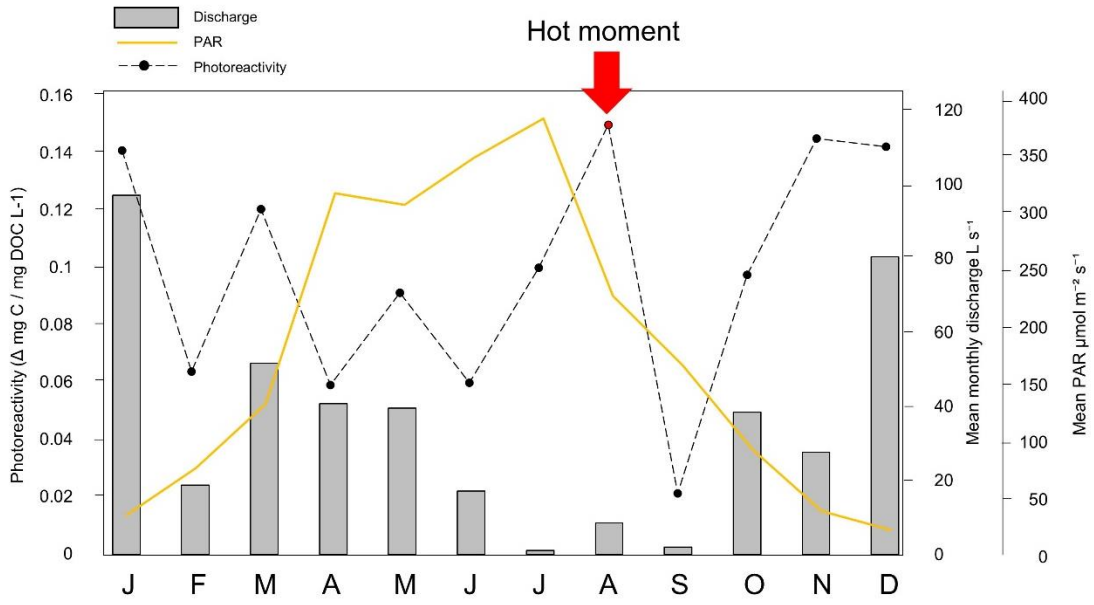

Figure 6.4 Potential hot moment for in-situ photo-processing of C in the Black Burn at Auchencorth Moss. Photoreactivity determined from the year-long study is shown in relation to measured mean monthly discharge and PAR data.

Photoreactivity in this study was measured across a one year period, which limits identification of hot moments for photo-processing. Although interannual variability in total aquatic C export was low in relation to other flux terms within the NECB at Auchencorth Moss during a 5 year study, both air temperature and precipitation were determined to be important drivers of C export (Dinsmore et al., 2013). The year in which this study was conducted was characterised by lower than average rainfall (1015 mm in 13 months, compared to a 6 year annual mean of 1155 mm). Higher mean annual rainfall could provide a greater soil flushing effect within the catchment whereby more photoreactive material would enter the aquatic environment. If this rainfall was timed in summer, hot moments for photo-processing may follow and thus it is important to measure photoreactivity over longer timescales to improve understanding of the likelihood of such occurrences.

One important finding to come from the Black Burn based studies is the significance of rainfall events and subsequent changes to discharge in delivering both higher concentrations of DOC and photoreactive C to peatland headwaters as reported in Chapter 3 and 4, respectively. During a winter rainfall event in which 19.6 mm of rainfall was recorded over 31 hours, a novel lignin phenol data set indicated that hydrological flow paths in the upper catchment were activated and woody, highly photoreactive material was subsequently delivered to the Black Burn. Ad:$Al_{v,s}$ data suggested that this material was less degraded compared to samples collected during the year-long study. This observation is in contrast to the findings of Ward et al. (2012) where Ad:Al ratios increased with discharge, indicating that rapidly mobilised lignin was more degraded than during base flow conditions. Although the study was not in a peat catchment, it demonstrates a need for further data regarding the impact of rainfall events in mobilising fresh, photoreactive material from different catchments, as there is likely to be considerable heterogeneity as a function of catchment specific characteristics, including topography and flow path configuration and soil type.

Antecedent moisture conditions may also play an important role in determining the potential flushing effect of rainfall events and delivery of photoreactive material to headwaters. During a summer rainfall event at the Black Burn, when 3.2 mm of rainfall was recorded, there was no discernible flushing effect and both discharge and sample photoreactivity remained low throughout the sample collection period. Clearly the magnitude and timing of this event was very different to the winter rainfall event and thus they are not directly comparable. The summer event sampled was preceded by a notable length (~ 2 weeks) of low discharge, then a flow event peaking at 12 L s^{-1} on the day before sample collection (Figure 4.9). Different event responses depending on dry or wet antecedent conditions have been observed for aquatic DOC concentrations during summer rainfall events in a comparable Scottish peatland catchment (Tunaley et al., 2016). Tunaley et al. (2016) determined that DOC peaks during summer events occurring in wet antecedent conditions were limited, whereas in dry antecedent conditions

small increases in discharge caused large increases in DOC concentrations due to flushing of SOC. Measuring photoreactivity across rainfall events with different antecedent moisture conditions would help towards identifying hot moments for aquatic photo-processing.

6.4 The importance of the photochemical pathway in peatland carbon budgets

Peatlands deliver photoreactive material to aquatic systems although, as previously discussed, the photoreactivity of this input varies in space and time. It is challenging to determine the overall importance of the photochemical pathway in peatland C budgets due to uncertainties in upscaling and lack of long term data sets regarding peatland aquatic C photoreactivity. However, despite these uncertainties, up-scaled C processing based on measurements at Cross Lochs during the in-situ field experiments conducted in Chapter 5 were compared to a recent NECB study at the same catchment, in which the site was determined to be a net C sink of −50 g C-CO_2 eq m^{-2} y^{-1} (Levy and Gray, 2015). The data from the present study suggest that the photochemical pathway contributes a source of C of ~0.10 ± 0.01 g C-CO_2 eq m^{-2} y^{-1}, accounting for 51% of total C processing in peatland pools. When combined with microbial processing estimates, the total source of C from peatland pools is ~0.20 ± 0.02 g C-CO_2 eq m^{-2} y^{-1}. Clearly this term is small in comparison to the overall NECB of the peatland, however peatland pools within the catchment account for < 3% of the total surface area. In catchments with higher areal coverage of pool systems, this term would contribute more to overall budgets and could contribute to a reduction of the C sink strength of peatlands, as suggested by Pelletier et al. (2014).

The connectivity of aquatic systems means that the C emissions associated with photo-processing of peatland derived material may not take place within peatland catchments, instead occurring later in the aquatic continuum (Figure 6.3). These ‘off-site’ emissions have implications for the C budgets of downstream environments, rather than for the peatland itself (Evans et al., 2015). In Scotland, the furthest distance from land to sea is < 80 km, with a maximum river length of 188 km (Harley et al., 2015) and thus transit time of peatland derived

C in the freshwater continuum is short compared to continental systems such as peatlands in Minnesota (Battaglia et al., 2012) and West Siberia (Sheng et al., 2004). This may mean that processing in estuarine systems and the marine environment is disproportionately more important for C derived from sites investigated in this study, particularly the Black Burn. CO_2 emissions from a mid-estuarine environment in Scotland were estimated at 13.8×10^6 kg C yr^{-1} (Harley et al., 2015) and significant removal of terrestrially derived DOC (including DOC from anthropogenic sources such as wastewater) has been observed in UK estuarine systems (Ahad et al., 2006; Spencer et al., 2007). Although flocculation to sediment and adsorption processes account for part of this loss (Amon and Meon, 2004; Spencer et al., 2007), oxidation via photochemical and microbial pathways has also been suggested to be considerable (Ahad et al., 2008). Determining the fate of peatland derived C and its potential importance in the C budgets of aquatic systems across the continuum of waters from source to sea should be an important future research focus.

6.5 Climate change and anthropogenic impacts on carbon photo-processing

DOC concentrations in freshwaters have doubled across the UK since the 1980s (Evans et al., 2005; Monteith et al., 2007; Watts et al., 2015). This observation is part of a wider trend across the Northern hemisphere in which DOC concentrations have increased in the majority of monitored surface waters in Europe and North America. Data from Chapters 3 and 4 showed that the magnitude of DOC photo-processing in headwater stream samples was controlled partly by initial DOC concentration. The results of this study therefore suggest that as more DOC is delivered to aquatic systems, the potential for C transformation via the photochemical pathway is increased. Using the predicted worst case climate scenario for Sweden until 2030, Weyhenmeyer et al. (2016) forecast a factor of 1.3 increase in a_{420} in freshwaters (a_{420} used here as a proxy for CDOM), suggesting that the chromophoric fraction of C most susceptible to photo-processing will increase. Other studies also predict a continuation of the upward trend in DOC concentration due to a range of climate related hydrological factors including

increased frequency and magnitude of drought (e.g. Tang et al., 2013), changes in water yield (e.g. Kicklighter et al., 2013) and timing and magnitude of precipitation (e.g. Weyhenmeyer et al., 2016).

Rainfall events, which are associated with increased mobilisation of C from the terrestrial to aquatic environment, were shown in Chapter 4 to load peatland headwater streams with photoreactive material, particularly in the winter. Anticipated climate changes have the potential to alter precipitation patterns (Edenhofer et al., 2014), with more intense summer rainfall events predicted in the UK by modelling studies (Fowler and Ekström, 2009; Kendon et al., 2014). In conjunction with light exposure and increased temperatures, these changes will affect soil decomposition rates and hydrological processes in peatland catchments (Capell et al., 2013) and will likely increase loading of DOC, including forms of photoreactive C, to aquatic systems (Clark et al., 2010; Monteith et al., 2007; Weyhenmeyer et al., 2016). Thus peatland catchments may be expected to act increasingly as a source of atmospheric C. Monitoring changes to DOC concentration and composition in relation to the timing of rainfall events will be important in understanding future changes to the magnitude of aquatic C processing.

Although rainfall events are likely to increase loading of DOC to aquatic systems as a function of climate change, the effect of climate induced temperature increases are less clear. Laudon et al. (2012) suggest that the long-term trajectory of aquatic DOC may depend largely on the mean air temperature (MAT). However, they identify areas with an MAT of 0 to 3°C as optimum for DOC production. Therefore, warmer conditions in the mid to high latitudes with a MAT above 3°C will likely result in decreasing DOC concentrations in the future due to increased rates of mineralisation, whereas in regions that have a MAT <0-3°C, DOC concentrations are predicted to increase (Laudon et al., 2012). Results from Chapter 3 showed that temperature increases resulted in enhanced photoreactivity of aquatic C in headwater stream samples. Thus, whilst the effect of warming on DOC concentrations may vary

regionally, data from this study suggest that higher MATs will increase the overall likelihood for photo-processing of aquatic DOC.

Climate warming in the high latitudes due to the effects of polar amplification is expected to result in permafrost degradation across regions of Arctic and sub-arctic peatland (Vonk et al., 2015). Permafrost thaw creates freshwater environments to which C mobilised from the surrounding SOC pool is delivered (Laurion et al., 2010; Vonk et al., 2015). Photochemical and microbial transformations in aquatic environments have the potential to release C to the atmosphere in the form of CO_2 and CH_4 (Laurion et al., 2010). Results from in-situ experiments in Chapter 5 showed that up to 45 g CO_2 eq m^{-2} yr^{-1} can be produced in the water column of peatland pools and that they act as hotspots of biogeochemical processing in relation to the wider peatland catchment. With an estimated surface permafrost C store (0–3 m depth) of 1035 ± 150 PgC (Schuur et al., 2015), the magnitude of C release from newly formed aquatic systems could be globally significant and permafrost thaw been identified as one of the key positive feedback mechanisms induced by climate change (Koven et al., 2011).

Results from Chapter 3 of this study which show considerable temperature sensitivity of photo-processing suggest that this pathway may be important at low latitudes, for example in aquatic systems draining tropical peatlands. Tropical systems contain 89,000 TgC and export considerable volumes of C to aquatic systems (Moore et al., 2013). A study of the River Congo, which drains one of the fourth largest wetland areas globally (Lawson et al., 2014), showed that aquatic C was highly photoreactive (Spencer et al., 2009). Median water temperatures in tropical systems are ~25°C, considerably higher than the median of ~14°C for temperate aquatic environments (Van Vliet et al., 2013). Given the difference in water temperature, in addition to the greater exposure to solar radiation received by aquatic C, photo-processing in tropical systems may be a globally significant C emissions source. Aquatic processing in tropical peatlands subject to disturbance, such a deforestation and drainage, may

be particularly important as 32% increases in the fluvial organic C flux have been reported from disturbed peatland systems in south-east Asia (Moore et al., 2013).

Many UK peatlands, including sites used in this study, have been subject to anthropogenic disturbance. Peatland disturbance takes numerous forms, including peat extraction, track construction, burning for maintenance of heather stands and optimise conditions for grouse, afforestation, artificial drainage and grazing by livestock (Parry et al., 2014). Such activities have been linked with a reduction in the C sequestration potential of peatlands (Turetsky et al., 2002; Yu et al., 2013) and there has been a move to restore peatlands to a more 'natural' state to avoid increased C losses. A key restoration technique used in many peatland catchments is to re-establish hydrological functioning through the blocking of drainage ditches (Parry et al., 2014; Wilson et al., 2011), which were originally cut to lower the water table in an attempt to make the land viable for agriculture. The aim of ditch blocking (using e.g. peat from the surrounding area, plastic piling or heather bales) is to increase the height of the water table, which results in water pooling behind the blocking material (Parry et al., 2014).

Results reported in Chapter 5 suggest that areas of standing water on the peat surface act as C reactors relative to the surrounding landscape. This view is supported by previous studies which have determined that natural peatland pools have higher CH_4 output and lower CO_2 uptake than terrestrial peatland environments (McEnroe et al., 2009; Pelletier et al., 2014). Artificial pools created by drainage ditch blocking are likely to function in a similar manner biogeochemically, acting as a net source of C to the atmosphere. Over time, these pools fill in with natural peatland vegetation and serve to increase the C sink of the peatland (Peacock et al., 2013). However, in the short term, such restoration measures may lead to an increase in C losses from peatland catchments and, due to the widespread implementation of such techniques, may have a significant impact on peatland C budgets. To counteract this potential negative consequence, preventative measures (such as overflow channels) can be employed to reduce the depth and area of pools formed in blocked ditches (Parry et al., 2014). A key

recommendation from this study is that preventative measures are employed to minimise the formation of artificial pools in all restoration activities where drainage ditch blocking is undertaken.

A suite of other peatland restoration methods are being implemented in addition to drainage ditch blocking. In the Flow Country of Northern Scotland, which encompasses the Cross Lochs site used in Chapter 5, a large scale forest to bog restoration programme coordinated by the RSPB is taking place (Krachler et al., 2016; Muller and Tankéré-Muller, 2012). This aims to revert 400 km^2 of land planted for commercial forestry in the 1980s to its former treeless peatland state (Muller and Tankéré-Muller, 2012). Clear cutting across large areas of peatland has been associated with short term increases in DOC export from peat. Export measurements from peatlands in Finland show average extra export of >400 kg ha yr^{-1} from fertile minerotrophic peatland forest sites in the three years post-felling (Nieminen et al., 2015). Such increases would result in DOC entering freshwaters which could be subject to photochemical or microbial processing. Therefore, whilst beneficial for the C balance of the peatland over the long term (Hargreaves et al., 2003), deforestation has the potential to result in short term C release from peatlands undergoing restoration.

Clear cutting will also increase light availability at the ground surface which would have previously been limited due to canopy light interception by the planted confers (Lieffers et al., 1999). This may lead to increased potential of photochemical transformation of C in the small pools and streams that form on the peat surface, which could contribute to an increase in emissions from the peatland. However, whilst unlikely to offset the enhanced C sequestration potential of a restored peatland, there is a dearth of studies which have monitored changes to light availability in relation to photochemical C processing in peatlands. Studies have instead focussed on changes to albedo in the wider peatland landscape in relation to clear cutting. (Lohila et al., 2010). Due to the lower albedo of conifer trees relative to peatland vegetation, removing trees from peatlands induces a negative radiative forcing (i.e. a cooling effect).

Therefore, in tandem with increased C storage, clear cutting of peatlands can help to mitigate climate change through changes in surface reflectivity (Betts, 2000).

One of the greatest uncertainties for the future importance of aquatic C photoprocessing is changes to insolation expected with climate change (Bais et al., 2015). High levels of UV radiation associated with ozone breakdown have been avoided through the successful implementation of the Montreal Protocol on Substances that Deplete the Ozone Layer in 1987 (Williamson et al., 2014). However, due to the long life time of chlorofluorocarbons, ozone depletion continues presently and is expected to ~2050 (Williamson et al., 2014). Increased UV associated with ozone depletion could result in higher than normal rates of photoprocessing occurring in aquatic systems over this recovery period. Future changes to cloud formation processes, aerosols and albedo will also affect insolation at the ground surface. A study by Bais et al. (2011) suggests that significant regional differences could emerge in insolation by 2100. Their model predicts that UV radiation will have increased in the tropics and decreased at polar latitudes by the end of the century. High uncertainty in future UV distribution is attributed to simulation of ozone and clouds which are poorly parameterised in global circulation models. Improvements in the parameterisations used in such models would narrow uncertainties and result in a better understanding of the potential changes to insolation and the implications this has for aquatic C processing on a global scale.

Chapter 7 Further Work and Conclusions

7.1 Further work

Biogeochemical cycling of aquatic C is a potentially important source of C to the atmosphere and, as such, further investigations are required to understand the processes that affect this cycle. A number of further field and laboratory studies, building on the results of this study, as outlined below.

7.1.1 Investigating the interaction and reactivity of POC and DOC

Results in Chapter 3 showed that the <0.2 μm fraction of peatland C contributed to gaseous photoproduction, although DOC production from POC was thought to increase DOC concentrations in light exposed unfiltered samples. DOC photoproduction from POC was again observed in the experiments reported in Chapter 5, however the effect of POC photolysis on gaseous production could not be determined due to the experimental set-up, as both DOC and POC were present in the sample. Although not detected in this study, POC production from DOC has also been observed upon light exposure (Porcal et al., 2014) and could present a loss pathway for DOC, either by full oxidation to CO_2 or by flocculation to sediments, in the peatland aquatic environment. To improve understanding of the interaction of POC and DOC and their relative contribution to gaseous photoproduction, further laboratory experiments could be undertaken whereby the particulate C retained on a 0.7 μm filter is re-suspended in deionised water and exposed to light in tandem with a filtered sample representing the DOC fraction and an unfiltered sample containing both POC and DOC. Tracking changes to C species in these three treatments during irradiation experiments using a mass budget approach would yield better understanding of the interplay between POC and DOC upon light exposure and the potential for pathways for C loss from peatland draining aquatic systems.

7.1.2 Continuous measurement of UV visible absorbance

Chapter 4 detailed changes in DOC concentration and composition during rainfall events, suggesting that these events may be important in replenishing the peatland aquatic environment with photoreactive C. However, sampling in this study was limited to two rainfall events of contrasting magnitude, with only the higher rainfall event being associated with input of photoreactive C. Recent developments have seen UV visible absorbance data collected at high temporal resolution in aquatic systems (<15 minutes), through use of in-situ field-based spectrophotometers (Avagyan et al., 2014; Grayson and Holden, 2012; Sandford et al., 2010). Using this method Grayson and Holden (2012) identified rainfall induced changes to absorbance characteristics of stream water prior to increased stream discharge in a UK peatland system. Obtaining high resolution absorbance data in peatland headwater systems over year-long cycles will allow the seasonal and rainfall driven trends in photoreactive material observed in this study to be corroborated. Furthermore, this method may also be able to provide new insights about the drivers of aquatic C cycling when coupled with PAR data and physio-chemical parameters including hydrological flow, temperature and pH (Sandford et al., 2010). High temporal resolution UV visible absorbance and C concentration measurements have the potential to improve estimates of downstream photoreactive C export in headwater catchments.

7.1.3 Isotopic characterisation of aquatic carbon species

Isotopic excursions have been widely used to indicate pathways of C degradation. In Chapter 5 $\delta^{13}C$ isotopes of DOC and DIC were used to determine the effect of light exposure on C cycling within peatland pool water samples, by comparison with unexposed control samples. This method revealed that the DIC pool was significantly moderated by light exposure, although the light effects on the DOC pool were less clear due to simultaneous effects of microbial activity. In order to improve understanding of the effect of light exposure on aquatic C cycling, an important future step would be to characterise the isotopic composition of

gaseous degradation products (CO_2 and CH_4; see Table A2, Appendix A for values measured in laboratory exposure experiments) and POC in addition to the dissolved forms (DOC and DIC) which were characterised in this study. If these analyses were undertaken with use of an additional third treatment in which water samples are sterilised prior to light exposure to remove microbial effects, the degree to which photo-processing and microbial processing contribute to overall C cycling could be distinguished more clearly.

Given the heterogeneity displayed between the two peatland pools investigated in this study, selection of a greater number of pools with varying DOC concentrations and surface areas is advised for future studies (Turner et al., 2016). This would reduce errors derived in upscaling attempts of the C cycling potential of peatland pool systems on a regional basis.

7.1.4 Characterising residence times of carbon in peatland draining aquatic systems

One of the factors that emerged as key in determining the photoreactivity of peatland derived aquatic C was residence time. In this study, it was inferred in Chapter 4 that photoreactivity per unit mass in the headwater stream samples was lower in summer because DOC had been subject to in-situ processing prior to sample collection during low flow conditions. Again in Chapter 5, the initial differences in δ^{13}C-DOC values between the two sample sites were taken to indicate that at Cross Lochs the samples had resided in the peatland pool for longer prior to experimental exposure and thus were less photoreactive. However, direct measurements of water residence time were not obtained at the sites. Previous studies in both lakes and headwater streams have also attributed observed DOC degradation rates, or lack thereof, to water residence times (Kothawala et al., 2015; Webster et al., 2008).

DOC input-output flux data analysed in relation to rainfall and discharge data in a variety of peatland draining aquatic systems would be particularly useful in order to constrain the time available for DOC processing. Whilst there are methods and models available to estimate water residence times (Birkel et al., 2014; Worrall et al., 2014), directly measurements of DOC

input-output would help to quantify catchment specific rates of aquatic C cycling. Incorporating measurements of $\delta^{18}O$ and $\delta^{2}H$ with C species data would give a comprehensive view of the coupling between hydrological processes and biogeochemical cycling in peatland catchments.

7.2 Conclusions

This study aimed to determine the importance of photo-processing in the C budgets of peatland draining aquatic systems by investigating the factors affecting photoreactivity of peatland derived C, the moments in time and space in which photoreactivity is highest and the importance of the process in relation to other C processing pathways. The key findings of the research in relation to this aim are summarised here.

Peatland derived aquatic carbon is highly susceptible to photo-processing.

The biogeochemical composition of C in peatland draining aquatic systems renders it susceptible to photo-processing, as it is enriched in aromatic, terrestrially derived material. Laboratory irradiation experiments conducted over 8 hours showed that the < 0.2 μm fraction was most photoreactive and that photoreactivity increased with water temperature, with significant implications for the many studies which do not make temperature corrections in photodegradation experiments. During ambient sunlight exposure, approximately 1.8 ± 0.4% of initial DOC in water samples was oxidised directly to CO_2 over exposure durations comparable to mean water transit times in the freshwater continuum and thus this pathway has the potential for significant C loss from peatland draining aquatic systems.

Spatial and temporal drivers affect the delivery of photoreactive carbon to peatland draining aquatic systems.

During a year-long study of a headwater stream and a reservoir, both located in catchments with high peatland cover, DOC photoreactivity was considerably lower at the reservoir system.

This was attributed to longer water residence times in the reservoir rendering a higher proportion of the DOC recalcitrant to photo-processing. Within the headwater stream system, seasonal cycles and rainfall events appeared to be major controls on export of photoreactive DOC from the catchment, with lignin phenol data suggesting that hydrological pathways in the upper catchment were activated during a heavy winter rainfall event, resulting in transport of fresh, photoreactive DOC from woody vegetation to the stream. Disparity between timing of most photoreactive C inputs to the stream and peaks in temperature and irradiance mean that photo-processing may not be important in some peatland aquatic C budgets for much of the year.

In comparison to microbial processing of carbon, photo-processing is an equally important carbon transformation pathway in peatland pools.

During experiments in which unfiltered water samples were exposed in-situ for 9 days at two peatland pool sites alongside unexposed control samples, photo-processing was determined to account for up to 51% of total C processing. However, due to interacting effects between photo-processing and microbial processing, the two pathways cannot be considered as separate and both contribute to significant processing of peatland aquatic C. Peatland pool environments within the one study catchment were estimated to reduce the overall C sequestration potential of the peatland by 0.20 g C-CO_2 eq m^{-2} yr^{-1}, despite pools accounting for <3% of the land surface area. Whilst this term is small in comparison with the overall peatland C budget, processing in aquatic systems may play an increasingly important role in the release of C from peatlands, especially under future climate change scenarios involving changes to temperature and hydrology.

References

Adams, H. E., Crump, B. C. and Kling, G. W.: Temperature controls on aquatic bacterial production and community dynamics in arctic lakes and streams, Environ. Microbiol., 12(5), 1319–1333, doi:10.1111/j.1462-2920.2010.02176.x, 2010.

Ahad, J. M. E., Ganeshram, R. S., Spencer, R. G. M., Uher, G., Gulliver, P. and Bryant, C. L.: Evidence for anthropogenic 14C-enrichment in estuarine waters adjacent to the North Sea, Geophys. Res. Lett., 33(8), doi:10.1029/2006GL025991, 2006.

Ahad, J. M. E., Barth, J. A. C., Ganeshram, R. S., Spencer, R. G. M. and Uher, G.: Controls on carbon cycling in two contrasting temperate zone estuaries: The Tyne and Tweed, UK, Estuar. Coast. Shelf Sci., 78(4), 685–693, doi:10.1016/j.ecss.2008.02.006, 2008.

Aitkenhead-Peterson, J. A., McDowell, W. H. and Neff, J. C.: Sources, Production, and regulation of allochthonous dissolved organic matter inputs to surface waters, in Aquatic Ecosystems: Interactivity of Dissolved Organic Matter, vol. 6, pp. 25–70., 2002.

Algesten, G., Sobek, S., Bergström, A. K., Ågren, A., Tranvik, L. J. and Jansson, M.: Role of lakes for organic carbon cycling in the boreal zone, Glob. Chang. Biol., 10(1), 141–147, doi:10.1111/j.1365-2486.2003.00721.x, 2004.

Amon, R. M. W. and Meon, B.: The biogeochemistry of dissolved organic matter and nutrients in two large Arctic estuaries and potential implications for our understanding of the Arctic Ocean system, in Marine Chemistry, vol. 92, pp. 311–330., 2004.

Anesio, A. M. and Graneli, W.: Increased photoreactivity of DOC by acidification: Implications for the carbon cycle in humic lakes, Limnol. Oceanogr., 48(2), 735–744, doi:10.4319/lo.2003.48.2.0735, 2003.

Anesio, A. M., Gran??li, W., Aiken, G. R., Kieber, D. J. and Mopper, K.: Effect of humic substance photodegradation on bacterial growth and respiration in lake water, Appl. Environ. Microbiol., 71(10), 6267–6275, doi:10.1128/AEM.71.10.6267-6275.2005, 2005.

Attermeyer, K., Tittel, J., Allgaier, M., Frindte, K., Wurzbacher, C., Hilt, S., Kamjunke, N. and Grossart, H.-P.: Effects of Light and Autochthonous Carbon Additions on Microbial Turnover of Allochthonous Organic Carbon and Community Composition, Microb. Ecol., 69(2), 361–371, doi:10.1007/s00248-014-0549-4, 2015.

Austnes, K., Evans, C. D., Eliot-Laize, C., Naden, P. S. and Old, G. H.: Effects of storm

events on mobilisaton and in-stream processing of dissolved organic matter (DOM) in a Welsh peatland catchment, Biogeochemistry, 99(1), 157–173, doi:10.1007/s10533-009-9399-4, 2010.

Avagyan, A., Runkle, B. R. K. and Kutzbach, L.: Application of high-resolution spectral absorbance measurements to determine dissolved organic carbon concentration in remote areas, J. Hydrol., 517, 435–446, doi:10.1016/j.jhydrol.2014.05.060, 2014.

Bais, A. F., Tourpali, K., Kazantzidis, A., Akiyoshi, H., Bekki, S., Braesicke, P., Chipperfield, M. P., Dameris, M., Eyring, V., Garny, H., Iachetti, D., Jöckel, P., Kubin, A., Langematz, U., Mancini, E., Michou, M., Morgenstern, O., Nakamura, T., Newman, P. A., Pitari, G., Plummer, D. A., Rozanov, E., Shepherd, T. G., Shibata, K., Tian, W. and Yamashita, Y.: Projections of UV radiation changes in the 21st century: Impact of ozone recovery and cloud effects, Atmos. Chem. Phys., 11(15), 7533–7545, doi:10.5194/acp-11-7533-2011, 2011.

Bais, A. F., McKenzie, R. L., Bernhard, G., Aucamp, P. J., Ilyas, M., Madronich, S. and Tourpali, K.: Ozone depletion and climate change: impacts on UV radiation., Photochem. Photobiol. Sci., 14(1), 19–52, doi:10.1039/c4pp90032d, 2015.

Ball, D. F.: Loss-on-ignition as an estimate of organic matter and organic carbon in non-calcareous soils, J. Soil Sci., 15, 84–92, doi:10.1111/j.1365-2389.1964.tb00247.x, 1964.

Bange, H. W. and Uher, G.: Photochemical production of methane in natural waters: Implications for its present and past oceanic source, Chemosphere, 58, 177–183, doi:10.1016/j.chemosphere.2004.06.022, 2005.

Bastviken, D., Tranvik, L. J., Downing, J. A., Crill, P. M. and Enrich-Prast, A.: Freshwater methane emissions offset the continental carbon sink., Science, 331, 50, doi:10.1126/science.1196808, 2011.

Battaglia, L. L., Woodrey, M. S., Peterson, M. S., Dillon, K. S. and Visser, J. M.: Wetland Ecosystems of the Northern Gulf Coast BT - Wetland Habitats of North America: Ecology and Conservation Concerns, in Wetland Habitats of North America: Ecology and Conservation Concerns, pp. 75–88. [online] Available from: http://books.google.com/books?hl=en&lr=&id=hvS5xljxuL4C&oi=fnd&pg=PA75&dq=wetlands+of+the+northern+gulf+coast&ots=7WFX45mHPY&sig=9u8MgWQLnMUlkBIBpIeqQ44QJ6c\npapers3://publication/uuid/C3759528-7679-4020-B4A4-E965E4CCEDC4, 2012.

Battin, T. J., Kaplan, L. a., Findlay, S., Hopkinson, C. S., Marti, E., Packman, A. I., Newbold, J. D. and Sabater, F.: Biophysical controls on organic carbon fluxes in fluvial networks, Nat. Geosci., 2(8), 595–595, doi:10.1038/ngeo602, 2009a.

Battin, T. J., Luyssaert, S., Kaplan, L. a., Aufdenkampe, A. K., Richter, A. and Tranvik, L. J.: The boundless carbon cycle, Nat. Geosci., 2(9), 598–600, doi:10.1038/ngeo618, 2009b.

Beetz, S., Liebersbach, H., Glatzel, S., Jurasinski, G., Buczko, U. and Höper, H.: Effects of land use intensity on the full greenhouse gas balance in an Atlantic peat bog, Biogeosciences, 10(2), 1067–1082, doi:10.5194/bg-10-1067-2013, 2013.

Bell, N. G. A., Michalchuk, A. A. L., Blackburn, J. W. T., Graham, M. C. and Uhrín, D.: Isotope-Filtered 4D NMR Spectroscopy for Structure Determination of Humic Substances, Angew. Chemie - Int. Ed., 54(29), 8382–8385, doi:10.1002/anie.201503321, 2015.

Benner, R. and Kaiser, K.: Biological and photochemical transformations of amino acids and lignin phenols in riverine dissolved organic matter, Biogeochemistry, 102, 209–222, doi:10.1007/s10533-010-9435-4, 2011a.

Benner, R. and Kaiser, K.: Biological and photochemical transformations of amino acids and lignin phenols in riverine dissolved organic matter, Biogeochemistry, 102(1), 209–222, doi:10.1007/s10533-010-9435-4, 2011b.

Benner, R., Louchouarn, P. and Amon, R. M. W.: Terrigenous dissolved organic matter in the Arctic Ocean and its transport to surface and deep waters of the North Atlantic, Global Biogeochem. Cycles, 19, 1–11, doi:10.1029/2004GB002398, 2005.

Bertilsson, S. and Jones, J. B.: Supply of dissolved organic matter to aquatic ecosystems: Autochthonous sources, in Aquatic Ecosystems: Interactivity of Dissolved Organic Matter, pp. 3–24., 2003.

Bertilsson, S. and Tranvik, L. J.: Photochemically produced carboxylic acids as substrates for freshwater bacterioplankton, Limnol. Oceanogr., 43(5), 885–895, doi:10.4319/lo.1998.43.5.0885, 1998.

Bertilsson, S. and Tranvik, L. J.: Photochemical transformation of dissolved organic matter in lakes, Limnol. Oceanogr., 45(4), 753–762, doi:10.4319/lo.2000.45.4.0753, 2000.

Betts, R. A.: Offset of the potential carbon sink from boreal forestation by decreases in surface albedo., Nature, 408(6809), 187–190, doi:10.1038/35041545, 2000.

Billett, M. F., Dinsmore, K.J., Garnett, M.H.: Should aquatic CO2 evasion be included in contemporary carbon budgets for peatland ecosystems?, Ecoystems, 18(3), 471–480, 2015.

Billett, M. F. and Harvey, F. H.: Measurements of CO2 and CH4 evasion from UK peatland headwater streams, Biogeochemistry, 114(1–3), 165–181, doi:10.1007/s10533-012-9798-9, 2013.

Billett, M. F., Deacon, C. M., Palmer, S. M., Dawson, J. J. C. and Hope, D.: Connecting organic carbon in stream water and soils in a peatland catchment, J. Geophys. Res. Biogeosciences, 111(2), doi:10.1029/2005JG000065, 2006.

Billett, M. F., Garnett, M. H. and Harvey, F.: UK peatland streams release old carbon dioxide to the atmosphere and young dissolved organic carbon to rivers, Geophys. Res. Lett., 34(23), 2–7, doi:10.1029/2007GL031797, 2007.

Billett, M. F., Charman, D. J., Clark, J. M., Evans, C. D., Evans, M. G., Ostle, N. J., Worrall, F., Burden, A., Dinsmore, K. J., Jones, T., McNamara, N. P., Parry, L., Rowson, J. G. and Rose, R.: Carbon balance of UK peatlands: current state of knowledge and future research challenges, Clim. Res., 45, 13–29, doi:10.3354/cr00903, 2010.

Billett, M. F. F., Palmer, S. M. M., Hope, D., Deacon, C., Storeton-West, R., Hargreaves, K. J. J., Flechard, C. and Fowler, D.: Linking land-atmosphere-stream carbon fluxes in a lowland peatland system, Global Biogeochem. Cycles, 18(1), GB1024, doi:10.1029/2003GB002058, 2004.

Birkel, C., Soulsby, C. and Tetzlaff, D.: Integrating parsimonious models of hydrological connectivity and soil biogeochemistry to simulate stream DOC dynamics, J. Geophys. Res. Biogeosciences, 119(5), 1030–1047, doi:10.1002/2013JG002551, 2014.

Blodau, C.: Carbon cycling in peatlands — A review of processes and controls, Environ. Rev., 10(2), 111–134, doi:10.1139/a02-004, 2002.

Bloom, A. A., Lee-Taylor, J., Madronich, S., Messenger, D. J., Palmer, P. I., Reay, D. S. and McLeod, A. R.: Global methane emission estimates from ultraviolet irradiation of terrestrial plant foliage., New Phytol., 187, 417–425, doi:10.1111/j.1469-8137.2010.03259.x, 2010.

C. Tunaley, D. Tetzlaff, J. Lessels, and C. S.: Linking high-frequency DOC dynamics to the age of connected water sources, Water Resour. Res., doi:10.1002/2015WR018419, 2016.

Capell, R., Tetzlaff, D. and Soulsby, C.: Will catchment characteristics moderate the

projected effects of climate change on flow regimes in the Scottish Highlands?, Hydrol. Process., 27, 687–699, 2013.

Catalán, N., Marcé, R., Kothawala, D.N., Tranvik, L. J.: Organic carbon decomposition rates controlled by water retention time across inland waters, Nat. Geosci., doi:doi:10.1038/ngeo2720, 2016.

Ciais, P., Sabine, C., Bala, G., Bopp, L., Brovkin, V., Canadell, J., Chhabra, a., DeFries, R., Galloway, J., Heimann, M., Jones, C., Quéré, C. Le, Myneni, R. B., Piao, S., Thornton, P., France, P. C., Willem, J., Friedlingstein, P. and Munhoven, G.: 2013: Carbon and Other Biogeochemical Cycles, Clim. Chang. 2013 Phys. Sci. Basis. Contrib. Work. Gr. I to Fifth Assess. Rep. Intergov. Panel Clim. Chang., 465–570, doi:10.1017/CBO9781107415324.015, 2013.

Clark, J. M., Lane, S. N., Chapman, P. J. and Adamson, J. K.: Export of dissolved organic carbon from an upland peatland during storm events: Implications for flux estimates, J. Hydrol., 347(3–4), 438–447, doi:10.1016/j.jhydrol.2007.09.030, 2007.

Clark, J. M., Bottrell, S. H., Evans, C. D., Monteith, D. T., Bartlett, R., Rose, R., Newton, R. J. and Chapman, P. J.: The importance of the relationship between scale and process in understanding long-term DOC dynamics, Sci. Total Environ., 408, 2768–2775, doi:10.1016/j.scitotenv.2010.02.046, 2010.

Cole, J. J., Prairie, Y. T., Caraco, N. F., McDowell, W. H., Tranvik, L. J., Striegl, R. G., Duarte, C. M., Kortelainen, P., Downing, J. A., Middelburg, J. J., Melack, J.: Plumbing the global carbon cycle: Integrating inland waters into the terrestrial carbon budget, Ecosystems, 10, 171–184, doi:10.1007/s10021-006-9013-8, 2007.

Cory, R. M. and McKnight, D. M.: Fluorescence spectroscopy reveals ubiquitous presence of oxidized and reduced quinones in dissolved organic matter, Environ. Sci. Technol., 39(21), 8142–8149, doi:10.1021/es0506962, 2005.

Cory, R. M., McKnight, D. M., Chin, Y. P., Miller, P. and Jaros, C. L.: Chemical characteristics of fulvic acids from Arctic surface waters: Microbial contributions and photochemical transformations, J. Geophys. Res. Biogeosciences, 112(4), doi:10.1029/2006JG000343, 2007.

Cory, R. M., Ward, C. P., Crump, B. C. and Kling, G. W.: Sunlight controls water column processing of carbon in arctic fresh waters, Science (80-.)., 345(6199), 925–928,

doi:10.1126/science.1253119, 2014.

Dawson, J.C.C., Bakewell, C., Billett, M. F.: Is in-stream processing an important control on spatial changes in carbon fluxes in headwater catchments?, Sci. Total Environ., 265(1–3), 27–39, 2001.

Dawson, J. J. C., Billett, M. F., Neal, C. and Hill, S.: A comparison of particulate, dissolved and gaseous carbon in two contrasting upland streams in the UK, J. Hydrol., 257(1–4), 226–246, doi:10.1016/S0022-1694(01)00545-5, 2002.

Dawson, J. J. C., Soulsby, C., Tetzlaff, D., Hrachowitz, M., Dunn, S. M. and Malcolm, I. A.: Influence of hydrology and seasonality on DOC exports from three contrasting upland catchments, Biogeochemistry, 90(1), 93–113, doi:10.1007/s10533-008-9234-3, 2008.

Dinsmore, K. J., Billett, M.F., Dyson, K.E.: Temperature and precipitation drive temporal variability in aquatic carbon and GHG concentrations and fluxes in a peatland catchment, Glob. Chang. Biol., 19(7), 2133–2148, doi:10.1111/gcb.12209, 2013.

Dinsmore, K. J. and Billett, M. F.: Continuous measurement and modeling of CO2 losses from a peatland stream during stormflow events, Water Resour. Res., 44(12), doi:10.1029/2008WR007284, 2008.

Dinsmore, K. J., Billett, M. F., Skiba, U. M., Rees, R. M., Drewer, J. and Helfter, C.: Role of the aquatic pathway in the carbon and greenhouse gas budgets of a peatland catchment, Glob. Chang. Biol., 16, 2750–2762, doi:10.1111/j.1365-2486.2009.02119.x, 2010.

Dinsmore, K. J., Billett, M. F. and Dyson, K. E.: Temperature and precipitation drive temporal variability in aquatic carbon and GHG concentrations and fluxes in a peatland catchment, Glob. Chang. Biol., 19, 2133–2148, doi:10.1111/gcb.12209, 2013.

Drewer, J., Lohila, A., Aurela, M., Laurila, T., Minkkinen, K., Penttilä, T., Dinsmore, K. J., McKenzie, R. M., Helfter, C., Flechard, C., Sutton, M. A. and Skiba, U. M.: Comparison of greenhouse gas fluxes and nitrogen budgets from an ombotrophic bog in Scotland and a minerotrophic sedge fen in Finland, Eur. J. Soil Sci., 61(5), 640–650, doi:10.1111/j.1365-2389.2010.01267.x, 2010.

Edenhofer, O., Pichs-Madruga, R. Sokona, Y., Farahani, E., Kadner, S., Seyboth, K., Adler, A., Baum, I., Brunner, S., Eickemeier, P., Kriemann, B., Savolainen, J., Schlömer, S., von Stechow, C., Zwickel, T. and Minx, J. C.: IPCC, 2014: Summary for Policymakers., 2014.

Eimers, M. C., Buttle, J. and Watmough, S. a: Influence of seasonal changes in runoff and extreme events on dissolved organic carbon trends in wetland- and upland-draining streams, Can. J. Fish. Aquat. Sci., 65(5), 796–808, doi:10.1139/f07-194, 2008.

Estapa, M. L. and Mayer, L. M.: Photooxidation of particulate organic matter, carbon/oxygen stoichiometry, and related photoreactions, Mar. Chem., 122(1–4), 138–147, doi:10.1016/j.marchem.2010.06.003, 2010.

Evans, C. D., Chapman, P. J., Clark, J. M., Monteith, D. T., Cresser, M. S.: Alternative explanations for rising dissolved organic carbon export from organic soils, Glob. Chang. Biol., 12(11), 2044–2053, doi:10.1111/j.1365-2486.2006.01241.x, 2006.

Evans, C. D., Monteith, D. T. and Cooper, D. M.: Long-term increases in surface water dissolved organic carbon: Observations, possible causes and environmental impacts, Environ. Pollut., 137(1), 55–71, doi:10.1016/j.envpol.2004.12.031, 2005.

Evans, C. D., Renou-Wilson, F. and Strack, M.: The role of waterborne carbon in the greenhouse gas balance of drained and re-wetted peatlands, Aquat. Sci., 1–18, doi:10.1007/s00027-015-0447-y, 2015.

Farjalla, V. F., Amado, A. M., Suhett, A. L. and Meirelles-Pereira, F.: DOC removal paradigms in highly humic aquatic ecosystems, Environ. Sci. Pollut. Res., 16(5), 531–538, doi:10.1007/s11356-009-0165-x, 2009.

Fellman, J. B., Hood, E., Edwards, R. T. and D'Amore, D. V.: Changes in the concentration, biodegradability, and fluorescent properties of dissolved organic matter during stormflows in coastal temperate watersheds, J. Geophys. Res. Biogeosciences, 114(1), doi:10.1029/2008JG000790, 2009.

Fellman, J. B., Hood, E. and Spencer, R. G. M.: Fluorescence spectroscopy opens new windows into dissolved organic matter dynamics in freshwater ecosystems: A review, Limnol. Oceanogr., 55, 2452–2462, doi:10.4319/lo.2010.55.6.2452, 2010.

Fenner, N., Freeman, C., Hughes, S. and Reynolds, B.: Molecular weight spectra of dissolved organic carbon in a rewetted Welsh peatland and possible implications for water quality, Soil Use Manag., 17(2), 106–112, doi:10.1079/SUM200162, 2001.

Fenner, N., Freeman, C. and Reynolds, B.: Observations of a seasonally shifting thermal optimum in peatland carbon-cycling processes; implications for the global carbon cycle and

soil enzyme methodologies, Soil Biol. Biochem., 37(10), 1814–1821, doi:10.1016/j.soilbio.2005.02.032, 2005.

Fiedler, S., Höll, B. S., Freibauer, A., Stahr, K., Drösler, M., Schloter, M. and Jungkunst, H. F.: Particulate organic carbon (POC) in relation to other pore water carbon fractions in drained and rewetted fens in Southern Germany, Biogeosciences Discuss., 5(3), 1615–1623, doi:SRef-ID: 1810-6285/bgd/2008-5-2049, 2008.

Fowler, H. J. and Ekstr??m, M.: Multi-model ensemble estimates of climate change impacts on UK seasonal precipitation extremes, in International Journal of Climatology, vol. 29, pp. 385–416., 2009.

Franke, D., Hamilton, M. W. and Ziegler, S. E.: Variation in the photochemical lability of dissolved organic matter in a large boreal watershed, Aquat. Sci., 74, 751–768, doi:10.1007/s00027-012-0258-3, 2012.

Freeman, C., Evans, C.D., Monteith, D.T., Reynolds, B., Fenner, N.: Export of organic carbon from peat soils., Nature, 412, 785, 2001.

Freeman, C., Fenner, N., Ostle, N. J., Kang, H., Dowrick, D. J., Reynolds, B., Lock, M. a, Sleep, D., Hughes, S. and Hudson, J.: Export of dissolved organic carbon from peatlands under elevated carbon dioxide levels, Nature, 430, 195–198, doi:10.1038/nature02707, 2004.

del Giorgio, P. a. and Cole, J. J.: Bacterial Growth Efficiency in Natural Aquatic Systems, Annu. Rev. Ecol. Syst., 29(1), 503–541, doi:10.1146/annurev.ecolsys.29.1.503, 1998.

Gordon, N. D., T. A. McMahon, B. L. Finlayson, C. J. Gippel, and R. J. N.: Stream Hydrology: An Introduction for Ecologists, Wiley., 2004.

Gorham, E.: Northern peatlands: role in the carbon cycle and probable responses to climatic warming, Ecol. Appl., 1(2), 182–195, doi:10.2307/1941811, 1991.

Grayson, R. and Holden, J.: Continuous measurement of spectrophotometric absorbance in peatland streamwater in northern England: Implications for understanding fluvial carbon fluxes, Hydrol. Process., 26(1), 27–39, doi:10.1002/hyp.8106, 2012.

Groeneveld, M. M., Tranvik, L. J. and Koehler, B.: Photochemical mineralisation in a humic boreal lake: temporal variability and contribution to carbon dioxide production, Biogeosciences Discuss., 12(20), 17125–17152, doi:10.5194/bgd-12-17125-2015, 2015.

Hader, D. P.: Effects of solar UV-B radiation on aquatic ecosystems., Adv. Space Res., 26(12), 2029–2040, doi:http://dx.doi.org/10.1016/S0273-1177(00)00170-8, 2000.

Häder, D.-P. and Sinha, R. P.: Solar ultraviolet radiation-induced DNA damage in aquatic organisms: potential environmental impact., Mutat. Res., 571(1–2), 221–233, doi:10.1016/j.mrfmmm.2004.11.017, 2005.

Häder, D.-P., Williamson, C. E., Wängberg, S.-Å., Rautio, M., Rose, K. C., Gao, K., Helbling, E. W., Sinha, R. P. and Worrest, R.: Effects of UV radiation on aquatic ecosystems and interactions with other environmental factors., Photochem. Photobiol. Sci., 14(1), 108–26, doi:10.1039/c4pp90035a, 2014.

Hahn, M. W.: Broad diversity of viable bacteria in "sterile" (0.2 ??m) filtered water, Res. Microbiol., 155(8), 688–691, doi:10.1016/j.resmic.2004.05.003, 2004.

Hamilton, J. D., Kelly, C. A., Rudd, J. W. M., Hesslein, R. H. and Roulet, N. T.: Flux to the atmosphere of CH4 and CO2 from wetland ponds on the Hudson Bay lowlands (HBLs), J. Geophys. Res., 99(D1), 1495–1510, doi:10.1029/93JD03020, 1994.

Hardacre, C.J., and Heal, M. R.: Characterisation of methyl bromide and methyl chloride fluxes at temperate freshwater wetlands, J. Geophys. Res., 118(2), 977–991, 2013.

Hargreaves, K. J., Milne, R. and Cannell, M. G. R.: Carbon balance of afforested peatland in Scotland, Forestry, 76(3), 299–317, doi:10.1093/forestry/76.3.299, 2003.

Harley, J. F., Carvalho, L., Dudley, B., Heal, K. V., Rees, R. M. and Skiba, U.: Spatial and seasonal fluxes of the greenhouse gases N2O, CO2 and CH4 in a UK macrotidal estuary, Estuar. Coast. Shelf Sci., 153, 62–73, doi:10.1016/j.ecss.2014.12.004, 2015.

He, W., Chen, M., Schlautmanb, M. A. and Hur, J.: Dynamic exchanges between DOM and POM pools in coastal and inland aquatic ecosystems: A review, Sci. Total Environ., 551–552, 415–428, 2016.

Hernes, P. J.: Photochemical and microbial degradation of dissolved lignin phenols: Implications for the fate of terrigenous dissolved organic matter in marine environments, J. Geophys. Res., 108, doi:10.1029/2002JC001421, 2003.

Hernes, P. J. and Benner, R.: Photochemical and microbial degradation of dissolved lignin phenols: Implications for the fate of terrigenous dissolved organic matter in marine environments, J. Geophys. Res., 108(C9), 3291, doi:10.1029/2002JC001421, 2003.

Hinton, M. J., Schiff, S. L. and English, M. C.: Sources and flowpaths of dissolved organic carbon during storms in two forested watersheds of the Precambrian Shield, Biogeochemistry, 41(2), 175–197, doi:10.1023/A:1005903428956, 1998.

Holden, J., Shotbolt, L., Bonn, A., Burt, T. P., Chapman, P. J., Dougill, A. J., Fraser, E. D. G., Hubacek, K., Irvine, B., Kirkby, M. J., Reed, M. S., Prell, C., Stagl, S., Stringer, L. C., Turner, A. and Worrall, F.: Environmental change in moorland landscapes, Earth-Science Rev., 82(1–2), 75–100, doi:10.1016/j.earscirev.2007.01.003, 2007.

Hong, J., Xie, H., Guo, L. and Song, G.: Carbon monoxide photoproduction: Implications for photoreactivity of arctic permafrost-derived soil dissolved organic matter, Environ. Sci. Technol., 48(16), 9113–9121, doi:10.1021/es502057n, 2014.

Hood, E., Fellman, J., Spencer, R. G. M., Hernes, P. J., Edwards, R., D'Amore, D. and Scott, D.: Glaciers as a source of ancient and labile organic matter to the marine environment., Nature, 462(7276), 1044–1047, doi:10.1038/nature08580, 2009.

Hope, D., Billett, M. F. and Cresser, M. S.: A review of the export of carbon in river water: Fluxes and processes, Environ. Pollut., 84(3), 301–324, doi:10.1016/0269-7491(94)90142-2, 1994.

Hudson, J. J., Dillon, P. J. and Somers, K. M.: Long-term patterns in dissolved organic carbon in boreal lakes: the role of incident radiation, precipitation, air temperature, southern oscillation and acid deposition, Hydrol. Earth Syst. Sci., 7(3), 390–398, doi:10.5194/hess-7-390-2003, 2003.

Jex, C. N., Pate, G. H., Blyth, A. J., Spencer, R. G. M., Hernes, P. J., Khan, S. J. and Baker, A.: Lignin biogeochemistry: from modern processes to Quaternary archives, Quat. Sci. Rev., 87, 46–59, doi:10.1016/j.quascirev.2013.12.028, 2014.

Jones, T. G., Evans, C. D., Jones, D. L., Hill, P. W. and Freeman, C.: Transformations in DOC along a source to sea continuum; impacts of photo-degradation, biological processes and mixing, Aquat. Sci., 1–14, doi:10.1007/s00027-015-0461-0, 2015.

Jorgenson, M.T., Racine, C.H., Walters, J.C., Osterkamp, T.E.: Permafrost Degradation and Ecological Changes Associated with a WarmingClimate in Central Alaska, Clim. Change, 48(4), 551–579, doi:10.1023/A:1005667424292, 2001.

Juutinen, S., V??liranta, M., Kuutti, V., Laine, A. M., Virtanen, T., Sepp??, H., Weckstr??m,

J. and Tuittila, E. S.: Short-term and long-term carbon dynamics in a northern peatland-stream-lake continuum: A catchment approach, J. Geophys. Res. Biogeosciences, 118(1), 171–183, doi:10.1002/jgrg.20028, 2013.

Kendon, E., Roberts, N. and Fowler, H.: Heavier summer downpours with climate change revealed by weather forecast resolution model, Nat. Clim. Chang., 4(June), 1–7, doi:10.1038/NCLIMATE2258, 2014.

Kicklighter, D. W., Hayes, D. J., Mcclelland, J. W., Peterson, B. J., Mcguire, A. D. and Melillo, J. M.: Insights and issues with simulating terrestrial DOC loading of Arctic river networks, Ecol. Appl., 23(8), 1817–1836, doi:10.1890/11-1050.1, 2013.

Koehler, A. K., Sottocornola, M. and Kiely, G.: How strong is the current carbon sequestration of an Atlantic blanket bog?, Glob. Chang. Biol., 17(1), 309–319, doi:10.1111/j.1365-2486.2010.02180.x, 2011.

Koehler, B., Von Wachenfeldt, E., Kothawala, D. and Tranvik, L. J.: Reactivity continuum of dissolved organic carbon decomposition in lake water, J. Geophys. Res. Biogeosciences, 117(1), doi:10.1029/2011JG001793, 2012.

Koehler, B., Landelius, T., Weyhenmeyer, G. a, Machida, N. and Tranvik, L. J.: Sunlight-induced carbon dioxide emissions from inland waters, Global Biogeochem. Cycles, 28, 696–711, doi:10.1002/2014GB004850.Received, 2014.

Kohler, S., Buffam, I., Jonsson, A. and Bishop, K.: Photochemical and microbial processing of stream and soil water dissolved organic matter in a boreal forested catchment in northern Sweden, Aquat. Sci., 64(3), 269–281, doi:10.1007/s00027-002-8071-z, 2002.

Korshin, G. V., Li, C. W. and Benjamin, M. M.: Monitoring the properties of natural organic matter through UV spectroscopy: A consistent theory, Water Res., 31(7), 1787–1795, doi:10.1016/S0043-1354(97)00006-7, 1997.

Kothawala, D. N., Ji, X., Laudon, H., ??gren, A. M., Futter, M. N., K??hler, S. J. and Tranvik, L. J.: The relative influence of land cover, hydrology, and in-stream processing on the composition of dissolved organic matter in boreal streams, J. Geophys. Res. G Biogeosciences, 120(8), 1491–1505, doi:10.1002/2015JG002946, 2015.

Koven, C. D., Ringeval, B., Friedlingstein, P., Ciais, P., Cadule, P., Khvorostyanov, D., Krinner, G. and Tarnocai, C.: Permafrost carbon-climate feedbacks accelerate global

warming., Proc. Natl. Acad. Sci. U. S. A., 108(36), 14769–74, doi:10.1073/pnas.1103910108, 2011.

Krachler, R., Krachler, R. F., Wallner, G., Steier, P., El Abiead, Y., Wiesinger, H., Jirsa, F. and Keppler, B. K.: Sphagnum-dominated bog systems are highly effective yet variable sources of bio-available iron to marine waters, Sci. Total Environ., 556, 53–62, doi:10.1016/j.scitotenv.2016.03.012, 2016.

Kritzberg, E. S., Cole, J. J., Pace, M. L., Granéli, W. and Bade, D. L.: Autochthonous versus allochthonous carbon sources to bacteria: Results from whole-lake 13C addition experiments, Limnol. Oceanogr., 49(2), 588–596, doi:10.4319/lo.2004.49.2.0588, 2004.

Lal, R.: Soil erosion and the global carbon budget, Environ. Int., 29(4), 437–450, doi:10.1016/S0160-4120(02)00192-7, 2003.

Lalonde, K., Vähätalo, A. V. and Gélinas, Y.: Revisiting the disappearance of terrestrial dissolved organic matter in the ocean: A δ13C study, Biogeosciences, 11(13), 3707–3719, doi:10.5194/bg-11-3707-2014, 2014.

Lapierre, J.-F., Guillemette, F., Berggren, M. and del Giorgio, P. a: Increases in terrestrially derived carbon stimulate organic carbon processing and CO2 emissions in boreal aquatic ecosystems., Nat. Commun., 4, 2972, doi:10.1038/ncomms3972, 2013.

Lapworth, D. J. and Kinniburgh, D. G.: An R script for visualising and analysing fluorescence excitation-emission matrices (EEMs), Comput. Geosci., 35(10), 2160–2163, doi:10.1016/j.cageo.2008.10.013, 2009.

Laudon, H., Buttle, J., Carey, S. K., McDonnell, J., McGuire, K., Seibert, J., Shanley, J., Soulsby, C. and Tetzlaff, D.: Cross-regional prediction of long-term trajectory of stream water DOC response to climate change, Geophys. Res. Lett., 39(17), doi:10.1029/2012GL053033, 2012.

Laurion, I., Vincent, W. F., MacIntyre, S., Retamal, L., Dupont, C., Francus, P. and Pienitz, R.: Variability in greenhouse gas emissions from permafrost thaw ponds, Limnol. Oceanogr., 55(1), 115–133, doi:10.4319/lo.2010.55.1.0115, 2010.

Lawson, I. T., Kelly, T. J., Aplin, P., Boom, A., Dargie, G., Draper, F. C. H., Hassan, P. N. Z. B. P., Hoyos-Santillan, J., Kaduk, J., Large, D., Murphy, W., Page, S. E., Roucoux, K. H., Sjögersten, S., Tansey, K., Waldram, M., Wedeux, B. M. M. and Wheeler, J.: Improving

estimates of tropical peatland area, carbon storage, and greenhouse gas fluxes, Wetl. Ecol. Manag., 1–20, doi:10.1007/s11273-014-9402-2, 2014.

Lee, H., Rahn, T. and Throop, H. L.: A novel source of atmospheric H2: Abiotic degradation of organic material, Biogeosciences, 9(11), 4411–4419, doi:10.5194/bg-9-4411-2012, 2012.

Leith, F. I., Garnett, M. H., Dinsmore, K. J., Billett, M. F. and Heal, K. V.: Source and age of dissolved and gaseous carbon in a peatland-riparian-stream continuum: A dual isotope (14C and δ13C) analysis, Biogeochemistry, 119, 415–433, doi:10.1007/s10533-014-9977-y, 2014.

Levy, P.E., and Gray, A.: Greenhouse gas balance of a semi-natural peatbog in northern Scotland, Environ. Res. Lett., 10, doi:doi:10.1088/1748-9326/10/9/094019, 2015.

Lieffers, V. J., Messier, C., Stadt, K. J., Gendron, F. and Comeau, P. G.: Predicting and managing light in the udnerstory of boreal forests, Can J. For. Res, (29), 796–811, 1999.

Limpens, J., Berendse, F., Blodau, C., Canadell, J. G., Freeman, C., Holden, J., Roulet, N. T., Rydin, H. and Schaepman-Strub, G.: Peatlands and the carbon cycle: from local processes to global implications - a synthesis., Biogeosciences, 5, 1475–1491, doi:10.5194/bgd-5-1379-2008, 2008.

Lohila, A., Minkkinen, K., Laine, J., Savolainen, I., Tuovinen, J. P., Korhonen, L., Laurila, T., Tiet??v??inen, H. and Laaksonen, A.: Forestation of boreal peatlands: Impacts of changing albedo and greenhouse gas fluxes on radiative forcing, J. Geophys. Res. Biogeosciences, 115(4), doi:10.1029/2010JG001327, 2010.

Lowe, W. H. and Likens, G. E.: Moving headwater streams to the head of the class, Bioscience, 55(3), 196–197, doi:10.1641/0006-3568(2005)055[0196:MHSTTH]2.0.CO;2, 2005.

Matilainen, A., Gjessing, E. T., Lahtinen, T., Hed, L., Bhatnagar, A. and Sillanp????, M.: An overview of the methods used in the characterisation of natural organic matter (NOM) in relation to drinking water treatment, Chemosphere, 83(11), 1431–1442, doi:10.1016/j.chemosphere.2011.01.018, 2011.

McEnroe, N. a., Roulet, N. T., Moore, T. R. and Garneau, M.: Do pool surface area and depth control CO2 and CH4 fluxes from an ombrotrophic raised bog, James Bay, Canada?, J. Geophys. Res. Biogeosciences, 114(1), 1–9, doi:10.1029/2007JG000639, 2009.

McKnight, D.M., Hood, E., Klapper, L.: Trace organic moieties of dissolved organic matter

inputs to surface waters, in Aquatic Ecosystems: Interactivity of Dissolved Organic Matter, edited by R. L. Findlay, S.E.G., Sinsabaugh, pp. 26–60, Elsevier Science, USA., 2003.

McKnight, D. M., Bencaia, K. E., Zeiiweger, G. W., Alken, G. R., Feder, G. L. and Thorn, K. A.: Sorption of Dissolved Organic Carbon by hydrous Aluminum and Iron oxides occurring at the confluence of Deer Creek with the Snake River, Summit County, Colorado, Environ. Sci. Technol., 26(7), 1388–1396, doi:10.1021/es00031a017, 1992.

McKnight, D. M., Boyer, E. W., Westerhoff, P. K., Doran, P. T., Kulbe, T., Andersen, D. T., E. W. Boyer, P. K. Westerhoff, P. T. Doran, T. Kulbe and Anderson, D. T.: Spectrofluorometric characterization of dissolved organic matter for indication of precursor organic material and aromaticity, Limnol. Oceanogr., 46(1), 38–48, doi:10.4319/lo.2001.46.1.0038, 2001.

McLeod, A. R., Fry, S. C., Loake, G. J., Messenger, D. J., Reay, D. S., Smith, K. A. and Yun, B.-W.: Ultraviolet radiation drives methane emissions from terrestrial plant pectins., New Phytol., 180, 124–132, doi:10.1111/j.1469-8137.2008.02571.x, 2008.

Messenger, D. J., McLeod, A. R. and Fry, S. C.: Reactive oxygen species in aerobic methane formation from vegetation., Plant Signal. Behav., 4, 629–630, doi:10.1111/j.1365-3040.2008.01892.x, 2009.

Met Office: Met Office Integrated Data Archive System (MIDAS) Land and Marine Surface Stations Data (1853-current), NCAS Br. Atmos. Data Cent. [online] Available from: http://catalogue.ceda.ac.uk/uuid/220a65615218d5c9cc9e4785a3234bd0, 2012.

Meyers-Schulte, K. J. and Hedges, J. I.: Molecular evidence for a terrestrial component of organic matter dissolved in ocean water, Nature, 321(6065), 61–63, doi:10.1038/321061a0, 1986.

Miller, W. L.: An overview of aquatic photochemistry as it relates to microbial production, Microb. Biosyst. New Front. Proc. 8th Int. Symp. Microb. Ecol., 1317–1324 [online] Available from: http://socrates.acadiau.ca/isme/Symposium07/miller.pdf, 1999.

Miller, W. L. and Zepp, R. G.: Photochemical producion of dissolved inorganic carbon from terrestrial matter: significance to the oceanic organic carbon cycle., Geophys. Res. Lett., 22(4), 417–420, 1995a.

Miller, W. L. and Zepp, R. G.: Photochemical production of dissolved inorganic carbon from

terrestrial organic matter: Significance to the oceanic organic carbon cycle, Geophys. Res. Lett., 22(4), 417, doi:10.1029/94GL03344, 1995b.

Molot, L. A. and Dillon, P. J.: Photolytic regulation of dissolved organic carbon in northern lakes, Global Biogeochem. Cycles, 11(3), 357–365, doi:10.1029/97GB01198, 1997.

Molot, L. A., Hudson, J. J., Dillon, P. J. and Miller, S. A.: Effect of pH on photo-oxidation of dissolved organic carbon by hydroxyl radicals in a coloured, softwater stream, Aquat. Sci., 67(2), 189–195, doi:10.1007/s00027-005-0754-9, 2005.

Monteith, D. T., Stoddard, J. L., Evans, C. D., de Wit, H. a, Forsius, M., Høgåsen, T., Wilander, A., Skjelkvåle, B. L., Jeffries, D. S., Vuorenmaa, J., Keller, B., Kopácek, J. and Vesely, J.: Dissolved organic carbon trends resulting from changes in atmospheric deposition chemistry., Nature, 450(7169), 537–540, doi:10.1038/nature06316, 2007.

Moody, C. S. and Worrall, F.: Sub-daily rates of degradation of fluvial carbon from a peat headwater stream, Aquat. Sci., doi:10.1007/s00027-015-0456-x, 2015.

Moody, C. S., Worrall, F., Evans, C. D. and Jones, T. G.: The rate of loss of dissolved organic carbon (DOC) through a catchment, J. Hydrol., 492, 139–150, doi:10.1016/j.jhydrol.2013.03.016, 2013.

Moore, S., Evans, C. D., Page, S. E., Garnett, M. H., Jones, T. G., Freeman, C., Hooijer, A., Wiltshire, A. J., Limin, S. H. and Gauci, V.: Deep instability of deforested tropical peatlands revealed by fluvial organic carbon fluxes., Nature, 493(7434), 660–3, doi:10.1038/nature11818, 2013.

Moore, T. R., Heyes, A. and Roulet, N. T.: Methane emissions from wetlands, southern Hudson Bay Lowland, J. Geophys. Res., 99(D1), 1455–1467, doi:10.1029/93jd02457, 1994.

Moran, M. A. and Zepp, R. G.: Role of photoreactions in the formation of biologically labile compounds from dissolved organic matter, Limnol. Oceanogr., 42, 1307–1316, doi:10.4319/lo.1997.42.6.1307, 1997.

Moran, M. A., Sheldon, W. M. and Zepp, R. G.: Carbon loss and optical property changes during long-term photochemical and biological degradation of estuarine dissolved organic matter, Limnol. Oceanogr., 45(6), 1254–1264, doi:10.4319/lo.2000.45.6.1254, 2000.

Muller, F. L. L. and Tankéré-Muller, S. P. C.: Seasonal variations in surface water chemistry at disturbed and pristine peatland sites in the Flow Country of northern Scotland, Sci. Total

Environ., 435–436, 351–362, doi:10.1016/j.scitotenv.2012.06.048, 2012.

Muller, R., Wiencke, C. and Bischof, K.: Interactive effects of UV radiation and temperature on microstages of Laminariales (Phaeophyceae) from the Arctic and North Sea, in Climate Research, vol. 37, pp. 203–213., 2008.

Nguyen, M.-L., Westerhoff, P., Baker, L., Hu, Q., Esparza-Soto, M. and Sommerfeld, M.: Characteristics and Reactivity of Algae-Produced Dissolved Organic Carbon, J. Environ. Eng., 131(11), 1574–1582, doi:10.1061/(ASCE)0733-9372(2005)131:11(1574), 2005.

Nieminen, M., Koskinen, M., Sarkkola, S., Laurén, A., Kaila, A., Kiikkilä, O., Nieminen, T. M. and Ukonmaanaho, L.: Dissolved organic carbon export from harvested peatland forests with differing site characteristics, Water. Air. Soil Pollut., 226(6), doi:10.1007/s11270-015-2444-0, 2015.

Nilsson, M., Sagerfors, J., Buffam, I., Laudon, H., Eriksson, T., Grelle, A., Klemedtsson, L., Weslien, P. and Lindroth, A.: Contemporary carbon accumulation in a boreal oligotrophic minerogenic mire - A significant sink after accounting for all C-fluxes, Glob. Chang. Biol., 14(10), 2317–2332, doi:10.1111/j.1365-2486.2008.01654.x, 2008.

Opsahl, S. and Benner, R.: Photochemical reactivity of dissolved lignin in river and ocean waters, Limnol. Oceanogr., 43, 1297–1304, doi:10.4319/lo.1998.43.6.1297, 1998.

Opsahl, S. P. and Zepp, R. G.: Photochemically-induced alteration of stable carbon isotope ratios (delta C-13) in terrigenous dissolved organic carbon, Geophys. Res. Lett., 28, 2417–2420 [online] Available from: <Go to ISI>://000171008500032, 2001.

Osburn, C.L., Morris, D.P.: Photochemistry of chromophoric dissolved organic matter in natural waters, in UV Effects in Aquatic Organisms and Ecosystems, pp. 185–218, The Royal Society of Chemistry, UK., 2003.

Palmer, S. M., Hope, D., Billett, M. F., Dawson, J. J. C. and Bryant, C. L.: Sources of organic and inorganic carbon in a headwater stream: Evidence from carbon isotope studies, Biogeochemistry, 52(3), 321–338, doi:10.1023/a:1006447706565, 2001.

Palmer, S. M., Evans, C. D., Chapman, P. J., Burden, A., Jones, T. G., Allott, T. E. H., Evans, M. G., Moody, C. S., Worrall, F. and Holden, J.: Sporadic hotspots for physico-chemical retention of aquatic organic carbon: from peatland headwater source to sea, Aquat. Sci., 1–14, doi:10.1007/s00027-015-0448-x, 2015.

Park, S., K. S. Joe, S. H. H. and H. S. K.: Characteristics of dissolved organic carbon in the leachate from Moonam Sanitary Landfill, Environ. Sci. Technol., 20, 419–424, 1999.

Parry, L. E., Holden, J. and Chapman, P. J.: Restoration of blanket peatlands, J. Environ. Manage., 133, 193–205, doi:10.1016/j.jenvman.2013.11.033, 2014.

Paul, A., Hackbarth, S., Vogt, R. D., Röder, B., Burnison, B. K. and Steinberg, C. E. W.: Photogeneration of singlet oxygen by humic substances: comparison of humic substances of aquatic and terrestrial origin., Photochem. Photobiol. Sci., 3, 273–280, doi:10.1039/b312146a, 2004.

Pawson, R. R., Evans, M. G. and Allott, T. E. H. A.: Fluvial carbon flux from headwater peatland streams: Significance of particulate carbon flux, Earth Surf. Process. Landforms, 37(11), 1203–1212, doi:10.1002/esp.3257, 2012.

Peacock, M., Evans, C. D., Fenner, N. and Freeman, C.: Natural revegetation of bog pools after peatland restoration involving ditch blocking-The influence of pool depth and implications for carbon cycling, Ecol. Eng., 57, 297–301, doi:10.1016/j.ecoleng.2013.04.055, 2013.

Peacock, M., Evans, C. D., Fenner, N., Freeman, C., Gough, R., Jones, T. G. and Lebron, I.: UV-visible absorbance spectroscopy as a proxy for peatland dissolved organic carbon (DOC) quantity and quality: considerations on wavelength and absorbance degradation., Environ. Sci. Process. Impacts, 10–12, doi:10.1039/c4em00108g, 2014.

Pelletier, L., Strachan, I. B., Garneau, M. and Roulet, N. T.: Carbon release from boreal peatland open water pools: Implication for the contemporary C exchange, J. Geophys. Res. Biogeosciences, 119(3), 207–222, doi:10.1002/2013JG002423, 2014.

Peuravuori, J. and Pihlaja, K.: Molecular size distribution and spectroscopic properties of aquatic humic substances, Anal. Chim. Acta, 337(2), 133–149, doi:10.1016/S0003-2670(96)00412-6, 1997.

Pickard, A.E., Heal, K.V., McLeod, A.R., Dinsmore, K. J.: Temporal changes in photoreactivity of dissolved organic carbon and implications for aquatic carbon fluxes from peatlands, Biogeosciences Discuss., doi:10.5194/bg-2016-296, 2016.

Pokrovsky, O. S., Viers, J., Shirokova, L. S., Shevchenko, V. P., Filipov, A. S. and Dupr??, B.: Dissolved, suspended, and colloidal fluxes of organic carbon, major and trace elements in

the Severnaya Dvina River and its tributary, Chem. Geol., 273(1–2), 136–149, doi:10.1016/j.chemgeo.2010.02.018, 2010.

Porcal, P., Dillon, P.J., Molot, L.A.: Seasonal changes in photochemical properties of dissolved organic matter in small boreal streams, Biogeosciences, 10, 5533–5543, doi:10.5194/bg-10-5533-2013, 2013.

Porcal, P., Dillon, P. J. and Molot, L. A.: Photochemical production and decomposition of particulate organic carbon in a freshwater stream, Aquat. Sci., 75(4), 469–482, doi:10.1007/s00027-013-0293-8, 2013.

Porcal, P., Dillon, P. J. and Molot, L. a.: Temperature Dependence of Photodegradation of Dissolved Organic Matter to Dissolved Inorganic Carbon and Particulate Organic Carbon, PLoS One, 10(6), e0128884, doi:10.1371/journal.pone.0128884, 2015.

Pribyl, D. W.: A critical review of the conventional SOC to SOM conversion factor, Geoderma, 156(3–4), 75–83, doi:10.1016/j.geoderma.2010.02.003, 2010.

Raich, J. W. and Schlesinger, W. H.: The Global Carbon-Dioxide Flux in Soil Respiration and Its Relationship to Vegetation and Climate, Tellus Ser. B-Chemical Phys. Meteorol., 44(2), 81–99, doi:10.1034/j.1600-0889.1992.t01-1-00001.x, 1992.

Raymond, P. A., Hartmann, J., Lauerwald, R., Sobek, S., McDonald, C., Hoover, M., Butman, D., Striegl, R., Mayorga, E., Humborg, C., Kortelainen, P., Durr, H., Meybeck, M., Ciais, P. and Guth, P.: Global carbon dioxide emissions from inland waters, Nature, 503, 355–359, doi:10.1038/nature12760, 2013.

Repo, M. E., Huttunen, J. T., Naumov, a. V., Chichulin, a. V., Lapshina, E. D., Bleuten, W. and Martikainen, P. J.: Release of CO2 and CH4 from small wetland lakes in western Siberia, Tellus, Ser. B Chem. Phys. Meteorol., 59(5), 788–796, doi:10.1111/j.1600-0889.2007.00301.x, 2007.

Robards, K., McKelvie, I. D., Benson, R. L., Worsfold, P. J., Blundell, N. J. and Casey, H.: Determination of carbon, phosphorus, nitrogen and silicon species in waters, Anal. Chim. Acta, 287(3), 147–190, doi:10.1016/0003-2670(93)E0542-F, 1994.

Roulet, N. and Moore, T. R.: Environmental chemistry: browning the waters., Nature, 444(7117), 283–284, doi:10.1038/444283a, 2006.

Sandford, R. C., Bol, R. and Worsfold, P. J.: In situ determination of dissolved organic

carbon in freshwaters using a reagentless UV sensor., J. Environ. Monit., 12(9), 1678–1683, doi:10.1039/c0em00060d, 2010.

Schindler, D. W. and Smol, J. P.: Cumulative effects of climate warming and other human activities on freshwaters of Arctic and subarctic North America., Ambio, 35(4), 160–168, doi:10.1579/0044-7447(2006)35[160:CEOCWA]2.0.CO;2, 2006.

Schuur, E. A. G., McGuire, A. D., Grosse, G., Harden, J. W., Hayes, D. J., Hugelius, G., Koven, C. D. and Kuhry, P.: Climate change and the permafrost carbon feedback, Nature, 520(January 2016), 171–179, doi:10.1038/nature14338, 2015.

Sharp, E. L., Parsons, S. A. and Jefferson, B.: The impact of seasonal variations in DOC arising from a moorland peat catchment on coagulation with iron and aluminium salts, Environ. Pollut., 140(3), 436–443, doi:10.1016/j.envpol.2005.08.001, 2006.

Sheng, Y., Smith, L. C., MacDonald, G. M., Kremenetski, K. V., Frey, K. E., Velichko, A. A., Lee, M., Beilman, D. W. and Dubinin, P.: A high-resolution GIS-based inventory of the west Siberian peat carbon pool, Global Biogeochem. Cycles, 18(3), doi:10.1029/2003GB002190, 2004.

Smith, V. H., Joye, S. B. and Howarth, R. W.: Eutrophication of freshwater and marine ecosystems, Limnol. Oceanogr., 51(1, part 2), 351–355, doi:10.4319/lo.2006.51.1_part_2.0351, 2006.

Sobek, S., Tranvik, L. J., Prairie, Y. T., Kortelainen, P. and Cole, J. J.: Patterns and regulation of dissolved organic carbon: An analysis of 7,500 widely distributed lakes, Limnol. Oceanogr., 52(3), 1208–1219, doi:10.4319/lo.2007.52.3.1208, 2007.

Spencer, R.G.M., Stubbins, A., Hernes, P.J., Baker, A., Mopper, K., Aufdenkampe, A.K., Dyda, R.Y., Mwamba, Vi.L. Mangangu, A.M., Wabakanghanzi, J.N., Six, J.: Photochemical degradation of dissolved organic matter and dissolved lignin phenols from the Congo River, J. Geophys. Res. Biogeosciences, 114(3), 1–12, doi:10.1029/2009JG000968, 2009.

Spencer, R. G. M., Ahad, J. M. E., Baker, A., Cowie, G. L., Ganeshram, R., Upstill-Goddard, R. C. and Uher, G.: The estuarine mixing behaviour of peatland derived dissolved organic carbon and its relationship to chromophoric dissolved organic matter in two North Sea estuaries (U.K.), Estuar. Coast. Shelf Sci., 74(1–2), 131–144, doi:10.1016/j.ecss.2007.03.032, 2007.

Spencer, R. G. M., Aiken, G. R., Wickland, K. P., Striegl, R. G. and Hernes, P. J.: Seasonal and spatial variability in dissolved organic matter quantity and composition from the Yukon River basin, Alaska, Global Biogeochem. Cycles, 22, doi:10.1029/2008GB003231, 2008.

Spencer, R. G. M., Stubbins, A., Hernes, P. J., Baker, A., Mopper, K., Aufdenkampe, A. K., Dyda, R. Y., Mwamba, V. L., Mangangu, A. M., Wabakanghanzi, J. N. and Six, J.: Photochemical degradation of dissolved organic matter and dissolved lignin phenols from the Congo River, J. Geophys. Res., 114, doi:10.1029/2009JG000968, 2009.

Spencer, R. G. M., Butler, K. D. and Aiken, G. R.: Dissolved organic carbon and chromophoric dissolved organic matter properties of rivers in the USA, J. Geophys. Res., 117, doi:10.1029/2011JG001928, 2012.

Stedmon, C. A., Thomas, D. N., Granskog, M., Kaartokallio, H., Papadimitriou, S. and Kuosa, H.: Characteristics of dissolved organic matter in baltic coastal sea ice: Allochthonous or autochthonous origins?, Environ. Sci. Technol., 41(21), 7273–7279, doi:10.1021/es071210f, 2007.

Stedmon, C. C. a, Markager, S. and Bro, R.: Tracing dissolved organic matter in aquatic environments using a new approach to fluorescence spectroscopy, Mar. Chem., 82(3–4), 239–254, doi:10.1016/S0304-4203(03)00072-0, 2003.

Steinberg, C. E. W., Meinelt, T., Timofeyev, M. a, Bittner, M. and Menzel, R.: Humic substances. Part 2: Interactions with organisms., Environ. Sci. Pollut. Res. Int., 15(2), 128–135, doi:http://dx.doi.org/10.1065/espr2007.07.434, 2008.

Stockley, R. A., Oxford, G. S. and Ormond, R. F. G.: Do invertebrates matter? Detrital processing in the River Swale-Ouse, Sci. Total Environ., 210–211, 427–435, doi:10.1016/S0048-9697(98)00029-1, 1998.

Stubbins, A., Law, C. S., Uher, G. and Upstill-Goddard, R. C.: Carbon monoxide apparent quantum yields and photoproduction in the Tyne estuary, Biogeosciences, 8(3), 703–713, doi:10.5194/bg-8-703-2011, 2011.

Sulzberger, B. and Durisch-Kaiser, E.: Chemical characterization of dissolved organic matter (DOM): A prerequisite for understanding UV-induced changes of DOM absorption properties and bioavailability, Aquat. Sci., 71, 104–126, doi:10.1007/s00027-008-8082-5, 2009.

Sutzkover-Gutman, I., Hasson, D. and Semiat, R.: Humic substances fouling in ultrafiltration processes, Desalination, 261(3), 218–231, doi:10.1016/j.desal.2010.05.008, 2010.

Tang, R., Clark, J. M., Bond, T., Graham, N., Hughes, D. and Freeman, C.: Assessment of potential climate change impacts on peatland dissolved organic carbon release and drinking water treatment from laboratory experiments, Environ. Pollut., 173, 270–277, doi:10.1016/j.envpol.2012.09.022, 2013.

Torseth, K., Aas, W., Breivik, K., Fjeraa, A. M., Fiebig, M., Hjellbrekke, A. G., Lund Myhre, C., Solberg, S. and Yttri, K. E.: Introduction to the European Monitoring and Evaluation Programme (EMEP) and observed atmospheric composition change during 1972-2009, Atmos. Chem. Phys., 12(12), 5447–5481, doi:10.5194/acp-12-5447-2012, 2012.

Tranvick, L. J. and Jansson, M.: Climate change (Communication arising): Terrestrial export of organic carbon, Nature, 415(6874), 861–862, doi:10.1038/415862a, 2002.

Tranvik, L. J., Downing, J. A., Cotner, J. B., Loiselle, S. A., Striegl, R. G., Ballatore, T. J., Dillon, P., Finlay, K., Fortino, K. and Knoll, L. B.: Lakes and reservoirs as regulators of carbon cycling and climate, Limnol. Oceanogr., 54, 2298–2314, doi:10.4319/lo.2009.54.6_part_2.2298, 2009.

Turetsky, M., Wieder, K., Halsey, L. and Vitt, D.: Current disturbance and the diminishing peatland carbon sink, Geophys. Res. Lett., 29(11), 7–10, doi:10.1029/2001GL014000, 2002.

Turner, T.E., Billett, M.F., Baird, A.J., Chapman, P.J., Dinsmore, K.J., Holden, J.: Regional variation in the biogeochemical and physical characteristics of natural peatland pools, Sci. Total Environ., 545–546, 84–94, 2016.

Turunen, J., Tomppo, E., Tolonen, K. and Reinikainen, A.: Estimating carbon accumulation rates of undrained mires in Finland – application to boreal and subarctic regions, The Holocene, 12(1), 69–80, doi:10.1191/0959683602hl522rp, 2002.

Vachon, D., Lapierre, J., del Giorgio, P. A.: Seasonality of photochemical dissolved organic carbon mineralization and its relative contribution to pelagic CO2 production in northern lakes, J. Geophys. Res. Biogeosciences, 121, doi:10.1002/ 2015JG003244, 2016.

Vähätalo, A. V. and Wetzel, R. G.: Long-term photochemical and microbial decomposition of wetland-derived dissolved organic matter with alteration of 13C:12C mass ratio, Limnol. Oceanogr., 53(4), 1387–1392, doi:10.4319/lo.2008.53.4.1387, 2008.

Vähätalo, A. V., Salkinoja-Salonen, M., Taalas, P. and Salonen, K.: Spectrum of the quantum yield for photochemical mineralization of dissolved organic carbon in a humic lake, Limnol. Oceanogr., 45(3), 664–676, doi:10.4319/lo.2000.45.3.0664, 2000.

Vecchio, R. Del and Blough, N.: Photobleaching of chromophoric dissolved organic matter in natural waters: kinetics and modeling, Mar. Chem., 78(4), 231–253, doi:10.1016/S0304-4203(02)00036-1, 2002.

Van Vliet, M. T. H., Franssen, W. H. P., Yearsley, J. R., Ludwig, F., Haddeland, I., Lettenmaier, D. P. and Kabat, P.: Global river discharge and water temperature under climate change, Glob. Environ. Chang., 23(2), 450–464, doi:10.1016/j.gloenvcha.2012.11.002, 2013.

Vonk, J. E., Tank, S. E., Bowden, W. B., Laurion, I., Vincent, W. F., Alekseychik, P., Amyot, M., Billet, M. F., Canário, J., Cory, R. M., Deshpande, B. N., Helbig, M., Jammet, M., Karlsson, J., Larouche, J., MacMillan, G., Rautio, M., Walter Anthony, K., K. P.: Reviews and Syntheses: Effects of permafrost thaw on arctic aquatic ecosystems, Biogeosciences Discuss., 12(13), 10719–10815, doi:10.5194/bgd-12-10719-2015, 2015.

Vonk, J. E., Tank, S. E., Mann, P. J., Spencer, R. G. M., Treat, C. C., Striegl, R. G., Abbott, B. W. and Wickland, K. P.: Biodegradability of dissolved organic carbon in permafrost soils and waterways: a meta-analysis, Biogeosciences Discuss., 12(11), 8353–8393, doi:10.5194/bgd-12-8353-2015, 2015.

Waldron, S., Scott, E. M. and Soulsby, C.: Stable isotope analysis reveals lower-order river dissolved inorganic carbon pools are highly dynamic., Environ. Sci. Technol., 41(17), 6156–6162, doi:10.1021/es0706089, 2007.

Wallage, Z. E., Holden, J. and McDonald, A. T.: Drain blocking: An effective treatment for reducing dissolved organic carbon loss and water discolouration in a drained peatland, Sci. Total Environ., 367(2–3), 811–821, doi:10.1016/j.scitotenv.2006.02.010, 2006.

Wallin, M. B., Weyhenmeyer, G. A., Bastviken, D., Chmiel, H. E., Peter, S., Sobek, S. and Klemedtsson, L.: Temporal control on concentration, character, and export of dissolved organic carbon in two hemiboreal headwater streams draining contrasting catchments, J. Geophys. Res. G Biogeosciences, doi:10.1002/2014JG002814, 2015.

Wang, Y., Hammes, F., Boon, N. and Egli, T.: Quantification of the filterability of freshwater bacteria through 0.45, 0.22, and 0.1 μm pore size filters and shape-dependent

enrichment of filterable bacterial communities, Environ. Sci. Technol., 41(20), 7080–7086, doi:10.1021/es0707198, 2007.

Wang, Z. P., Xie, Z. Q., Zhang, B. C., Hou, L. Y., Zhou, Y. H., Li, L. H. and Han, X. G.: Aerobic and anaerobic nonmicrobial methane emissions from plant material, Environ. Sci. Technol., 45(22), 9531–9537, doi:10.1021/es2020132, 2011.

Ward, N. D., Richey, J. E. and Keil, R. G.: Temporal variation in river nutrient and dissolved lignin phenol concentrations and the impact of storm events on nutrient loading to Hood Canal, Washington, USA, Biogeochemistry, 111(1–3), 629–645, doi:10.1007/s10533-012-9700-9, 2012.

Watts, G., Battarbee, R. W., Bloomfield, J. P., Crossman, J., Daccache, A., Durance, I., Elliott, J. A., Garner, G., Hannaford, J., Hannah, D. M., Hess, T., Jackson, C. R., Kay, A. L., Kernan, M., Knox, J., Mackay, J., Monteith, D. T., Ormerod, S. J., Rance, J., Stuart, M. E., Wade, A. J., Wade, S. D., Weatherhead, K., Whitehead, P. G. and Wilby, R. L.: Climate change and water in the UK - past changes and future prospects, Prog. Phys. Geogr., 39(1), 6–28, doi:10.1177/0309133314542957, 2015.

Webster, K. E., Soranno, P. a., Cheruvelil, K. S., Bremigan, M. T., Downing, J. a., Vaux, P. D., Asplund, T. R., Bacon, L. C. and Connor, J.: An empirical evaluation of the nutrient-color paradigm for lakes, Limnol. Oceanogr., 53(3), 1137–1148, doi:10.4319/lo.2008.53.3.1137, 2008.

Weishaar, J. L., Aiken, G. R., Bergamaschi, B. A., Fram, M. S., Fujii, R. and Mopper, K.: Evaluation of specific ultraviolet absorbance as an indicator of the chemical composition and reactivity of dissolved organic carbon., Environ. Sci. Technol., 37, 4702–4708, doi:10.1021/es030360x, 2003.

Weyhenmeyer, G. A., Fröberg, M., Karltun, E., Khalili, M., Kothawala, D., Temnerud, J. and Tranvik, L. J.: Selective decay of terrestrial organic carbon during transport from land to sea, Glob. Chang. Biol., 18(1), 349–355, doi:10.1111/j.1365-2486.2011.02544.x, 2012.

Weyhenmeyer, G. A., Prairie, Y. T. and Tranvik, L. J.: Browning of boreal freshwaters coupled to carbon-iron interactions along the aquatic continuum, PLoS One, 9(2), doi:10.1371/journal.pone.0088104, 2014.

Weyhenmeyer, G. A., Müller, R. A., Norman, M. and Tranvik, L. J.: Sensitivity of freshwaters to browning in response to future climate change, Clim. Change, 134(1–2), 225–

239, doi:10.1007/s10584-015-1514-z, 2016.

Wiesenburg, D. A. and Guinasso Jr., N. L.: Equilibrium solubilities of methane, carbon monoxide, and hydrogen in water and sea water, J. Chem. Eng. Data, 24(4), 356–360, doi:10.1021/je60083a006, 1979.

Williamson, C. E., Zepp, R. G., Lucas, R. M., Madronich, S., Austin, A. T., Ballaré, C. L., Norval, M., Sulzberger, B., Bais, A. F., McKenzie, R. L., Robinson, S. A., Häder, D.-P., Paul, N. D. and Bornman, J. F.: Solar ultraviolet radiation in a changing climate, Nat. Clim. Chang., 4(6), 434–441, doi:10.1038/nclimate2225, 2014.

Wilson, L., Wilson, J., Holden, J., Johnstone, I., Armstrong, A. and Morris, M.: Ditch blocking, water chemistry and organic carbon flux: Evidence that blanket bog restoration reduces erosion and fluvial carbon loss, Sci. Total Environ., 409(11), 2010–2018, doi:10.1016/j.scitotenv.2011.02.036, 2011.

Wollheim, W. M., Stewart, R. J., Aiken, G. R., Butler, K. D., Morse, N. B. and Salisbury, J.: Removal of terrestrial DOC in aquatic ecosystems of a temperate river network, Geophys. Res. Lett., 42(16), 6671–6679, 2015.

Worrall, F., Burt, T.P., Adamson, J.: The rate of and controls upon DOC loss in a peat catchment, J. Hydrol., 321(1–4), 311–325, 2006.

Worrall, F., Howden, N.J.K., Burt, T. P.: A method of estimating in-stream residence time of water in rivers, J. Hydrol., 274–284, doi:doi:10.1016/j.jhydrol.2014.02.050, 2014.

Worrall, F. and Moody, C. S.: Modeling the rate of turnover of DOC and particulate organic carbon in a UK, peat-hosted stream: Including diurnal cycling in short-residence time systems, J. Geophys. Res. Biogeosciences, 1–13, doi:10.1002/2014JG002671.Received, 2014.

Worrall, F., Reed, M., Warburton, J. and Burt, T.: Carbon budget for a British upland peat catchment, Sci. Total Environ., 312(1–3), 133–146, doi:10.1016/S0048-9697(03)00226-2, 2003.

Worrall, F., Burt, T. and Adamson, J.: Can climate change explain increases in DOC flux from upland peat catchments?, Sci. Total Environ., 326(1–3), 95–112, doi:10.1016/j.scitotenv.2003.11.022, 2004.

Worrall, F., Armstrong, A. and Holden, J.: Short-term impact of peat drain-blocking on

water colour, dissolved organic carbon concentration, and water table depth, J. Hydrol., 337(3–4), 315–325, doi:10.1016/j.jhydrol.2007.01.046, 2007.

Yallop, A. R., Clutterbuck, B. and Thacker, J.: Increases in humic dissolved organic carbon export from upland Peat catchments: The role of temperature, declining sulphur deposition and changes in land management, Clim. Res., 45(1), 43–56, doi:10.3354/cr00884, 2010.

Yu, Z., Beilman, D. W. and Jones, M. C.: Sensitivity of Northern Peatland Carbon Dynamics to Holocene Climate Change, in Carbon Cycling in Northern Peatlands, edited by L. D. Baird, A.J., Belyea Belyea, L.R., Comas, X., Reeve, A.S., Slater, pp. 55–69, American Geophysical Union., 2013.

Yu, Z. C.: Northern peatland carbon stocks and dynamics: A review, Biogeosciences, 9(10), 4071–4085, doi:10.5194/bg-9-4071-2012, 2012.

Zepp, R.: Solar UVR and aquatic carbon, nitrogen, sulfur and metals cycles, in UV Effects in Aquatic Organisms and Ecosystems, edited by H. Heibling, E.W., Zagarese, pp. 137–185, The Royal Society of Chemistry, Cambridge. [online] Available from: http://www.ncbi.nlm.nih.gov/entrez/query.fcgi?db=pubmed&cmd=Retrieve&dopt=AbstractPlus&list_uids=10095496579689450330\nhttp://books.google.com/books?hl=en&lr=&ie=UTF-8&id=45pupaUl_jUC&oi=fnd&pg=PA137&dq=macrophyte*+remote+sensing+amazon*&ots=bLTejyBZBr&si, 2003.

Zhang, Y., Xie, H. and Chen, G.: Factors affecting the efficiency of carbon monoxide photoproduction in the St. Lawrence estuarine system (Canada), Environ. Sci. Technol., 40(24), 7771–7777, doi:10.1021/es0615268, 2006.

Zhang, Y., Liu, X., Osburn, C. L., Wang, M., Qin, B. and Zhou, Y.: Photobleaching Response of Different Sources of Chromophoric Dissolved Organic Matter Exposed to Natural Solar Radiation Using Absorption and Excitation-Emission Matrix Spectra, PLoS One, 8(10), doi:10.1371/journal.pone.0077515, 2013.

Appendix A Biogeochemical Characterisation of Peatland Pool Sites

2 L water samples were collected from the peatland pools at Red Moss of Balerno and Cross Lochs, Forsinard on 3 April and 17 March 2015, respectively. Biogeochemical properties of the water samples were measured upon return to the laboratory (Table A1), with considerable variation emerging between the sites. Red Moss had significantly higher DOC concentrations and thus the sites were employed in Chapter 5 to represent high and low DOC peatland pools.

Table A1. Biogeochemical properties of bulk water samples collected from peatland pools at Red Moss and Cross Lochs. Values represent the mean of triplicate measurements.

	Red Moss	**Cross Lochs**
DOC mg L^{-1}	30.5	4.90
DIC mg L^{-1}	1.30	0.76
POC mg L^{-1}	3.46	3.46
$SUVA_{254}$	4.73	3.16
E4:E6	6.22	3.50
E2:E3	4.46	5.15

Using the same method described in Chapter 5 unfiltered peatland pool samples were decanted into Tedlar gas bags, with UV exposed and control samples employed (n=2). The bags were then placed in the laboratory irradiation facility described in Chapter 2 and irradiated with UVB Q Panel lamps at 0.3 mV for 8 h. After irradiation samples were prepared for analyses described in Chapter 5, section. In addition to the analyses performed in Chapter 5, $\delta^{13}C\text{-}CO_2$ and $\delta^{13}C\text{-}CH_4$ analyses were undertaken. Isotopic data for C species: DOC, DIC, CO_2 and CH_4 in UV exposed and control samples are presented below (Table A2).

Table A2. Stable carbon isotope data (all expressed in per mil ‰) and publication codes (where available) from the laboratory experiment trial run. RM denotes Red Moss, the '+' indicates light treatment and the second number refers to the replicate. Control (dark) treatments are denoted by '-'. CL denotes Cross Lochs.

Sample	δ^{13}C-DOC	Publication code	δ^{13}C-DIC	Publication code	δ^{13}C-CO_2	δ^{13}C-CH_4
RM+1	-28.99	S-177801	-23.75	SE164835	-21.51	-44.85
RM+2	-29.03	S-177802	-23.61	SE164836	-22.21	-39.93
RM-1	-29.01	S-177803	-22.30	SE164837	-20.23	-35.46
RM-2	-29.07	S-177804	-22.58	SE164838	-17.78	-32.19
CL+1	-26.05	S-177813	-13.41	SE164831	-13.48	-51.43
CL+2	-26.20	S-177814	-16.08	SE164832	-14.42	-51.28
CL-1	-26.15	S-177815	-16.88	SE164833	-12.27	-51.41
CL-2	-26.02	S-177816	-14.67	SE164834	-14.11	-51.74

Appendix B Selection of Lamps for Irradiation Experiments

UV lamps were used in initial irradiation experiments, as UV is the part of the spectrum most strongly associated with a photochemical effect. The output of UV-B 313 and UV-A 351 lamps were measured using a double monochromator scanning spectroradiometer (Model SR9910-V7; Irradian, UK) and compared to natural sunlight (Figure B1).

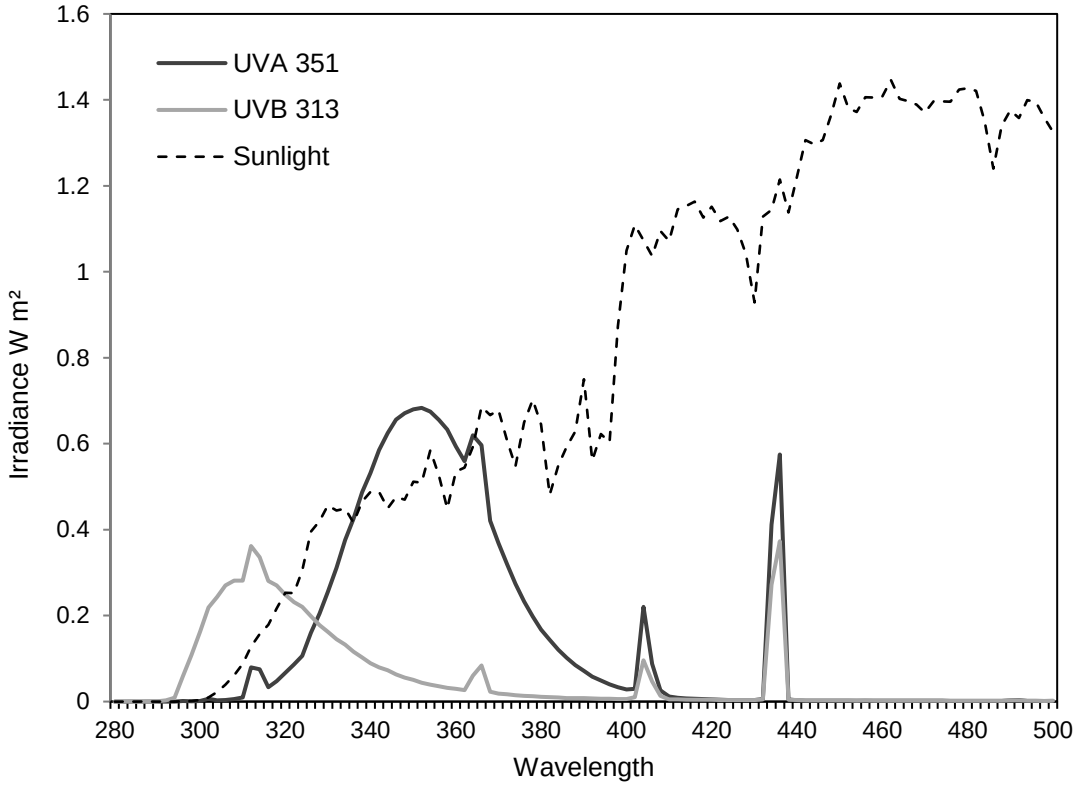

Figure B1. Irradiance (W m^2) of UVB 313 and UVA 351 lamps in comparison to natural sunlight from 280-500 nm.

Using a water sample with a DOC concentration of 23.3 mg L^{-1} collected from the Black Burn in January 2014, photoreactivity, here measured as gaseous photoproduction, was tested upon exposure to both lamp types at a range of temperatures (Table B1). The difference in headspace concentrations of CO_2 and CO were recorded and subject to analysis using a two-way, paired Student's t-test.

Table B1. Irradiation induced difference in headspace concentration of CO_2 and CO (ppm) in experiments using UVB-313 and UVA-351 lamps, at temperatures: 12, 16 and 20°C. Data represent the mean of four replicates.

		Temperature °C		
		12	**16**	**20**
ΔCO_2	UVB	1271	1562	1910
	UVA	1381	1511	1747
	t-test p-value	0.23	0.57	0.07
ΔCO_2	UVB	96	129	157
	UVA	102	139	144
	t-test p-value	0.38	0.06	0.27

These results indicate that over 8 hours irradiation, there is a slight, but statistically insignificant difference in sample photoreactivity as a function of using UVB-313 lamps with a total UV irradiance of 10.8 W m², in comparison to UVA-351 lamps with a total UV irradiance of 28.6 W m^2. UV-B lamps were employed in laboratory experiments going forward and a broadband sensor was employed to ensure consistent output from the lamp over 8 h.

Appendix C Exposure Time Experiments

Duration experiments were conducted using water samples filtered to 0.7 μm collected from the Black Burn at Auchencorth Moss in June 2013. Sample DOC and DIC concentrations were 9.7 mg L^{-1} and 18.2 mg L^{-1}, respectively. Exposure intervals of 1, 2, 4, 8 and 16 hours were selected to determine the timescale over which significant differences would emerge due to irradiation treatment (Figure C1).

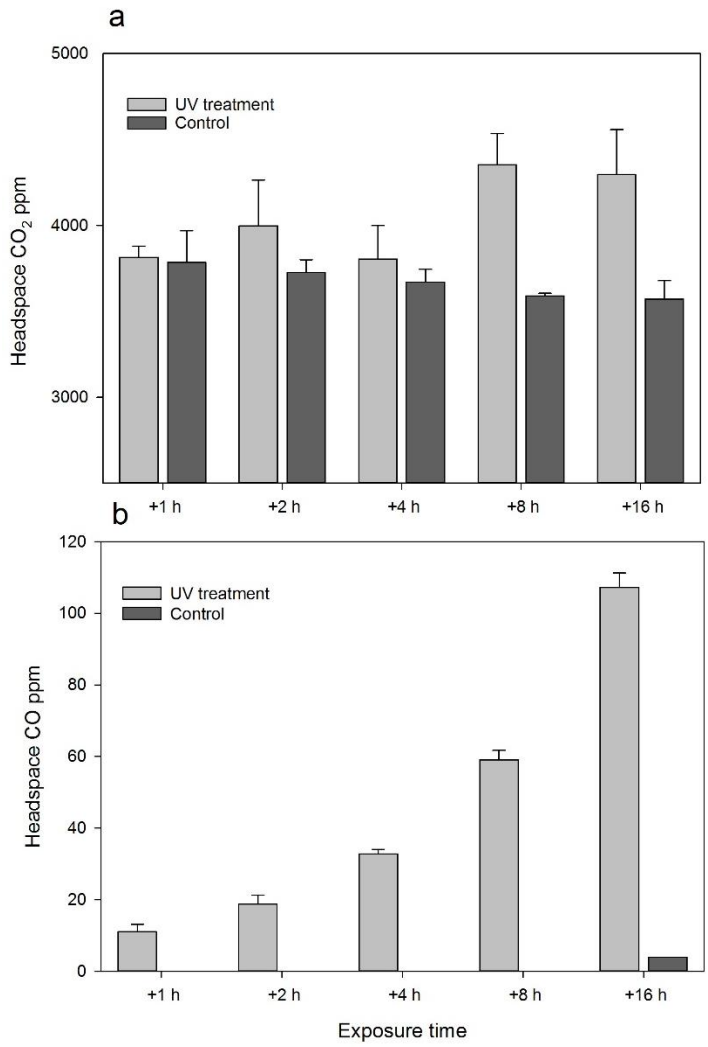

Figure C1. Difference in headspace gas concentration for a) CO_2 and b) CO in UV treatment and control samples at increasing exposure times (n=4). Error bars show the standard deviation of the mean.

Headspace concentrations of CO were significantly different between treatments after 1 hour of irradiation (Table 2.2), however CO_2 headspace concentrations did not become significantly different until 8 hours of irradiation. As CO_2 was one of the key photoproducts of interest, 8 hours was selected as a standard irradiation time going forward.

Appendix D Lignin Phenol Data from the Black Burn

Table D1. Lignin phenol data collected from the Black Burn over the year-long sampling campaign, winter rainfall event and summer rainfall event.

Campaign		C:V	S:V	P:V	Al:Ad_{vs}	Λ_{11}
Year-long	May 14	0.38	0.71	1.63	0.97	1.23
	Jun	0.50	1.32	1.23	1.16	1.44
	Jul	0.63	1.48	2.03	0.75	1.04
	Aug	0.45	1.21	1.50	1.02	1.83
	Sep	0.44	1.32	1.55	1.32	0.84
	Oct	0.51	1.42	1.11	1.14	1.99
	Nov	0.29	0.32	1.00	1.09	1.69
	Dec	0.26	0.41	0.88	1.13	1.54
	Jan	0.22	0.49	1.03	1.19	1.29
	Feb	0.44	0.84	1.56	1.03	1.18
	Mar	0.58	1.54	1.56	0.96	1.44
	Apr	0.59	1.42	1.77	0.91	1.22
	May 15	0.31	0.57	0.96	1.30	1.75
Winter event	11:00	0.45	1.23	0.89	1.05	2.40
	12:00	0.47	1.29	0.89	1.04	1.87
	17:00	0.25	1.35	1.47	0.57	0.83
	20:00	0.56	1.21	1.03	1.11	2.33
	22:00	0.21	0.91	1.39	0.61	0.89
	01:00	0.45	1.19	0.83	1.04	1.96
	06:00	0.43	1.20	0.83	1.05	1.84
	14:00	0.32	1.35	0.86	0.73	2.31
Summer event	14:30	0.82	1.07	1.11	1.54	1.69

17:30	0.67	1.08	1.34	1.15	0.64
18:30	0.75	1.25	1.41	1.14	0.72
20:30	0.61	1.09	1.41	1.09	0.69
22:30	0.90	1.46	1.27	1.41	1.23
03:30	0.67	1.09	1.47	1.26	0.80
06:30	0.53	1.14	1.37	1.16	0.93

Appendix E Spectrofluorescence Data from Year-long Samples

An R script was used to process the excitation-emission matrix data for monthly samples collected in the year-long campaign from the Black Burn and Loch Katrine (Lapworth and Kinniburgh, 2009). The script produced a table of intensity values (mean, max, min, Σ and SD) for fulvic-like (FA), tryptophan (TPH) and tyrosine (TY) components in water samples (Figure D1).

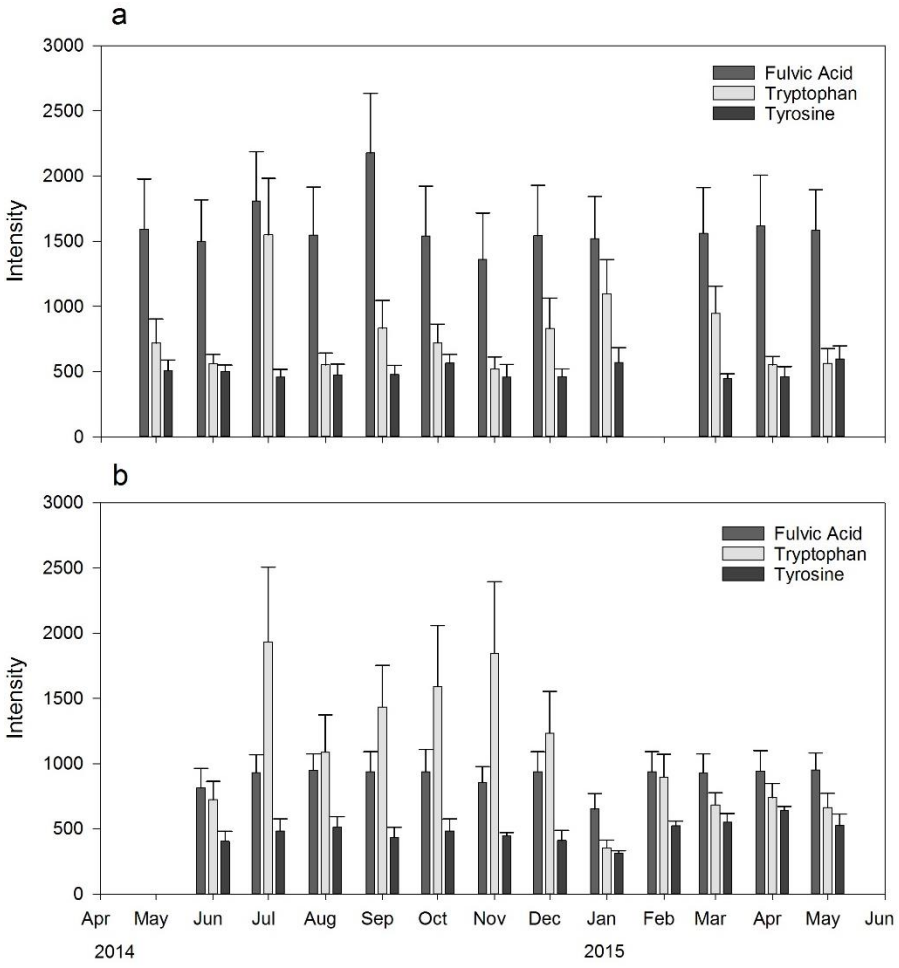

Figure E1. The mean intensity values for fulvic-like (FA), tryptophan (TPH) and tyrosine (TY) components for samples collected from a) the Black Burn and b) Loch Katrine. The error bars show the standard deviation of the mean.

Data are missing for February at the Black Burn and May 2014 at Loch Katrine, due to insufficient sample for analysis (all spectrofluoresence data were collected in April 2015, using samples filtered to 0.2 μm, and thus there was not an opportunity to collect extra sample to represent monthly conditions).